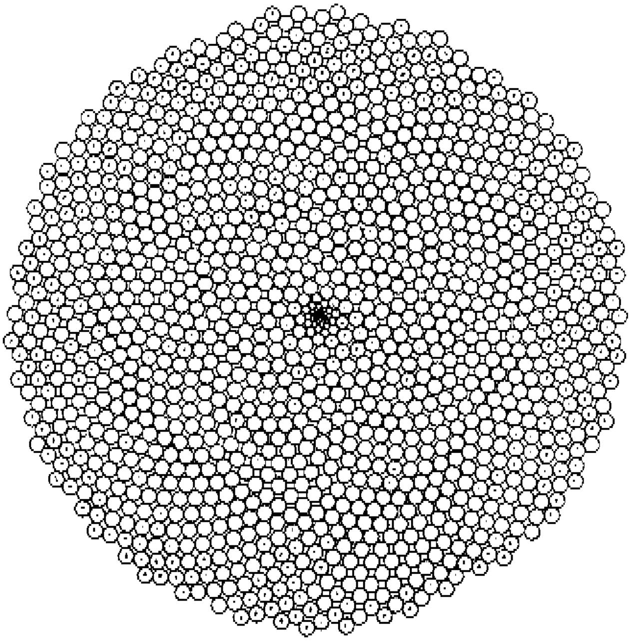

PATTERNS AND MORPHOLOGY OF BUILDING ELEMENTS FOR CLOSE-PACKING OF DOME SURFACES AFTER

PHYLLOTACTIC PATTERNS FOR DOMES

THE EXAMPLE OF PHYLLOTAXIS AND MORPHOGENESIS OF PRIMORDIA ON THE APEX OF COMPOSITES

PROEFSCHRIFT

ter verkrijging van de graad van doctor aan de Technische Universiteit Eindhoven,
op gezag van de Rector Magnificus, prof.dr. J.H. van Lint,
voor een commissie aangewezen door het College van Dekanen in het openbaar te verdedigen op
woensdag 21 december 1994 om 14.00 uur

door

Frank Maria Jozef van der Linden
geboren te Eindhoven

Dit proefschrift is goedgekeurd door de promotoren:
prof.ir H. Wagter
en
prof.dr.ir. H.S. Rutten.

Phyllotactic Patterns for Domes

PHYLLOTACTIC PATTERNS FOR DOMES

 Printed in Holland by Wibro, Helmond.
Information address: Vondelstraat 31, 5671 VA Nuenen, The Netherlands.

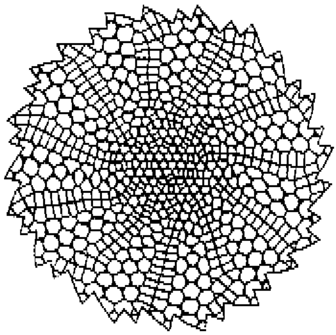

PHYLLOTACTIC PATTERNS FOR DOMES

to Karianne, Mick, and Otto

Frank M. J. van der Linden

CONTENTS

MATHEMATICAL-BIOLOGICAL MODELING (2-4)

WITHIN AN ARCHITECTONICAL CADRE (1,5)

APPENDAGES (i-v)

CONTENTS

CHAPTERS 1-5

APPENDAGES i-v

1 INTRODUCTION

TERMINOLOGY

"Patterns and morphology of building elements for close-packing of dome-shaped receptacles after the model of phyllotaxis and morphogenesis of primordia on the apex of composites."

patterns	repeated regularities within a structure
structure	coherent whole
morphology	elementary geometry, form qualities
building elements	prefabricated parts of a building
close-packing	maximum dense stacking
dome	hemispherical to paraboloid shaped shell
phyllotaxis	patterns in plant part positioning
morphogenesis	arising of shapes, development of shapes
primordia	minuscule appendages in genesis of plants
apex	growth top of a plant stem
composites	plants with compound flowers on a flower head
Euclidian geometry	geometry of point, line, plane, and solid
fractal structures	structures with self-similarity
self-similarity	repeated form similarity in different size scales of a structure
gnomonical structures	structures, which grow with maintainance of form
Fibonacci sequence	1, 2, 3, 5, 8, ...
Lucas sequence	1, 3, 4, 7, 11, ...

ARCHITECTONICAL CONTEXT

There exist different architectonic schools or traditions that lay claim to the metaphor of Nature and organical shape: the nineteenth century English Arts and Crafts tradition, the American tradition of Louis Sullivan, the Catalonian modernistic tradition (Gaudi and others), the ArtNouveau/Jugendstil tradition, and the anthroposophic tradition. These traditions not only caused a widespread differentiation of forms in the decorative art but also in the spatial effect of volumes, both in exterior and interior. With functionalism and the expulsion of ornament, the sensitivity for such shapes (and for their quality in architectural junction details and implementation) has decreased or even been lost.

The withdrawal of the monopoly of the functionalistic-modernistic paradigm leaves room for a multitude of shapes and creates a need for a new naturalistic metaphor that, without losing its ties with the past, can mean a new impuls for another definition of decorative art: no longer superficial but rooted in the basic structure.

The models presented here offer the opportunity, with the use of advanced technology, to generate a virtually unlimited series of new shapes that are based upon the principles of natural growth processes. With it, the designer is offered a multitude of choices. By means of some simple manipulations, the architect can adapt the variety that is produced to his own wishes, continuously explore and interpret new shapes. At this moment designers have at their disposal classical works like the habitually cited "On Growth and

Form" by d'Arcy W. Thompson. Whereas these classics are still a rich source of inspiration, since their time new insights have been developed about shapes produced by natural growth processes. This project refers to the newest insights in biological morphology (see the mathematical-biological articles) and elaborates these in an architectonical sense.

In summary, the aim is a contemporary structural design and ornamental art in architecture that is derived from the way shapes and patterns are generated in Nature. The motive is a fascination by the beauty of natural shapes and growth processes in which the simplicity of developmental principles is coupled to the profusion of form variations that arise from them. To realize the dream of an Architec-Nature, mathematical-biological investigations may be applied to the architecture of buildings by developing a new shape-grammar that can be made accessible to every designer.

Formulation of the problem

The mechanical constructing and assembling of elements of domes is usually done in enclosing shells (like those by Nervi) or in semi-regular bodies made of regular polygons (like those by Buckminster-Fuller). These methods are interpretations of static natural patterns, as they arise from material deposition (in the non-living Nature).

In the case of cast concrete or very large elements (in size scale just below the entire building), talking about elements is hardly relevant and a pattern genesis is hardly distinguishable.

In the case of relatively small elements one has to keep to dome-shapes, derived from Platonic and Archimedical bodies (respecitively regular and semi-regular polyhedra). The profusion in tesselations can be descibed by a few characteristics of shape, material, and environment (think of crystallization). However, in the developing structure lies the limitation of its static character.

In dynamical, living structures, pattern generation is governed by the already formed part of the expanding whole - more specified by (i) messages and (ii) transformation:
(i) The structure incorporates genetic and environmental information and thereby continually redefines and narrows the limiting conditions for further growth. While I adapt this principle, I shall disregard the biochemical and genetical details and replace these by the simplest possible mathematical instructions. This is justified, because the genetic mechanisms contain a good deal of evolutionary historical ballast that is irrelevant to the architectural principle, and they are still incompletely analyzed.
(ii) Insight in biological and architectonical principles is indispensable in understanding the influence of a structure's enlargement on pattern genesis. Interpretation of phyllotactic patterns leads to new design premises for building elements (and their assembly methods), such as certain principles for position, shape, and dimension of close-packed units.

Three objectives are now outlined:
(i) designing a model that generates phyllotactic patterns starting from parameters recognizable in biology

(ii) formulation of the meaning and possibilities to derive building element-forms and -patterns from the phyllotaxis of composites
(iii) description of principles for architecture and construction. NB. The concept of architecture is being used here in the meanings of structure (as in: the architecture of a tree, the architecture of a computer) and cultural manifestation (compare: the architecture of Wim Quist, the architecture of the Shakers).

(Light supportive constructions as those from Frei Otto fall outside the problem matter since in these, the external appearance of a naturally grown product is imitated on scale and repetition of components. Algorithmic element ordening to achieve patterns is not the aim there.)

Starting points

The traditional architect occupies a prominent place in the building process. In that position he will usually not be inspired by the way (green) Nature approaches the problem of constructing shape. On the one hand this is understandable when one considers that a building does not arise according to the limiting laws of natural growth. On the other hand this is remarkable since the human being is essentially a part of Nature.

The current building practices are alarming when looked upon from the perspective of the environmental issue. The traditional architect will have to change his attitude. He will have to gain more insight in mechanisms prevalent in Nature. For this I do not think so much about copying outward appearances, but more about harmonization in the sense of working according to biological mechanisms. Particularly in the designing phase of a building project the architect has the authority to contribute to improvements of the current situation.

Recently, a development in mathematics has been initiated that can be important for future constructing practices or respectively the pre-manufacturing of parts. The mathematician Benoit B. Mandelbrot is the founder of *fractal geometry* which states that Nature is not built-up of perfect straight lines, sheer planes, and regularly bordered solids.

Parallel to this development, the *L-systems* of biologist Aristid Lindenmayer were elaborated. L-systems are algorithms that generate geometric branching structures as they occur in plants. An important blank space in the L-systems lies in the old question of the orientations in certain spatial structures. L-systems are essentially lodged in a plane: it requires additional tricks to make them three-dimensional

Since the early seventies I am studying the Fibonacci sequence in connection with the pattern formation of primordia on the flower heads of composites. My interest was stimulated after being told that the majority of all plants carries these patterns, indeed 'hidden' along the stem (S. van der Vorst). In the first instance, my problem was: *"Draw in a simple way the pattern of a sunflower head."*. By simple I mean: 'blind', not using (intuitively) strange parameters and complex mathematical functions, but elementary geometry and indivisible algorithms. A professional computer produced the first simple constructions (R. Barluschke). Since the appearance of relatively popular computers, I myself was able to test assumed algorithms instantly. Feedback with systematic biology became necessary (A. Lindenmayer). While the yet simplified phyllotaxis model was build up from a center, I called it 'Dislodgement Model' (F. van der Blij). After criticisms concidering the singular character of this model (no thing can arise from a *point*) I transformed it into the 'Stack and Drag Model' (K. Bachmann).

The viability of the *phyllotaxis generator* is ensured by the following qualities:

(i) The model uses an absolute minimum of the hereditary information in plants. Except geometrical basics, only assumptions reflecting true biological growth are used as input.

(ii) The model re-establishes the L-systems through a structural extension in the third dimension.

(iii) The model generates fractal structures with Euclidic building blocks. In other words, gnomonic structures are being created with spherical units which are defined with conceptions from the special literature (see *references* in the articles) and recent investigations (such as *numerical canalization*, J. Battjes). This means that designed fractal structures are founded on a biologically justified model. It has to be noted that the current fractal-theories are facing a problem: although results seem to be very true to Nature, the mechanisms that underlie these mostly deviate strongly from the (bio)fysical and (bio)chemical mechanisms which give natural fractals. For the time being, scientifically based fractals are exceptional.

INTRODUCTION: FIGURES

In the first seven figures, 'Architec-Nature' is shown as reflections or settings in different contexts *(see Architectonical context)*. This architecture can be tied to a people, a person, a philosophy of life, a tradition, constructive principles, mathematical rules. The remaining figures show work of the author, in which the Dislodgement Model and the Stack and Drag Model can be concidered in the perspective of a continued line of investigation.

INLEIDING: FIGUREN

De eerste zeven figuren tonen 'Architec-Natuur' als reflecties of situeringen in verschillende contexten *(zie Architectonische context)*. Deze architectuur kan zijn gebonden aan een volk, een persoon, een levensovertuiging, een traditie, constructieve principes, wiskundige regels. De resterende figuren tonen werk van de auteur, waarbij het Verdringingsmodel en het Stapel- en Trekmodel kunnen worden beschouwd in het perspectief van een doorgezette lijn van onderzoek.

Fig 1 **Gotiek** - expressie, bepaald door in de architectuurhistorie uitzonderlijke inspiratie vanuit met name religieuze, experimenteel-constructieve, licht-technische, kunstzinnige, prestigieuze en politieke motieven.
Fig 2 **Dogon** - een integratie van cultuur (Mali) en ornament over een lange reeks van jaren.
Fig 3 **Steiner** - architectuur als onderdeel van een levensovertuiging, 'natuur-architectuur' in vorm ('organisch') en materiaal (hout).
Fig 4 **Gaudi** - integratie van constructie en ornament.
Fig 5 **Nervi** - integratie van geabstraheerde organische-vormentaal en constructie.
Fig 6 **Buckminster-Fuller** - anonieme architectuur met veel regelmaat / weinig afwijkingen. De strenge geometrie is geïnspireerd door vooral de dode natuur (kristallijne structuren) en vertoont dislocaties.
Fig 7 **Frei Otto** - lichte, constructieve structuren met architectonische elementen voor trek en druk.

Fig 8 Eindproject van de auteur aan de TUE, architectonisch ontwerpen: De tekening toont *(boven)* een 'woonberg' bovenop een *(onder)* vloerconstructie van een voorgestelde parkeerkelder bij het stadhuis. Het streven was een veelduidige architectuur, waarbij het hand-in-hand-gaan van constructieve vormregelmaat en functionele bestemming intrinsiek domineert. Stedebouwkundige situatie, gebruiksfuncties, constructie, materialen en architectuur zijn duidelijk aanwijsbaar geïntegreerd: de (geometrische) hoek, die de beide hoofdassen (Wal - Paradijslaan) maken, definieert een gecompliceerd dualisme. Met andere woorden, de architectuur wordt bepaald door het onderscheid (programmatisch:) openbare functies - wonen, (constructief:) kolommen - schijven, (technologisch:) beton - baksteen, (Gestalt:) plein en wand - 'berg', (stedebouwkundig:) sociaal-culturele functies - wonen.
Fig 9 Onderzoek naar krachtenspel en vervormingen *-kracht en vorm-* in een fragment van de constructie van Fig 8.
Fig 10 De computer als laboratorium: rekenkundig vergelijk van phyllotactische plantetop-patronen en bouwkundige dome-patronen.
Fig 11 Bolstapelingen als uitgangspunt voor oppervlaktepatronen.
Fig 12 3D-simulatie van bloemhoofd in vroege ontwikkelingsfase van *Microseris Pygmaea*. Het Stapel- en Trek-model maakt zeer nauwkeurige simulaties mogelijk. De structuur is vergaand vergelijkbaar (zie bijlage iv RESULTS) met SEM's (Scanning Electron Microscope-opnamen) in de vakliteratuur.
Fig 13 Dome-patronen: primaire (*boven:* elementen vormen een helices-patroon) en secundaire (gegroepeerde elementen vormen een zes-rotatie-symmetrisch patroon).
Fig 14 Halfregelmatig patroon, naar analogie van de levende natuur (phyllotaxis): een algehele orde, waarbij (incidentele) dislocaties niet voorkomen *(vergelijk met Fig 6, Buckminster Fuller)*.
Fig 15 Variaties in element-definitie en domevorm. De structuren zijn alle ontwikkeld met het programma 'ApexD', volgens het Verdringingsmodel.

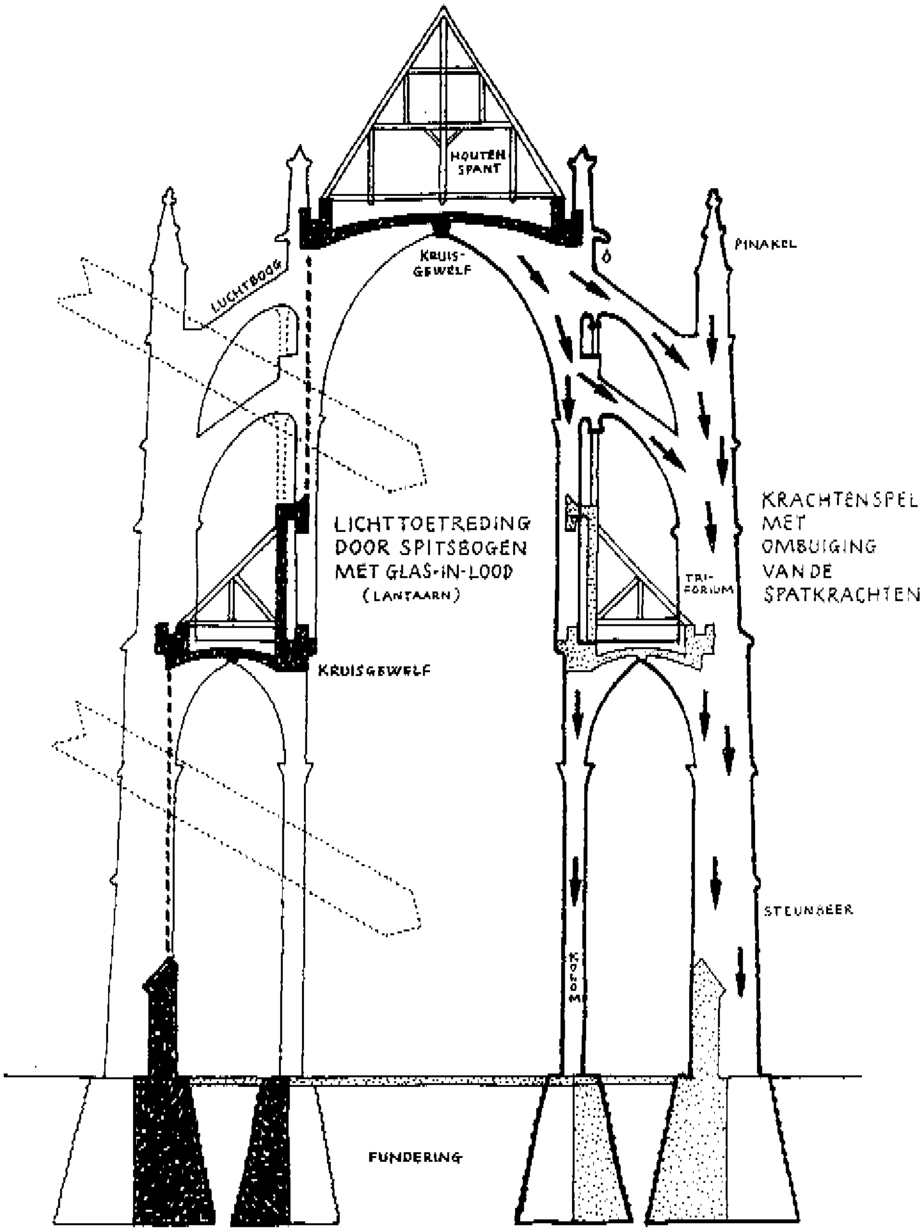

Fig 1 Gothic - expression after an excessive inspiration by religious, experimental-constructive, lighttechnical, artistic, prestigious, and political motives.

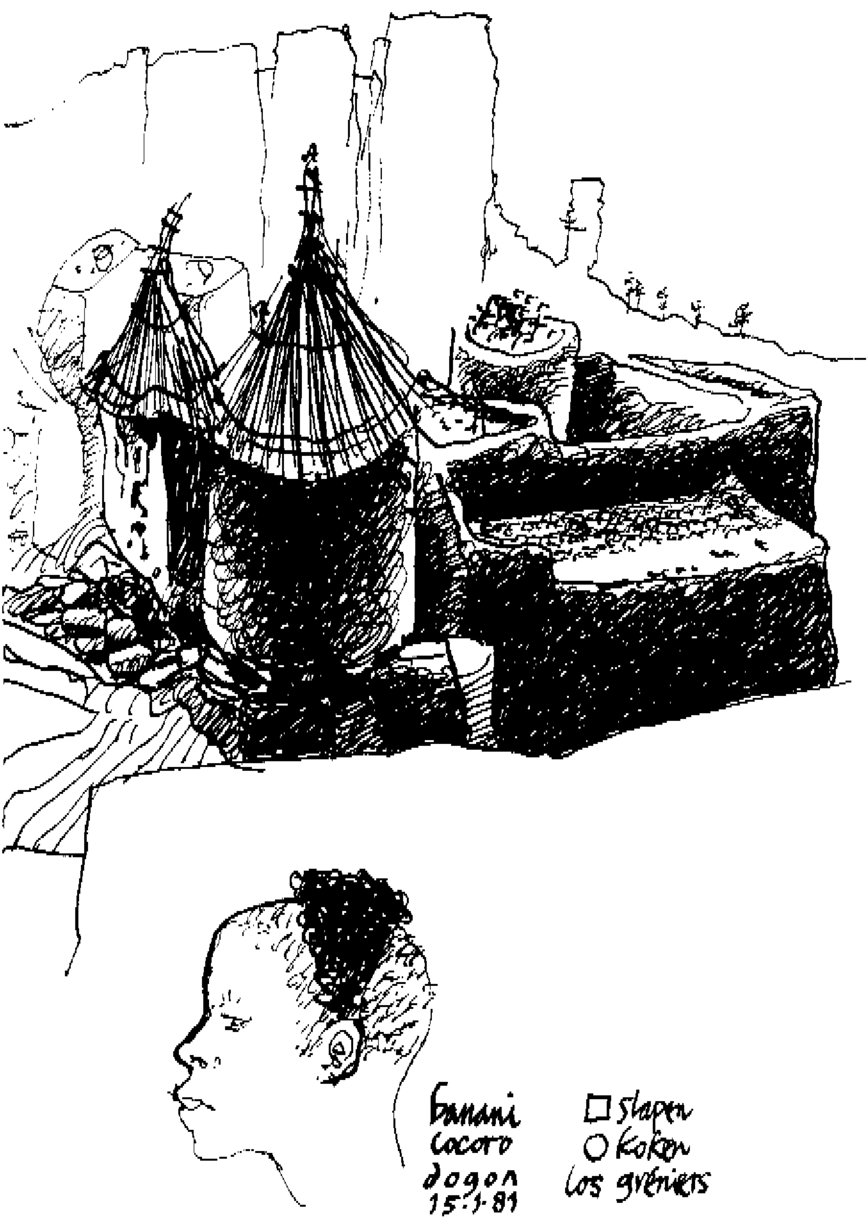

Fig 2 Dogon - an integration of culture (Mali) and ornament in a period of many years.

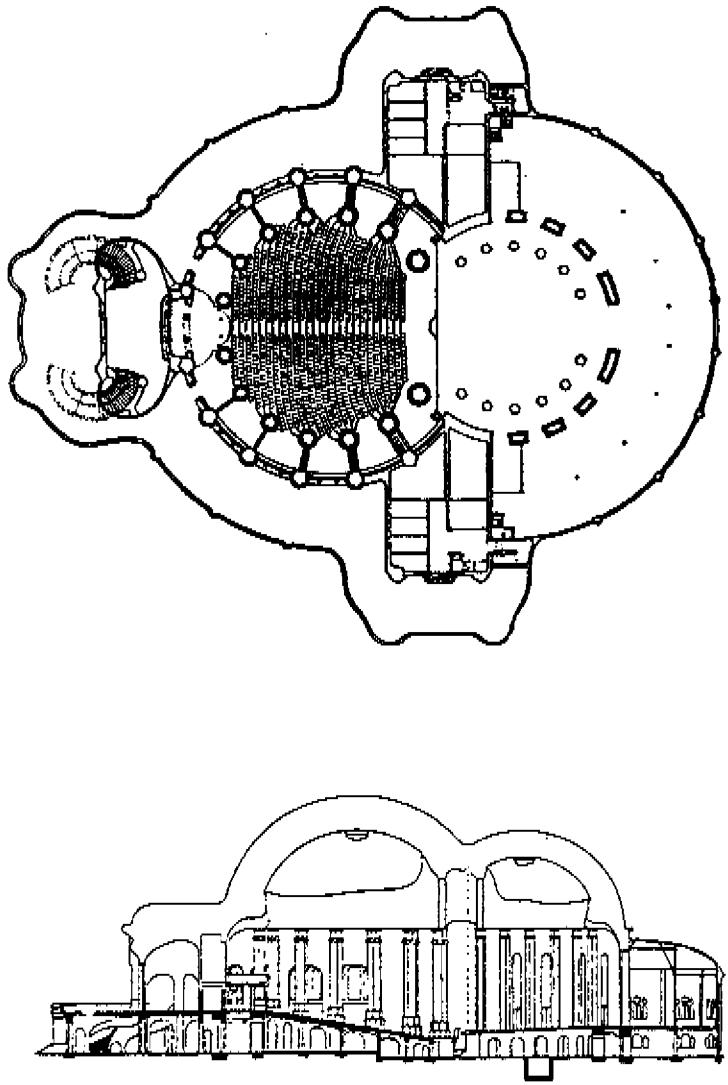

Fig 3 **Steiner - architecture as a part of a philosophy of life, 'nature-architecture' in shape ('organic') and material (wood).**

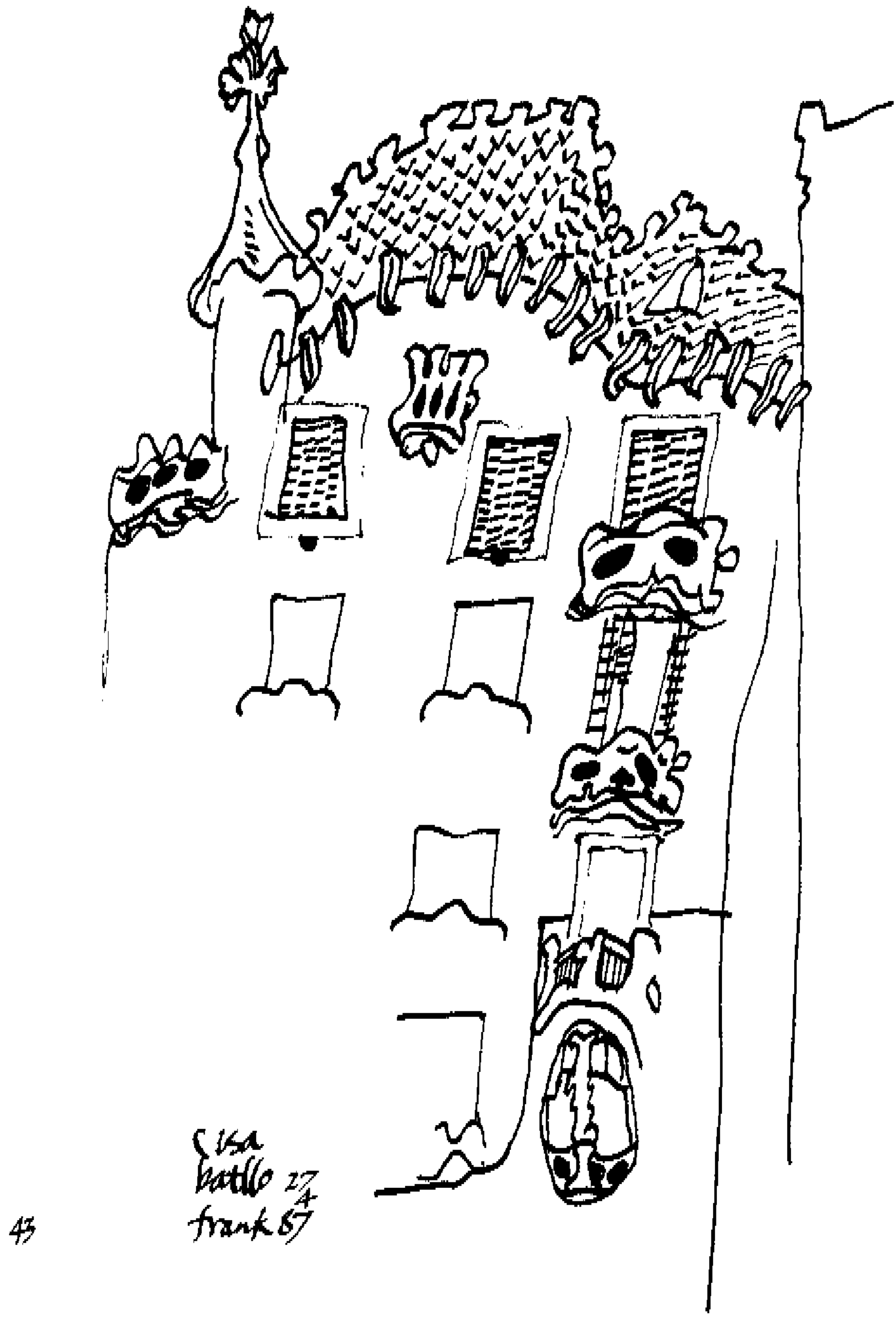

Fig 4 Gaudi - integration of construction and ornament.

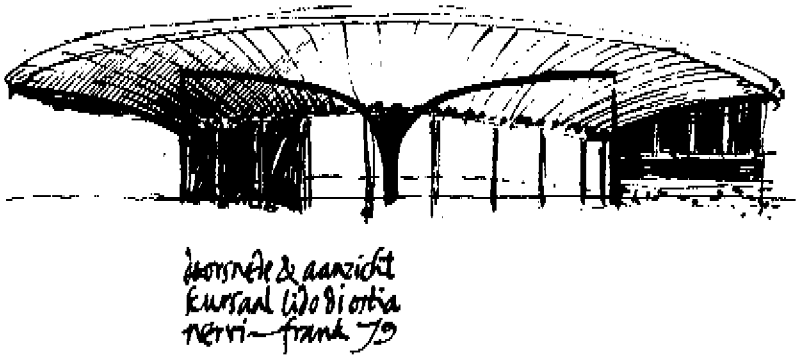

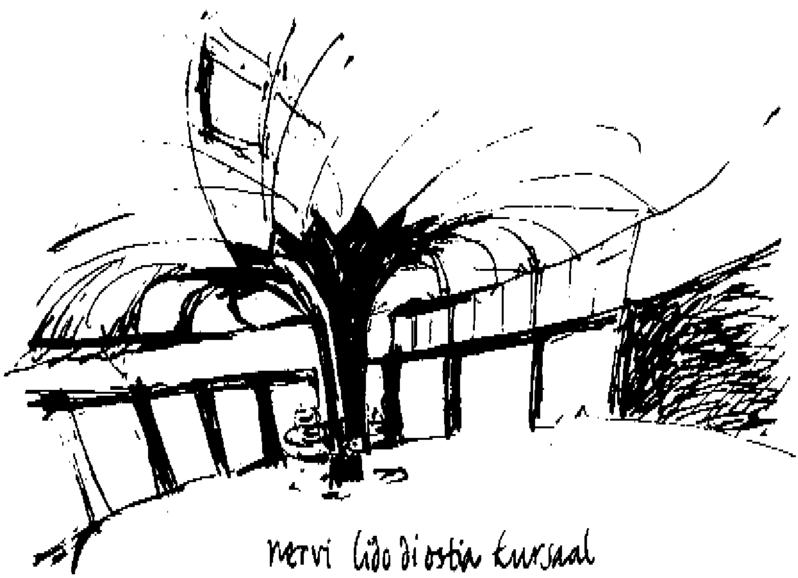

Fig 5 **Nervi** - integration of abstracted organic form language and construction.

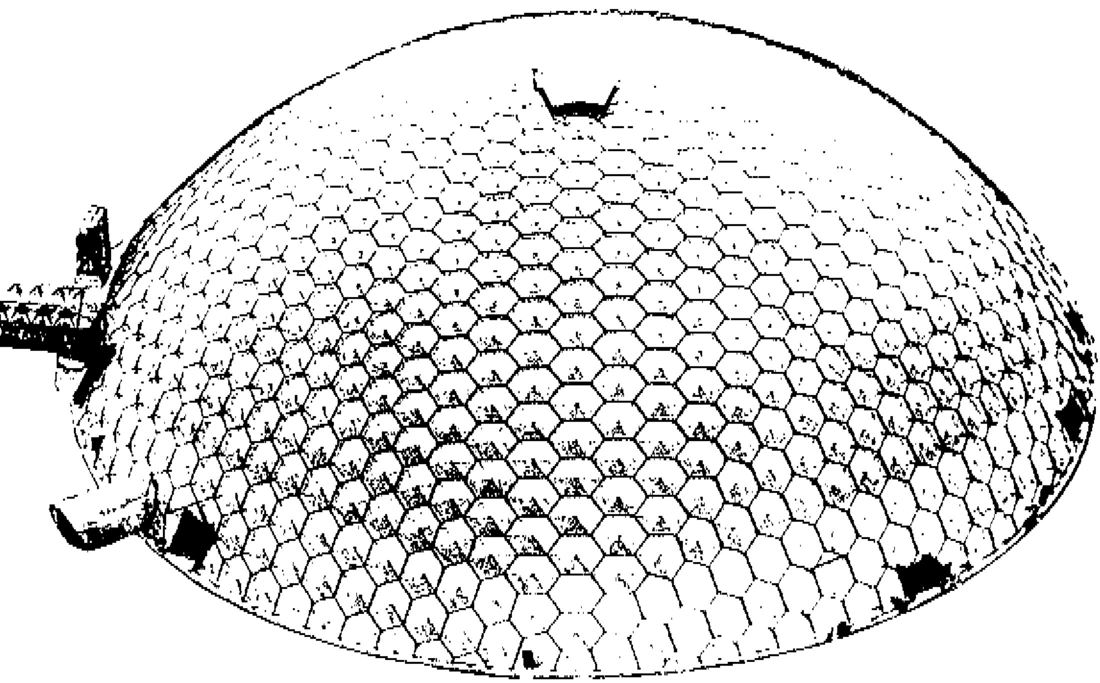

Fig 6 **Buckminster-Fuller** - anonymous architecture with much regularity and a few anomalies. Showing dislocarions, the rigid geometry seems to be inspired by crystallic structures.

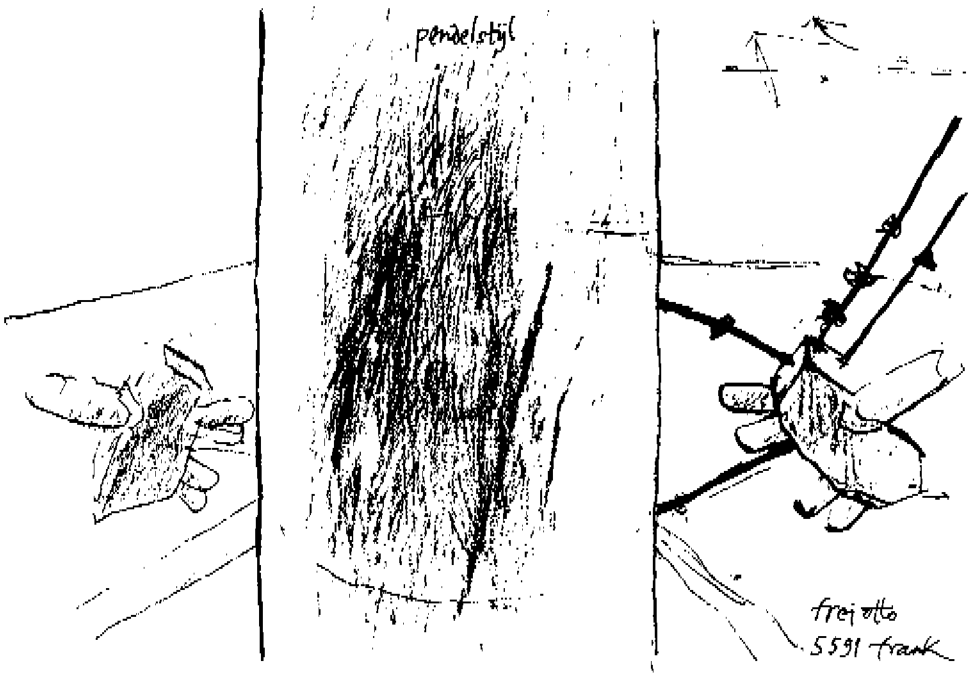

Fig 7 **Frei Otto** - light bearing structures with architectonical elements for different kinds of forces.

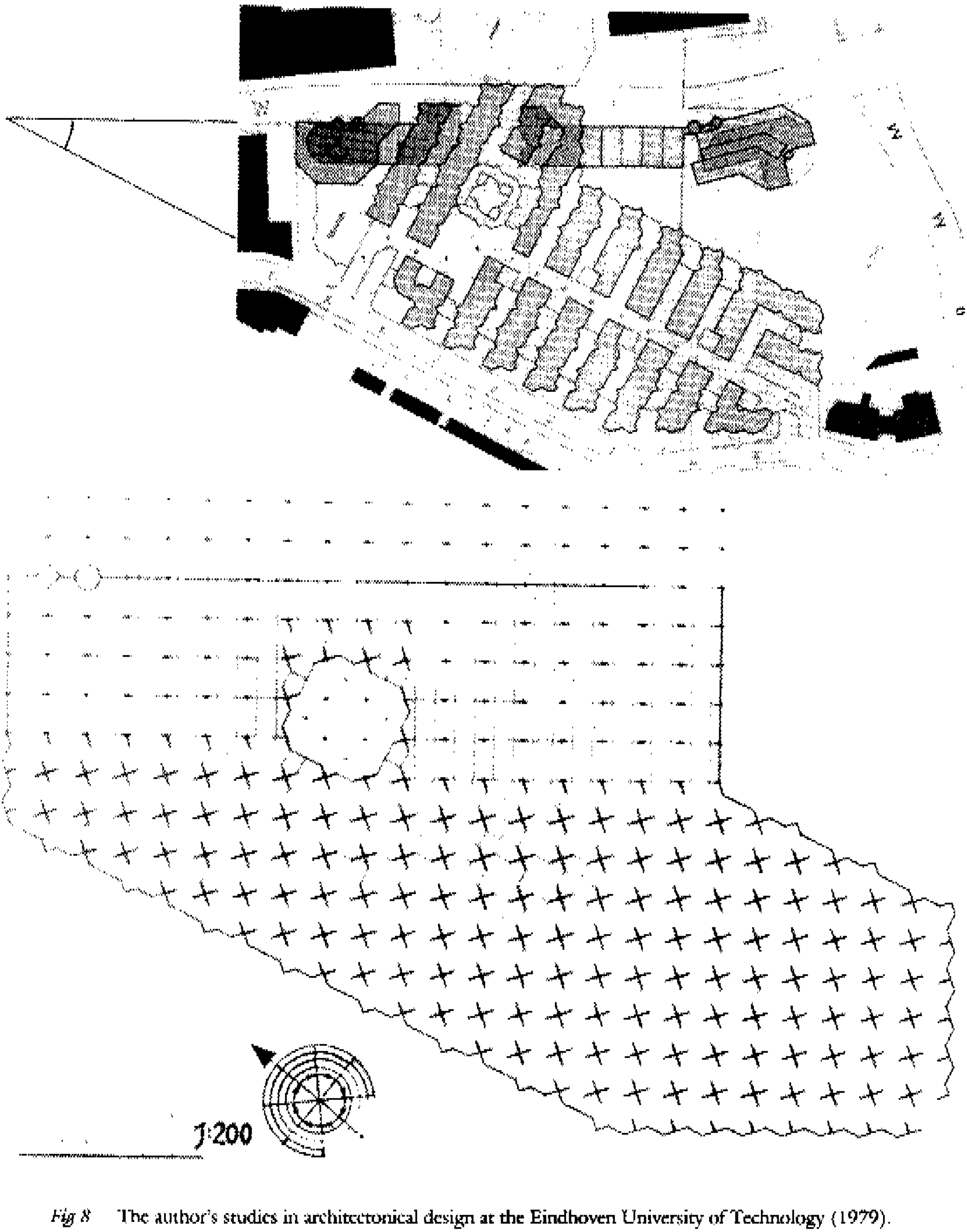

Fig 8 The author's studies in architectonical design at the Eindhoven University of Technology (1979). The drawings show *(top)* building structures on top of *(below)* the ground level floor construction of an underground parking near the city hall. The project's aim was achieving an ambiguous architecture which shows an intrinsic dominant harmony of constructive regularity and functional destination. The architecture may be characterized by the differences (programmatic:) public functions - housing, (constructive:) columns - walls, (technological:) concrete - brick, (Gestalt:) square and wall - 'mountain', (town-planning:) social-cultural functions - housing.

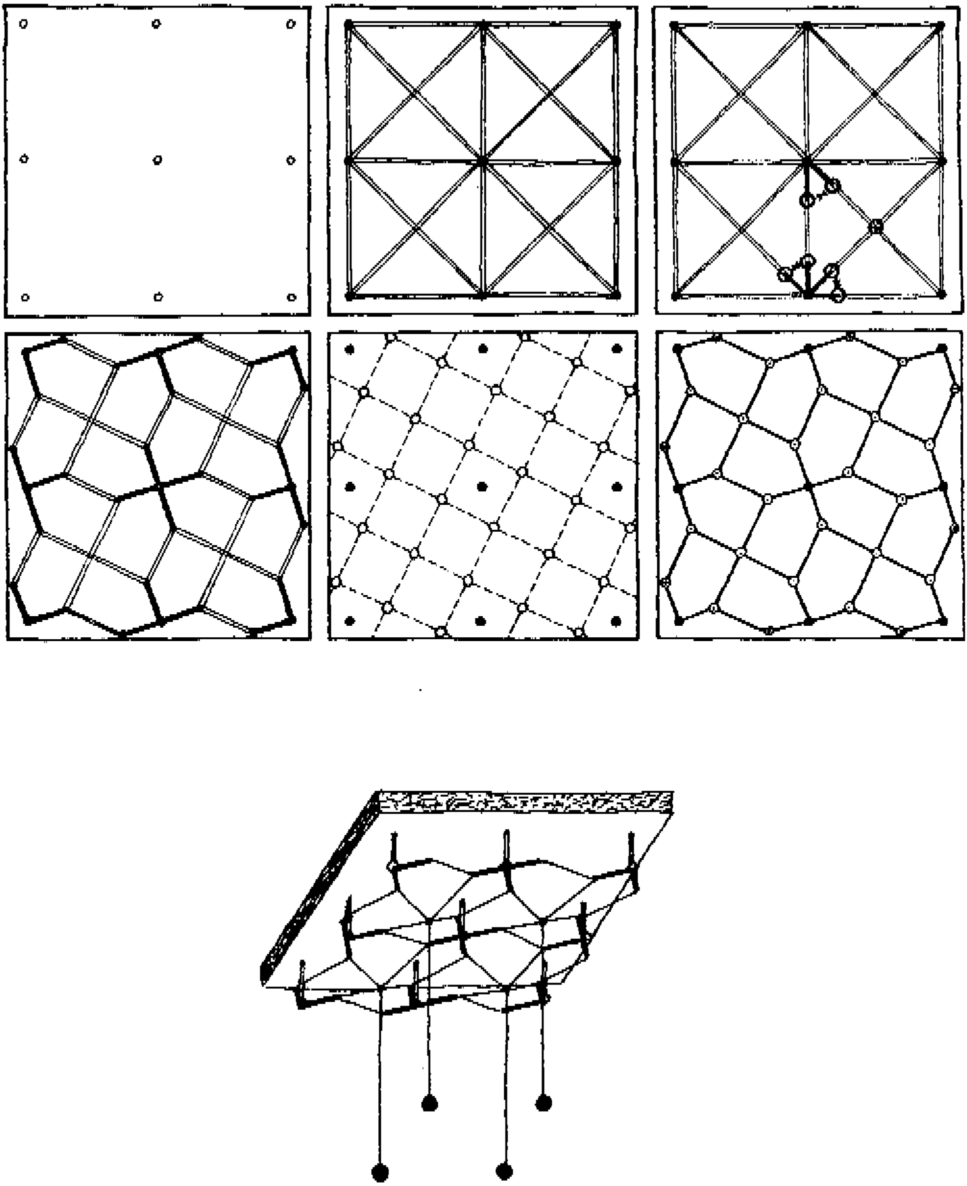

Fig 9 Analysis of the forces and deformations *-force and form-* in part of the construction of Fig 8.

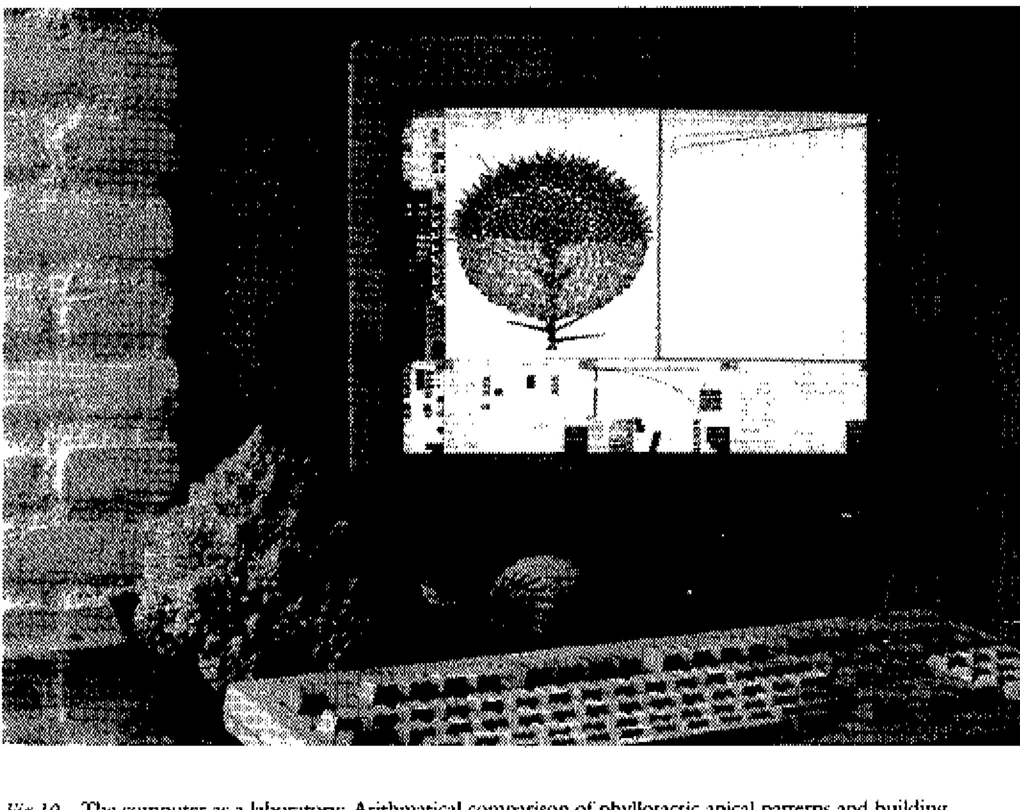

Fig 10 The computer as a laboratory: Arithmatical comparison of phyllotactic apical patterns and building dome patterns.

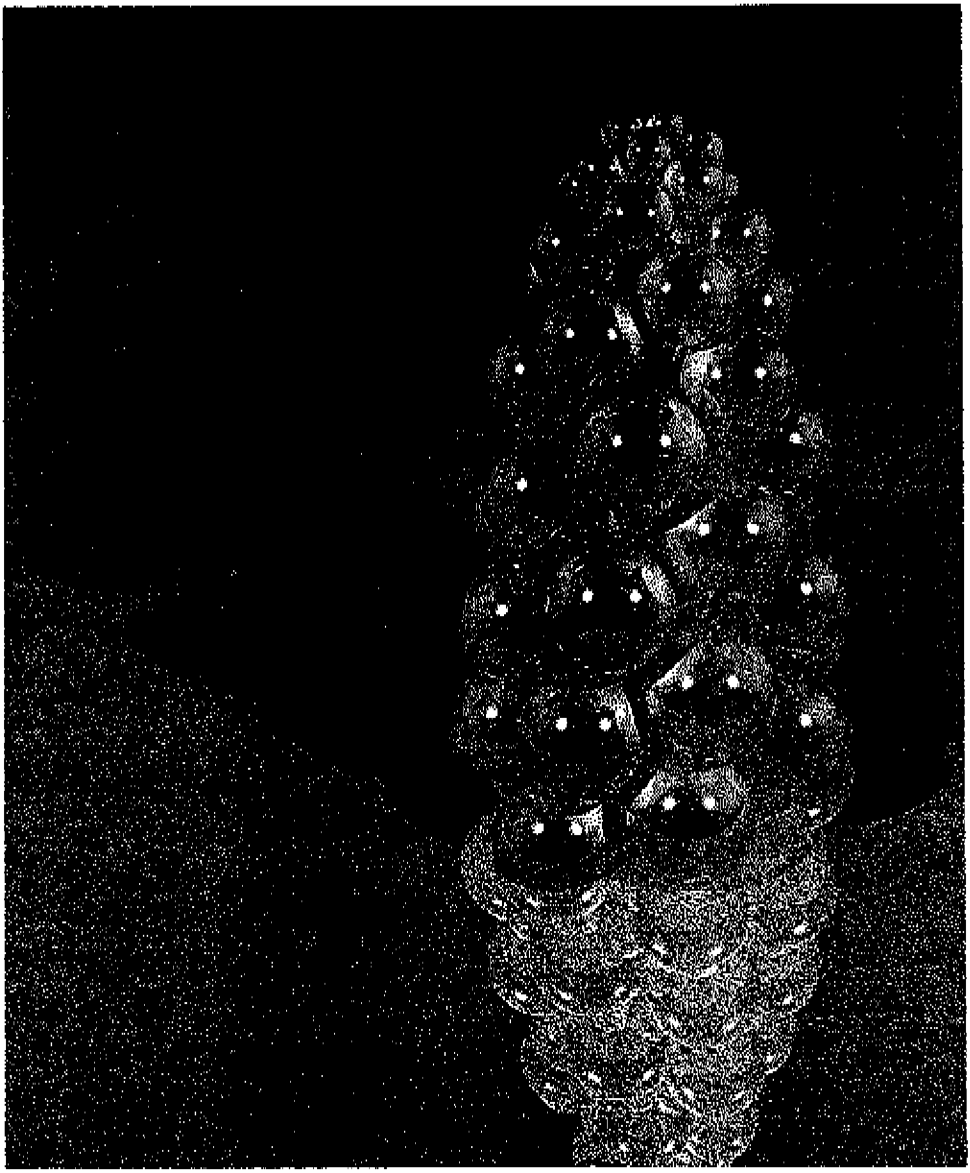

Fig 11 Spheres stackings as the starting point towards surfacial patterns.

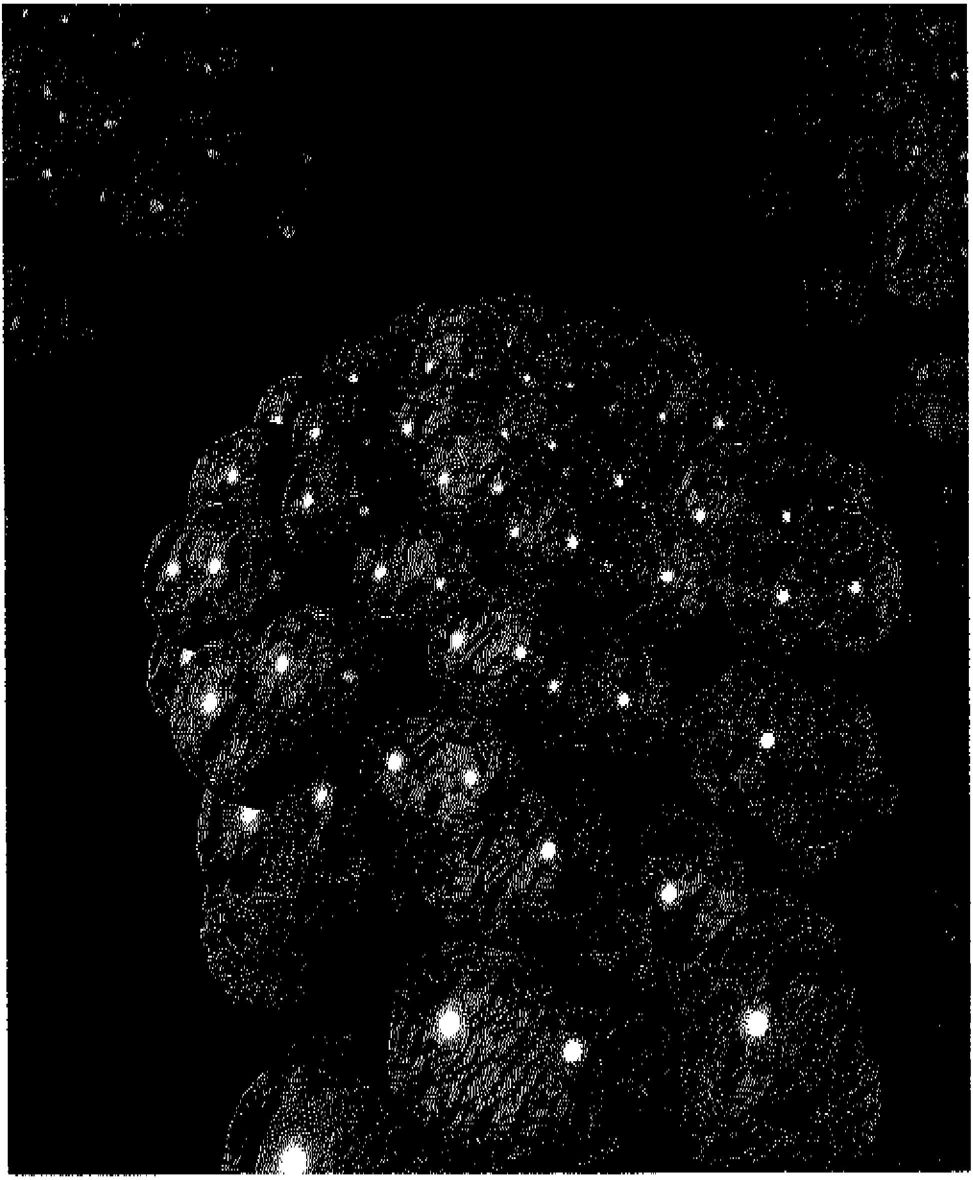

Fig 12 3D-simulation of a flower head in early development of *Microseris Pygmaea*. The Stack and Drag Model provides close approximations (see compared SEM's in appendage).

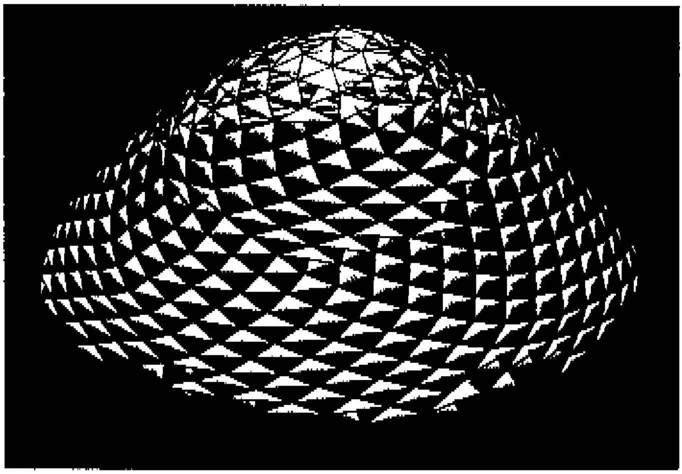

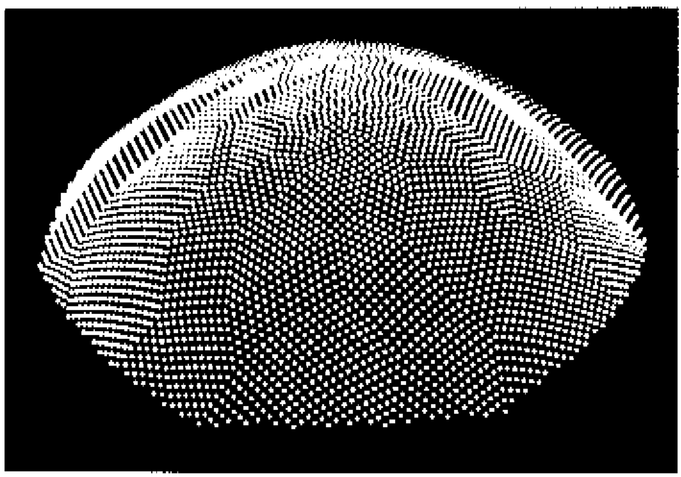

Fig 13 Dome patterns: primary (*top:* units are arranged in helices) and secondary (clustered units form a six-rotation symmetrical pattern).

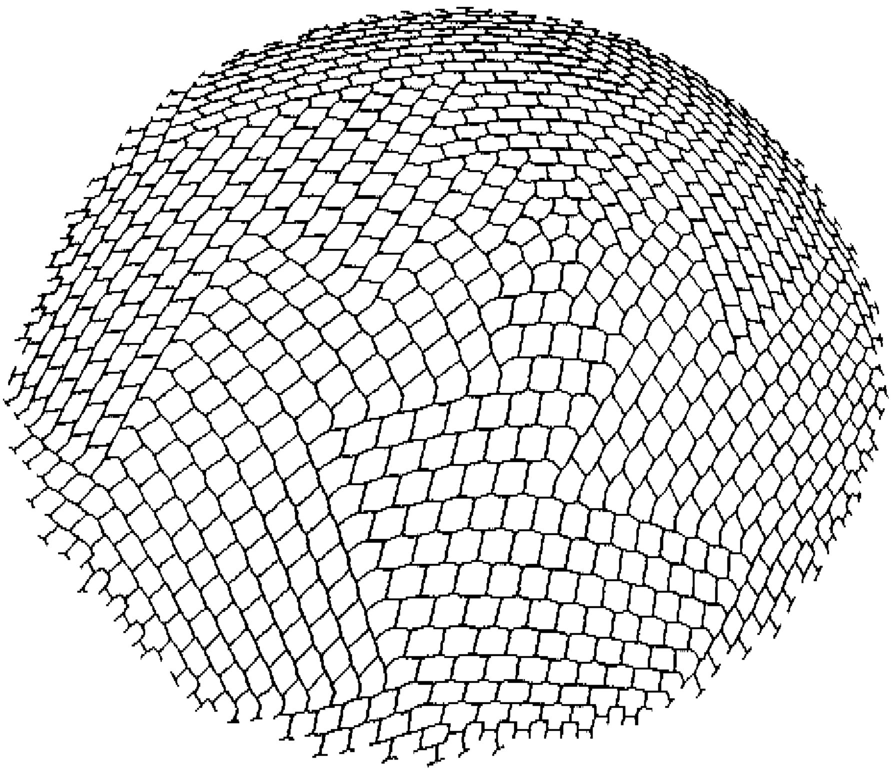

Fig 14 Semiregular pattern, showing a whole order without the occurrence of dislocations *(see also Fig 6)*.

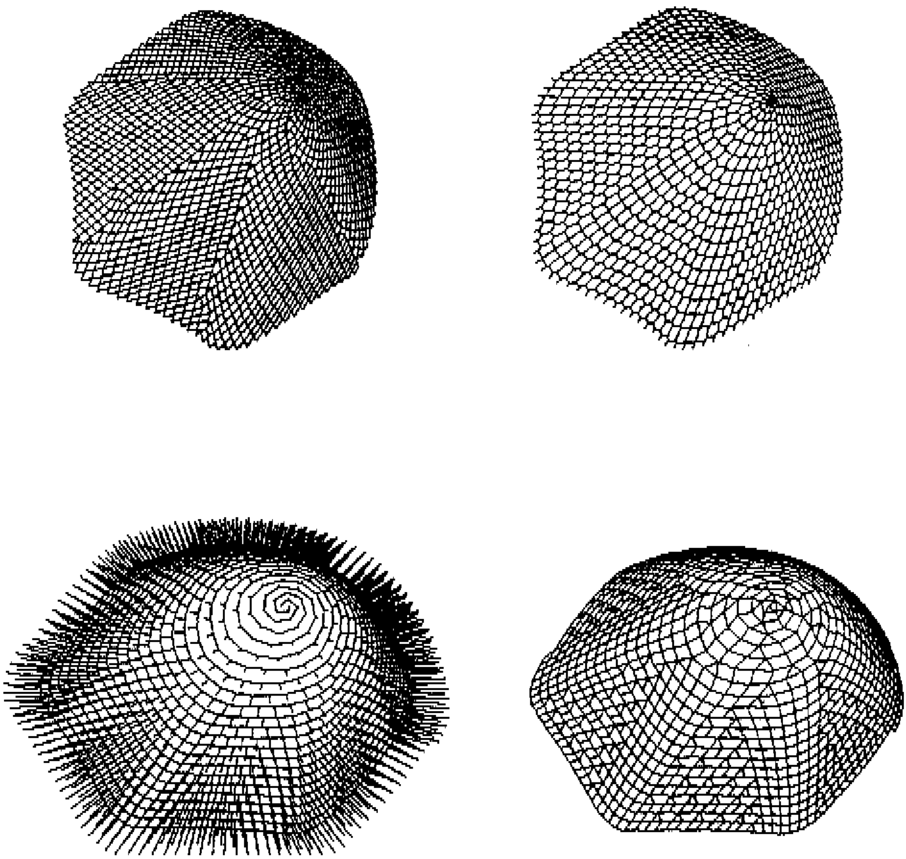

Fig 15 Variations in unit-definition and dome shape. All of the structures have been developed with the program 'ApexD' of the Dislodgement Model.

1 INLEIDING

Terminologie

"Patronen en morfologie van bouwelementen voor close-packing van dome-oppervlakken naar voorbeeld van phyllotaxis en morfogenese van primordia op de apex van composieten."

patronen	zich herhalende regelmatigheden binnen een structuur
structuur	samenhangend geheel
morfologie	vormleer, vormeigenschappen
bouwelementen	te prefabriceren delen van een gebouw
close-packing	maximaal dichte stapeling
dome	schaal in de vorm van een halve bol tot paraboloïde
phyllotaxis	patronen in plaatsing van plantedelen
morfogenese	vormontstaan, vormontwikkeling
primordia	minuscule uitsteeksels van planten in aanleg
apex	groeitop van een plantestengel
composieten	planten met samengestelde bloemen op een bloemhoofd
Euclidische geometrie	meetkunde van punt, lijn, vlak, lichaam
fractale structuren	structuren met self-similarity
self-similarity	in zichzelf gelijkvormige structuren
gnomonische structuren	structuren, die groeien met vormbehoud
reeks van Fibonacci	1, 2, 3, 5, 8, ...
reeks van Lucas	1, 3, 4, 7, 11, ...

Architectonische context

Er bestaan verschillende architectonische scholen of tradities, die zich beroepen op de metafoor van natuur en organische vormen: de negentiende eeuwse Engelse Arts and Crafts traditie, de Amerikaanse traditie van Louis Sullivan, de Catalaanse modernistische traditie (Gaudi e.a.), de ArtNouveau/Jugendstil traditie, de anthroposofische traditie. Deze tradities veroorzaakten niet alleen een grote differentiatie van vormen in de ornamentiek, maar ook in de ruimtelijke uitwerking van volumes, zowel exterieur als interieur. Met het functionalisme en de verbanning van het ornament is de gevoeligheid voor dergelijke vormen (en voor de kwaliteiten in detaillering en uitvoering daarvan) verschraald of zelfs verloren gegaan.

Nu het terugtreden van de alleenheerschappij van het functionalistisch-modernistisch paradigma de ruimte open laat voor een veelvoud aan vormen, is er behoefte aan een nieuwe naturalistische metafoor, die, zonder haar binding met het verleden te verliezen, een nieuwe impuls kan betekenen voor een ander begrip van ornamentiek: niet meer oppervlakkig, maar geworteld in de tectoniek.

De hier gepresenteerde modellen bieden de mogelijkheid, bij aanwending van vooruitstrevende technologie, een bijna eindeloze reeks nieuwe vormen te genereren, die gestoeld zijn op principes van natuurlijke groeiprocessen. Daarbij wordt de ontwerper een veelvoud aan keuzes geboden. Door middel van enkele eenvoudige ingrepen kan de architect de geproduceerde variëteit volledig naar zijn hand zetten, steeds nieuwe vormen exploreren en interpreteren. Op dit moment beschikken ontwerpers over klassieke werken, zoals het altijd opnieuw aangehaalde "On Growth and Form" van d'Arcy W. Thompson. Terwijl deze klassiekers nog steeds een rijke bron vormen van inspiratie, zijn er inmiddels nieuwe inzichten ontstaan over vormen, die het gevolg zijn van natuurlijke groei. In dit project wordt een beroep gedaan op de allernieuwste inzichten in de biologische morfologie (zie de beide mathematisch-biologische artikelen) en worden architectonische consequenties voorgesteld.

Samenvattend: het streven is een eigentijdse ornamentiek en tectoniek in de architectuur van gebouwen, die is afgeleid van de wijze waarop vormen en patronen worden gegenereerd in de natuur. Het motief is fascinatie door de schoonheid van natuurlijke vormen en groeiprocessen, waarbij eenvoud van principes gepaard gaat met rijkdom van de ontstane vormvariaties. Om de droom van een architec-natuur te realiseren wordt voorgesteld, mathematisch-biologische onderzoekingen toe te passen in de architectuur door een nieuwe vormgrammatica te ontwikkelen, die voor iedere ontwerper toegankelijk kan worden gemaakt.

Probleemomschrijving

Het construeren en detailleren van domemantels gebeurt meestal in omvattende schalen (als van Nervi) of in halfregelmatige lichamen, opgebouwd uit regelmatige veelhoeken (als van Buckminster-Fuller). Genoemde methoden kunnen worden vergeleken met natuurlijke processen, waarbij patronen ontstaan door materiaalafzetting op een overigens statische structuur.

In het geval van gegoten constructies en bij zeer grote bouwonderdelen (in de orde van grootte juist onder die van het gehele gebouw) is nauwelijks een patroonvormend proces te onderscheiden.

In het geval van relatief kleine elementen is men gehouden aan domevormen, afgeleid van de Platonische en de Archimedische lichamen (resp. regelmatige en halfregelmatige veelvlakken). De grote verscheidenheid aan patronen is terug te voeren tot enkele kenmerken in vorm, materiaal en omgeving (denk aan kristallisatie). Er schuilen echter beperkingen in het statische karakter van de zich ontwikkelende structuur.

In dynamische, levende structuren wordt patroonvorming echter sterk bepaald door het reeds gevormde deel van het uitdijende geheel - en meer specifiek door (i) boodschappen en (ii) vormverandering:
(i) De structuur draagt erfelijke en van de omgeving afgeleide informatie over, waarbij zij voortdurend additionele randvoorwaarden stelt voor verdere groei. Dit principe pas ik in zoverre toe, dat ik de biochemische en genetische details negeer en ze vervang door de eenvoudigst mogelijke wiskundige instructies. Dit is verantwoord, daar de genetische mechanismen veel evolutionair-historische ballast bevatten, die voor het architectonische principe betekenisloos is en daarenboven nog niet geheel is geanaliseerd.
(ii) Begrip van de invloed van vergroting van een structuur op patroonvorming vraagt inzicht in biologische en architectonische principes. Via interpretatie van phyllotactische patronen ontstaan nieuwe ontwerpuitgangspunten voor bouwvormen en -methodieken.

Hier kan men denken aan close-packings van elementen volgens zekere principes voor positie, vorm en maat.

Drie doelen tekenen zich nu af:
(i) ontwikkelen van een theorie en afleiden van een model, dat phyllotactische patronen genereert vanuit in de biologie herkenbare parameters
(ii) formuleren van betekenis en mogelijkheden, om bouwelementvormen en -patronen te ontlenen aan de phyllotaxis van composieten
(iii) beschrijven van uitgangspunten voor architectuur en constructie. *NB.* Het begrip architectuur wordt hier gebezigd in de betekenissen van opbouw (als in: de architectuur van een boom, de architectuur van een computer) en van culturele uiting (vergelijk: de architectuur van Wim Quist, de architectuur van de Shakers)

(Lichte draagconstructies als van Frei Otto vallen buiten het probleemveld. Daar worden gegroeide structuren als natuurlijke producten op schaal nagebootst. Algoritmische plaatsing van onderdelen, met als resultaat patronen, staat dan niet op de eerste plaats.)

Uitgangspunten

De traditionele architect bezet een prominente plaats in het bouwproces. Hij laat zich daarin meestal niet inspireren door de manier, waarop de (groene) natuur het probleem van het construeren van vormen benadert. Enerzijds is dat begrijpelijk, wanneer men bedenkt, dat een gebouw niet ontstaat binnen de beperkende regels van natuurlijke groei. Anderzijds is het opmerkelijk, daar de mens zelf in zijn wezen een deel van de natuur uitmaakt.

De huidige bouw baart zorg, wanneer men haar gadeslaat in het perspectief van de milieuproblematiek. De traditionele architect zal zijn attitude moeten wijzigen. Hij zal meer inzicht moeten krijgen in mechanismen in de natuur. Daarbij denk ik niet zozeer aan het overnemen van uiterlijke verschijningsvormen, maar meer aan harmonisatie in de zin van werken volgens biologische mechanismen. Met name in de ontwerpfase van een bouwproject heeft de architect de macht, een bijdrage te leveren aan verbetering van de huidige situatie.

Recentelijk is in de wiskunde een ontwikkeling in gang gezet, die belangrijk kan zijn voor het toekomstige bouwen, respectievelijk voor prefabricage van onderdelen. De wiskundige Benoit B. Mandelbrot is de grondlegger van de *fractale geometrie*, die ervan uitgaat, dat de natuur niet is samengesteld met perfect rechte lijnen, zuivere vlakken en regelmatig begrensde lichamen.

Parallel aan deze ontwikkeling zagen de *L-systems* van Aristid Lindenmayer het licht. L-systems zijn algoritmen, die geometrische vertakkingsstructuren genereren, zoals de groene natuur die ons openbaart. Een belangrijke witte plek in de theorie ligt in het oude vraagstuk van het ontstaan van zekere ruimtelijke patronen. Immers, de L-systems blijven principieel steken in het platte vlak: slechts met kunstgrepen "piept" men eruit, de derde dimensie in.

Sinds het begin van de zeventiger jaren bestudeer ik de Fibonacci-reeks in relatie met de patroonvorming bij primordia op het bloemhoofd van composieten. Mijn verwondering werd gestimuleerd na het vernemen van het feit, dat het grootste deel van alle planten deze patroonvorming kent, weliswaar 'verborgen' langs de stengel (S. van der Vorst). In eerste instantie was mijn opgave: *"Teken het patroon van een zonnebloemhoofd op een gemakkelijke manier."*. Met *gemakkelijk* bedoel ik: 'blind', zonder (intuïtief) vreemde gegevens, zonder ingewikkelde wiskundige functies, met elementaire geometrie, met ondeelbare algoritmes. Een professionele computer bracht het tot de eerste eenvoudige constructies (R. Barluschke). Vanaf de verschijning van relatief populair rekentuig (PC's) kon ik vermoede algoritmes direct zelf toetsen. Daarbij was feedback met de systematische biologie noodzakelijk (A. Lindenmayer). Omdat het inmiddels vereenvoudigde phyllotaxis-model was opgebouwd vanuit een centrum noemde ik het 'Verdringingsmodel' (F. van der Blij). Kritiek op het model aangaande het singuliere karakter ervan (uit een *punt* kan niets ontstaan) leidde tot het 'Stapel- en Trek-model' (K. Bachmann).

De levensvatbaarheid van de *phyllotaxisgenerator* is verzekerd door de volgende eigenschappen:
(i) Het model gebruikt een absoluut minimum aan specifieke erfelijke gegevens in planten. Behalve geometrische grondbeginselen worden als "input" slechts aannames gebruikt, die een afspiegeling zijn van werkelijk biologische groei.
(ii) Het model blaast de L-systems nieuw leven in, door een structurele uitbreiding in de derde dimensie.
(iii) Het model genereert fractale structuren met Euclidische bouwstenen. Anders gezegd: met bolvormige elementen worden gnomonische structuren gevormd. Deze elementen worden gedefinieerd vanuit begrippen uit de vakliteratuur (zie references in de artikelen) en recente onderzoeken (zoals numerieke canalisatie, J. Battjes). Dit betekent, dat een biologisch verantwoord model ten grondslag ligt aan ontworpen fractale structuren. Opgemerkt dient te worden, dat de actuele fractal-theorieën met een probleem kampen. Resultaten schijnen weliswaar zeer natuur-getrouw te zijn - echter, de mechanismen, die aan de resulaten ten gronslag liggen, wijken vaak sterk af van de (bio)fysische en (bio)chemische mechanismen die natuurlijke fractals opleveren. Wetenschappelijk gefundeerde fractals zijn vooralsnog zeldzaam.

2 CREATING PHYLLOTAXIS: THE DISLODGEMENT MODEL

ABSTRACT

Assuming that neither the Fibonacci sequence nor any numerical ratio or angular deflection is specified in the genetic material of a plant cell, there must be an arranging mechanism effecting the sequence mentioned. Considering the ubiquity of the Fibonacci numbers in nature, embracing many species of flora, we expect a very simple geometrical law to be responsible. Success in finding such a law does not constitute a proof, but it is at the least an indication that we should look here with mathematician's rather than biologist's eyes.

The idea may seem self-evident. However, in the literature it has not yet been honored as the basis for constructing the phyllotaxis in centric, planar models. It is shown here that for the construction of a phyllotactic structure, no special angles or distances need be defined; natural growth functions can be used; planar, cylindrical, conical, and paraboloid constructions are possible within the same model; and constructions leading to accessory sequences and multijugate sequences can also be carried out.

THE ORDERED STRUCTURE OF A PLANT

A given plant has an underlying 'ordered structure' that runs on through the entire individual [5]. This structure can be considered the bearer of all forms of appendages that the plant can produce. When the plant develops a flower, this will be placed and built up according to the plant's own individual structure.

A flower or fruit will enable the plant to reproduce. It is important for the plant to produce large numbers of offspring, since much of the reproductive material will be lost. Reproductive units are small in size and large in number. The underlying structure of a plant will become clearly visible where these units are arranged closely together, in the flower head, for example. The sunflower has a flower head (capitulum) with hundreds, often over a thousand, florets, which can produce as many seeds (achenes). These seeds are arranged according to a spiral system. From the center outwards, congruous spirals run both to the left and to the right. 'On the way out', spirals will be replaced by others, with their number increasing abruptly. The ring in which spirals go over into other spirals is clearly demonstrable (Fig 1).

In the year 1202, Fibonacci (Leonardo di Pisa) described a numerical sequence with opening terms 1 and 2. Each term is the sum of the previous two terms, which are natural numbers. Thus it runs 1, 2, 3, 5, 8, 13, 21, 34, 55, 89, ... A large proportion of the seed-bearing plants have an ordered structure having to do with congruous spirals. The number of spirals turning to the left and to the right are consecutive terms in the sequence, which is called the ***Fibonacci sequence*** or the ***main sequence***. The most important ***accessory sequence,*** the ***Lucas sequence*** (named after Eduard Lucas and described in 1877), also occurs, although considerably less often. It starts with the terms 1 and 3. Accessory sequences have different opening terms from those of the main sequence, but the same rule of continuation (see Section OTHER SEQUENCES). Plants without spiral arrangements either have a different structure or form a special group within the ordered structures mentioned [1]. They may show, for example, opposite leaf arrangements, whorls, umbels. The ordered structure is called ***phyllotaxis***.

UNLIMITED AND LIMITED PHYLLOTAXIS

As the support of the phyllotactic structure, we take a radially symmetrical covering surface around axis Z.

Model A

A special case is the covering surface with $z=0$, which is a flat disk. This case is practicable if a structure continues to expand radially, so that the phyllotaxis is unlimited, as in a flower head.

The flower head is to be conceived as a flat, round disk tapering into a stem in the center (Fig 2). Primordia will develop from cell regions, which in turn arise from the center of the disk. Cells will be pushed apart in a radial direction, with their substratum growing radially also: all primordia-forming cells remain directly attached to it. In sunflowers, cell regions are pushed apart before primordia arise. As a result, the first primordia arise on the rim of the disk. Each primordium goes through its own growing process, subject to genetic code and environmental conditions, but its dimensions are limited. Thus, parastichies (contact spirals) will develop in numbers that are dependent on the number of units and their size. The spirals go over into other spirals in concentric, annular areas. The number of peripheral spirals stands in direct relation to the number of units that fit in the perimeter of the capitular disk. The number of ray flowers is determined by the number of spirals at the disk's periphery. In the model, the perimeter is unlimited, so the maximum number of parastichies is also unlimited (Fig 3a).

Model B

If, during the development of primordia, a structure extends axially, that is, in the z direction, and the radial expansion is limited, we speak of limited phyllotaxis. The number of helices that a cylinder can contain is limited; the pattern becomes rigid.

Structures that ostensibly deviate from model *A* and model *B* but evidently answer to (spiral) phyllotaxis are, for example, radially asymmetrical plants or plant parts (such as flattened cacti) and certain succulents [e.g., saxifraga have their leaf tips lying in a horizontal plane, but not the leaf attachments to the stem, so they correspond to model *B* (Fig 3b)]. Flowers and flower heads are the results of appendage differentiations after a growth process in obedience to the rules of model *B*. In the case of flower heads, changes can be considered a *B*-*A* transition (Fig 4).

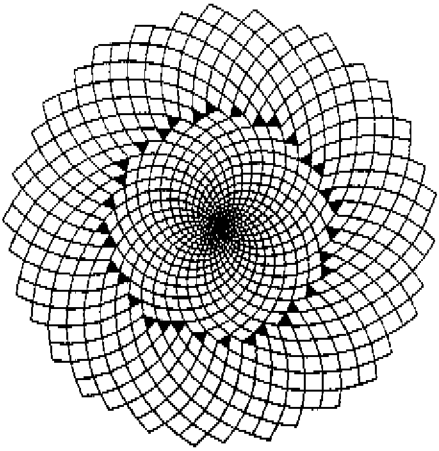

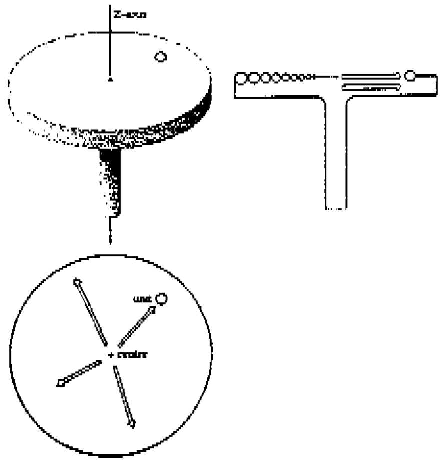

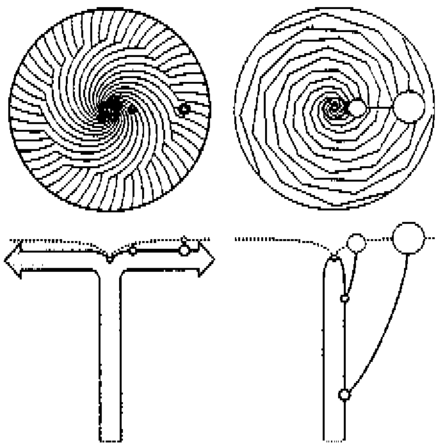

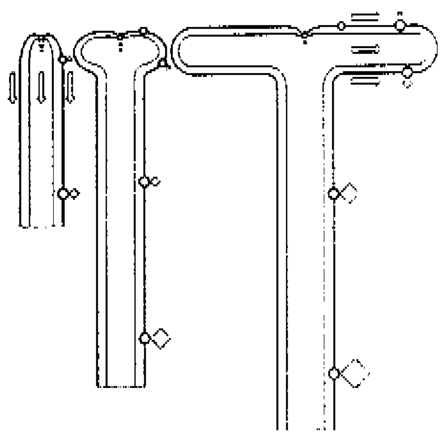

1 2
3 4

Fig 1 The ring in which spirals go over into other ones is clearly demonstrable. (Spirals show connections between adjacent seeds.)

Fig 2 The flower head is to be conceived as a flat, round disk, tapering into a stem in the center. A unit is defined here as a region of cells, which will produce a primordium.

Fig 3 *(left)* The perimeter is unlimited in the model, therefore so is the maximum number of parastichies. *(right)* Leaf tips lie in a horizontal plane, but not the leaf attachments on the stem. The number of parastichies is limited by the perimeter of the stem.

Fig 4 In flower heads, changes can be considered a transition limited/unlimited phyllotaxis. Notice the apex to be the center of expansion for successively the stem and the capitular disk. Notice also the (radial) elongation of the disk's under-surface, without supply of primordia. A seed and a leaf are indicated as a triangle and a square respectively.

Basic principles with regard to the arrangement of primordia

The simplest form to be chosen for a unit (either a single primordium or a sphere of influence consisting of cells) in a two-dimensional model is the circle. A single unit will develop [subject to a growth function of the form given below (see Section Concepts) and through the time instants indicated] as a growing circle (Fig 5). The time between the inception of two units in the growing point, the plastochron, is presumed to be constant: Δt. So at t_2 (after $2.\Delta t$) there are two units, consecutive in size, and a third one emerges.

The smallest of the first two units is lying against the growing point. For the place of origin of the third unit, there are two principal possibilities: It develops either in a peripheral position or between the two existing units, assuming that the circles must touch but not overlap. At this stage, a genetic or environmental datum will be important. Will the unit develop in a symmetrical position (a,b) or will it take an aymmetrical direction (c,d,e) (Fig 6)?

For all variants except d, the continuation of the growth process is evident. In a, c, and e, the growing point remains peripheral, the structure being linear, alternately, and spiral (the basis for ferns), respectively. In b, the two previous units are pushed apart. In the remaining case, d, the growing point is situated centrally in an asymmetrical structure. All of these cases occur, but for the reasons mentioned only variant d will be examined.

At t_3 (after $3.\Delta t$), the next unit will emerge. The place of origin will be central, that is, between the existing units. As it is growing, the youngest unit will have to obtain a place. After it has touched on all three previous units, two of these will have to part. This parting can happen in three different ways (Fig 7), of which two occur in nature: d_1 and d_3 . Configuration d_2 is not consistent after the former choice (d). In case d_2 , the youngest unit separates two immediate predecessors, which is consistent with b, not d.

Case d_3 will lead to a simple spiral (with the younger units central), or to anomalies (see Section Other sequences). Case d_1 is very common and leads to phyllotaxis according to Fibonacci numbers. This is the variant we will examine first, because here we find the problem in question.

What are the advantages of variant d_1 as opposed to variant d_3?

(i) The overall system aims at a minimum average surface per unit. In a growing system, the place of units, in relation to one another, will change in such a way that each unit will keep as close as possible to the growing point. The choice between rolling aside to the left or to the right under the influence of the forces from the neighborhood is made for the direction that will keep the system as compact as possible (Fig 8). The older, peripheral unit will then lie against the youngest neighboring units available, that is, as close as possible to the growing point.

(ii) The smaller the unit, the higher the rate of expansion. Bigger, older units are therefore more easily moved than smaller ones. (In rigid systems, there is no structural displacement at all.)

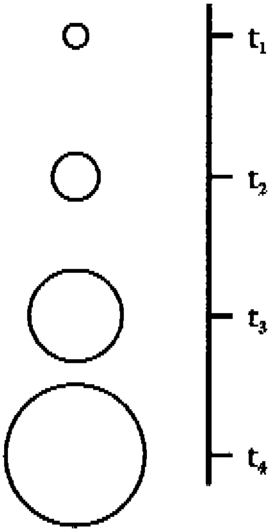

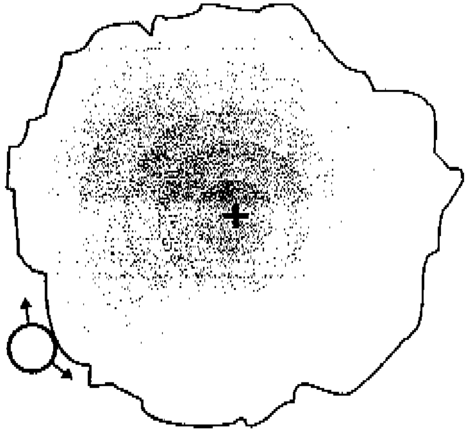

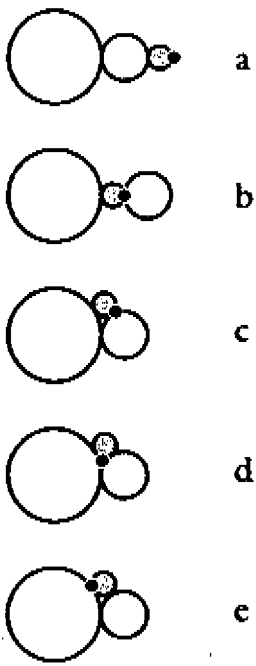

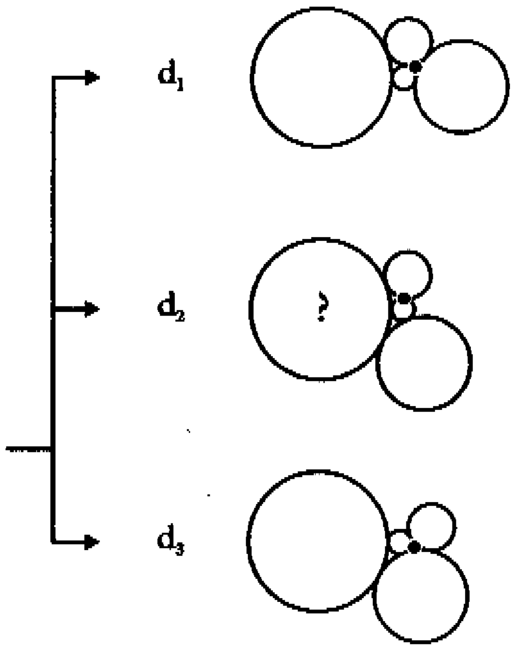

5 8
6 7

Fig 5 A single unit will develop as a growing circle.
Fig 6 The third unit will develop in a symmetrical position (a,b) or it will take an asymmetrical direction (c,d,e). (The center of the apex is indicated by a dot.)
Fig 7 The configuration d_2 is not consistent after choice (d). The tinted units are of form b in Fig 6.
Fig 8 The choice between rolling aside to the left or to the right under the influence of the forces from the neighborhood is made for the direction that will keep the system as compact as possible.

Comparison of the model at t_3 with that at t_4 shows that the structure of t_3, in its entirety, fits into that of t_4, although turned at a certain angle (Fig 9). This follows directly from the starting point: The structures are drawn at certain points in time, that is, every time a unit has reached the size of its predecessor. At any of these points in time, a new unit emerges in the growing point. When a unit has reached the size of its predecessor, the same holds for every other unit too. However complex the model drawing may become, a structure will always fit onto every previous structure. So we have properties of what has been called 'gnomonic growth' [6]. The gnomon here is the oldest, biggest unit. In a recursive model, we could add this gnomon to an existing structure (see next section).

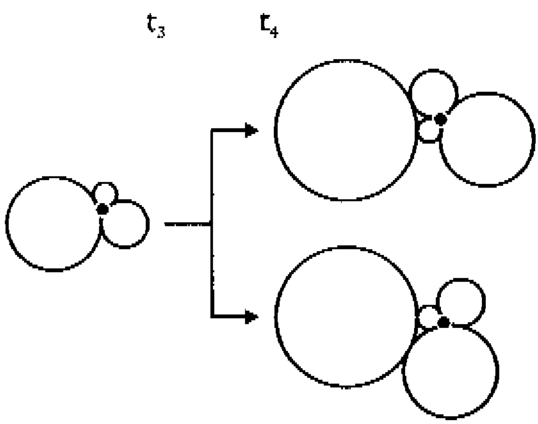

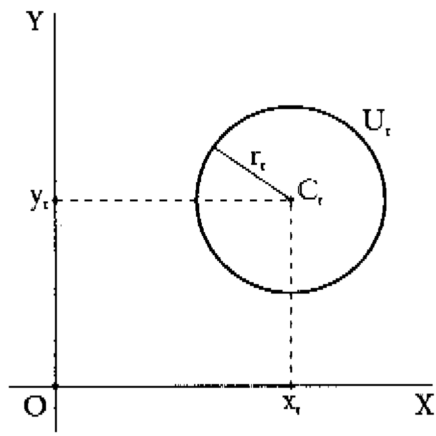

Fig 9 *(left)* Comparison of the model at t_3, with that at t_4, shows, that the structure of t_3, in its entirety, fits into that of t_4, although turned at a certain angle.

Fig 10 The growth model is constructed in relation to a rectangular coordinate system *XOY*, with *O* for the growing point.

Concepts

The growth model is constructed in relation to a rectangular coordinate system XOY, with O for the growing point (Fig 10).

Let the unit of time Δt, the plastochron, be 1. t is a natural number. U_t is a construction unit with age $t.\Delta t = t$; U_t is a circle with radius r_t and center C_t (x_t, y_t). The growth of a unit is usually slow at first, fast later, and then slow again, which results in the S-curve (Fig 11). U_0 has a radius $r_0 > 0$: Either units (with $t < 0$, out of the model) may grow underneath the XOY surface before popping or there may be a limited number of units (the structure being drawn more plastochrons after the last unit arose). An individual unit will grow according to the equation

$$r_t = R \,/\, \{1 + e^{c.(t'-t)}\}$$

in which R is the (limit) radius of a mature unit, e the Euler number $e = 2.71828\ldots$, c the growth constant, and t' the half-life, the time a unit takes to reach radius $R/2$.

Because the growth model has gnomonic properties (see Section BASIC PRINCIPLES and Fig 12a), the drawing of structure$_t$ can be turned in such a way that it fits onto the drawing of structure$_{t-1}$. Thus, structure$_t$ can be constructed starting from structure$_{t-1}$.

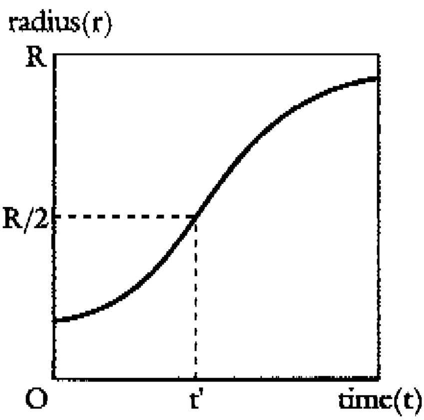

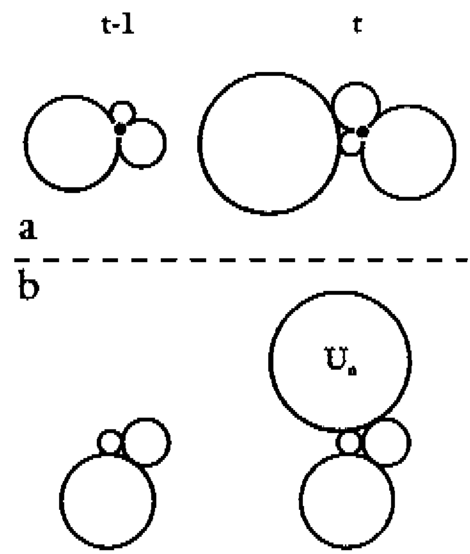

Fig 11 The growth of a unit is usually slow at first, fast later and then slow again, following the 'S-curve'.
Fig 12 *(right)* *(a)* The tinted circle, like the other ones, grows and a new circle arises in the center. The drawing of the structure$_t$ can be turned in such a way that it fits onto the drawing of structure$_{t-1}$. *(b)* The 'additive model': the biggest unit U_n, the gnomon (tinted), must be added to the periphery at a place to be determined.

The biggest unit U_t , the gnomon, must be added to the periphery at a point to be determined. We now have an 'additive' or 'inverted' model. In this model, t is replaced by n (Fig 12b). Each of the units has dimensions

$$r_n = R \;/\; \{1 + e^{c.(n'-n)}\}$$

in which n' is the ordinal number of the unit with radius $R/2$.

Finally, two other concepts are essential: support circle and mutual secondary support circle. With $n>2$, a unit U_n always touches on two (or more, theoretically) younger units, which are situated closer to the growing point. These two units are the 'support units' of U_n . In the circles model, we call these ***support circles*** *(*U_p and U_q). The values p and q are dependent on n. For the sake of unambiguous definition of U_p and U_q , we state: C_q is in a 'positive' position in relation to C_n . Angle C_qOC_n is positive, while C_q can be found within 180° from C_n by circling OC_q from OC_n with center O counterclockwise (Fig 13).

Both (primary) support circles U_p and U_q in turn have two support circles each, when $n>5$ (Figs 14 and 16). In relation to the unit considered, U_n , these four support circles are called ***secondary support circles***. Two of the four circles mostly coincide, resulting in the ***mutual secondary support circle*** U_z . If such is not the case, there are two alternatives.

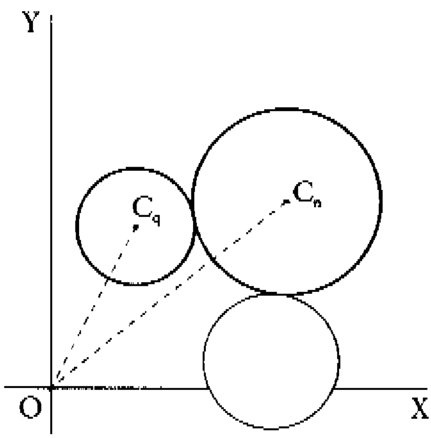

Fig 13 C_q is in 'positive' position in relation to C_n : C_q can be found within 180° from C_n by circling OC_q counterclockwise from OC_n with center O.

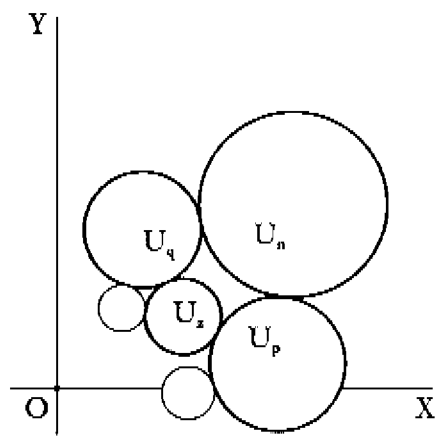

Fig 14 Both (primary) support circles U_p and U_q have two support circles each, when $n>5$. Mostly, two of the four circles coincide: U_z , the mutual secondary support circle (tinted).

Either one of the two (primary) support circles has the other primary support circle for one of its (secondary) support circles (Fig 15), or none of the primary and secondary support circles coincide (Fig 16). The configuration last mentioned occurs only rarely in model A (unlimited phyllotaxis), namely after irregular growth or growth distortions, but is more usual in model B (limited phyllotaxis), where unit growth function and curving of the apex compete. The latter phenomenon is also responsible for the appearance of many different patterns (see Section LIMITED PHYLLOTAXIS).

UNLIMITED PHYLLOTAXIS

First we will look into the growth model in which each unit, in a period of time $\Delta t = 1$ (plastochron), grows to such an extent that it reaches the size of its (older) predecessor. In a growing structure, at time t, we examine the situation close to the oldest unit (aged t). U_t is supported by U_p and U_q . (The units with ordinal numbers $p+1$ and $q+1$, elsewhere in the structure, are also outlined in Fig 17a). At time $t+1$, all units have grown (Fig 17b). The configuration that has now developed near U_{t+1} is identical to the configuration with U_{p+1} and U_{q+1} at time t. Thus, U_{t+1} could have been drawn directly into Fig 17a. The dimensions of U_{t+1} follow from the growth function given, and its place can be constructed: U_{t+1} touches the support circles U_{p+1} and U_{q+1} 'on the outside'. The structure in its entirety, however, has been turned in relation to growing point O.

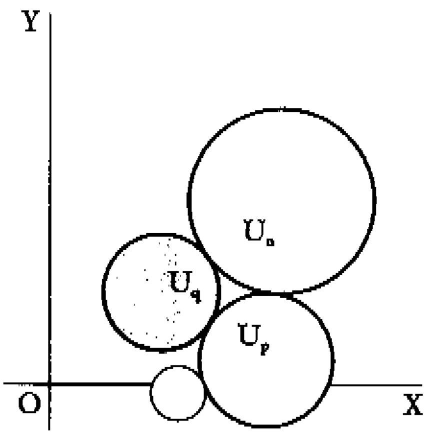

Fig 15 One of the two (primary) support circles (U_p here) has the other one (U_q , tinted) for one of its own (secondary) support circles.

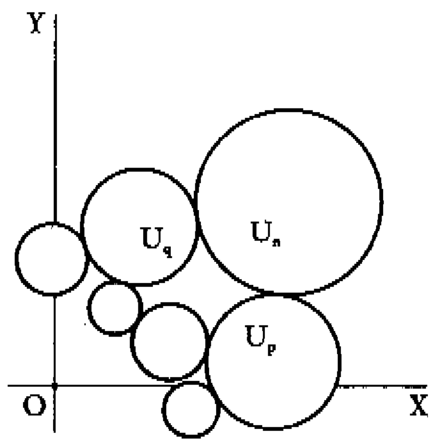

Fig 16 None of the primary and secondary support circles coincide.

After this, the model will be developed according to the inversion $t \rightarrow n$. Ever bigger units are added to the periphery of an otherwise static structure, the additive model. For simplicity, the growing point is redefined as the point of contact of the first two circles. For each unit U_n , a series of data can be arranged in a matrix. The first three units are defined (U_0 is defined as the center; r_1 and r_2 are deduced from the growth function). The givens in the matrix agree with the structure drawn in Fig 18. The matrix is

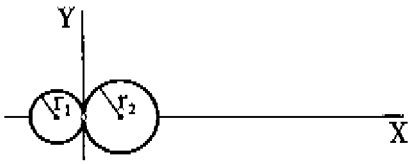

n	r	p	q	x	y
0	0	0	0	0	0
1	r_1	0	0	$-r_1$	0
2	r_2	1	0	$+r_2$	0

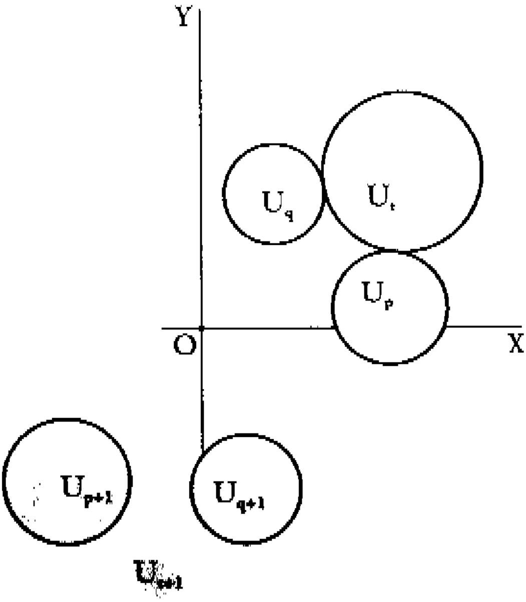

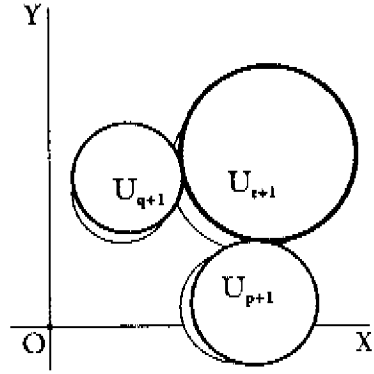

18

17a 17b

Fig 17a At time t, U_t is supported by U_p and U_q. The units with ordinal numbers $p+1$ and $q+1$ (elsewhere in the structure) have also been outlined.

Fig 17b At time $t+1$, all units have grown. The new configuration could have been constructed into Fig 17a, where U_{p+1} and U_{q+1} are units in the structure at time t. (The size of U_{t+1} follows from the growth function. The place in Fig 17a is indicated as a tinted area.)

Fig 18 The first three units are defined (r_1 and r_2 to be deduced from the growth function). For simplicity, the growing point (+) is redefined as the point of contact of the first two circles.

If the two support circles of unit U_n, being U_p and U_q, are known, this enables us to localize unit U_{n+1} on the basis of the algorithm described in the growth model (see above). By analogy it holds that

$$n:=n+1,\ p:=p+1,\ \text{and}\ q:=q+1.$$

With the data $C_p(x_p, y_p), r_p$; $C_q(x_q, y_q), r_q$; and r_n, we calculate $C_n(x_n, y_n)$. Point C_n is determined through calculation of one of the two intersections of two circles with centers C_p and C_q and radii r_p+r_n and r_q+r_n (Fig 19). In Fig 12b the third unit is constructed this way.

While determining C_4, we encounter a problem. Initially, U_4 (or U_{3+1}) touches U_3 (or U_{2+1}) and U_2 (or U_{1+1}), intersecting U_1. Intersection is not allowed; according to case d_1 in Fig 7, U_1 and U_2 become the support circles of U_4. (In Fig 12b, the fourth unit is constructed).

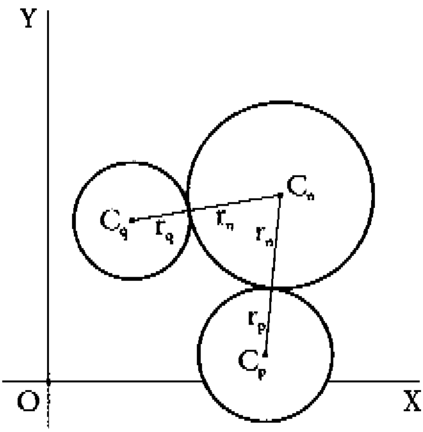

Fig 19 Point C_n can be determined through calculation of one of the two intersections of two circles with centers C_p and C_q, and radii (r_p+r_n) and (r_q+r_n).

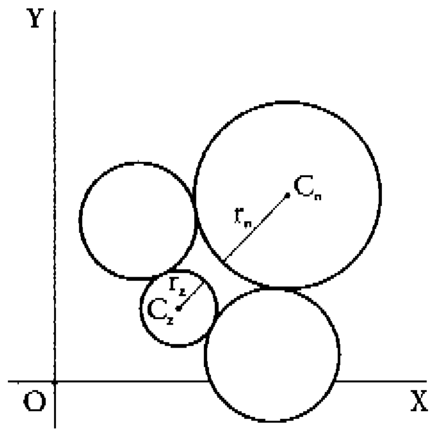

Fig 20 If there is a mutual secondary support circle U_z of the unit constructed, this could intersect the circle just found.

In general, if there is a mutual secondary support circle U_z of the unit constructed, this could intersect the circle just found (Fig 20). Therefore, we must examine whether (if a circle U_z exists) C_nC_z is smaller than the sum of the radii of the circles involved, r_n+r_z. If it is (Fig 21a), the unit to be constructed rolls off along the secondary support circle, notably in the direction of the ***youngest*** unit (see Section BASIC PRINCIPLES). In other words, U_z dislodges the oldest of U_p and U_q. The calculation for the intersection of two circles is to be repeated, but now for the youngest of the two support circles and the mutual secondary support circle. So:

if $C_nC_z < r_n+r_z$ then if $q > p$ then $q := z$
else if $p > q$ then $p := z$ (Fig 21b).

Now that the new unit has been fixed, the next unit can be found in the same way.

The mutual secondary support circle (when $p_q=q_p=z$) is not the only candidate to intersect a 'new' circle. If $p=p_q$ or $q=q_p$, the unit with ordinal number $n-|p-q|$ is the candidate, being the biggest neighbor of U_n. In the final case, one of the ordinal numbers p_q and q_p is possible. So (let f be the ordinal number of a possible intersecting unit):

if $p_q = q_p$ then $f = p_q = q_p$
else if $p = p_q$ or $q = q_p$ then $f = n-|p-q|$
else if $p_q > q_p$ then $f = p_q$
else if $q_p > p_q$ then $f = q_p$.

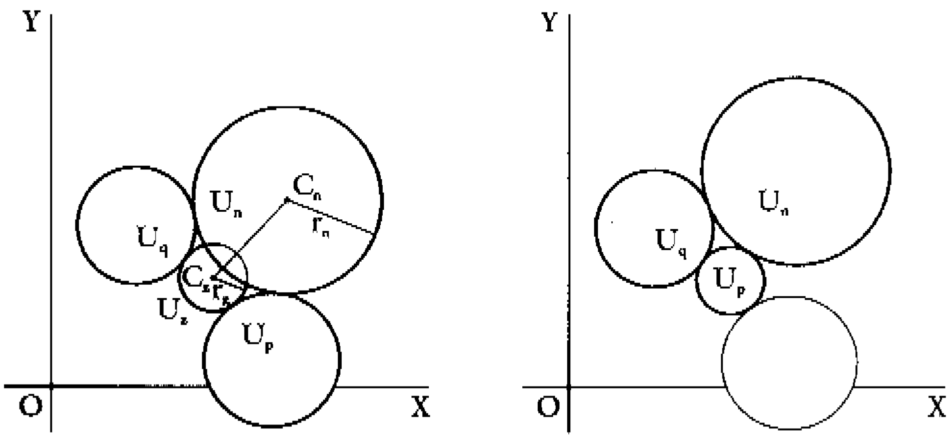

Fig 21 (*a*) C_nC_z is smaller than the sum of the radii of the circles involved, r_n+r_z.

(*b*) U_n is pushed aside by U_z. U_z separates U_n from U_p, the oldest of the support circles U_p and U_q, thereby becoming the new U_p for U_n.

The place of the third unit indicates the turning direction of an imaginary, flowing curve through the centers of all circles constructed and yet to be constructed. This curve is called the primary or generating spiral. It depends on the definition of the first two support circles whether the generating spiral will be turning to the left or to the right. U_1 has U_0 for its only support circle. U_2 has U_0 and U_1 as its support circles. If $p_2=0$ and $q_2=1$, the generating spiral will turn clockwise; if $p_2=1$ and $q_2=0$, it will not.

As from $n=4$, subsequent units along the spiral will not touch one another. That is why, neither in a flower head nor in the model, the generating spiral (in fact, the first contact spiral) will be visible as a sequence of primordia or units. Other contact spirals will develop: a spiral trio, turning in the same direction, as well as a spiral duo, turning in the opposite direction. These spirals will disappear according as the model contains more units. They make place for eight and five spirals, respectively. Thus, the terms of the Fibonacci sequence will be developed successively, as numbers of contact spirals.

The route that a unit travels, from growing point to periphery, turns out to run in a radial direction. In the tangential direction, the unit will experience forces that push it alternately to the left and to the right. As a result, the unit takes a zigzag path. Examples of unlimited phyllotactic circle patterns in the main sequence are shown in Figs 22, 23.

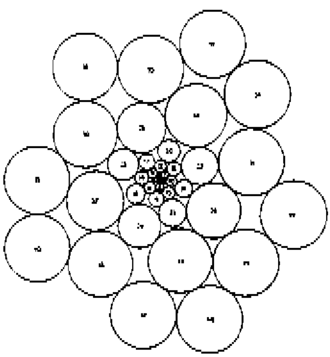

Fig 22 In this structure of 42 circles in unlimited phyllotaxis, Fibonacci numbers in the centre (3,5) and in the periphery (8,5) are distinguishable.

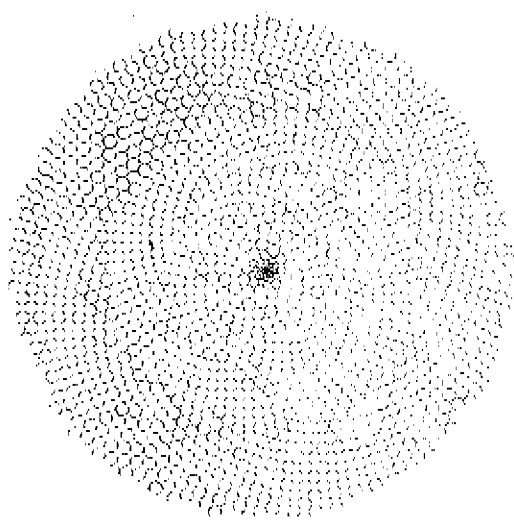

Fig 23 This example of unlimited phyllotaxis shows numbers (55,89) on the rim. ($n=1300$)

Other Sequences

The model described leads to numbers of spirals according to the Fibonacci sequence. The fact that plants showing accessory sequences (see Section THE ORDERED STRUCTURE OF A PLANT) form a minority growing ***amidst*** other plants with Fibonacci phyllotaxis indicates that we can speak of anomalies. The Lucas sequence (1, 3, 4, 7, 11, 18, 29, 47, ...) is the first accessory sequence. The second accessory sequence (1, 4, 5, 9, 14, 23, 37, 60, ...) starts with yet other terms.

If we depart from configuration d in Fig 6, d_1 in Fig 7 follows the algorithm deduced (see Section UNLIMITED PHYLLOTAXIS). Initially, U_4 (or U_{3+1}) touched U_3 (or U_{2+1}) and U_2 (or U_{1+1}), intersecting U_1. The biggest of U_2 and U_3, being U_3, is dislodged by U_1. The configuration leads to Fibonacci numbers after repeated application of the algorithm (Fig 24). If, directly after t_3 (with d in Fig 6), we introduce a deviation, then the only possibility would be d_3 in Fig 7. In this case, the smallest of U_2 and U_3, being U_2, is dislodged by U_1. Continuation with the algorithm leads to the Lucas sequence (Fig 25). Instead, continuation with a second deviation (which resembles the first, because there are no alternative possibilities), and then with the usual algorithm, leads to the second accessory sequence. (U_5 touches U_2 and U_4. If U_1 intersects U_5, it will dislodge the smallest of U_2 and U_4, which is U_2.) After having applied the deviation three times, followed by the usual algorithm from t_7, we find the third accessory sequence. Accessory sequences after the first rarely occur. If the deviation described should go on repeating itself, we could no longer speak of a deviation (resulting in an anomaly), but rather of another algorithm. In choices, younger, smaller units are dislodged here. The result would be a simple spiral, with the younger units in the center (compare with Fig 6, case e, where units arise peripherally).

A quite different deviation can be found in the existence of multiplied sequences, such as the bijugate sequence (2, 4, 6, 10, 16, 26, 42, 68, ...). This sequence arises when the growing point produces two similar primordia every plastochron. At $t=1$, two circles with radius R_1 and centers $C_1(R_1, 0)$ and $C_1'(-R_1, 0)$ are drawn. At $t=2$, a third circle U_2 touches U_1 and U_1', just following the rules. The choice for y_2 to be positive or negative is arbitrary. Symmetrically around the X axis (for U_2 and the fourth unit U_2' arise at once), U_2' is drawn. U_3 may intersect U_1'. The choice of which direction U_3 rolls off in predicts the turning direction of the two (identical) generating spirals in the ultimate structure. U_3' is drawn symmetrically in relation to the growing point O. The place of U_4 is determined by using the algorithm starting from U_3. U_4' is the symmetry of U_4. Succeeding units are drawn consequently. In a flat plane, the result is a flower head with spirals in the numbers mentioned here (Fig 26). In limited phyllotaxis, opposite leaves appear on a stem. The angle between two successive pairs of units depends on the form of the covering surface (see Section LIMITED PHYLLOTAXIS).

In the same way, multijugate sequences are possible. For any n, unit U_n is settled and units U_n, U_n', U_n'', ... require rotation-symmetry around point O. In addition, deviations are easily possible in structures with multijugate sequences. From the bijugate sequence we get 2, 6, 8, 14, 22, 36, 58, 94, ...

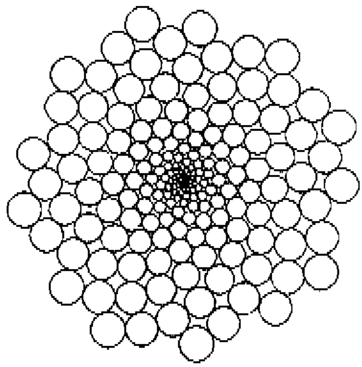

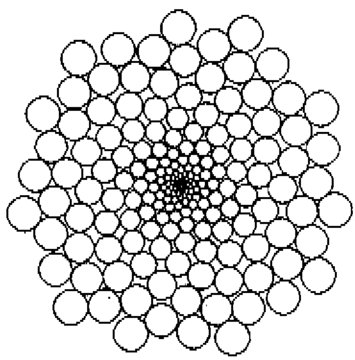

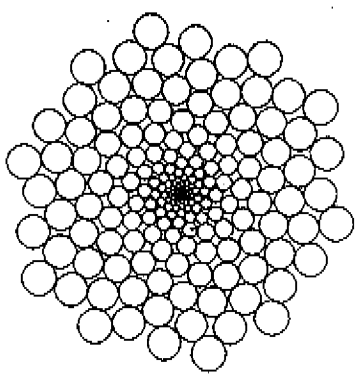

Fig 24 If we depart from Fig 9, then the topmost configuration at t_4 leads to Fibonacci numbers after repeated application of the algorithm in Section OTHER SEQUENCES.
Fig 25 Directly after t_3 , we introduce a deviation. Continuation with the algorithm leads to Lucas numbers.
Fig 26 When the growing point produces two similar primordia every plastochron, the doubled Fibonacci sequence arises.

VARIATIONS

The dislodgement model as described above leads to a set of circle-disks in orderly, natural patterns. Variations within a structure can develop through changes in the form of the building block. So far, we have spoken of circles. It would seem obvious that the unit should be given a flexible wall. The tendency to reach a compact main form leads to compression of 'weak' circle forms to soap-bubble-like units, with the spaces between them becoming smaller or disappearing and the wall material becoming rigid.

A close-packed honeycomb structure can be constructed by drawing the mutual tangents or polar lines of all circles between their intersections with other tangents (Fig 27). Where optional problems arise, the key is minimum use of material, that is, ***minimum distances***. A rough approximation of a soap-bubble structure can be reached through the method described below. In the case that there is no mutual secondary support circle, three circles touch one another to form an intercellular space. Between these circles, a point can be determined on the basis of their reciprocal radii. Let the ordinal numbers of the circles be $i = n, p$, and q, respectively; then the radius is r_i , and the coordinates of the center are x_i and y_i . The x coordinate of the point in question is

$$x = \Sigma(x_i/r_i) \, / \, \Sigma(1/r_i)$$

The point will be relatively far from the centers of the smaller circles (Fig 28). In the second case possible, four circles touch one another around the intercellular space. A point is calculated four times for three circles each time. Two mutually connecting lines between the points qualify as partitions, the shortest sum of which requires a minimum of material for the buildup of the five walls concerned (Fig 29). In the final case possible, five circles form the intercellular space. Now, after analogous calculations, seven points result in seven partition walls (Fig 30). Examples of unlimited phyllotactic patterns with varied building blocks are shown in Figs 31-35.

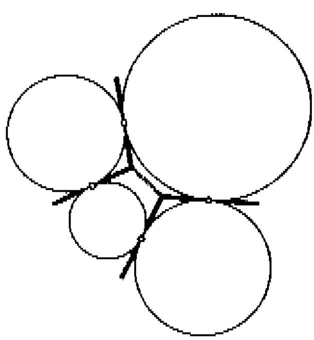

Fig 27 A 'close-packing' honeycomb structure can be constructed by drawing the mutual tangents or polar lines of all circles 'between' their intersections with other tangents.

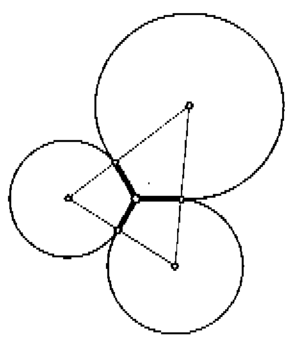

Fig 28 Between three circles, each of their points of contact is connected with a fourth point, which is determined by the reciprocal radii and the centers.

Limited phyllotaxis

The three-dimensional structure mentioned in Section UNLIMITED AND LIMITED PHYLLOTAXIS can be constructed on a supportive surface defined in advance. Just as in the flat plane of model *A*, we constructed the centers of circular units, we construct the centers of spherical units on the paraboloid surface area of model *B*. The flat structure of the flower head will go over into the cylindrical structure of the stem: Spirals go over into helices. The dislodgement theory described also holds good for model *B*. Unit radii grow according to the growth curves mentioned (Fig 36), as the circles of the two-dimensional model are in fact spherical cross sections through the flat plane. Examples of limited phyllotactic patterns with varied building blocks are shown in Figs 37-44.

The entire plant body

Where a plant shows characteristics of fractals (geometric structures between the Euclidean dimensions), Mandelbrot [3] provides us with an interesting area of study. Lindenmayer [2] describes algorithms to generate ramifications and budding from a single, simple building block. Prusinkiewicz and Hanan [4] combine fractal plant growth with L-systems in computer graphics. Here, combination with the dislodgement model will lead to a correct interpretation of the profusion of phyllotactic patterns in the plant world.

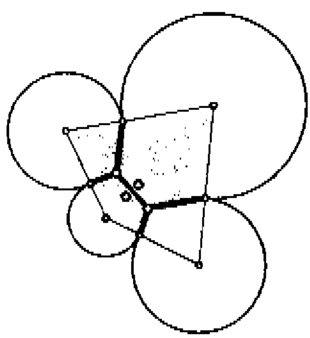

Fig 29 Four times a point is calculated, for three circles each time. The shortest sum of partitions requires a minimum of material for the build-up of the five walls concerned.

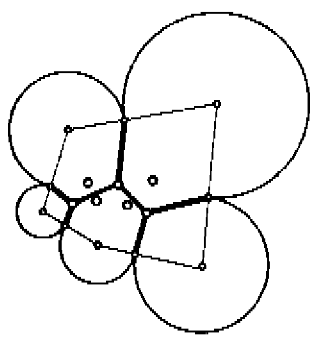

Fig 30 Five circles form the intercellular space. Seven points result in seven partition walls.

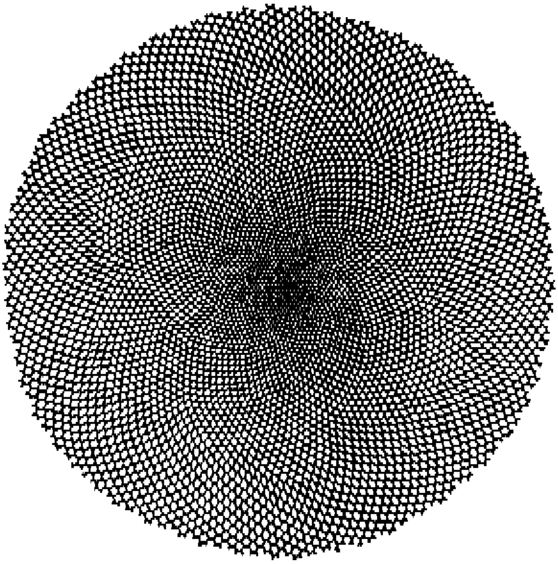

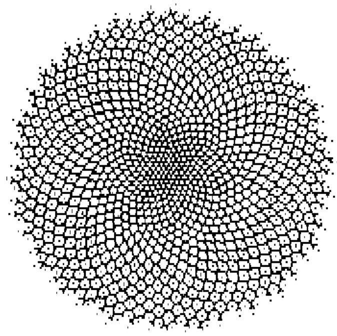

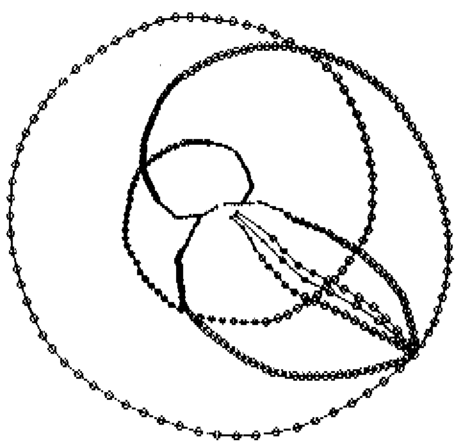

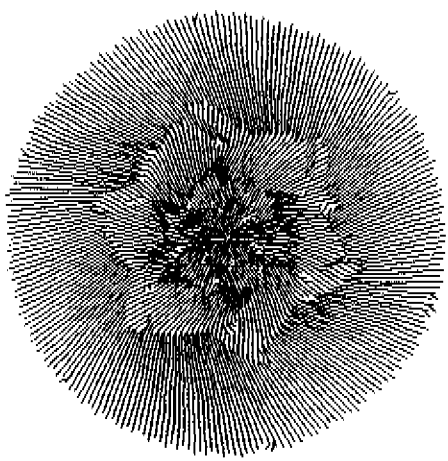

31 32
33 34

Fig 31 Seeds can be simulated by using several parameters, which determine points between circles.

Fig 32 In this structure ($n=5000$), (89,144) is passing into (233,144) on the rim.

Fig 33 From Fig 32, only one of the following spiral numbers is shown: 34, 55, 89, 144, 233, 377, 610. Each number has its own ring, in which their spirals are easily visible. The higher numbers are not visible as contact spirals yet.

Fig 34 Connections between circle centers are drawn. Units with ordinals n and z are connected. If z does not exist, then unit n is connected with the smallest primary support circle. The result is a hidden structure.

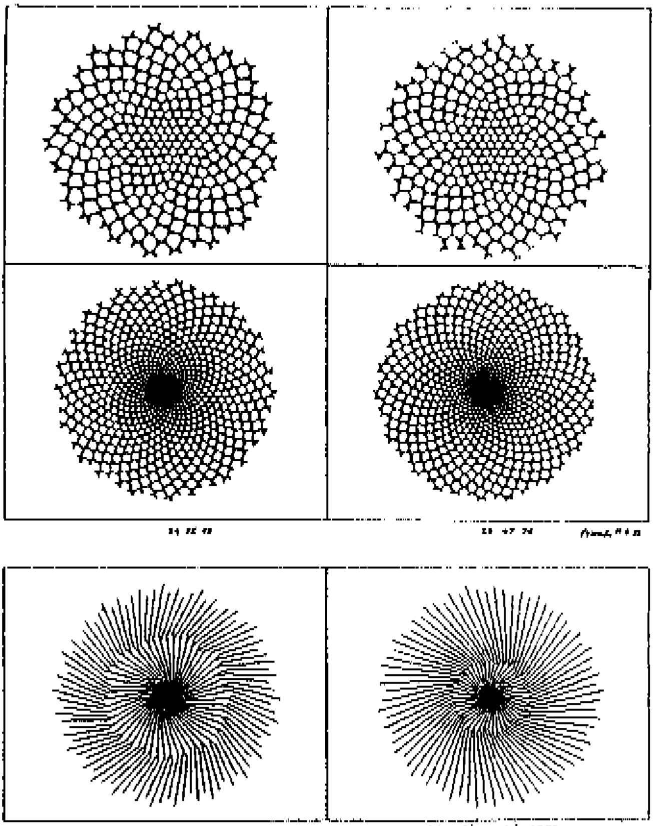

Fig 35 Structures with Fibonacci numbers *(left)* and Lucas numbers are generated, while using different S-curves. $n = 300$ *(top)* and 1000.

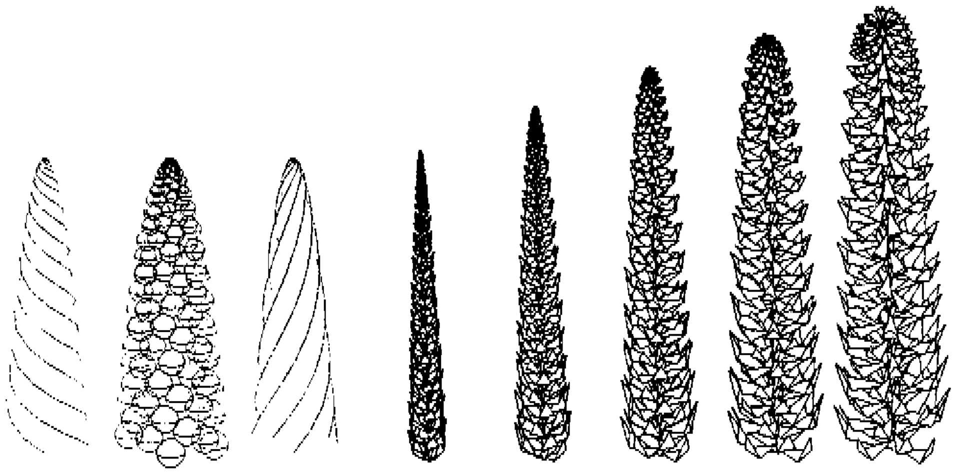

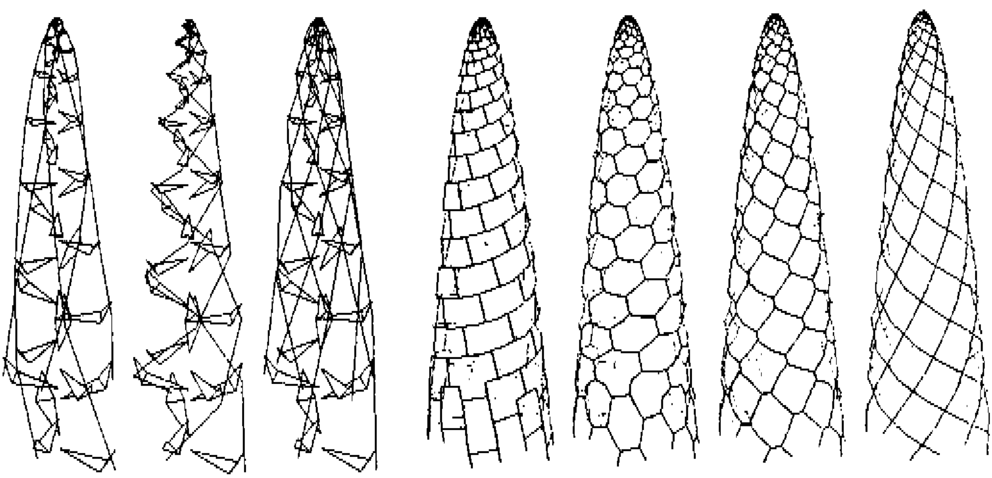

36 37
38 39

Fig 36 The dislodgement theory described also holds good for model *B*. Spirals go over into helices.
Figs 37-44: Examples of limited phyllotaxis. Using parameters to determine geometrical appendages and tilings, plant structures are plotted by computer. By connecting the centers of certain spheres, hidden

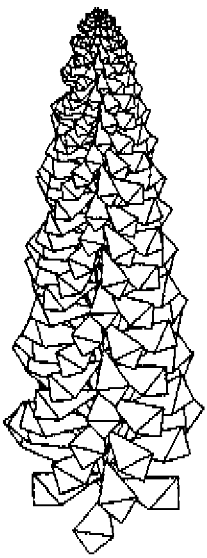
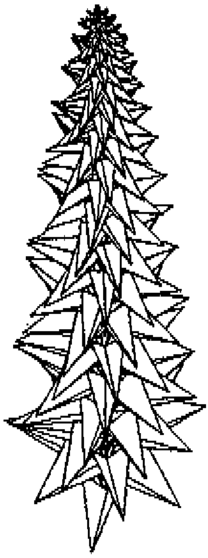
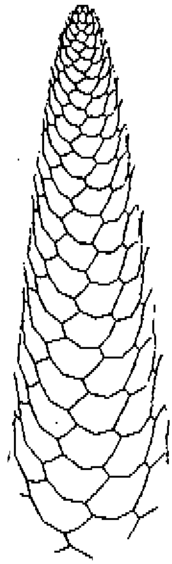
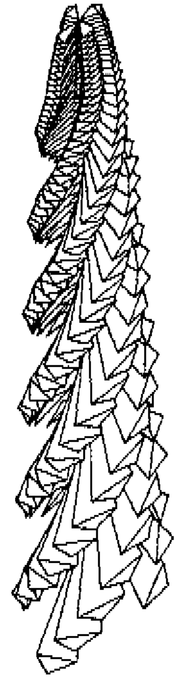
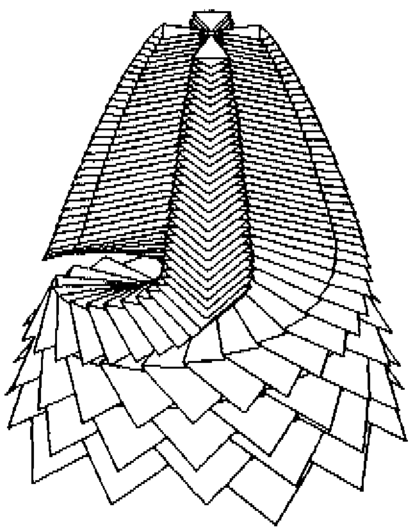
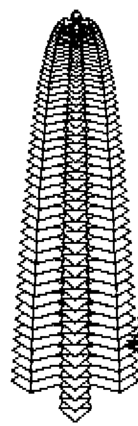
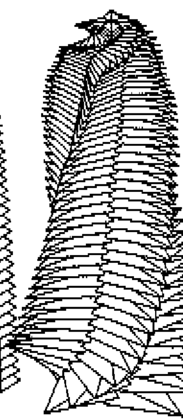


40 41
42 43

patterns can be revealed (Figs 36,37). Varying the building blocks leads to alternatives (Figs 39,40,44) or, together with translations, to change with time in a single individual (Fig 38). Figs 41-43 show deviated patterns on several receptacles (see Sections CONCEPTS and OTHER SEQUENCES).

References

(1) R.V. Jean, Phyllotactic pattern generation: a conceptual model, Ann. Bot. (London) 61:293-303 (1988)

(2) A. Lindenmayer, Development algorithms: lineage versus interactive control mechanisms, in Development Order: Its Origins and Regulation, S. Subtelny and P.B. Green, Eds., Alan R. Liss, N.Y., 1982, pp. 219-245

(3) B.B. Mandelbrot, The Fractal Geomery of Nature, Freeman, N.Y., 1983, pp. 151-165

(4) P. Prusinkiewicz and J. Hanan, Lindenmayer Systems, fractals and plants, Lect. Notes, Uni. of Regina, Canada, 1988, pp. 23-28

(5) O. Schüepp, Geometrical constructions on phyllotaxis, 16 mm movie, no. 10997

(6) d'Arcy W. Thompson, On Growth and Form, Cambridge University Press, London, 1917, pp. 759-766

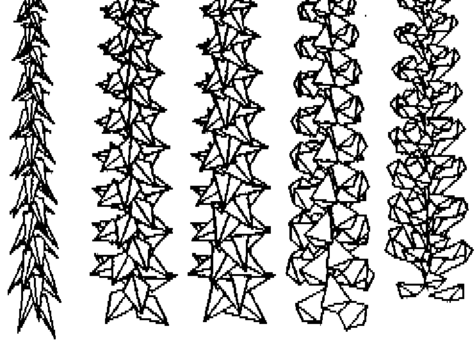

Fig 44

3 PHYLLOTACTIC PATTERNS FOR DOMES

ABSTRACT

The naked eye misleads us, when we wish to understand geometry and patterns in Nature. The basis of visible natural structures lies in the repeated application of very simple procedures [1],[2],[3]. If we want to work in harmony with Nature, our technicity should strive to work according to her ways and to her rules.

In growth, we can distinguish expanding and stacking. In many organisms, we observe a relatively smooth overall expanding. In the contrary, in the snail house, material is added only on the outside. Plants show patterns in the placement of appendages. The author found a very simple algorithm, that leads to these ***phyllotactic*** patterns [4]. The ***Dislodgement Model*** explains phyllotaxis via an inversion from expanding to stacking. This inversion is allowed, while plants follow the rules of gnomonic growth [5]. Now, we have a tool to reproduce natural stackings.

The section BASIC PRINCIPLES FOR THE ARRANGEMENT OF UNITS in the present article is a revised version of part of '*Creating Phyllotaxis: The Dislodgement Model*' [4].

INTRODUCTION

In the past, Nature has always provided many solutions for questions induced by man. In technology, but also in architecture and in constructions, engineers borrowed ideas, which were presented by Nature in one of two distinguishable (but not strictly separate) categories: dead and living matter. In living matter we traditionally englobe vegetal and animal reign.

There are good reasons to try and imitate Nature as provider of technical solutions.
(i) Nature ***evolved*** solutions. These solutions are in perfect balance with their neighbourhood. Species in plants and animals occupy their own unique niche in an ecosystem. Their bodies and habits consist of very well adapted details. Many of these details have a counterpart in man's technology. The difficulty lies mainly in seeing, ***where*** and ***when*** to choose and use ***which*** natural 'invention'.
(ii) The fractal identity of natural phenomena is approached by computer. Until only a few years ago it was impossible to simulate certain processes, like growth of structures in a more or less chaotic manner [6]. For example, we can now provide descriptions of transitions between turbulent and laminar flows.. In the many cases, that Nature develops complex structures, simple algorithms are 'looped' again and again, thousands and millions of times. What the engineer perceives, is an indefinite accumulation of micro-events, not the natural algorithms which underlie those events. Until now, application of natural algorithms was not in sight. But with the growing understanding of these algorithms [7], it becomes 'natural' to introduce them in our artificial world. Solutions and optimizations in solutions are calculated by computer.

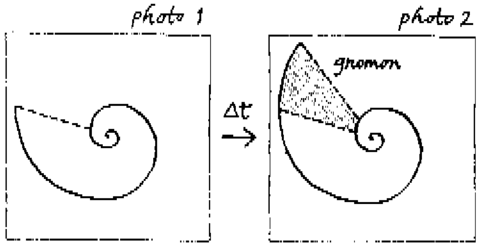

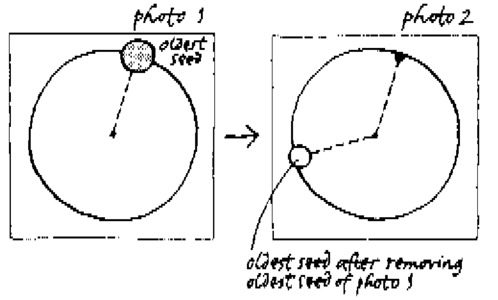

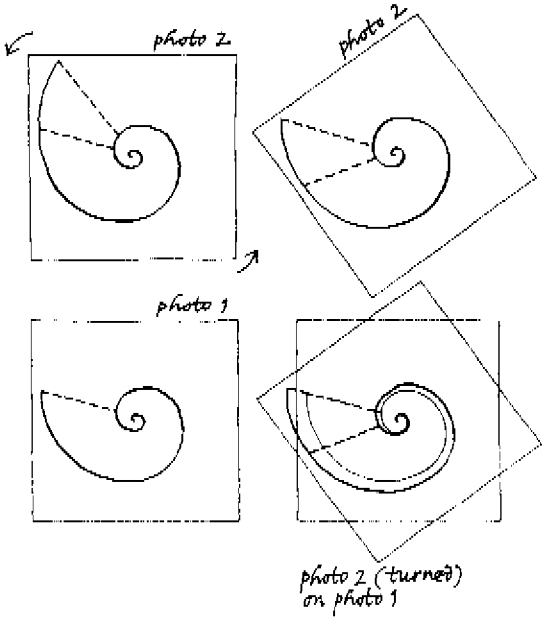

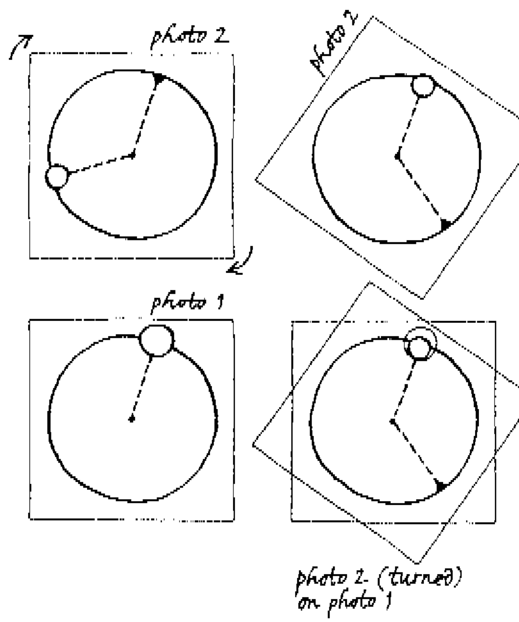

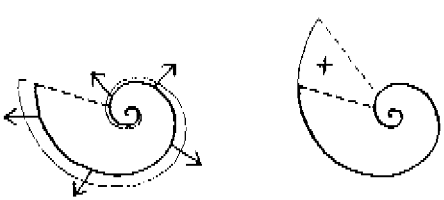

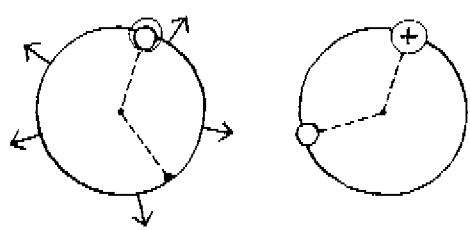

Fig 1 Gnomon in the snail house
Fig 2 Turning the snail house photographs
Fig 3 Expansion versus stacking

Fig 4 The capitular gnomon
Fig 5 Turning the sunflower disk photographs
Fig 6 Reversions

Naturalness is not simple to reproduce. In the past, the metaphor of plant growth has been used in architectural design. But the metaphor was paradoxical. 'Organic architecture' was not natural. To use Victor Papanek's words [8]: *'Designers and artists especially have looked to nature, but their viewpoints have often been clouded by a romantic longing for the re-establishment of some sort of primeval Eden, a desire to get back to 'basics' and escape the depersonalizing power of the machine, or by a sentimental mystique about closeness to the soil.'*

Biological building as understood here is more than the use of natural materials and natural manifestations. It has to imply natural algorithms as well. Important concepts in the new biological architecture are: gnomonic growth, self-similarity, expanding and stacking. These concepts will be exposed at greater length in the sequel.

There are reasons to reject certain natural phenomena for application in building. Application of rules in plant growth is not in agreement with the way we make buildings. How could we *'grow'* a building, while we always *stack* it? It seems obvious, to reject growth as a building principle. We will show a way of interpreting the phenomena of phyllotactic patterns in plants.

The snail

When a snail grows, material is added at the open outside of its house. We speak of a growing house. Growing implies stacking here. The way of stacking is simple. the snail itself grows in the three spatial directions, while keeping its general form. The snail secretes chitin in one single way all the time. So the rings of material grow and a rectilinear, spiral or helical cone is the result. (A *spiral* turns around a point in a flat plane. A *helix* screws around a line perpendicular on that plane.) In a time Δt the house grows. Some molluscs like Nautilus, add chambers, which are similar but not congruent.

When we make a photograph of a growing house before and after the time interval Δt, we see the difference in the added part called *gnomon* [Fig 1]. But when we rotate the second photograph, we can fit it on the first one. We can look at the house as if it has been expanded [Fig 2].

When we take photographs after equal time intervals, we can make a movie of an expanding snail house. The building material seems to be plastic [Fig 3].

The sunflower

To reconstruct the growth process of a sunflower, the best way is to reverse it. Let us consider a full grown head *(capitulum)*. We reverse the growth process as follows.

We take a photograph before and after picking the oldest seed from the disk [Fig 4]. It is located on the perimeter. The second seed to be removed is the oldest of the remaining seeds. It is situated elsewhere on the perimeter. *The close-packing of seeds retains its circular form* while we are picking more and more seeds. Every time we make a picture. (At last, the disk becomes less circular.)

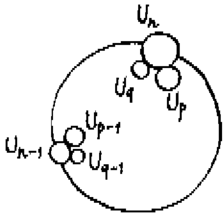

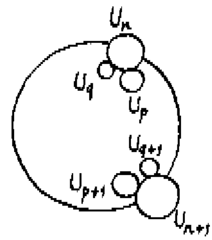

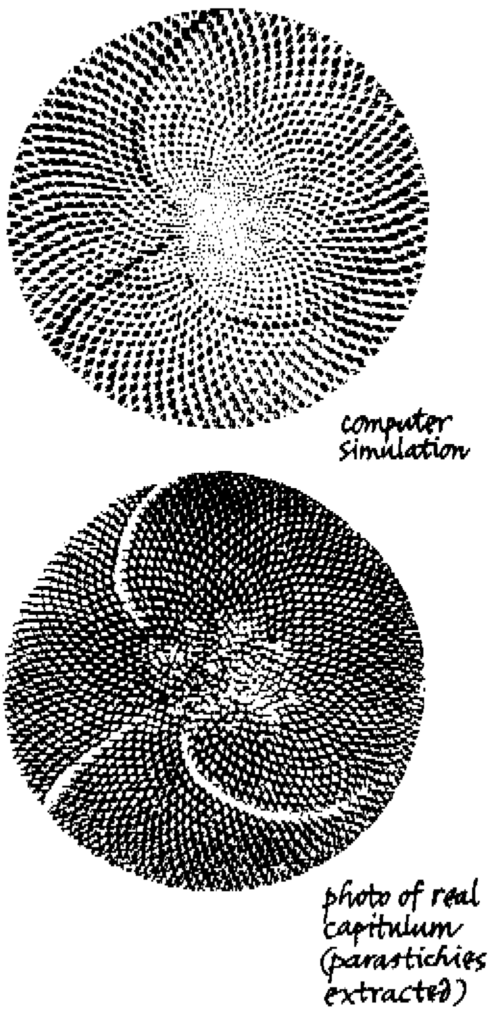

n	1	1	2	3	5	8	13	21	34
$\frac{n}{n-1}$		1	2	1·5	1·66..	1·6	1·625	1·615..	1·619..

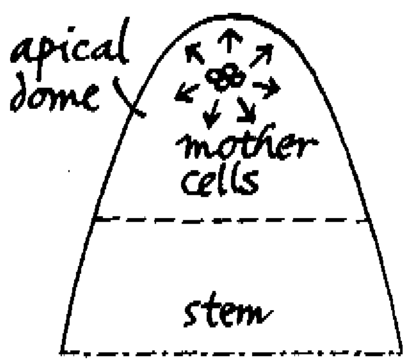

Fig 7 (*see also Figs 4-6*) Support units; U_{n-1} has age U_n-Δt = U_n-plastochron

Fig 9 Parastichies (spiral ordered seeds)

Fig 8 The algorithm: $n := n+1;\ p := p+1;\ q := q+1$

Fig 10 The Golden Section

Fig 11 Plant top

As we turned photographs to get the snail house animation, we turn them now for the sunflower head movies. The last taken photograph will be the first one in the animation. As a result, we are able now to see the growth process of the capitulum. the gnomon here is a seed [Fig 5]. (The central seed should be of age one ***plastochron*** or younger. (The plastochron is the time between the arising of two primordia or newly formed appendages (seeds here). In other cases, that is when the capitulum has central seeds which are roughly fully grown, the experiment has the same significance. However, we cannot explain the animation now as an image of a normal growing capitulum, for the size of central units will always differ from that of natural ones.)

What is the meaning of the time interval between two images of the resulting movies? In the case of the snail house, we chose an arbitrary period of time. But it is important, to repeat that period exactly. The snail house grows in a continuous way. Material is not packed in units, arising in the centre with time intervals. For the sunflower we choose the plastochron. In the animation, there are as many photographs as there are seeds. After p.Δt there are p seeds. (The ***parastichies***, or spirals of adjacent seeds on the capitulum, are discontinuous, and even somewhat subjective. The existence of a plastochron illustrates the discontinuous character of the parastichies.)

Expansion versus stacking

First, we reversed the stacking of a snail house in an expansion. After that, we regarded the expanded sunflower head as a stacking structure [Fig 6]. Actually, we picked seeds from a static structure to simulate shrinking. To get growth, we reversed the film.

When we try to 'build' a capitulum, the size of any seed is deduced from a growth function. A seed of age t has a known size. The location of a seed to be added is related to the location of the seed of age one plastochron younger. That seed has neighbours with a known age. Now, seeds one plastochron older than these neighbours are the neighbours of the seed to be added [Fig 7].

When we apply the algorithm described here [Fig 8] hundreds or thousands times we get phyllotactic patterns. These patterns are found in every green structure. When a plant forms appendages, it orders them in spirals on a flower head (parastichies) or in helices along the stem.

In most cases, the numbers of spirals are terms of the Fibonacci sequence, running 1, 1, 2, 3, 5, 8, 13, ... [Fig 9]. Of course, the terms are natural numbers. (The 'Golden Section', which is approached by the quotient of two Fibonacci numbers [Fig10], is all but natural!) Typically, phyllotactic patterns are generated by centric growing structures. The patterns are visible on stems (cylinders), in flowers, flower heads, in/on fruits. They arise in the apical dome of the plant. The apical dome is the 'vital tip' of the stem. Here lie the ***mother cells***, which are responsible for the properties and the displacement directions of their new cells, which produce new plant parts ***(primordia)***. The apical dome as well as the stem ***following*** it can be regarded as a receptacle for a phyllotactic pattern [Fig 11].

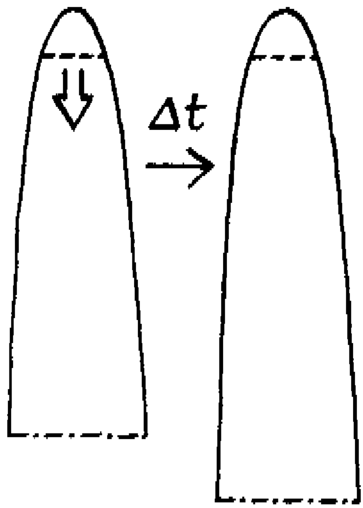

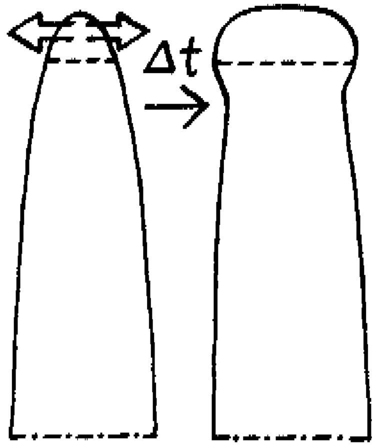

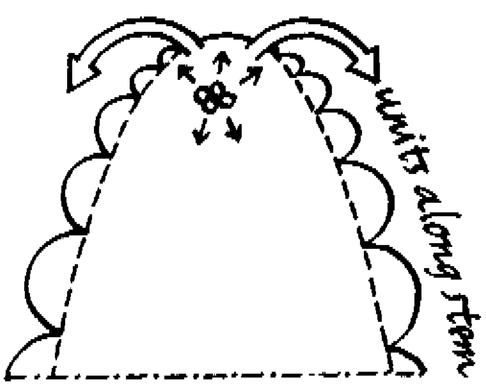

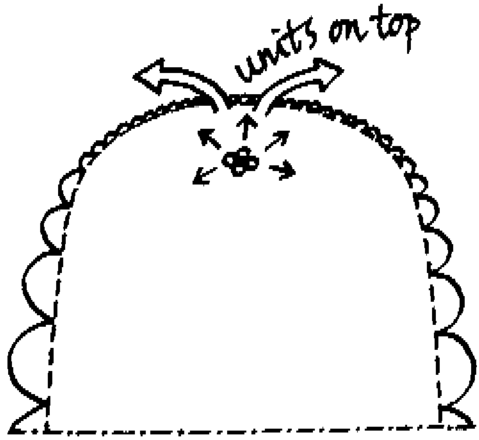

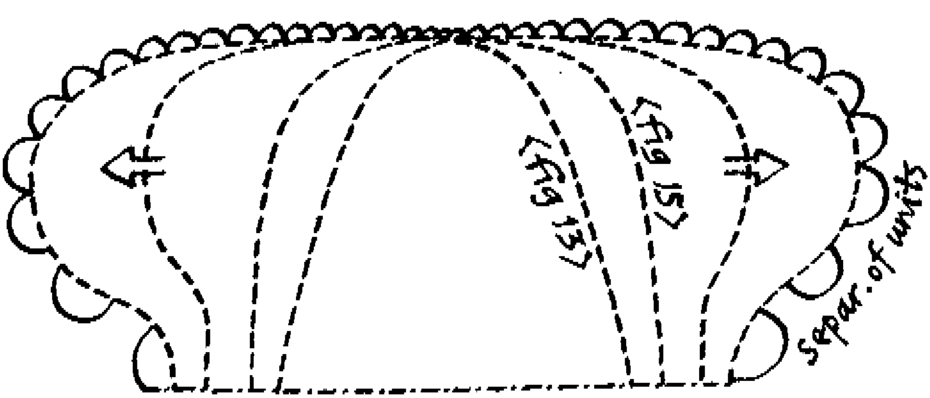

Fig 12 Indeterminate growth
Fig 13 Units along the stem
Fig 16 Radial expansion

Fig 14 Determinate growth
Fig 15 Units on the top

Phyllotactic patterns on a green receptacle

(Where we speak of a 'unit', we mean a single primordium or a sphere of influence consisting of cells, which become a primordium.)

In the vegetative phase, a plant extends axially. This way of growing is called *indeterminate growth* [Fig 12][9]. Primordia develop from cell regions in the apex (the mother cells). Units move outwards from the apex and they come to lie along the stem [Fig 13]. Near the top, the stem has a small perimeter. The number of helices that a cylinder can contain is limited, it depends on the number of units that fit around the stem tip. Below the tip, the just formed pattern is topological rigid. As a result, in this phase Fibonacci numbers are low and leaves may be opposite.

In plant life, one can distinguish different but stable phases. The transition from one equilibrium to another takes place as a sudden event, a *catastrophe* [10]. From vegetative to floral phase, the apex usually changes
(i) the direction of growth (from axial to radial),
(ii) the size of primordia (from big to small),
(iii) the form of primordia (from leaf to seed),
(iv) the plastochron (from long to short).

In the new stage one speaks of *determinate growth* [Fig 14]. Units will be pushed apart in a radial direction. Their substratum grows radially too: all primordia-forming cells remain directly attached to it [Fig 15].

In sunflowers, cell regions are pushed apart a long time (many plastochrons) before primordia are visible. As a result, the first primordia arise on the rim of the disk [Fig 16]. Each primordium goes through its own growth process, subject to genetic code and environmental conditions, but its dimensions are limited. Thus, parastiches (contact spirals) will develop in numbers that are dependent on the number of units and their size. The spirals go over into other spirals in concentric, annular areas [Fig 17]. The number of peripheral spirals stands in direct relation to the number of units that fit in the perimeter of the capitular disk. The number of ray flowers is determined by the number of spirals at the periphery of the disk. The *generative spiral* (the imaginary spiral, which connects succesive primordia) is traceable through the entire plant [11].

Basic principles for the arrangement of units

The simplest form to be chosen as a unit in a two-dimensional model is the circle. A single unit will develop (subject to a growth function) as a growing circle [Fig 18]. The time between the inception of two units in the growing point is presumed to be constant: Δt (plastochron). So at t_2 (after 2. Δt), there are two units, consecutive in size, while a third unit emerges.
The smallest of the first two units is lying against the growing point. For the place of origin of the third unit, there are two principal possibilities: It develops either in a

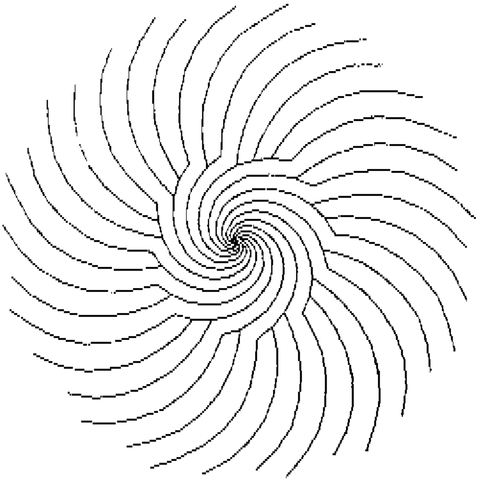

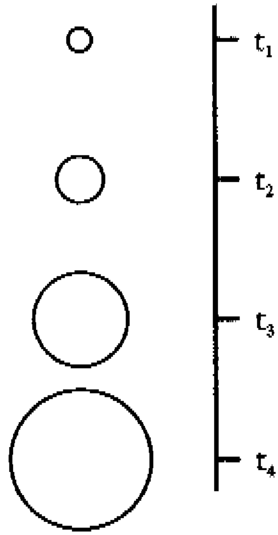

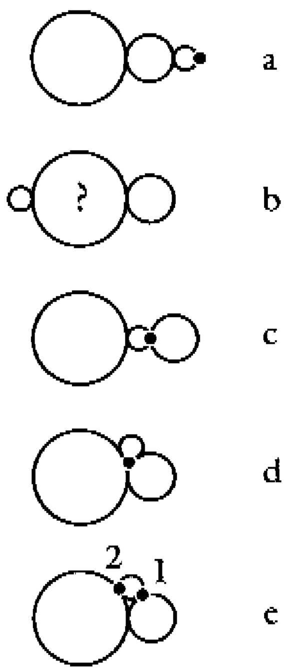

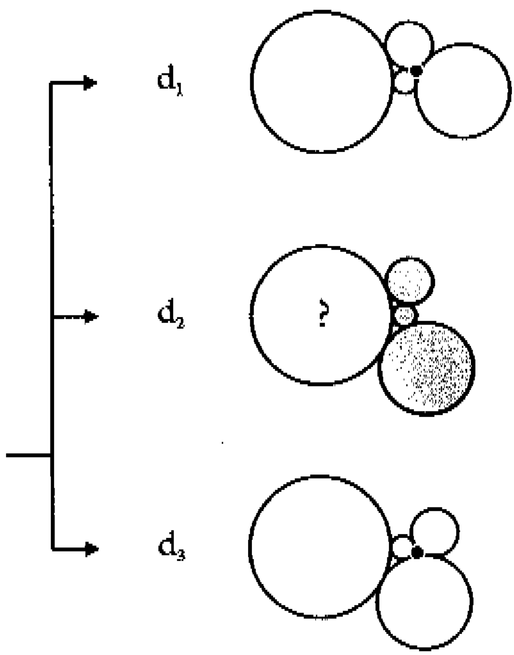

Fig 17 The ring in which spirals go over into other ones is clearly demonstrable.

Fig 19 The third unit will develop in a symmetrical peripheral position (a, b), it will push apart symmetrically the previous two units (c), or it takes an asymmetrical direction (d, e). (The centre of the apex is indicated by a dot.)

Fig 18 A single unit will develop as a growing circle.

Fig 20 The configuration d_2 is not consistent after the former choice (d).

peripheral position or between the two existing units, assuming that the circles must touch but not overlap. At this stage, a genetic or environmental datum will be important. Will the unit develop in a symmetrical position (a,b,c) or will it take an asymmetrical direction (d,e) [Fig 19]? Case b does not reflect a centric growth structure. For all remaining variants except d, the continuation of the growth process is evident. In a and e, the growing point remains peripheral, the structure being linear, alternately (1) and spiral (2), respectively. In c, the two previous units are pushed apart. In the remaining case, d, the growing point is situated centrally in an asymmetrical structure. For the reasons mentioned only variant d will be examined.

At t_3 (after 3. Δt), the next unit will emerge. The place of origin will be central, that is, between the existing units. As it is growing, the youngest unit will have to obtain a place. After it has touched on all three previous units, two of these will have to part. This parting can happen in three different ways [Fig 20], of which two occur in Nature: d_1 and d_3. Configuration d_2 is not consistent with the former choice (d). In case d_2, the youngest unit separates two immediate predecessors, which is consistent with c, not d.

Case d_3 will lead to a simple spiral (with the younger units central), or to anomalies. Case d_1 is very common and leads to phyllotaxis according to Fibonacci numbers.

What are the advantages in energy and space of variant d_1 as opposed to variant d_3?
(i) The overall system aims at a minimum average surface per unit. In a growing system, the place of units, in relation to one another, will change in such a way that each unit will keep as close as possible to the growing point. The choice between rolling aside to the 'left' or to the 'right' under the influence of the forces from the neighbourhood is made for the direction that will keep the system as compact as possible [Fig 21]. The older, peripheral unit will then lie against the youngest neighbouring units available, that is, as close as possible to the growing point.
(ii) The smaller the unit, the higher the rate of expansion. Bigger, older units are therefore more easily moved than smaller ones. (In rigid systems, there is no structural displacement at all.)

Comparison of the model at t_3 with that at t_4 shows that the structure of t_3, in its entirety, fits into that of t_4, although turned at a certain angle [Fig 22]. This follows directly from the starting point: the structures are drawn at certain points in time, that is, every time a unit has reached the size of its predecessor. At any of these points in time, a new unit emerges in the growing point. When a unit has reached the size of its predecessor, the same holds for every other unit. However complex the model drawing may become, a structure will always fit onto every previous structure.

So we have properties of gnomonic growth. As outlined above, the gnomon here is the oldest, largest unit. In a recursive model, we could add this gnomon to an existing structure. The circles in the two dimensional structure described above are to be regarded as cross sections of spheres. When the XY-plane is curved to (for instance) a paraboloid receptacle with axis Z, we can construct a threedimensional structure. Spheres are packed from the tip downwards. Spirals go over into helices.

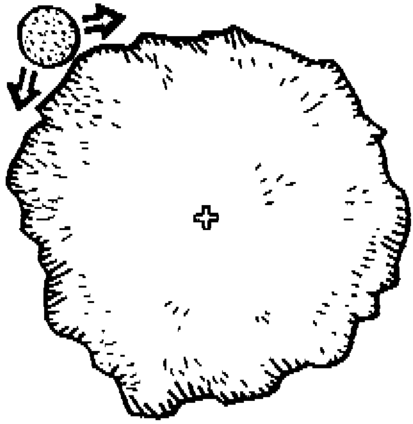

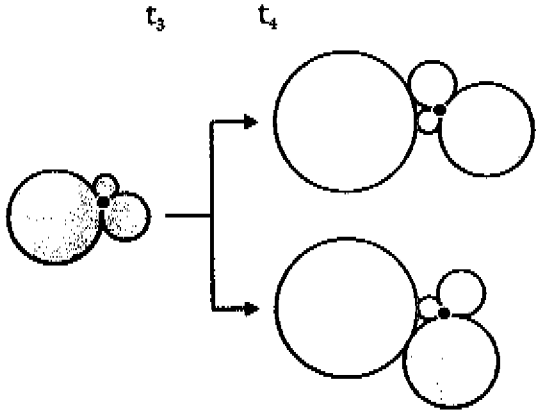

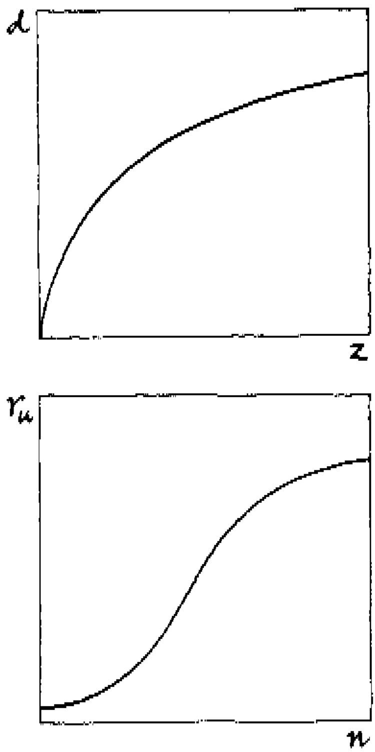

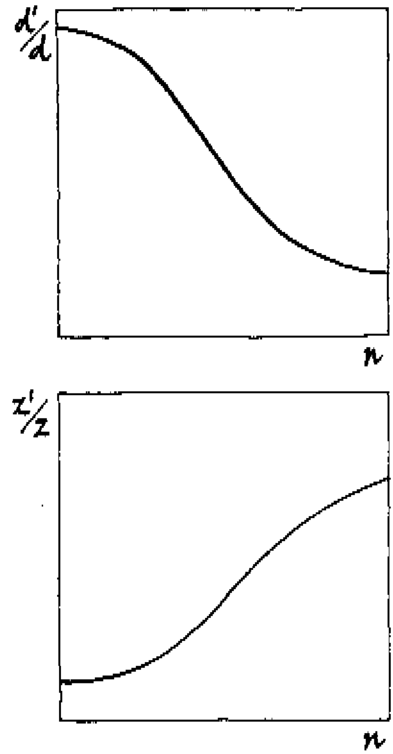

Fig 21 The system should be as compact as possible.

Fig 23 Receptacle *(top)* and unit growth

Fig 22 Comparison of the model at t_3 with that at t_4 shows, that the structure of t_3, in its entirety, fits into that of t_4, although turned at a certain angle.

Fig 24 Radial *(top)* and axial translations

Utilisation

The *Dislodgement Model* described here, may have a notable meaning in building domes and other applications. The reversion dynamic/static, growing/stacking, may remove old barriers.

Fibonaccian patterns are not necessarily a result of smooth growth. We are able now to get them by stacking building blocks. It is possible to generate tilings for dome surfaces to cover them. The units of these tilings are closely packed when we follow the *Dislodgement Model*. The sizes of the units can be chosen freely (for example similar); there is no necessity to use natural growth curves like the S-curve [Figs 23,24]. In constructions, it is possible to stack units to get domes. While Buckminster Fuller worked out Euclidean solutions for dome constructions [12][13][14], the present method opens a fractal way of constructing and covering domes [Figs 25,26]. Recent experiments show, that phyllotactic patterns can be synthesized in a purely physical environment [15]. This indicates (1) the value of these patterns for the close-packing of surfaces and (2) the value of the *Dislodgement Model* as a *'contact-pressure model'* [16],[17].

Until now, gnomonical stackings were of the snail house type or of the ring type (where added material is wrapping the whole structure). The gnomon increased in size. For this reason, the built result was not very compact and it was seldom useful. Close-packing problems are among the hardest unsolved questions in geometry [18]. The *Dislodgement Model* results in extremely compact structures in any convex shape.

The computer programs

A computer program, called *'ApexD'*, has been developed. Essentially, it has a biological basis. The program is divided into two modes 'Create' and 'Shape'. In 'Create', one defines the form of the receptacle and the growth curve. There are variables like the number of units, the influence of different aged units, the relation in size of unit and receptacle, etc.. After calculating the pattern, there is a very wide variation of results. The only unchangeable thing is the topological relationship of units. Once in program part 'Shape', one is free to choose in size and form of appendages, in axial and radial translations, being defined by mathematical curves.

A demonstration version of *'ApexD'* is already obtainable. Another program, *'ApexS'*, has been developed recently [19]. The *'Stack and Drag Model'* builds a growing structure upwards from two cotyledons. It has more biological significance, while the *Dislodgement Model* may be more valuable for engineers.

Acknowledgements

I like to thank Myriam Daru for her proof-reading, Roger V. Jean for his correspondences and reviewing the *Dislodgement Model*, and my cousin Frank J. van der Linden for his valuable contributions. I owe the late Aristid Lindenmayer very much for the many discussions and my introduction in the science of biology.

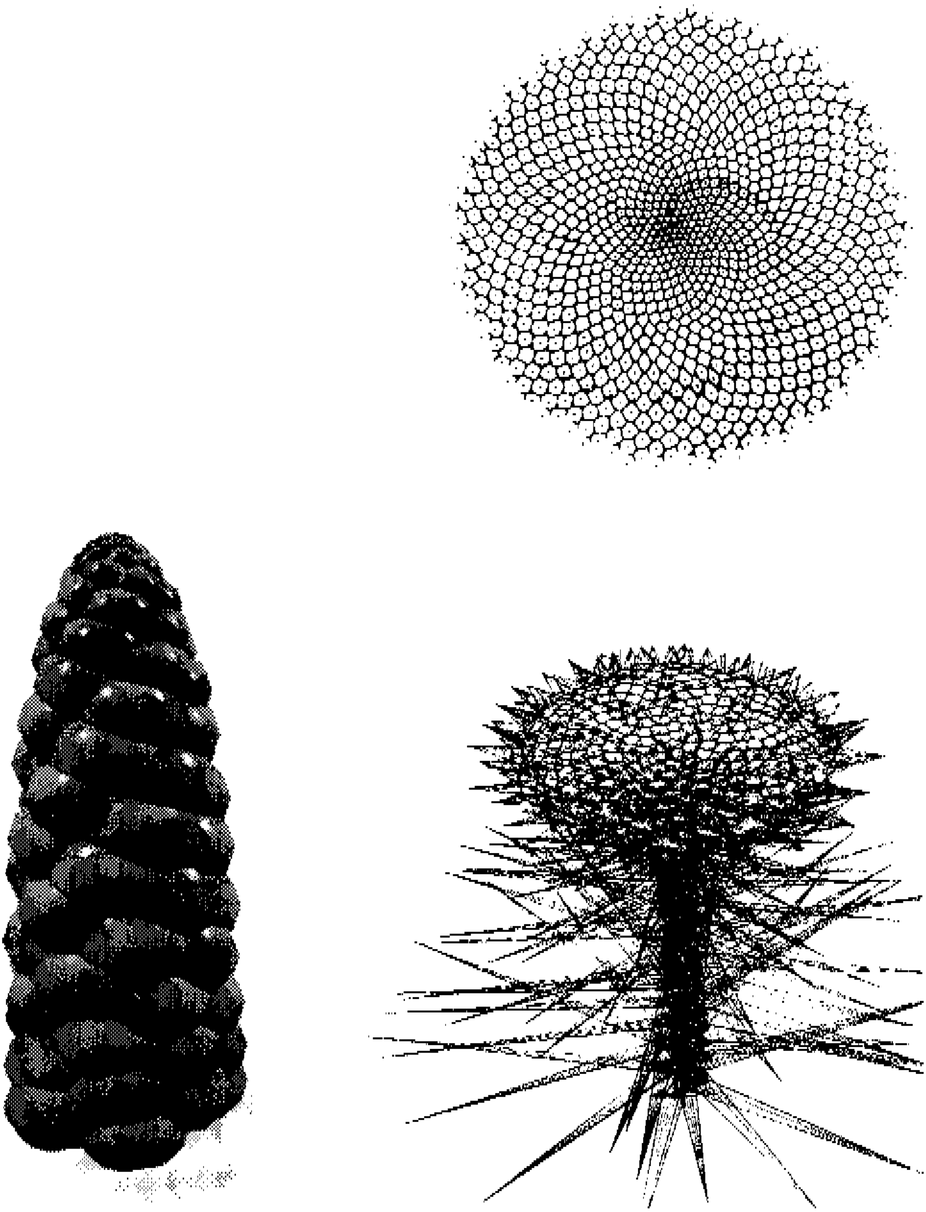

Fig 25 Computer simulations of Fibonaccian plant patterns (with growing units) (solid model by Lucien Havermans)

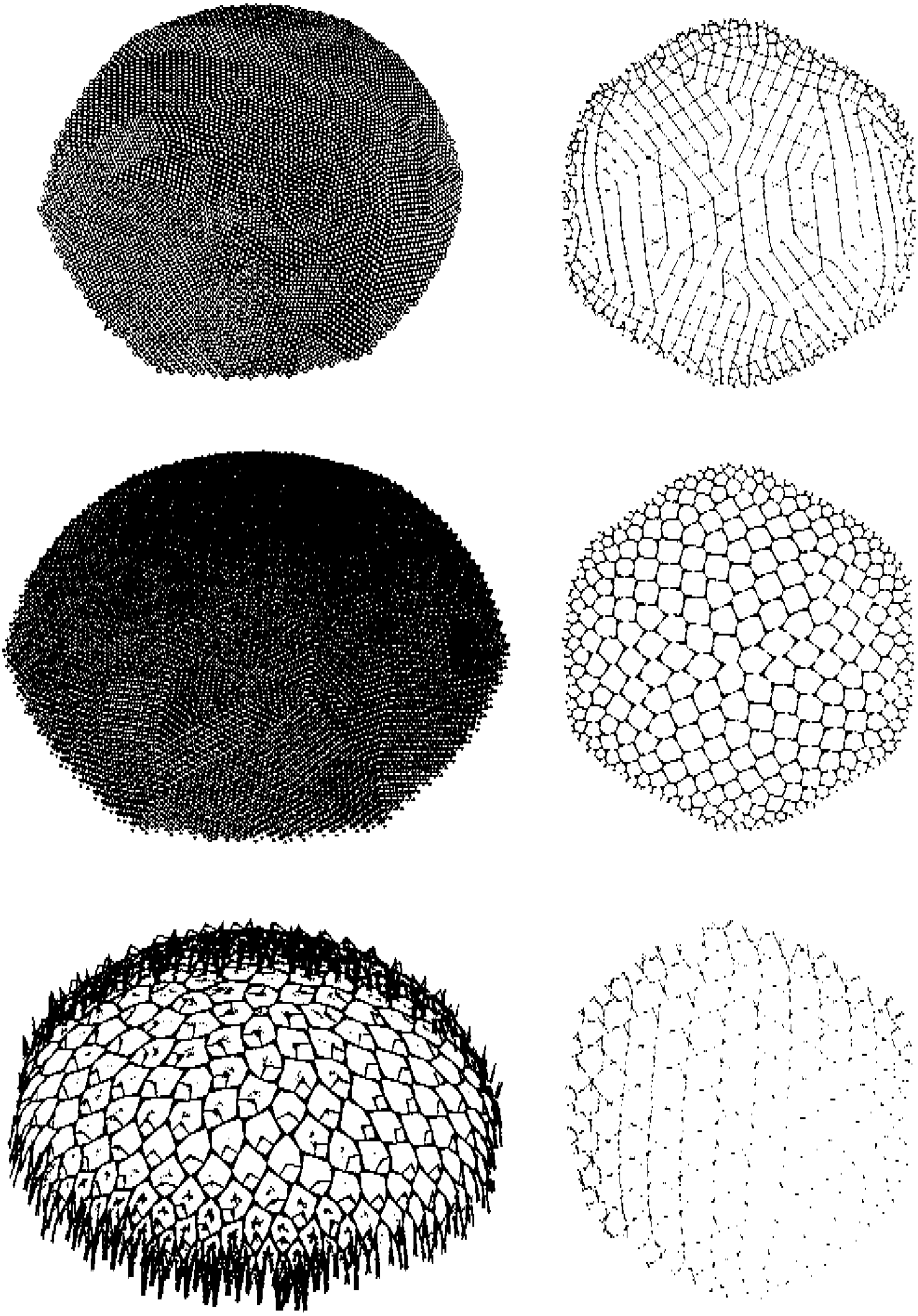

Fig 26 Examples of Fibonaccian dome patterns (with various building blocks)

References

(1) Prusinkiewicz, P. and Lindenmayer, A., *The Algorithmic Beauty of Plants*, Springer Verlag, New York, 1990

(2) Mandelbrot, B.B., *The Fractal Geometry of Nature*, Freeman and Company, New York, 1983

(3) Rozenberg, G., Salomaa, A., and others, *The Book of L*, Springer Verlag, Berlin, 1986

(4) Van der Linden, F.M.J., *Creating Phyllotaxis: The Dislodgement Model*, Mathematical Biosciences, (vol 100, no 2), Elsevier Science Publ. Co., New York, 1990, 161-199

(5) Thompson, d'Arcy W., *On Growth and Form*, Cambridge Universiry Press, Cambridge, 1917, 759-766.

(6) Briggs, J. and Peat, F.D., *Turbulent Mirror, An Illustrated Guide to Chaos Theory and the Science of Wholeness*, Harper & Row, New York, 1989

(7) Stevens, P.S., *Patterns in Nature*, Little, Brown and Company, Boston, 1974

(8) Papanek, V., *Design for the Real World*, Pantheon Books, New York, 1971, 187-188.

(9) Steeves, T.E. and Sussex, M., *Patterns in Plant Development*, Cambridge University Press, Cambridge, 1989, 181-183

(10) Lyndon, R.F., *Plant Development*, The Cellular Basis, Unwin Hyman Ltd, Boston, 1990, 54

(11) Meicenheimer, R.D., *Relationships between Shoot Growth and Changing Phyllotaxy of Ranunculus*, American Journal of Botany, (vol 66, no 5), 1979, 568-569

(12) Miyazaki, K., *An Adventure in Multidimensional Space, The Art and Geometry of Polygons, Polyhedra, and Polytopes*, John Wiley & Sons, New York, 1983, 40-50

(13) Senechal, M., Fleck, G., and others, *Shaping Space, A Polyhedral Approach*, Birkhäuser, Boston, 1988

(14) Williams, R., *The Geometrical Foundation of Natural Structure*, Dover Publications, New York, 1972

(15) Douady, S. and Couder, Y., *Phyllotaxis as a Physical Self-Organized Growth Process*, Physical Review Letters, (vol 68, no 13), The American Physical Society, 1992, 2098-2101

(16) Schwendener, S., *Mechanische Theorie der Blattstellungen*, Leipzig, 1878

(17) Mitchison, G.J., *Phyllotaxis and the Fibonacci Series*, Science, (vol 196, April), American Association for the Advancement of Science, 1977, 270-275

(18) Stewart, I., *How to Succeed in Stacking (a solution by Wu-Yi Hsiang)*, New Scientist, (13, July), 1991, 29-32

(19) Van der Linden, F.M.J., *Creating Phyllotaxis: The Stack and Drag Model*, Mathematical Biosciences (in preparation), Elsevier Science Publ. Co., New York, 1994

4 CREATING PHYLLOTAXIS: THE STACK AND DRAG MODEL

ABSTRACT

The genesis of phyllotaxis, the origin of the pattern of appendages on the surface just below the apical extreme of many plants, is an old unsolved puzzle. While many models generate helices, the present one is the first to achieve this in an integral construction from seed to flower. Combination of the principle of gnomonic growth, where consecutive additions have comparable positions, with a dragging principle, where the developing zone follows the apical tip, provides a powerful tool in simulating a wide range of phyllotactic manifestations. The influence of three vital parameters for primordial size, compressibility, and canalization (or annular arrangement) helps in understanding the problem's nature.

INTRODUCTION

Observed patterns and some divergent models

Most plant bodies show a radial symmetry as a consequence of their axial development. Primordia (early appendages) are ordened in various phyllotactic patterns such as distichous (or opposite), decussate (or cross-opposite), in whorls, or in parastichies (or spirals and helices). Therefore it seems defendable to start a simulation for pattern generation from a centric growth principle. Investigations on pattern formation of epidermic cells in vegetative ontogeny [5,16,48] centric experiments [11], and centric surface models [15,17,52] show that use of (centric) surface models may be sensible in some cases. However, studies on floral ontogeny [13,18], and surgical experiments [20,21] clearly contradict a purely centric theory.

Differences with other models

This paper presents a phyllotactic model of which the stacking principle is traditional to some degree [24,34,58] but with a dragging principle prohibiting primordium stacking below certain regions. Use of a dragging aspect as a counterpart of gravity and adhesion is justifiable, for new material arises continuously at the top of the stem while the epidermic and lower layers have to follow. In the model, this dragging causes canalization of organ numbers or the tendency of organ numbers to remain constant in spite of genetic or environmental variation [4]. Canalization has not been incorporated in phyllotactic models for complete plant bodies before. The arranging in concentric circles of primordia on the shoot apex is again responsible for annular differentiation of flower parts [8].
In contrast to existing theories which are based on observed geometrical consequences (like the Fibonacci angle of 137.5°) [1,3,7,10,22,24,26,34,41,42,43,45,46,55,56,58] the

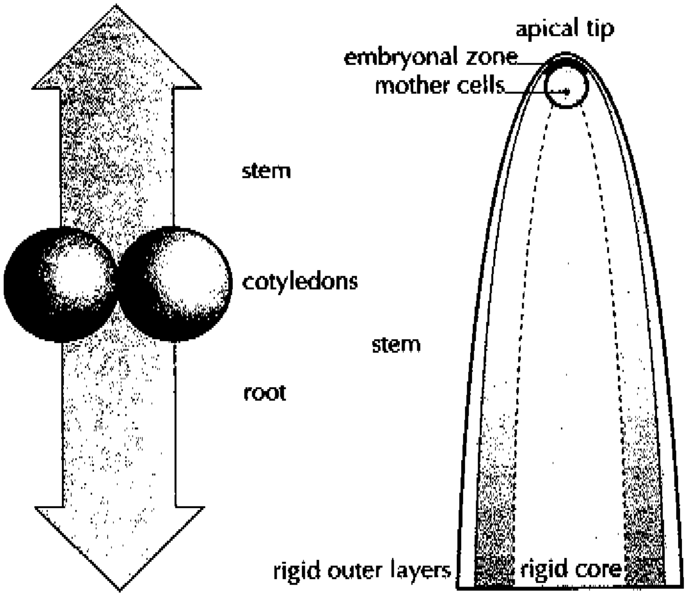

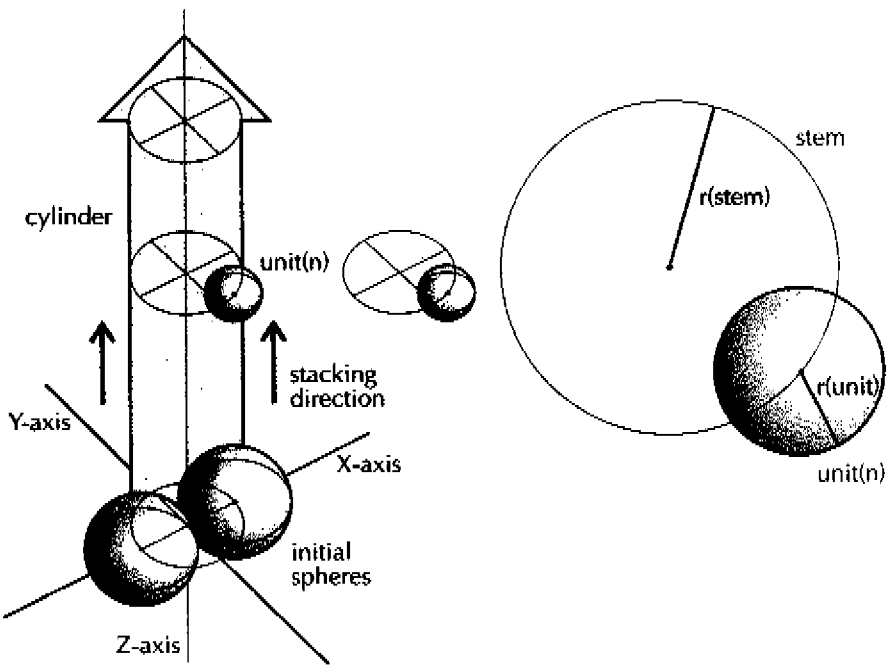

Fig 1 The origins of vegetative phyllotaxis. *(left)* Basically, dicotyledons show horizontal and vertical symmetry. Only dicotyledons, and only the shoot is subject of study. *(right)* Just below the extreme top a cluster of cells with an active envelope is continuously pushed forward by the elongating and multiplying shoot cells.

Fig 2 The Stack and Drag Model: initiation and relation *r*(unit)/*r*(stem) in the vegetative stage.

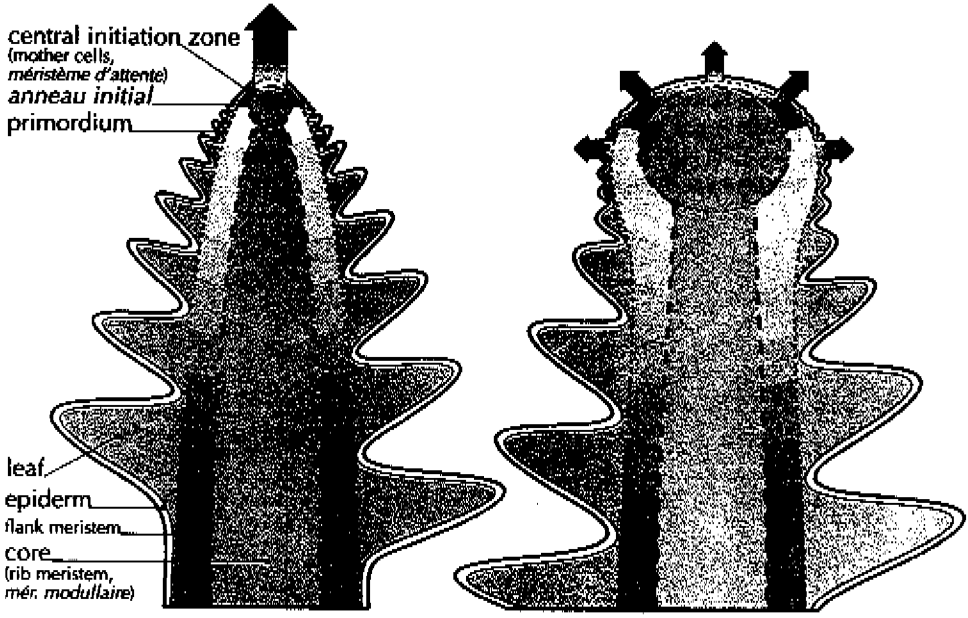

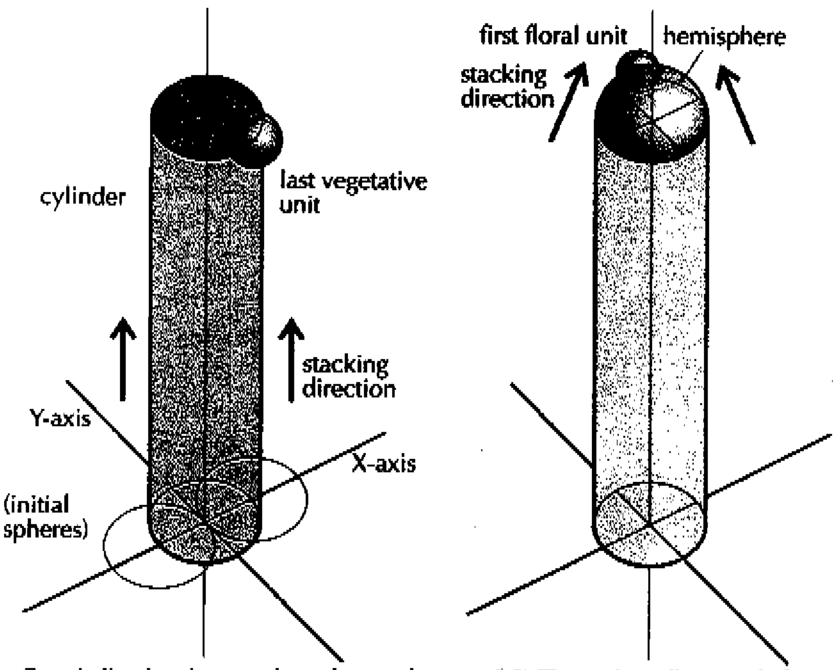

Fig 3 Growth directions in vegetative and generative stage.*(left)* The mother cells are pushed upwards, thereby dragging their mitotic active envelope which is annular shaped [6]. The very top is quiet and does not generate primordia. *(right)* While the apical dome expands reproduction organs are generated. In flower heads, as shown, the active ring remains behind some time before it rapidly closes on the top while primordia arise as surfacial little hemispheres.

Fig 4 The Stack and Drag Model: from vegetative to generative stage.

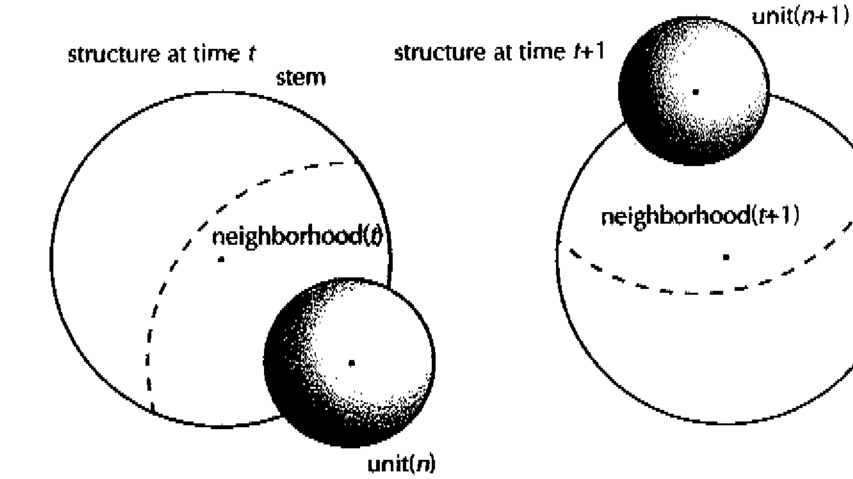

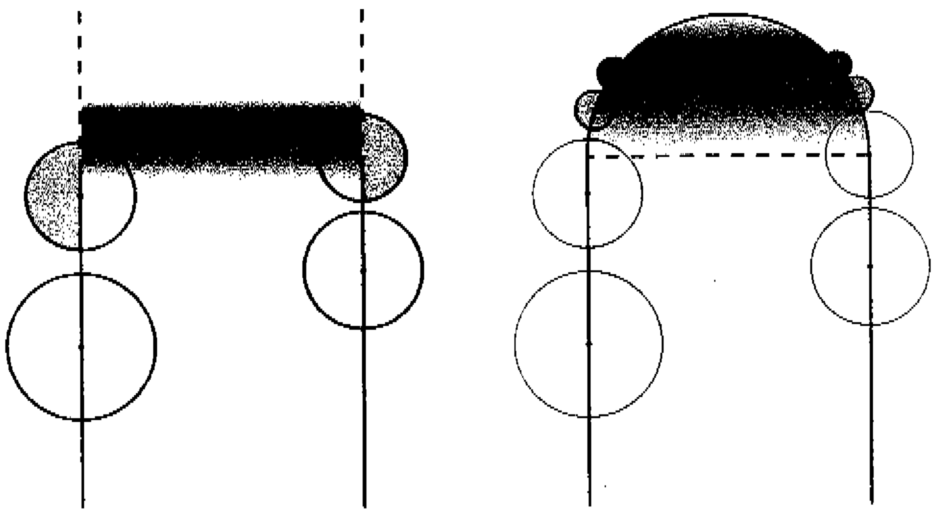

Fig 5 At a point in time $t+1$ a new primordium will become visible, but where? In looking back at the structure at time t we see that the new primordium there arose between or against two support units of which we know the ordinal numbers p and q. Because, when turned, structure($t+1$) fits on structure(t), the new primordium will arise in neighborhood($t+1$). Thus, at time $t+1$, we choose support units with an age of one plastochron younger (or: with ordinal numbers $p+1$ and $q+1$) than the support units of the primordium that just arose. If positioning is impossible for any reason, we have to shift the new unit (see below).

Fig 6 Transition from vegetative to generative stage, interpreting Buvat's concept. *(left)* A new unit may arise in the initiation zone *(grey)* when there is no room left between the neighboring units just below it. Units may not arise significantly lower than the preceeding ones. The initiation zone has a width that relates closely the upper unit sizes. In vegatative structures, represented in the cylinder-stage of the model, the initiation zone is relatively wide. *(right)* Determinate growth: The cylinder is closed by the apical hemisphere, being filled in with primordial units which meet at a point not necessarily lying exactly on the Z-axis. Unit radii are related to the cylinder radius. (see also fig 10)

Stack and Drag Model uses the gnomonic growth property[1] [50] which makes the introduction of distances or angles to control correct unit positioning redundant.

Goals and limitations of the theory

To demarcate the field of study ramifications [40] are excluded. The model strives for
(i) continuity in development from cotyledons to inflorescences and flowers (any initiating rule is consequently repeated from the very start, regardless of the motive behind it),
(ii) a very limited set of easily recognizable parameters frequently mentioned in the literature,
(iii) numerical and graphical output which is easily comparable with observations reported in the literature[2] [3,27,32],
(iv) solutions of some open problems in phyllotaxis [14,25,27,44],
(v) consistency, according to recommendations for phyllotaxis theories [44).

Approach and biological evidence

Cotyledons, stem, and flowering

The Stack and Drag Model follows a tradition in the geometry of close-packings of spheres in nonliving structures[3] [9,35,57]. The stacking is from two initial, similar, and touching spheres as cotyledons upwards. A phyllotactic unit is defined as a primordium or a sphere of influence including primordium forming cells. Primordial units may be shaped as spheres and arise one after one with a nearly constant time interval (plastochron). The vegetative stem (fig 1) is presented as an infinite cylinder (fig 2).

The switch from vegetative to generative growth (flowering) [8] (fig 3) is simulated by ending the cylinder stacking. Now, an apical hemisphere with radius 1 becomes the bearer of primordial spheres with constant radii [4] (fig 4). For flower heads, the distance ratio becomes relatively small just before flowering and units are nearly constant in size. In simulations of vegetative structures and flowers, units will soon fill up the hemisphere.

The gnomonic principle: biological justification and application in the model

In investigations and modeling in phyllotaxis, primordia are identified by numbering them in a logical way [13]. In general, it is discussable whether the numbers represent the actual succession of inception or not [4], but it is often visible that successive numbered primordia are embedded in resembling regions, or: subsequently arising primordia lean against subsequent environments. This empirical rule is equivalent with the ascertainment that a plant grows gnomonically. Any primordium has generally the same difference in ordinal or age compared with its lower contacts as the preceding primordium. This holds for all primordia. Small positional and dimensional adjustments are of second order. In vegetative plant structures the gnomonical way of growing is obvious, but in generative ones it is not. However, phyllotactic pattern generation takes place in early stages in plant development, while primordia are not differentiated and the apical dome keeps its form more or less, so there is gnomonical growth.

In the plant, the inception of a new primordium is a local event which depends on certain circumstances like gravitation, surface tension, expansion, and chemical influences. More important here is the ascertainment, that (i) circumstances are broadly stable in time and (ii) heredity plays a modest part[4]. In order ro predict the site at which a new unit arises, the Stack and Drag Model makes use of the gnomonic growth principle. In other words, the place of a new unit in a configuration at a certain point in time tells much about the place of the next unit to arise (fig 5). By applying the gnomonic property, modeling is possible without the instant need of knowledge of underlying mechanisms. The Stack and Drag Model neither follows any of three well-known hypotheses, nor excludes them: (i) New primordia should arise as far as possible from just born ones [23,34,45], which implies an inhibitor mechanism. Many phyllotactic patterns seem to obey this theory, but other ones, like the monostichous spiral, contradict it [27]. (ii) New primordia should arise at the first available space [49], which implies a tension-field theory. (iii) New primordia are positioned by mechanical pressure of its contacts [1,47]. This does not account for the initiating location of a new primordium.

Disconnection of pattern formation and structural growth

During formation of phyllotactic patterns, the plant is growing. In the model, pattern generation is separated from structure expansion. The geometric relations between neighboring units and stem radius just at the inception of a new unit form the basis for the consequently arising patterns in which the stem width is measured by the distance ratio r(unit)/r(stem). Thus, instead of increasing the cylinder radius, the size of the units is decreased. The maximum distance ratio is presumed 1, defining the initial cotyledons, and it diminishes while stacking new spheres[5]. The stem's absolute thickening has no topological significance. The settling height for new spheres depends on the upper units configuration.

The place of a new spherical unit is calculated as if it were the last (top) one to be constructed. At the very moment of placing the unit the growth process is simulated topologically. So, results of arising, developing, and topological consequence are copied while at the same time the possibility to stack more units on the structure is maintained by its cylindrical shape. This is achieved by positioning units locally correct, with their sizes not related to each other but to their receptacle. Because in the model the stem is cylindrical with radius 1, calculating correct unit sizes is easy. When these are known for initiating primordia of any ordinal number, a construction or even a growth simulation for a certain point in time of development can be executed[6]. To understand the relative sizing in the model, we should imagine the development on the apical dome as follows (fig 6): not the extreme top of the apical dome, being a point, is the growth center but the perimeter of the mother cells determines a ring of development. In fact, there can never be a growth center without dimensions. One should rather speak of an expanded point.

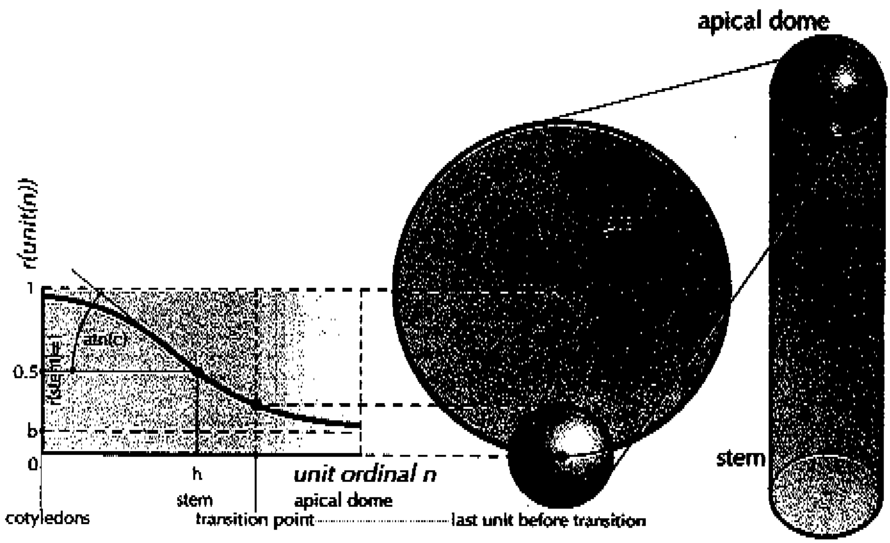

Fig 7 The relation ***unit radius - stem radius***. The unit shown is the last vegetative one, lying on the cylinder. Unit sizes are defined by the S-curve [51].

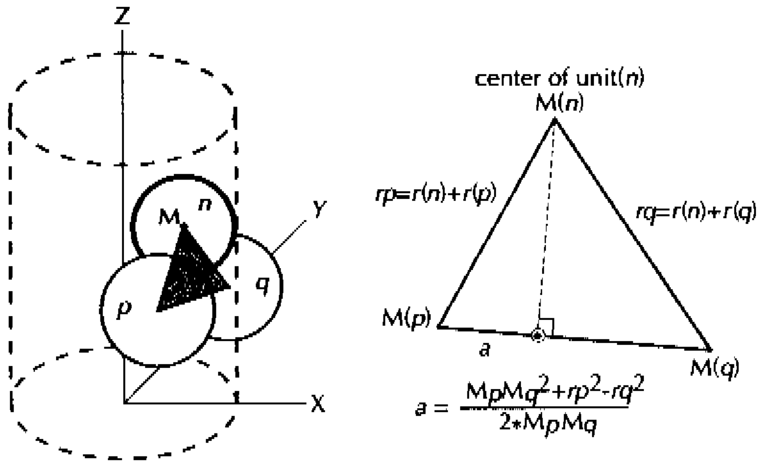

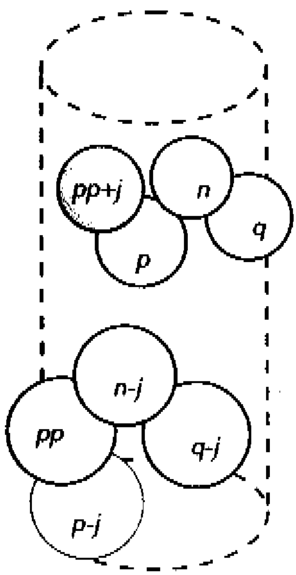

Fig 8 Unit(*n*) will have contacts(*p*) and (*q*) when the previous unit(*n*-1) had units(*p*-1) and (*q*-1) as its contacts. Unit(*p*) lies counterclockwise around the positive *Z*-axis against unit(*n*). *mpq*=*d*(*M*(*p*),*M*(*q*)); *rp*=*r*(*n*)+*r*(*p*); *rq*=*r*(*n*)+*r*(*q*). The center of unit(*n*) *M*(*n*) is the intersection of a circle with center (*xm*,*ym*,*zm*) with the cylinder. If a neighboring unit intersects unit(*n*) it will replace unit(*p*) or unit(*q*).
Fig 9 The highlighted unit(*pp*+*j*) will be counted, for unit(*n*-*j*) has unit(*pp*) as one of its support units. Increase of *j* means decrease of sensitivity.

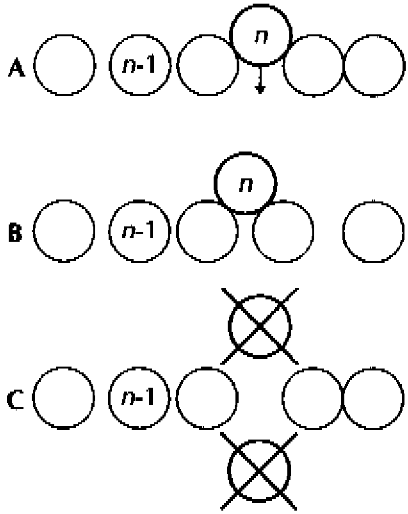

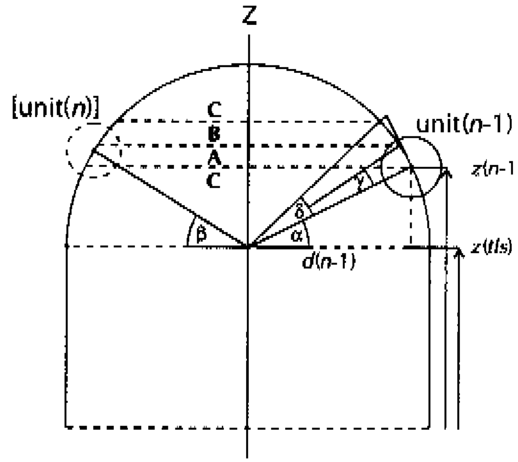

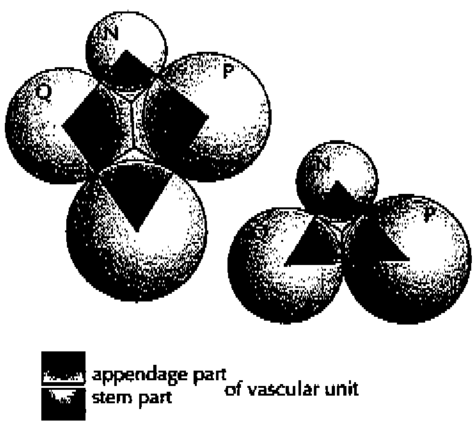

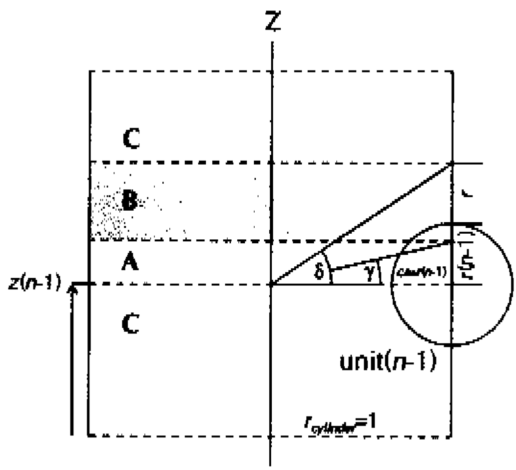

Fig 10 (left, top: sideview of unrolled cylinder) A new unit which fits or nearly fits between its predecessors (A, canalization zone) will be part of the existing ring. When it has been located significantly higher (B, free positioning zone) after lack of space below, it will be the first unit in a new ring. Extreme high or low positions indicate an error (C, upper and lower error zone).
(right, below: vertical section through cylinder) Besides by $z(n\text{-}1)$, the upper border of the canalization ring (A) is settled by $ca.r(n\text{-}1)$, or angle γ. The maximum height for origin of units is determined by angle δ in

$$\tan(\delta) = r + r(n\text{-}1)\} \; / \; r_{cylinder} \, .$$

A unit which has been placed in (B) remains its calculated position. Higher ca values will narrow the ring.
(right, top: vertical section through hemisphere) The ring's shifting is defined by angles α and β in

$$\tan(\alpha) = \{ z(n\text{-}1) - z(tls) \} \; / \; d(n\text{-}1) \quad \text{and} \quad \tan(\beta) = \{ z - z(tls) \} \; / \; d \, .$$

z is height of unit(n); $z(n\text{-}1)$ is height of unit(n-1); $z(tls)$ is height of the last vegetative unit; r is radius of unit(n); ca is canalization factor.
Fig 11 (left, below) Differentiations by the vascular unit [29].

The three S-curves

The model makes use of three S-curves[7] [51]: the unit growth curve and two translating curves simulating axial and radial growth. The moment of the transition from indeterminate (vegetative) to determinate growth is preset. Contrary to the number of vegetative units, the exact number of units that fit on the apical hemisphere is not predictable.

Differentiation and the relationship between pattern, shape, and color

Closely connected with the expansion of a plant structure in radial and axial directions is the differentiation of primordial parts[8]. In general, differentiation in living structures can be explained by positioning signals [59]. Below, it will be shown how to get some essential shape and color differentiations as a byproduct after translations. As a consequence, the Stack and Drag Model relates pattern (phyllotaxis), shape (differentiation), and coloring to each other.

MODEL DESCRIBTION

The model comprises two main processes: (i) Creating Patterns in which spheres of different sizes are positioned using the same algorithm thourough the entire construction and (ii) Shaping Structures in which spheres are translated in order to simulate axial and radial growth. In part (i) a growth curve[9] defines sphere radii in relation to receptacle radius (fig 7) and in part (ii) two similar curves define translations in the distinguishable stem parts.

Creating patterns

Sizes of spheres as phyllotactic units are calculated; their centers are situated at distance 1 from the Z-axis. The stacking direction is upwards from two initial, touching spheres (fig 2). These two spheres, representing cotyledons, have unit radius 1. Units are constructed using positioning algorithms of the Dislodgement Model[10] (fig 8). After the last unit on the cylindric stem, spheres close the surface in a transition from vertical to horizontal: the apical hemisphere with radius 1 (fig 4). The parameters used are: (i) *tls*, number of spheres on the cylinder, initiating spheres included, (ii) *exp*, expansion: spheres are compressible to repulsive, dependent on age, (iii) *sens*, sensitivity: the placement of spheres depends on past configurations (fig 9), and (iv) *canal*, canalization: the ring in which a sphere is allowed to be constructed, is chosen narrow to wide[11] (fig 10).

Shaping structures

After the pattern-forming on the receptacle we displace units in axial and radial directions[12]. To simulate flowering according to the catastrophe theory [51], the three curves for unit growth, axial translations and radial translations, must work closely together. The distance ratio r(unit)/r(stem) is of decisive importance here. At the time of inflorescence, high values result in flowers and low values result in flower heads.

When spherical units are replaced by stemsurface-filling polygons, or vascular units[13] [28,29,38], differentiation is simulated. To understand this, we consider a given unit with both of its two support units and more lower units if necessary (fig 11). The lower part of the top unit develops as an appendage and the top parts of the lower units will be contributors of stem filling parts. The length and top position of the appendage may be changed by specific parameters which are related to radial or axial translations. Use of these parameters leads to remarkable results when simply relating them with unit positions. In this way, differentiation and corresponding coloring in the distinguishable 'plant' parts arise spontaneously, conditioned by the S-curves. Adjacent polygons form a honeycomb structure, like in pineapple.

RESULTS

The Dislodgement Model [52] was sufficient for simulations with recognizable positioning of individual primordia on early flower heads [2].

In the Stack and Drag Model[14] variable values for some vegetative and floral structures have been compared (Table I). The computer program is able to produce very different phyllotactic patterns along the vegetative axis as well as in flowers and in flower heads. Helices appear almost exclusively in Fibonacci numbers (1,1,2,3,5,8,13,...) while successive units make XY-projected angles of -137.5°, starting from right angles or the decussate arrangement at the base. Accessory series of the Fibonacci sequence may arise as sudden anomalies without particular parameter presettings. Canalization which is induced by the mechanism as depicted in (fig 10) results in rings of units in fixed numbers like Fibonacci terms. The preference for fixed numbers in canalization follows from the preference for these numbers in parastichies. In contradistinction to stability for fixed numbers in parastichies, units often show canalization in deviations close to those numbers.

The early development of the composite flowering head of Microseris pygmaea [3] is simulated after parameter settings in column comp/micr.

The column cost/costus shows simulation values for Costus (Costaceae). Spiromonostichy in the species Costus scaber can be regarded as an unsolved problem for 120 years [27]. The apical dome is enclosed by sickle-shaped bract primordia, which show a lower and a simultaneously developing higher part. The higher part of a given bract overlaps the lower part of a previous bract. In the terms of our model, two spheres of influence define one primordium.

Synthetic phyllotactic shift by gibberellic-acid [32] is simulated (see veg/gibb).

The Lucas sequence (1,3,4,7,11,18,...) is generated under comp/lucas. It is not directly deduceable from the parameter values that Lucas numbers will arise. Appearance of the numbers is caused by an early stacking accident [12].

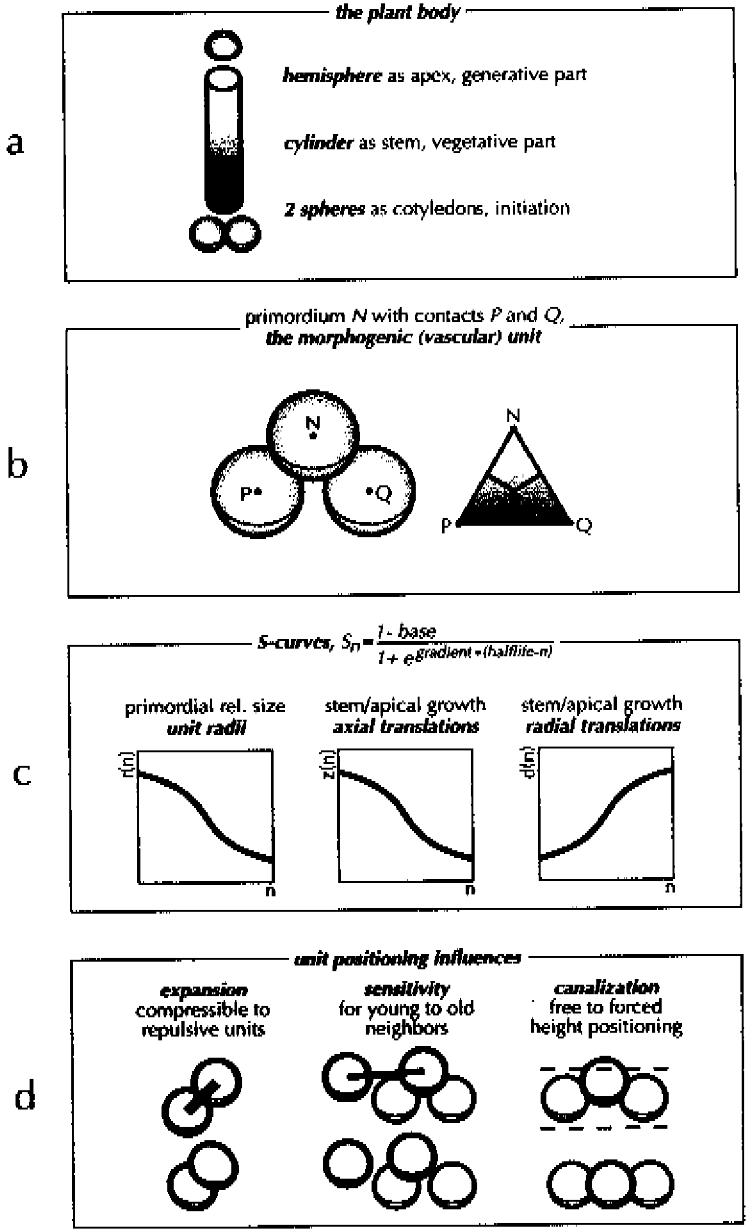

Fig 12 Basics in the Stack and Drag Model. *(a)* The three parts of a plant reflected by the model. *(b)* Two spheres P and Q determine the location of a third one N. Translations determine shape and color of the vascular unit PQN. *(c)* The unit growth curve *(left)* is important for pattern development and the other curves define the receptacle's growth. *(d)* Three pattern defining parameters simulate different levels of interaction between units.

Discussion

The model

The Stack and Drag Model has been built on three basic size/shape principles (fig 12a,b,c):

(i) There are three plant parts: the initiating cotyledons (presented by two spheres), the vegetative stem (presented by a cylinder), and the generative apex (presented by a hemisphere).

(ii) Plant appendages are regarded in relation to internodial stem parts. A primordial unit is always combined with two supporting lower units. Adjoining parts of these three spheres form the vascular unit [38].

(iii) Three interacting S-curves determine the growth of primordia and plant body: one for unit growth, one for axial expansion, and one for radial expansion.

The parameters

Three parameters may be isolated to produce a wide range of recognizable phyllotactic patterns: b determines the minimum relative size of a primordial unit (fig 7), exp gives the compressibility of units, and canal is a measure for the sharpness of the annular dragging zone in which units may arise (fig 12d). Another three parameters are of less importance: h and c determine together with b the path of the S-curve for the size of early primordial units and tls is the number of vegetative units which indirectly defines the unit size just before inflorescence and the unit growth rate.

The drag component

The status of the drag parameter canal is a moot point. As depicted above, in the small physical scale of phyllotactic pattern formation we realized the necessity for a pendant of gravity. We interpreted Buvat's embryonal ring as a zone of pressure from the hypodermic shoot apical meristem on the epidermic layers and combined this with the assumption that outer layers have to follow after central elongation. The biological nature of the drag parameter has to be specified.

Branching

Bud formation will be possible by permitting a structure to branch outside its cylindrical casing. Fractal theories which obtain branching patterns are not satisfying because they lack sufficient biological evidence. An approach might be integrating the L-systems [30] or vice versa. On the contrary, fractal properties should be results like the angle of 137.5° is.

Phyllotaxis and differentiation

The Stack and Drag Model tries to reduce the question of the origin of phyllotaxis to the question of primordial differentiation. What we know about differentiation in a developing living structure is that, given the potential of any embryonic cell to specialize in any adult's organ function, morphological changes of cell clusters are strongly directed by chemical diffusions and physical tensions from their environment. The geometrical orientation of cell clusters in their environment (phyllotaxis) is crucial for the way these influences act upon them [19]. Phyllotaxis is governed by annular differentiation of the apex and after that, differentiation of primordia is governed by phyllotaxis [8].

We may consider physical and chemical forces to indirectly shape the shoot apex including the arising primordia on it. Shape influences differentiations and therefore new initiating points for primordia. If the shape is known and the influence of forces is translated into universal geometrical parameters, a continuation of the process of pattern development can be deduced.

Although the true character of differentiation is still unknown, we do have knowledge of the character of the arising phyllotactic patterns. By reducing the number of parameters to only recognizable geometrical ones, the problems of differentiation and phyllotaxis have been disconnencted. The ***a-b-c-model*** for specification of organ identity in flower development [8,19] seems to link up closely with this conclusion and may be useful in future development of determinate differentiation in the Stack and Drag Model.

Acknowledgements

I like to thank Konrad Bachmann for his push towards the present model and his proof-reading, Johannes Battjes for the feed-back from his observations and interpreting, Roger Jean for the exchange of some opposite thoughts, Lo Camps for his proof-reading, Harry Wagter and Jan Houben for their willingness to support my study.

TABLE I: ***Comparison of parameters (vertical) in the Stack and Drag Model for some structures (horizontal).***

The third row ***(tl)*** shows the number of units on entire structures as calculation results.

	veg			flow					comp				spike	cost	fruit
	dec	***gibb***	***canal***	***8532***	***52***	***333***	***1313***	***wild***	***lucas***	***sun1***	***sun2***	***micr***	***maize***	***costus***	***pinapp***
tl	50	40	113	32	24	16	79	142	55	105	5939	67	311	202	261
tls	50	40	30	10	10	5	20	100	20	20	80	10	*300*	*200*	200
exp	*0.70*	*1.27*	0.50	1.10	1.10	0.80	1.05	1.00	1	1.00	0.95	*0.77*	*1.10*	*1.40*	1.05
sens	0.90	0.96	1.00	0.95	0.95	1.00	0.90	0.96	0.96	1.00	0.98	0.90	0.90	0.95	0.96
canal	0	0.30	*1.00*	*0.70*	*0.85*	*0.58*	*0.65*	0.70	0.50	*0*	*0*	0.20	*0.90*	0	*0.09*
base	1	0.63	0.15	*0.24*	*0.28*	*0.33*	*0.16*	*0.19*	*0.17*	*0.13*	*0.015*	*0.17*	0.42	0.50	0.16
blife	0.52	0.50	0.30	0.60	0.50	0.40	0.50	0.90	*0*	10	0.44	0.80	0.05	*0.15*	*0.05*
const	*0.10*	*-1.22*	*0.17*	*0.49*	*0.69*	*0.69*	0.34	0.22	0.22	*0.27*	*0.07*	0.27	0.17	*0.10*	*0.34*
see fig		*13*		*14*	*15a*	*15b*		*16*	*17*		*18*	*19*		*20*	

tl (-) calculated number of spheres on the cylinder and the hemisphere
tls (-) number of spheres to be constructed on the cylinder
exp (0.5..1..1.5) units are compressible to repulsive
sens (0...1) units are settled with feed back with existing structure to strong sensitivity
canal (0...1) units are stacked (leaning on neighbors) to dragged (by Buvat's ring)
base (0...1) growth function minimum
blife (0...1...) ordinal of unit with 0.5 x stem radius related to ***tls***
const (0...1) growth function steepness

Notes and remarks

veg/***dec*** Decussate leaf positioning with stem torsion caused by the phyllotactic pattern.
veg/***canal*** Strong canalization leads to distinct whorls with many primordia when unit ***const*** is kept small. One of the rings has 16 (doubled Fibonacci number) units.
flow/***1313*** Flower with numeric canalization 13-13-8-5. Units in a canalized ring may show inequality in form and function.
comp/***sun1*** Composite with a low number of florets.
spike/***maize*** Grains are in 5x2 columns.
fruit/***pinapp*** A pineapple is regarded as a thickened stem. Leaves on the fruit are small.

(i) Only pattern defining parameters have been shown.
(ii) ***blife*** may surpass 1. This is due to the definition of ***blife***, being related to the vegetative number of units.
(iii) Combinations of pattern characterising values are printed in italics.
(iv) All patterns have been generated in one-and-the-same single process. All structures have been translated, differentiated, and colored in one single progression. All figures are output of the program *ApexS* and have been drawn after one single command. Pattern calculation speed on a PC (*486/DX-66*) is approximately 60 units per second.

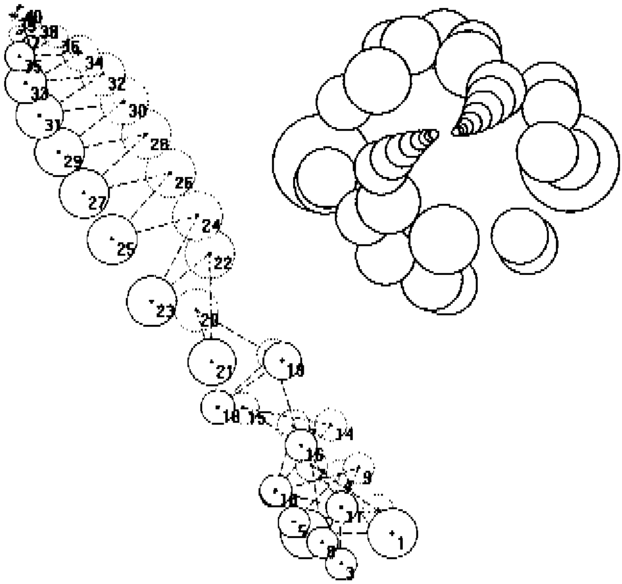

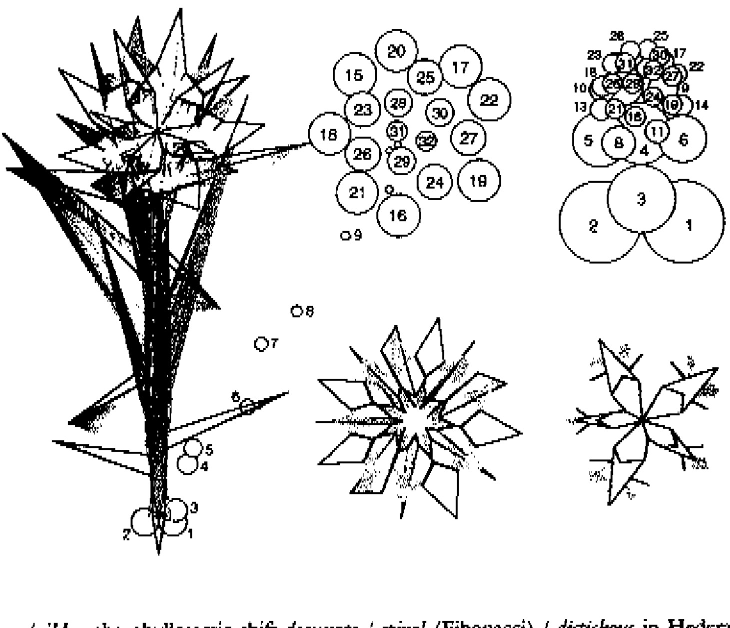

Fig 13 veg/*gibb* - the phyllotactic shift *decussate / spiral* (Fibonacci) / *distichous* in Hedera Helix L. after injection with gibberelin-acid [32]. *(right)* top view of the stacking, with spheres drawn small to show pattern change.

Fig 14 flow/*8532* - flower, showing 8-5-3-2 canalization. Strong canalization with high unit *const* results in a simple flower with distinguishable parts. *(top)* translated polygons/leaves with spheres pattern *(left)* and calculated stacking *(right)*. *(bottom)* top view of the flower parts which are divided between canalization rings. Note that (i) phyllotaxis is decussate near the cotyledons, (ii) sepals, petals, and stamens/carpels show a three-division, and (iii) the flower is singular mirror-symmetrical.

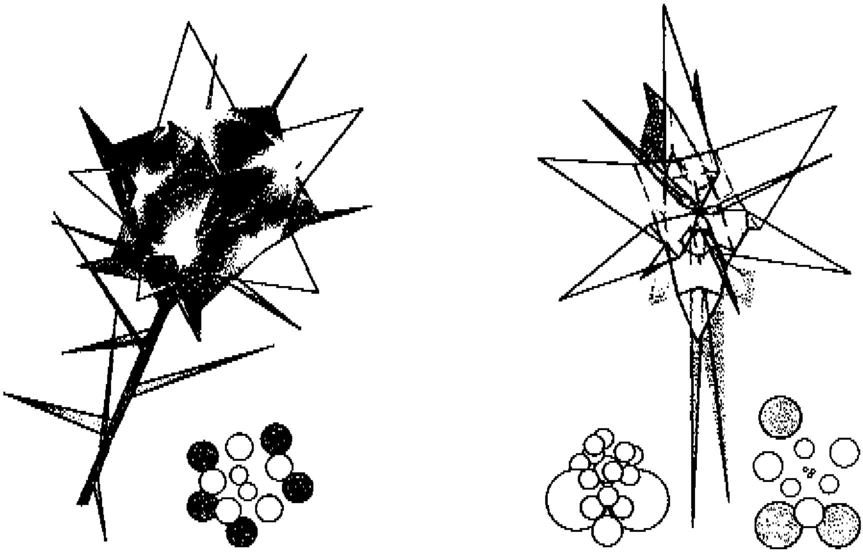

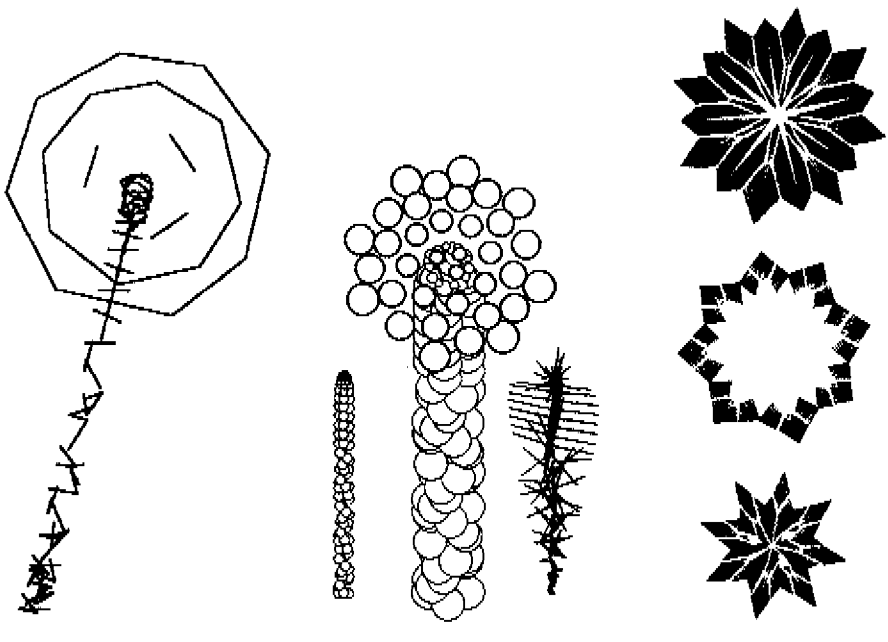

Fig 15 (*a*) flow/52 - 5-2 flower after 10 vegetative units. *(left)* flower scheme after translations of the calculated units. *(b)* flow/333 - 3-3-3 flower after only 5 stem units (cotyledons included) with a total of 16 units. *(left)* calculated untranslated stacking, showing all units. *(right)* scheme, showing the dissimilarity of the four whorls of flower parts, although there may be a 6-petals-symmetry.
Fig 16 flow/*wild* - wild phyllotaxis, with very regular flower. *(left)* connections between units and one of both contacts, showing a stem pattern transition wild-decussate. *(bottom)* calculated stacking, translated spheres, leaves. *(right)* (parts of) sepals, petals, stamens, and carpels.

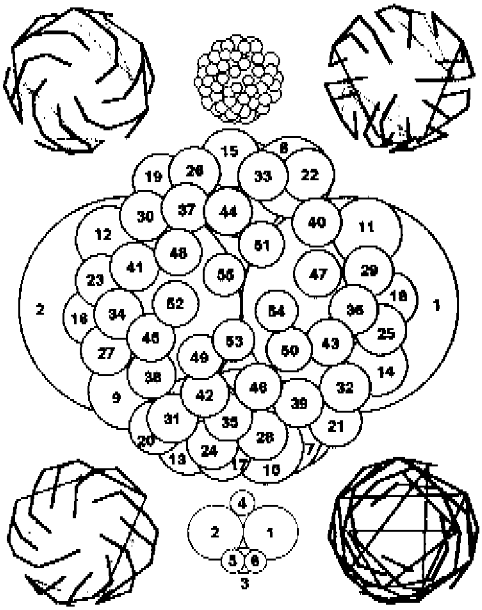

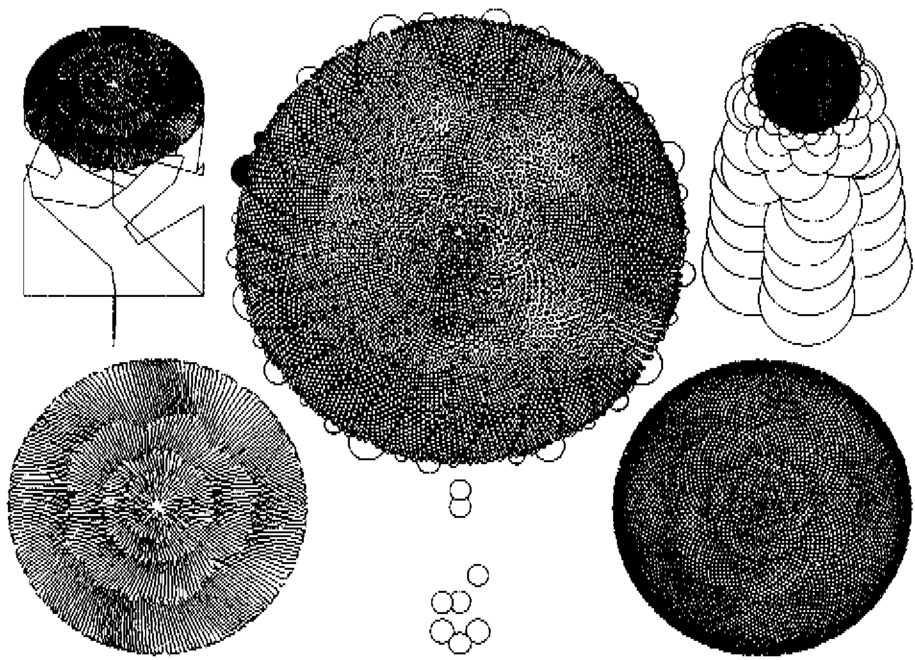

Fig 17 comp/***lucas*** - deviation of the Fibonacci phyllotaxis [12]. ***(center, bottom)*** the early deviation at ***n***=6, which causes the Lucas phyllotaxis. ***(center, top)*** follow-up from ***n***=6. ***(corners)*** connections of centers of units: ***n-p, n-q, n-p(q), p-q***.

Fig 18 comp/***sun2*** - composite with a very high number of florets. ***(left)*** possible vascular pattern: oblique, untranslated, and transparant top view, translated. ***(right)*** calculated spheres packing and top view of flower head with seeds. ***(center)*** axial and radial translations, with every 13th unit highlighted.

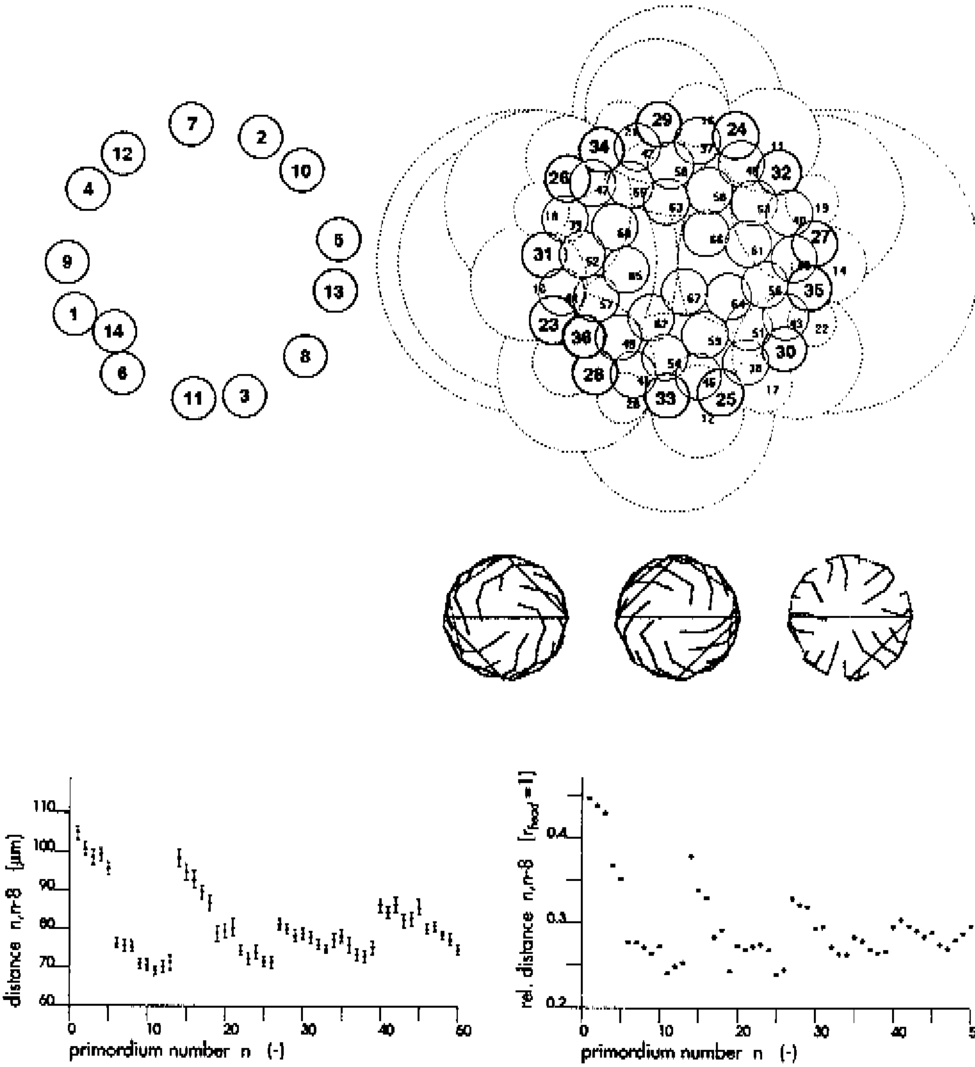

Fig 19 comp/*micr* - topological/graphical results: simulation, compared with observations in flower heads of Microseris pygmaea D. Don [3]. A special problem is the canalization jump after the first annular arrangement of 13 primordia. Observations are compared with simulation results.

(a) topological: canalization jump out of the basical capitulum ring with 13 primordia. *(left)* model according to observations [3]. *(top right)* computed pattern, including (highlighted) 13-ring and canalization jump. *(bottom right)* three patterns with unit centers connected.

(b) graphical: characteristic patterns in threedimensional distances between primordia. *(left)* relations according to observations [3]. *(right)* 3-dimensional distances between units (*n*) and (*n*-8).

Notes: (i) Distances are dimensioned differently; in the model, they are related to the (untranslated) cylinder radius. (ii) The simulation is done for an embryonal stage, so (radial) translations are little. (iii) In order to get optimal approximations the author follows this procedure: Simulating is started by assuming rough values and fine-tunig is done by a trial and error procedure. Once graphs get similar, the characteristic values of the model parameters are known.

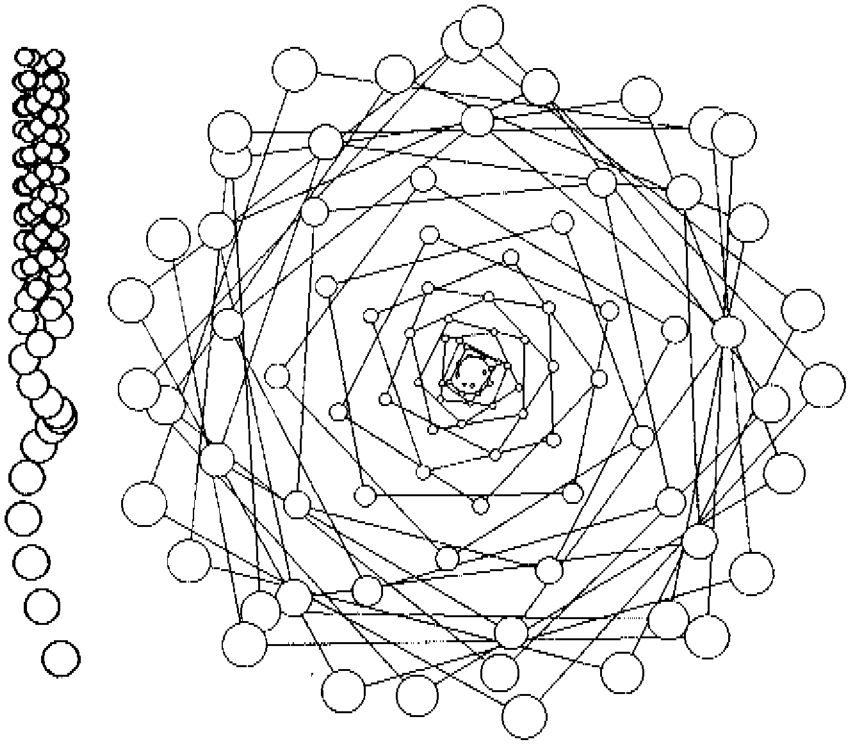

Fig 20 cost/*costus* - small divergence angles; scarcely translated structure showing the small torsion as a phyllotactic, not physiologic, quality in Costus scaber [27]. Because of it's embracing sickle shape, a primordium is defined here by two units. *(right)* schematic presentation with connections between centers of subsequent units. Note that always one of both near lower units is not a direct contact.

Footnotes

(1) A structure grows gnomonically, if it keeps its form during the process. An example is shown by the snail which grows its shell by secreting ever larger amounts of chitin on the open side of the helical tube [54]. A more basic example is the planar stacking of growing circles from a center outwards. Every circle is constructed against its predecessor in the same rotation direction around the initial circles. The result is a simple spiral of circles with increasing size. The Dislodgement Model [52,53] obeys a slightly more complicated mechanism. Every new circle is initially constructed in a consequent position in relation to its predecessor. The structure's disc shape is maintained by adjusting locations when neighboring circles should intersect the new one.

(2) The Stack and Drag Model resembles the Dislodgement Model but has more biological justification because it shows (i) a stacking from base to top, (ii) a predefined transition vegetative-generative stage, and (iii) restricted settling of primordia in a zone.

(3) Filling surfaces and bodies with circles and spheres has an long tradition which can be traced back to Plato, Archimedes, Kepler, Kelvin.

(4) Phyllotaxis shows an important phenomenon: different species may show the same phyllotaxis, and within a species or even an individual plant, different but stable phyllotactic patterns are possible. This indicates a geometric constraint to have dominance over differentiation determining forces. An example of species overriding geometry is the ubiquity of Fibonacci numbers with typical anomalies like the Lucas numbers. In cases, where phyllotaxis is unstable, the geometric constraint may be subsidiary to genetic or environmental variations.

(5) Just below the apical tip lies a central cell region with relatively low mitotic activity: the 'mother cells' [31] or the 'méristème d'attente' [6,36,39]. This region is accompanied with another hypodermic one with high mitotic activity in which primordia are initiated (Buvat's 'anneau initial'). Its annular shape causes canalization. In flowers, stamen and carpel primordia are initiated in a spiral sequence, e.g. Ranunculus acris [33].

(6) The Stack and Drag computer program is not only capable of producing images of the stacking-iterations during calculation and the calculation results but also shows the growth process from cotyledons expanding to flowering adults.

(7) The vegetative apex promotes longitudinal growth and the reproductive apex produces a meristematic envelop with a large surface area from which the parts of a flower or flowers develop [37]. The transition vegetative to reproductive apex is gradual [14].

(8) Many characteristics of flowers are related to the phyllotaxis of floral organs [14].

(9) The S-Curve is defined by parameters b (minimum), h (halflife), and c (gradient).

S-Curve: $$S_n = (1-b) / (1+e^{c(h-n)})$$

in which n is ordinal number, e=2.71828... (the Euler number), b is base or minimum of relative sphere radius, h is halflife or the ordinal of the sphere with radius 0.5, c is growth constant or gradient. A unit, defined as a primordium or sphere of influence including primordium forming cells, is represented as a sphere with its center on a cylindrical or hemispherical receptacle with radius 1.

Unit Radii: $R_n = 1 - S_n$

(10) In the Dislodgement Model, checks are needed to trace units as intersecting candidates [52,53]. The Stack and Drag Model uses some of these checks and decides which one of the support units has to be dislodged. If $p=p(n)$ and $q=q(n)$ are the ordinals of the support units of unit(n), then (i) unit(p) may be replaced by one of the following units with ordinals $p+n-q$, $q+q-p$, $p+q-n$, $p(q)+n-q$, $p(p)+n-p$, and (ii) unit(q) may be replaced by one of the units with ordinals $q+n-p$, $p+p-q$, $q+p-n$, $q(p)+n-p$, $q(q)+n-q$.

(11) The expansion factor declines downwards along the receptacle. One of the consequences is that misplacement of units caused by the static character of unit configurations in the simulation is neutralized [4]. High sensitivity means, that only the location of the upper spheres predict the settling of a new sphere. Low sensivity means, that lower spheres on the cylinder influence the settling of a new sphere. Strong canalization is caused by a narrow placement zone.

(12) Translation depends on unit ordinal or age, n, but also on distance to Z-axis, d, and on height from *XY*-plane, z. Stem growth causes shifting in the phyllotactic pattern. Translations follow the S-curve *(fig 7)*, being a function of n, but also of z or d, respectively.

Axial Translations: $Ax_n = (1-S_n) \, . \, z_n^{LinkZ}$

in which z_n is relative height ($0<=z_n<=1$) and *LinkZ* causes displacements to depend on n to z_n ($0<=LinkZ<=10$). Parameter *LinkZ* leaves the dependence open for there is no evidence to exclude either n or z. Note that axial translations and unit sizes use similar graphs, when *LinkZ*=0.

Radial Translations: $Rad_n = S_n \, . \, d_n^{LinkD}$

in which d_n is relative distance ($0<=d_n<=1$) and *LinkD* causes displacements to depend on n to d_n ($0<=LinkD<=10$). Notice, that radial translations and unit sizes use horizontally mirrored graphs, when *LinkD*=0.

(13) For defining leaf and internode as one unit, see also the ***'leaf-skin model'*** and the ***'phytonic model'*** in [44].

(14) The computer program *ApexS*, which generates patterns and structures, is sized approximately 400 KByte. It runs in the *Windows-3.1* environment of personal computers.

References

(1) I. Adler, A Model of Contact Pressure in Phyllotaxis, J. Theor. Biol. 45:1-79 (1974).

(2) J. Battjes and F.M.J. van der Linden, Positioning of Primordia on Early Flower Heads of Microseris Pygmaea: A Comparision of SEM's and Simulations by the Dislodgement Model, unpublished results (1992).

(3) J. Battjes, N.O.E. Vischer, and K. Bachmann, Capitulum Phyllotaxis and Numerical Canalization in Microseris Pygmaea, Am. J. Bot. 80(4):419-428 (1993).

(4) J. Battjes, thesis, Amsterdam Univ. (1994), pp.43,44,110-122.

(5) D.W. Bierhorst, On the Stem Apex, Leaf Initiation, and Early Leaf Ontogeny in Filicalean Ferns, Am. J. Bot. 64(2):125-152 (1977).

(6) R. Buvat, Structure, évolution et functionnement du méristème apical de quelques dicotylédones, Ann. Sci. Nat. Bot. 11.13:199-300 (1952).

(7) A.H. Church, The Principals of Phyllotaxis, Annals of Bot. 18:227-243 (1904).

(8) E.S. Coen and E.M. Meyerowitz, The War of the Whorls: Genetic Interactions Controlling Flower Development, Nature 353:31-37 (1991).

(9) H.S.M. Coxeter, Regular Polytopes, Dover, New York (1963).

(10) R. Dixon, The Mathematical Daisy, New Scientist 17:792-795 (1981).

(11) S. Douady and Y. Couder, Phyllotaxis as a Physical Self-Organized Growth Process, Phys. Rev. Lett. 68(13):2098-2101 (1992).

(12) P.K. Endress, Patterns of Floral Construction in Ontogeny and Phylogeny, Biol. Journ. Linnean Soc. 39:153-175 (1990).

(13) R.O. Erickson, The Geometry of Phyllotaxis, in The Growth and Functioning of Leaves, J.E. Dale and F.L. Milthorpe, Eds., Cambr. Univ. Press (1983), pp.53-88.

(14) A. Fahn, Plant Anatomy - 4th ed., Pergamon Press, Oxford (1990), pp.65,413.

(15) C. Goodall, Eigenshape Analysis of a Cut-Grow Mapping for Triangles, and its Application to Phyllotaxis in Plants, SIAM J. Appl. Math. 51(3):775-798 (1991).

(16) P.B. Green, Surface of the Shoot Apex: a Reinforcement-Field Theory for Phyllotaxis, Journ. of Cell Sci. Suppl. 2:181-201 (1985).

(17) P.B. Green, A Theory for Inflorescence Development and Flower Formation based on Morphological and Biophysical analysis in Echeveria, Planta 175:153-169 (1988).

(18) W.A. Van Heel, Androecium Development in Actinidia Chinesis and A. Melanandra (Actinidiaceae), Bot. Jahrb. Syst. 109:17-23 (1987).

(19) J. Heslop-Harrison, Sex Expression in Flowering Plants, Brookhaven Symp. Biol. 16:109-125 (1964).

(20) L.F. Hernandez and J.H. Palmer, Regeneration of the Sunflower Capitulum after Cylindrical Wounding of the Receptacle, Am. J. Bot. 75:1253-1261 (1988).

(21) G.S. Hicks and I.M. Sussex, Development In Vitro of Excised Flower Primordia of Nicotiana Tabacum, Can. J. Bot. 7:133-139 (1970).

(22) M. Hirmer, Zur Kenntnis der Schraubenstellungen im Pflantzenreich, Planta 14:132-206 (1931).

(23) W. Hofmeister, Allgemeine Morphologie der Gewächse, Engelmann, Leipzig (1868).
(24) R.V. Jean, Mathematical Approach to Pattern and Form in Plant Growth, Wiley-Interscience, N.Y. (1984).
(25) R.V. Jean, A Basic Theorem on and a Fundamental Approach to Pattern Formation on Plants, Math. Biosci. 79(2):127-154 (1986).
(26) W.L. Kilmer, On Growing Pine Cones and other Fibonacci Fruits - McCulloth's Localized Algorithm, Math. Biosci. 11:53-57 (1971).
(27) B.K. Kirchoff and R.Rutishauser, The Phyllotaxy of Costus (Costaceae), Bot. Gaz. 151(1):88-105 (1990).
(28) P.P. Larson, Development and Organization of the Primary Vascular System in Populus Deltoides According to Phyllotaxis, Am. J. Bot. 62:1084-1099 (1975).
(29) P.P. Larson, Vascularization of Developing Leaves of Gledistsia Triacanthos, Am. J. Bot. 71:1201-1220 (1984).
(30) A. Lindenmayer, Development Algorithms: Lineage versus Interactive Control Mechanisms, in Development Order: Its Origins and Regulation, S. Subtelny and P.B. Green, Eds., Alan R. Liss, N.Y. (1982), pp.219-245.
(31) R.F. Lyndon, The Shoot Apex, in Cell Division in Higher Plants, M.M. Yeoman, Ed., Acad. Press, London (1976), pp.285-314.
(32) J. Marc and W.P. Hackett, Gibberellin-induced reorganization of Spatial Relationships of Emerging Leaf Primordia at the Shoot Apical Meristem in Hedera helix L., Planta 185:171-178 (1991).
(33) R.D. Meicenheimer, Relationships between Shoot Growth and Changing Phyllotaxy of Ranunculus, Am. J. Bot. 66(5):557-569 (1979).
(34) G.J. Mitchison, Phyllotaxis and the Fibonacci Series, Science 196:270-275 (1977).
(35) K. Miyazaki, An Adventure in Multidimensional Space, John Wiley and Sons (1986).
(36) A. Nougarède, Organisation et functionnement du méristème apical des végétaux vasculaires, in Travaux Dédiés au Lucien Plantefol, Masson et Cie, Paris (1965).
(37) W.R. Philipson, The Ontogeny of the Shoot Apex in Dicotyledones, Biol. Rev. 24:21-50 (1949).
(38) G.A. Pieters and M.E. Van der Noort, The Morphogenic Unit: The Essence of Morphogenesis, Dept. of Plant Physiol. Research, Agricult.University Wageningen (The Netherlands), manuscript (1978).
(39) L. Plantefol, Hélices Foliaires, Point Végétatif et Stèle chez les Dicotylédones. La Notion d'Anneau Initial., Rev. gén. Bot. 54:49-80 (1947).
(40) P. Prusinkiewicz and A. Lindenmayer, The Algorithmic Beauty of Plants, Springer Verlag (1990), pp.99-118.
(41) F.J. Richards, Phyllotaxis: It's Quantitative Expression and Relation to Growth in the Apex, Philos. Transact. of the Royal Soc. of London B235:509-564 (1951).
(42) P.H. Richter and R. Schranner, Leaf Arrangement: Geometry, Morphogenesis, and Classification, Naturwissenschaften 65:319-327 (1978).
(43) D.W. Roberts, A Contact Pressure Model for Semi-Decussate and Related Phyllotaxis, J. Theor. Biol. 68:583-597 (1977).

(44) R. Rutishauser and R. Sattler, Complementarity and Heuristic Value of Contrasting Models in Structural Botany 1, Bot. Jahrb. Syst. 107:415-455 (1985).
(45) J.C. Schoute, Beiträge zur Blattstellungslehre, Réqueil des Traveaux Bot. Neérlandais 10:153-324 (1913).
(46) O. Schüepp, Konstruktionen zur Blattstellungstheorie, I, Berichte der Deutsche Bot. Gesellschaft 41:255-262 (1923).
(47) S. Schwendener, Mechanische Theorie der Blattstellungen, Leipzig (1878).
(48) R.H. Smith and T. Murashige, In Vitro Development of the Isolated Shoot Apical Meristem of Angiosperms, Am. J. Bot. 57:562-568 (1970).
(49) M. Snow and R. Snow, On the Determination of Leaves, New Phytol 46:5-19 (1947).
(50) d'Arcy W. Thompson, On Growth and Form, Cambr. Univ. Press, London (1917), pp.759-766.
(51) J.H.M. Thornley and K.E. Cockshull, A Catastrophe Model for the Switch from Vegetative to Reproductive Growth in the Shoot Apex, Ann. Bot. 46:333-341 (1980).
(52) F.M.J. Van der Linden, Creating Phyllotaxis: The Dislodgement Model, Math. Biosci. 100(2):161-199 (1990).
(53) F.M.J. Van der Linden, The Dislodgement Model Improved, manuscript (1994).
(54) F.M.J. Van der Linden, Phyllotactic Patterns for Domes, Int. J. Space Structures 9(1):9-19 (1994).
(55) G. Van Iterson, Mathematische und Mikroskopisch-Anatomische Studien über Blattstellungen, Gustav Fischer Verlag, Jena (1907).
(56) H. Vogel, A Better Way to Construct the Sunflower Head, Math. Biosci. 44:179-189 (1979).
(57) R. Williams, The Geometrical Foundation of Natural Structure, Dover Publications, N.Y. (1979).
(58) R.F. Williams and E.G. Brittain, A Geometric Model of Phyllotaxis, Austr. J. Bot. 32:43-72 (1984).
(59) L. Wolpert, The Shape of Things to Come, New Scientist June:38-42 (1992).

5 SUMMARY / INFERENCES

THE STATE OF THE ART IN BIOLOGY

Until now, one had to rely on secondary phenomena to explain phyllotactic patterns.I will name three in particular:
(i) Certain consequences (e.g. the mean angle between 2 consecutive primordia on a flower head) of an unknown mechanism were the starting points of a synthesis. An explanation was then sought through intuitive assumptions in hereditary characteristics.
(ii) The Lucas sequence was, along with other sequences, perceived as the consequence of a peculiar phyllotaxis rather than an abberation of the Fibonaccian phyllotaxis.
(iii) A canalized capitulum, whereby primordia are generated in rings of similar elevation, was based on a first canalized ring.

(The conformity in each of these 3 deviations is: a configuration is not stored as such in genetic material. What we, as humans, consider to be forms are the more or less consistent results of blind processes, however 'stunning' and impressive those may be.)

Especially among geometrists, computer-controlled generators are designed. For those however, the following shortcomings can be mentioned:
(i) a separated approach for 2- and 3-dimensional structures
(ii) the impossibility of varying the size of the elements
(iii) the impossibility of Nature related abberations
(iv) an uncompromising bond to an exact, fictitious angle that in Nature only occurs as a mean angle.

GENERAL EXAMINATION OF THE NEW THEORIES

The Dislodgement Model stems from the principle of reversal, meaning that stacking starts at the top of a receptacle which will then gradually be covered. The results of this kind of pattern development are strongly in line with published results (e.g. J. Battjes and F.M.J. Van der Linden, unpublished results, with examples in this thesis). However, the reveral is unnatural. Many biologists therefore feel that this stacking principle is not acceptable. The Dislodgement Model (like all published models to date) furthermore does not include the phenomenon of canalization. Finally, although an approach to flowering patterns has been incorporated in the improved version of the Dislodgement Model, this model essentially generates only vegetative patterns.

The Stack and Drag Model neutralizes these shortcomings. Important is that close-packings, even in composites, are hardly found. This indicates a drag component in the pattern development. In other words, primordia do not initiate at low levels, but are generated within a certain annular zone which is continuously dragged upwards behind the apex.

Morpho-biological examination of the theories

Below, each of the models will be examined and tested for applicability in building, both architectonically and constructively, and for their different meaning for dome shaped buildings. In the Dislodgement Model, a convex surface (in this case the apex of a composite) becomes filled with units. These units arise from, respectively dislodge one another from, a growth center. In the Stack and Drag model, not a growth center (or top) is the starting point of a dome stacking, but a basis (or periphery). Not the structure lying beneath this basis, but the basis itself is essential for pattern development above.

Phyllotaxis is 'superficial'.

Biologists do not unanimously agree on the statement that *"In a developing plant, pattern formation takes place from the structure's surface."* Nevertheless, I think that the biological significance as depicted in 'Creating Phyllotaxis: The Stack and Drag Model' may help understanding the character of phyllotactic pattern formation. What then is the analogy between phyllotaxis and constructional work? An application of the knowledge about biological patterns will be literally superficial. Like Nature employs a thin, non-constructional layer, so building phyllotactic patterned domes should deal with wrapping, not with mechanical construction. Thus the impact of the phyllotaxis theories would likely be confined to (decorative) architecture, so we should be conservative in conclusions towards applications in (supportive) constructions. Furthermore, we confine ourselves to paraboloids and hemispheres as (apical) tips or domes.

Categorizing domes by distinguishing element types

Thesis: 'Phyllotactic patterns show a hierarchical build-up.'

(i) In vegetative, scarcely canalized structures, there is no hierarchy at all (Fig 1).
(ii) In composites, groups of stacked primordia may form sharply defined geometrical figures. Both in Nature as in the Dislodgement Model (and in the Stack and Drag Model in the case of canalization factor 0), these figures are clearly visible. Since these semi-regular polygons are repeated in a (6-) rotation symmetry, a secondary pattern arises (Fig 2).
(iii) In singular flowers with strong canalization, rings of units are formed. This phenomenon is coupled with differentiations in sepals, petals, stamens and carpels. There is no prove, but most investigators agree with the assumption that, besides genetic factors, chemical hypodermic messages determine the ring's qualities (see 'Creating Phyllotaxis: The Stack and Drag Model'), so we may state that the ring plays has a vital significance in primordial initiation and development. The Stack and Drag Model generates patterns on the basis of controlled stacking, which means that units are placed within certain limits. (The Dislodgement Model lacks the possibility to design singular flowers.) In biology the mechanism behind this limitation is called canalization. Canalization can be understood by means of the following thought-experiment. Depart from a cylinder, rounded with a hemisphere (see 'Creating Phyllotaxis: The Stack

AND DRAG MODEL', Figs 3, 4, 6, and 10). Within the hemisphere is a zone from where new cells generate and differentiate: the mothercells. New organs arise in the apex (shoot tip, the hemisphere) of the stem (the cylinder). They do not arise at the apical tip but at the surfacial ring-shaped edge of the aforementioned zone. The tip of the rounded cylinder is therefore not the center of origin of units. This point will have to be pulled apart to create a ring from which new units may arise. The strip-width of the ring can vary from wide to small. A small ring results in strong canalization (Fig 3).

CONCLUSIONS RELATING TO BUILDING CONSTRUCTION

Based on the aforementioned categories of element types in the hierarchical construction of phyllotactic patterns, we can now relate their significance to building applications:

(i) Building elements are directly derived from phyllotactic units.

(ii) Building elements are clusters of smaller, phyllotactic units in that these units are gathered in larger, semi-regular polygons (trapezoids and rhomboids). Under the condition of a constant unitradius application is possible. To achieve this in the Dislodgement Model, unit radii have to be independent from the local receptacle radius (see 'THE DISLODGEMENT MODEL IMPROVED' for the variable in question). The Dislodgement Model indeed uses paraboloid receptacles, but this receptacle's shape is not a dominant phyllotaxis determining factor (see also reference Meicenheimer). Other receptacles, such as the hemisphere and the chainline-rotated dome are as much possible, with similar results.

(iii) Building elements are derived from ringshaped units. Strong canalization results in an equable basis for the hemisphere (dome). Additional stacking furthermore provides strong structural uniformity by rings which arise with decreasing numbers of units (often according to the Fibonacci-sequence). The unitradii decrease towards the tip. The total number of phyllotactic units on the dome can be relatively low, for instance 50. For dome-designs we use the hemisphere or any other convex receptacle, not the cylinder.

In living organisms, growth is achieved by replacing and adding amounts of material. On early flower heads, these amounts seem to be bundled in hemispherical units which are then stacked in (phyllotactic) patterns. In fact, these units are shaped and developed by differentiation and growth of outer cell layers. Both the Dislodgement Model and the Stack and Drag Model combine structural expanding with unit stacking (see 'PHYLLOTACTIC PATTERNS FOR DOMES').

A building arises through an essentially different kind of growth process, yet the stackingmodels can be used. First, phyllotactic patterns maintain their order after their genesis; unit positions are freezed to topologically rigid patterns. In general, this means that phyllotactic patterns are independent from structural growth. Secondly, the freedom in exploration that these models offer results in a very wide range of patterns since parameters that in Nature can never go beyond certain threshold values, are now open to experimentation. For instance: instead of a natural growth curve, a constant value or a shrink function can be applied.

Conclusions derived from phyllotaxis development span the gap between traditional building techniques and (for now) experimental constructions, junction details, and methods for engineering. For the first time, building engineers have at their disposal a methodology inspired by green Nature to fill a given dome-surface with elements of predescribed dimensions. The objective is to reach an optimum in density, regularity, and beauty. The designer uses one of the CAD-programs *ApexD* and *ApexS* with an input of biologically recognizable variables like:

(i) the mantle-surface's shape (for example hemisphere, flat plane, cone, paraboloid)
(ii) the close-packing element's shape (for example circle-disc, comb, rectangle, rhomb)
(iii) the intercellulars' shapes (depending on the element form and size or vice versa)
(iv) the element's size (for example constant, or according to a possibly irregular course)
(v) the geometric relations between elements (for example connected centers).

SOFTWARE

The programs *ApexD* and *ApexS* provide projections of three-dimensional structures and numeric and graphic results. These are the first generators of this kind and systematic biologists will recognize the parameters used. The programs can have architectonical (or at least decorative) or constructional (structural) implications. The software which has been developed in ***Visual Basic for MS-Windows*** is very compact and will run on a personal computer in the ***MS-Windows*** environment. Results can be downloaded in packages as ***AutoCAD*** and ***3D-Studio***.

UTILISATION

The building practice needs simple methodologies for the production of elements. Phyllotactic structures provide these through building elements that are derived from spheres of influence like rounds. The specific (gnomonic) ordening of these building elements produces fractal structures, resulting in an application of a fractal theory in building practices. Potential interested parties can be found among commissioners of middlesized to large dome-like constructions and manufacturers of light concrete elements in light supporting-constructions.

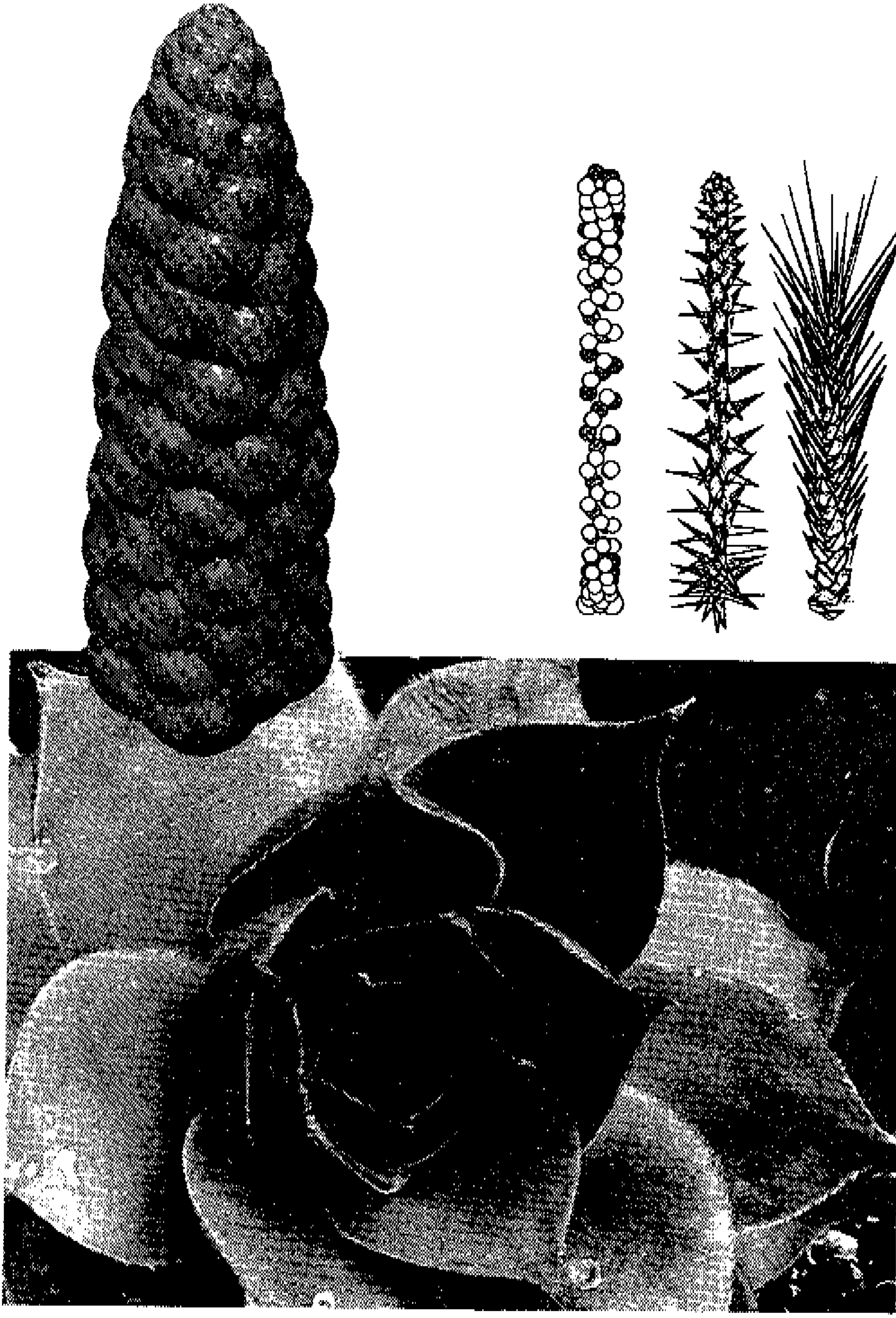

Fig 1 *(top left)* Top-down spheres stacking according to the Dislodgement Model.
(top right) Bottom-up vegetative spheres stacking in the Stack and Drag Model and two manifestations.
(photograph) Vegetative plant structure.

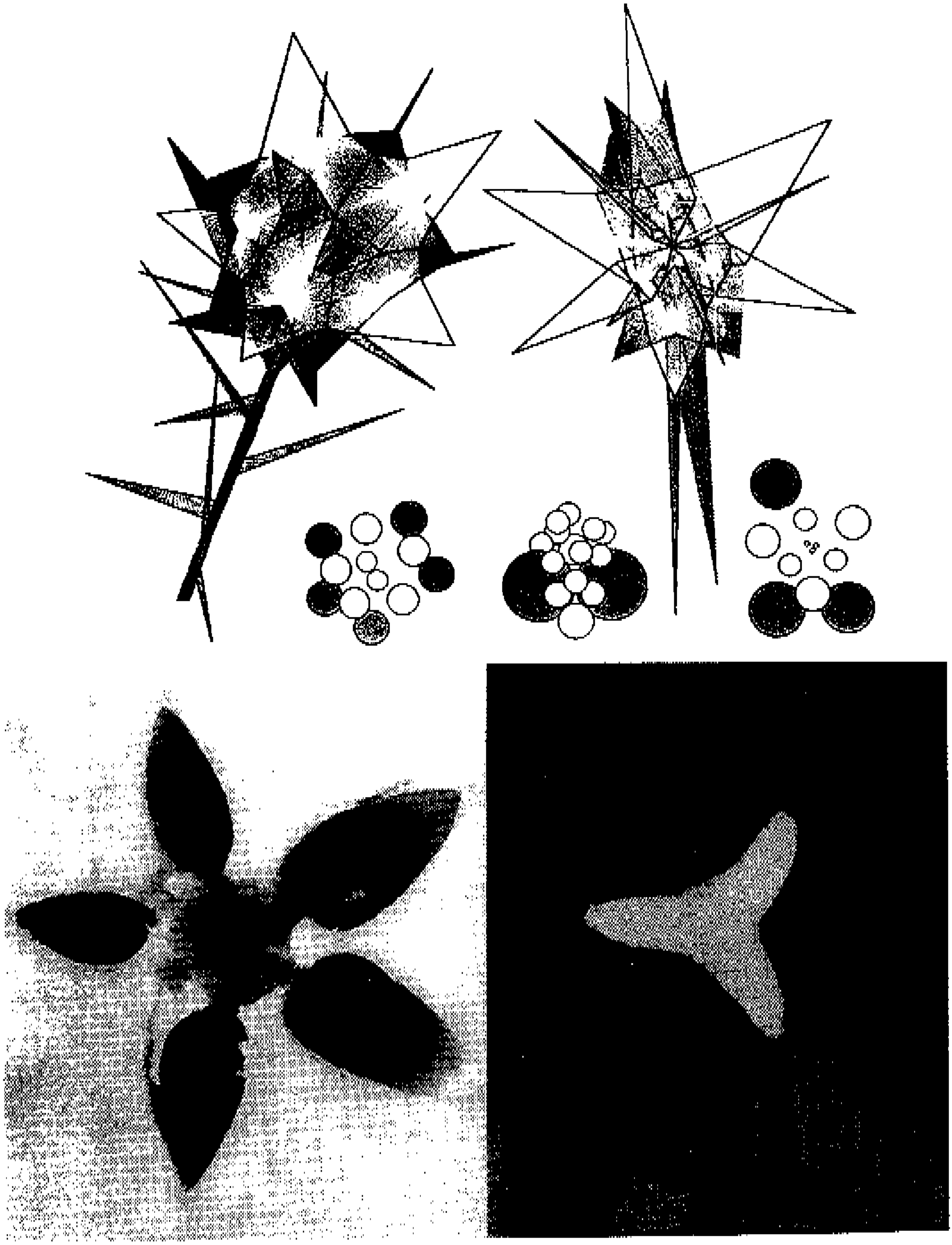

Fig 3 ***(top)*** Flower structures *52* and *333* (see chapter 4 on the Stack and Drag Model and appendage iv 'RESULTS'). A six symmetry can be regarded as a repeated three symmetry. Flowers show characteristic conversions of rings with 8, 5, 3, and 2 parts. The Stack and Drag Model simulates these easily.
(photographs) Fruit and flower core with 5 and 3-3-3 ring symmetry, respectively.

5 SAMENVATTING / GEVOLGTREKKINGEN

De stand van zaken in de biologie

Tot op heden was men voor het verklaren van de onderzochte patronen gehouden aan secundaire verschijnselen. We noemen er drie.
(i) Zekere gevolgen van een mechanisme (zoals de gemiddelde hoek tussen twee na elkaar ontstane primordia, in zekere patronen) lagen aan het startpunt van een synthese. Men zocht naar verklaringen, door intuïtieve aannames te doen in overerfelijke eigenschappen.
(ii) De Lucasreeks werd -samen met andere optredende reeksen- gezien als het gevolg van een bijzondere phyllotaxis, in plaats van als een afwijking van de Fibonacci-phyllotaxis.
(iii) Een bloemhoofd met canalisatie, waarbij primordia ontstaan in ringen van gelijke hoogte, werd geconstrueerd met als uitgangspunt een eerste, gecanaliseerde ring.

(Overeenkomst tussen deze drie dwalingen is: een vorm is niet als zodanig in erfelijk materiaal opgeslagen. Wat wij, als mensen, als vormen beschouwen, zijn min of meer consistente resultaten van blinde processen, hoe 'mooi' en indringend die resultaten ook mogen zijn.)

Vooral onder geometrie-onderzoekers vindt men modellenmakers, die komen tot computergestuurde generators. Echter, hier kan men de volgende beperkingen noemen:
(i) gescheiden benadering voor 2- en 3-dimensionale structuren
(ii) onmogelijkheid van variatie in grootte van elementen
(iii) onmogelijkheid van (met de natuur verwante) afwijkingen
(iv) starre binding aan een exacte, fictieve hoek, die in de natuur slechts voorkomt als gemiddelde hoek.

Algemene beschouwing van de nieuwe theorieën

Het Verdringingsmodel gaat uit van een omkering, ofwel: een stapeling start in de top van een te bedekken manteloppervlak. Het resultaat van patroonontwikkelingen vertoont sterke overeenkomst met gepubliceerde waarnemingen, echter de methode is tegennatuurlijk. Daarom is de omkering voor vele biologen niet acceptabel. Voorts omvat het model (zomin als alle totdantoe gepubliceerde modellen), het verschijnsel canalisatie niet. En tenslotte, samenhangend met genoemde tekortkomingen, genereert het model in principe uitsluitend vegetatieve patronen. Overigens, in de verbeterde versie is een benadering van bloeipatronen ingebouwd.

Het Stapel- en TrekModel heft de feilen op. De stapeling voltrekt zich opwaarts vanaf twee bollen (zaadlobben) als basis. Belangrijk uitgangspunt is, dat maximaal-dichte stapelingen, zelfs in composieten, nauwelijks worden waargenomen. Dit duidt op een trek-aandeel in de patroonontwikkeling. Hiermee wordt bedoeld: primordia ontstaan niet laag op de structuur, maar worden binnen een zekere ringvormige zone gevormd. Deze zone wordt voortdurend opwaarts getrokken, achter de apex aan.

Morfo-biologische beschouwing van de theorieën

Hierna worden beide modellen beschreven naar en getoetst op enerzijds de toepasbaarheid in het bouwen, architectonisch en constructief, anderzijds de verschillen in betekenis voor het bouwen.In het Verdringingsmodel wordt een convex oppervlak (in dit geval de apex van een composiet) gesloten met elementen. Deze elementen ontstaan in, respectievelijk verdringen elkaar vanuit, een groeikern.In het Stapel- en Trek-model is in plaats van een groeikern (de top of het centrum) een contour (de basis of de periferie) het vertrekpunt van een dome-stapeling. Overigens is de basis zelf - niet de voorgeschiedenis ervan - voor de verdere patroonontwikkeling essentieel.

Phyllotaxis is 'oppervlakkig'.

Biologen zijn niet eensgezind in de uitspraak *"In een zich ontwikkelende plant vindt patroonvorming plaats vanuit de oppervlakte van de structuur."*. Niettemin ben ik van mening, dat de biologische verantwoording, zoals het Stapel- en Trek-model die biedt, het karakter van phyllotactische patronen inzichtelijker maakt. Vervolgens kunnen we een analogie met het bouwen afleiden. Een toepassing zal letterlijk oppervlakkig zijn. Zoals het in de natuur gaat om een dun, niet constructief-structureel laagje, zal het in het bouwen gaan om bekleden en niet om construeren. Aldus is de impact van de theorieën waarschijnlijk beperkt tot architectuur en moeten we terughoudend zijn in conclusies richting constructieve toepassingen. Daarbij komt, dat we ons beperken tot (apicale) toppen, of domes.

Categorisering van domes door onderscheid in element-types

These: "Phyllotactische patronen vertonen een hiërarchische opbouw."

(i) In vegetatieve, weinig gecanaliseerde structuren is er van een hiërarchie geen sprake (Fig 1).

(ii) In composieten kunnen groepsgewijs gestapelde primordia scherp afgebakende geometrische figuren vormen. Zowel in de natuur als in het Verdringingsmodel (en in het Stapel- en Trek-model bij canalisatiefactor=0) zijn deze figuren duidelijk waarneembaar. Omdat de geometrische figuren zich hier herhalen in een (6-)rotatiesymmetrie, ontstaat een secundair patroon (Fig 2).

(iii) In enkelvoudige bloemen met sterke canalisatie worden kransen gevormd. Dit gaat gepaard met differentiaties als kelkbladen, kroonbladen, meeldraden en stampers. Er is geen bewijs, maar de meeste onderzoekers delen de aanname, dat, naast overerfelijke factoren, chemische, hypodermische boodschappen de eigenschappen van de ring bepalen (zie 'Creating Phyllotaxis: The Stack and Drag Model'). We kunnen dus stellen, dat de ring van vitaal belang is voor wat betreft ontstaan en ontwikkeling van primordia. Het Stapel- en Trek-model genereert patronen op basis van geleide stapeling, wat wil zeggen, dat elementen kunnen worden geplaatst binnen zekere grenzen. (Binnen het Verdringingsmodel zijn enkelvoudige bloemen niet gedefinieerd.) In de biologie wordt het mechanisme achter deze beperking canalisatie genoemd. Canalisatie kan worden begrepen via het volgende gedachtenexperiment. Ga uit van een met een halve bol afgeronde cilinder (zie 'CREATING PHYLLOTAXIS: THE STACK AND DRAG MODEL', Fig 3, 4, 6 en 10). Binnen de halve bol ligt een zone, waarvanuit nieuwe cellen worden gevormd en gedifferentieerd: de moedercellen. Nieuwe organen ontstaan in de apex (groeitop, de halve bol) van de stengel (de cilinder). Ze ontstaan niet in een punt, maar aan de rand van de genoemde zone. Het toppunt van de afgeronde cilinder is dus niet het ontstaanspunt. Dit punt moet uiteen worden getrokken om een ring te krijgen, waar nieuwe elementen kunnen ontstaan. De strook-breedte van de ring kan ruim tot iel zijn. Een iele ring heeft sterke canalisatie tot gevolg (Fig 3).

CONCLUSIES VOOR HET BOUWEN

Overeenkomstig de categorisering boven behandeld, kunnen we voor bouwkundige toepassingen een onderscheid maken:

(i) Bouwelementen zijn direct afgeleid van phyllotactische eenheden.

(ii) Bouwelementen zijn clusters van kleinere, phyllotactische eenheden - dus: units van het model worden samengenomen tot grotere, halfregelmatige vormen (trapezia en parallellogrammen). Voorwaarde voor toepassing is een constante elementradius. Om dat in het geval van het verdringingsmodel te bereiken, moeten elementradii tevens onafhankelijk zijn van de dragerradius ter plaatse (zie voor de variabele in kwestie het Verdringingsmodel). Het verdringingsmodel gebruikt weliswaar paraboloïde mantels, maar de mantelvorm is geen dominante phyllotaxis-bepalende factor. Andere manteloppervlakken, zoals de halve bol en de 'kettinglijn-dome' zijn evenzeer mogelijk, met overeenkomstige resultaten.

(iii) Bouwelementen zijn afgeleid van ringvormige eenheden. Een sterke canalisatie heeft een regelmatige basis voor de halve bol (dome) als gevolg. Verdere stapeling geeft sterke regelmaat in de structuur. Er ontstaan ringen van afnemende aantallen elementen (vaak volgens Fibonacci-aantallen). De elementradii nemen ditmaal af richting toppunt. Het totaal aantal elementen op de halve bol kan relatief laag zijn, bijvoorbeeld 50. Voor dome-ontwerpen gebruiken we slechts de halve bol of een ander convex oppervlak, zonder de cilinder.

In levende organismen wordt groei bereikt door het vervangen en toevoegen van hoeveelheden materiaal. Op bloemhoofdjes in aanleg schijnen deze hoeveelheden te zijn gebundeld in halfbolvormige eenheden, die vervolgens worden gestapeld tot (phyllotactische) patronen. In feite worden deze eenheden gevormd en ontwikkeld door differentiatie en groei van buitenste cellagen. Zowel het Verdringingsmodel als het Stapel- en Trekmodel combineren structurele uitdijing met stapeling (zie 'PHYLLOTACTIC PATTERNS FOR DOMES').

Een gebouw ontstaat via een wezenlijk anderssoortig groeiproces; toch zijn de stapelingsmodellen bruikbaar. Ten eerste, phyllotactische patronen handhaven hun regelmaat na hun ontstaan. De posities van eenheden worden bevroren in topologisch starre patronen. In het algemeen houdt dit in, dat phyllotactische patronen onafhankelijk zijn van structurele groei. Ten tweede resulteert de vrijheid, die de modellen bieden, in een zeer groot bereik van patronen: parameters, die in de natuur nooit buiten zekere grenswaarden kunnen komen, staan voor experimenten open. Bijvoorbeeld: in plaats van een natuurlijke groeicurve kan een constante waarde of een krimpfunctie worden aangewend.

Gevolgtrekkingen, afgeleid van phyllotactische ontwikkeling, slaan een brug tussen de traditionele bouwmethodieken en (nog) experimentele constructies, detailleringen en uitvoeringswijzen. Voor het eerst hebben bouwkundigen de beschikking over een door de groene natuur geïnspireerde methodiek, om een gegeven dome-oppervlak te vullen met elementen van voor te schrijven grootte. Doel is daarbij een optimum te bereiken in dichtheid, regelmaat en schoonheid. De ontwerper gebruikt een van de CAD-programma's *ApexD* en *ApexS* met vanuit de biologie herkenbare variabelen, zoals:

(i) de vorm van het manteloppervlak (bv. halve bol, plaat, kegel, paraboloïde)
(ii) de vorm van het close-packing element (bv. cirkelschijf / bol, raat, rechthoek, ruit)
(iii) de vorm van intercellulairen (afhankelijk van element-vorm en -grootte of andersom)
(iv) de elementgrootte (bv. constant, of volgens een eventueel onregelmatig verloop)
(v) de geometrische relaties tussen elementen (bv. verbindingen tussen middelpunten).

SOFTWARE

De programma's *ApexD* en *ApexS* geven projecties van driedimensionale structuren en numerieke en grafische resultaten als uitvoer. Ze zijn de eerste generators in hun soort. Systematisch biologen herkennen de gebruikte parameters. De ontwerpen kunnen architectonische (of minstens: artistieke en decoratieve) of constructieve (structurele) betekenis hebben. De programmatuur, ontwikkeld in *Visual Basic for MS-Windows*, is zeer compact en werkt op een personal computer in de *MS-Windows*-omgeving. Men kan resultaten inlezen in paketten als *AutoCAD* en *3D-Studio*.

UTILISATIE

De bouwpraktijk behoeft eenvoudige methodieken voor het produceren van elementen. De bouwstenen van de phyllotactische structuren zijn afgeleid van invloedssferen, ofwel bollen. Het specifiek (gnomonisch) ordenen van deze bouwstenen levert fractale structuren op, zodat er een toepassing ontstaat van een fractal-theorie in de bouwpraktijk. Potentiële belanghebbenden kunnen worden gevonden onder opdrachtgevers van middelgrote tot grote dome-achtige constructies en fabrikanten van lichte betonelementen in lichte draagconstructies.

i THE DISLODGEMENT MODEL IMPROVED

ABSTRACT

With the introduction of the Stack and Drag Model [Van der Linden, 1994], we now may simulate a wide range of vegetative and generative phyllotactic patterns without excluding one of three well-known hypotheses[1].

However, the Dislodgement Model [Van der Linden, 1990] should not be set aside since

(i) While in each of the models the gnomonic principle [Thompson, 1917] has been approached from a different point of view, the construction of the Dislodgement Model is purely centric and therefore relatively simple.
(ii) The Dislodgement Model is based on very simple planar-geometrical postulates.
(iii) We believe that expanding from a centre adjusts an initial ordering.
(iv) In some cases, we see inversions in structures [Tappan, 1980].

A primordium, or a sphere of influence with appendage-forming cell clusters, is called *unit* in the model. A unit is represented as a sphere on a receptacle. Below, we show some improvements on the existing dislodgement theory [Van der Linden, 1990], which describes the separation of centrally arising units on a flat or curved surface. The process is simulated by a static construction, while between time intervals Δt = *plastochron* a structure has to be turned to fit the preceeding one [Van der Linden, 1994]. (A plastochron is the time between the inception of succesive primordia.) At the same time a new unit is added on the outside. Recently, the significance of contact pressure from the center was indicated by physical Fibonacci pattern formation [Douady and Couder, 1991].

INTRODUCTION

In the Dislodgement Model, the stacking of units is from the growth tip out-/downwards (Fig 1). At the start of the construction a close relation in size between units and receptacle does not exist. The receptacle may be a flat plane, a paraboloid, or any convex rotation symmetrical 3-dimensional surface. To get a relationship in size between units and receptacle we will introduce a *limiter* (see UNIT GROWTH). Close size relations between units and stem result in early growth patterns and almost cotyledons. The radii of the stacked spheres will approach, but not overgrow, the receptacle's radius. Like the Stack and Drag Model, the Dislodgement Model makes use of three S-curves [Thornley and Cockshull, 1980]. The first one is the unit growth curve. The other ones are translating curves to simulate structural growth by expansions in axial and radial directions. The total of units in the entire structure is known at the start. Differences between the models are (TABLE I):

TABLE I - COMPARISON	
Dislodgement Model	*Stack and Drag Model*
The centric dislodgement process is reversed to a stacking in a static structure. After the construction of unit(*n*), structure(*n*) must be rotated around the *z*-axis to simulate growth.	Annular stacking; structure(*n*) and structure(*n*-1) have same positions.
planar >>> covering ('folding')	3-dimensional
top >>> down	bottom >>> up
predefined number of units for whole structure	only number of vegetative units is preset *
moment of transition depends on S-curves	moment of transition depends on event *
increasing relation $R(u)$-$R(s)$ towards base	full relation $R(u)$-$R(s)$
no canalization, no regular flowers	canalization, regular flowers
result of construction is a dense close-packing	result of construction may be more loose
top configuration of units is very regular	top configuration is not predictable **
base configuration of units is problematical	base configuration of units is predefined

* The generative stage starts instantly after the placement of all vegetative units.

** In apical domes with many primordia, as in composites, this corresponds with the observed chaotic patterns in the center of bigger flower heads.

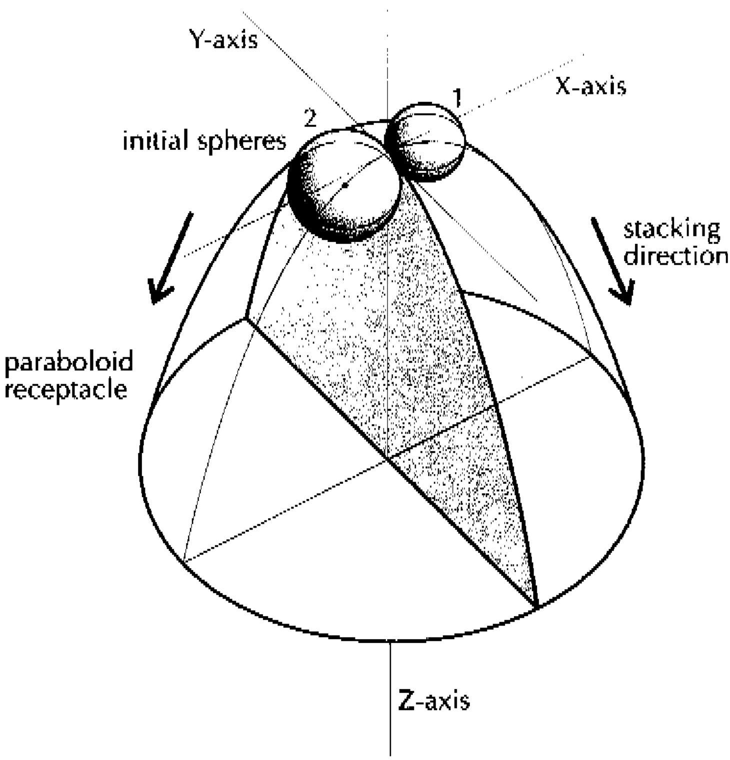

Fig I Initiation in the Dislodgement Model.

Unit growth

Compared with the Dislodgement Model [Van der Linden, 1990], there are two important improvements: the change of the growth function (see below), and the use of this function for translations (see Discussion). Around a Z-axis, a parabole with its top in the perpendicular *XY*-plane, is rotated as a receptacle (Fig 1). After this, we establish the total number of units with which we will build up the structure. The growth curve of units is defined as:

$$S_n = b + (1\text{-}b) \,/\, (1+e^{c.(b-n/tl)})$$

in which S is unadjusted (see below) sphere radius ($0 \leq S \leq 1$), n is ordinal number, b is base (minimum radius), e is the Euler number $e = 2.71828...$, c is gradient constant, b is halflife (the time a unit takes to reach radius $R/2$ - in terms of stacking: the ordinal number of the unit with radius $R/2$), and tl is the total number of units in the structure. Touching spheres are calculated; their centres lie on the receptacle. The stacking direction is out- and downwards from two initial, touching spheres (Fig 1). Sphere radii, including the first ones, are calculated by the growth curve (S) and the distance of the predecessing unit to the receptacle's axis (d). To establish a dependence of unit radii on the receptacle's width, we introduce a limiter (L):

$$L_n = S_n \,.\, rd \,.\, (R_{max}\text{-}d_n\text{-}1)$$

in which L is the limiter, S is unadjusted sphere radius, n is ordinal number, rd is radius-distance ratio, R_{max} is maximum unadjusted radius, and d is distance. Note, that L increases following the unit growth curve. In fact, another function might be considered here. Now, the adjusted radius is defined by:

$$R_n = S_n \,.\, (R_{max}\text{-}L_n)$$

in which R is unit radius, n is ordinal number, S is unadjusted sphere radius, R_{max} is maximum unadjusted radius, and L is limiter. The algorithm which sites new spheres in successive neighborhoods (see below) is

$$n{:}=n+1,\ p{:}=p+1,\ q{:}=q+1$$

in which n is the ordinal of the last unit placed, and p and q are the ordinals of the units, against which that unit is leaning. The sphere with ordinal $n+1$ is lying in the neighborhood, that is just one plastochron younger ($n+1$) than the last neighborhood. Instead of '*neighborhood (n)*' we may read '*configuration of units around unit (n)*', or '*environment around unit (n)*'. (The meaning of ordinal difference in relation to the plastochron is described in [Van der Linden, 1990].)

Structural growth

After the pattern-forming on the receptacle we simulate growth of the structure by axial and radial unit translations. Translation depends on unit ordinal n (or age), on distance d (to Z-axis) and on height z (from XY-plane). Stem growth causes shifting in the phyllotactic pattern. Translations follow the S-curve, being a function of n, but also of z or d, respectively.

Axial Translations: $Ax_n = (1\text{-}S_n).z_n^{LinkZ}$

in which z_n is relative height ($0<z_n\leq 1$) and *LinkZ* causes displacements to depend on n to z_n ($0\leq LinkZ\leq 10$). Notice, that axial translations and unit sizes use similar graphs, when $LinkZ=0$.

Radial Translations: $Rad_n = S_n.d_n^{LinkD}$

in which d_n is relative distance ($0<d_n\leq 1$) and *LinkD* causes displacements to depend on n to d_n ($0\leq LinkD\leq 10$). Note that radial translations and unit sizes use horizontally mirrored graphs when $LinkD=0$. For a more detailed explanation, see [Van der Linden, 1994].

Discussion

Although the Stack and Drag Model appears to produce recognizable results, we suggest that this model should be used for a first arrangement only. Stacking from the base is combined with dragging by Buvat's top ring. Immediately after a primordium has been surrounded by neighbors, an early pattern has been established. From this point, the whole structure shows a remarkable lack of tensions. In other words, the initial stacking along and even towards the Z-axis is followed by a translation from it. So, the pattern will show little changes while the structure expands. We may continue with expansion, not unit generation, as described in the Dislodgement Model which follows the principle of contact pressure [Schwendener, 1878]. Investigations on floral ontogeny [Van Heel, 1987; Endress, 1990] and surgical experiments [Hicks and Sussex, 1970; Hernandez and Palmer, 1988] clearly pledge against a purely centric dislodgement theory. Investigations on pattern formation of epidermic cells in vegetative ontogeny [Smith and Murashige, 1970; Bierhorst, 1977; Green 1985], centric experiments [Douady and Couder, 1991], and centric surface models [Green 1988; Goodall 1991] show that use of (centric) surface models may be sensible in some cases.

Footnote

[1]Three hypotheses are concerned with primordial positioning:

(i) *New primordia will arise as far as possible from just born ones.*
[Hofmeister, 1868; Schoute, 1913; Mitchison, 1977]

(ii) *New primordia will arise at the first available space.*
[Snow and Snow, 1947]

(iii) *New primordia are positioned by mechanical pressure of its contacts.*
[Schwendener, 1878; Adler, 1974]

REFERENCES

(1) S. Douady and Y. Couder, Phyllotaxis as a Physical Self-Organized Growth Process, Phys. Rev. Lett. 68(13):2098-2101, 1992

(2) C. Goodall, Eigenshape Analysis of a Cut-Grow Mapping for Triangles, and its Application to Phyllotaxis in Plants, SIAM J. Appl. Math. 51(3):775-798, 1991

(3) P.B. Green, Surface of the Shoot Apex: a Reinforcement-Field Theory for Phyllotaxis, Journ. of Cell Science Suppl. 2:181-201, 1985

(4) P.B. Green, A Theory for Inflorescence Development and Flower Formation based on Morphological and Biophysical analysis in Echeveria, Planta 175:153-169, 1988

(5) W.A. Van Heel, Androecium Development in Actinidia Chinesis and A. Melanandra (Actinidiaceae), Bot. Jahrb. Syst., 109:17-23, 1987

(6) L.F. Hernandez and J.H. Palmer, Regeneration of the Sunflower Capitulum after Cylindrical Wounding of the Receptacle, Am. Journ. Bot., 75:1253-1261, 1988

(7) G.S. Hicks and I.M. Sussex, Development In Vitro of Excised Flower Primordia of Nicotiana Tabacum, Can. Journ. Bot. 48:133-139, 1970

(8) R.F. Lyndon, The Shoot Apex, in Cell Division in Higher Plants, M.M. Yeoman, Ed., Academic Press, London, pp.285-314, 1976

(9) S. Schwendener, Mechanische Theorie der Blattstellungen, Leipzig, 1878

(10) R.H. Smith and T. Murashige, In Vitro Development of the Isolated Shoot Apical Meristem of Angiosperms, Am. Journ. Bot. 57:.562-568, 1970

(11) H. Tappan, The Paleobiology of Plant Protists, W.H. Freeman and Company, pp. 855-925, fig 10.45, 1980

(12) d'Arcy W. Thompson, On Growth and Form, Cambridge University Press, London, pp.759-766, 1917

(13) J.H.M. Thornley and K.E. Cockshull, A Catastrophe Model for the Switch from Vegetative to Reproductive Growth in the Shoot Apex, Annals Bot. 46:333-341, 1980

(14) F.M.J. Van der Linden, Creating Phyllotaxis: The Dislodgement Model, Math. Biosci. 100(2):161-199, 1990

(15) F.M.J. Van der Linden, Creating Phyllotaxis: The Stack and Drag Model, Manuscript, 1994

ii COMPUTER PROGRAM *'APEXS'*: KEY ALGORITHMS

1 Introduction

As a counterpart of purely argumentation theories, modeling is essential in science. The modern laboratory *computer* enables us to test a hypothesis by repeating phyllotactic modeling algorithms again and again. I have concluded to show my experiments in detail by supplying the core of the developed software as a section in this thesis.

In order to prevent this section to be a desert island, it has been purified by removing user interface and disturbing 'noise', and explicit connections with the theory are provided. For a right understanding and definitions, see 'Basics in the Stack and Drag Model', in Chapter 4, p.12 of this book.

Software development is done in *Visual Basic 3.0* in the *MS-Windows 3.1* environment, using a *486DX*-processed personal computer.

NB ***'ApexS'*** belongs to the Stack and Drag Model. The kernal calculation files of ***'ApexD'*** of the Dislodgement Model are basically different from the present ones.

[1] INLEIDING

Als tegenhanger van zuiver bewijsvormende theorieën is modelleren in de wetenschap essentieel. Het moderne laboratorium *computer* maakt het mogelijk, een hypothese te testen door algoritmen in het phyllotactisch modelleren telkens opnieuw uit te voeren. Ik heb besloten, om mijn experimenten gedetailleerd te tonen door het hart van de ontwikkelde reken-programmatuur op te nemen als een hoofdstuk in dit proefschrift.

Om te voorkomen, dat dit hoofdstuk een onbewoond eiland wordt, is het gezuiverd van gebruikersprogrammering en storende 'ruis' en zijn er expliciete verbindingen met de theorie verschaft. Voor een goed begrip en definities, zie 'BASICS IN THE STACK AND DRAG MODEL' in hoofdstuk 4, p.12 van dit boek.

Programma's zijn ontwikkeld in *Visual Basic 3.0* in de *MS-Windows 3.1* omgeving, met gebruik van een *486DX*-gestuurde 'personal computer'.

NB 'ApexS' behoort tot het Stack and Drag Model. De centrale RekenFiles van programma *'ApexD'*, behorend bij het Dislodgement Model, verschillen fundamenteel van de navolgende.

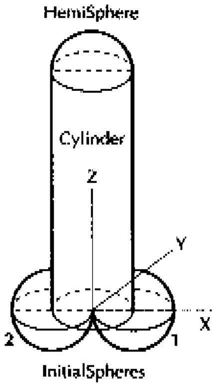

a. InitialSpheres:

n	1	2
d	1	1
x	1	-1
y	0	0
z	0	0
p	0	1
q	0	0
r	(1)	(1)

b. PatternCalculation:
Left:
InitialSpheres, r =1 (cotyledons)
- other radii are possible
Cylinder, r =1 (stem)
- contains tls units
HemiSphere, r =1 (apex)
- contains a previously unknown number of units
Center and right:
p: Support unit*(p)* lies in clockwise direction against unit*(n)*. Unit*(q)* is the other contact.

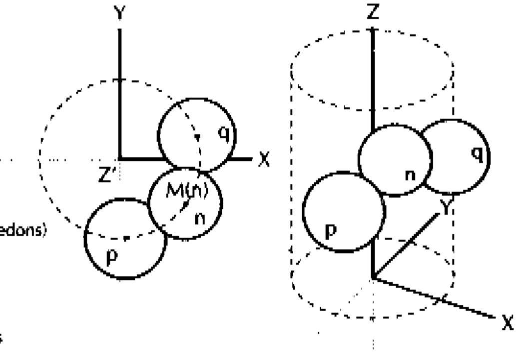

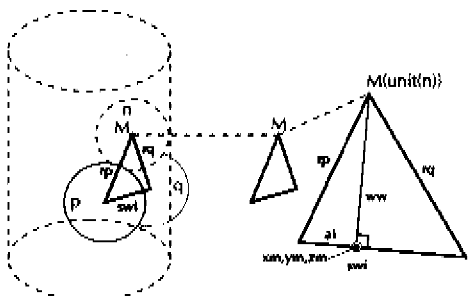

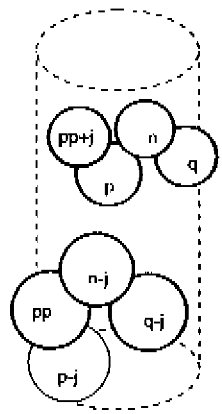

c. ProposeSphere:
[1] $ww^2 = rp^2 - ai^2$
[2] $ww^2 = rq^2 - (swi-ai)^2$
[1],[2] $ai = (swi^2+rp^2-rq^2) / (2*swi)$

d. Sensitivity: *(right)*
The highlighted unit*(pp+j)* will be counted, for unit*(n-j)* has *pp* as one of its support units. Increase of *j* means decrease of sensitivity.

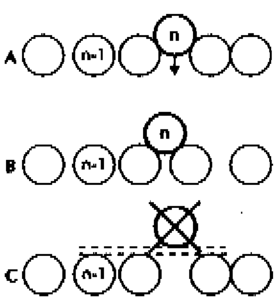

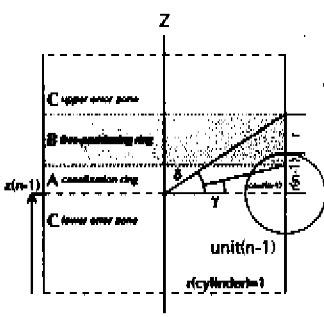

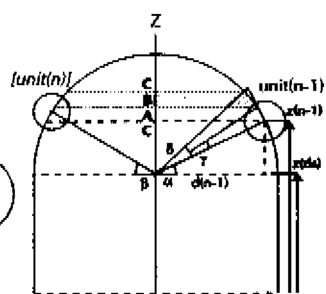

e. Canalization:
Left (side view): A new unit, which fits, or nearly fits, between its predecessors (A) will be part of the existing ring. When it has been located significantly higher (B) (after lack of space below), it will be the first unit in a *new* ring. Extreme high (C) or low positions indicate an error. (This kind of error may occur in Nature as well.)
Center (cylinder, cross section): Besides z(n-1), ca=r(n-1), or angle γ, settles the upper border of the *canalization ring.* Angle δ, in *tan(δ)=(r+r(n-1))/r(cylinder)* determines the upper border. A unit, which has been *proposed* within the ring, remains its calculated position. Higher *ca* values will narrow the ring.
Right (hemisphere, cross section): Angles α in *tan(α)=(z(n-1)-z(tls))/d(n-1)* and β define a horizontal shift of the ring.

3 Pattern Calculation in 'ApexS'

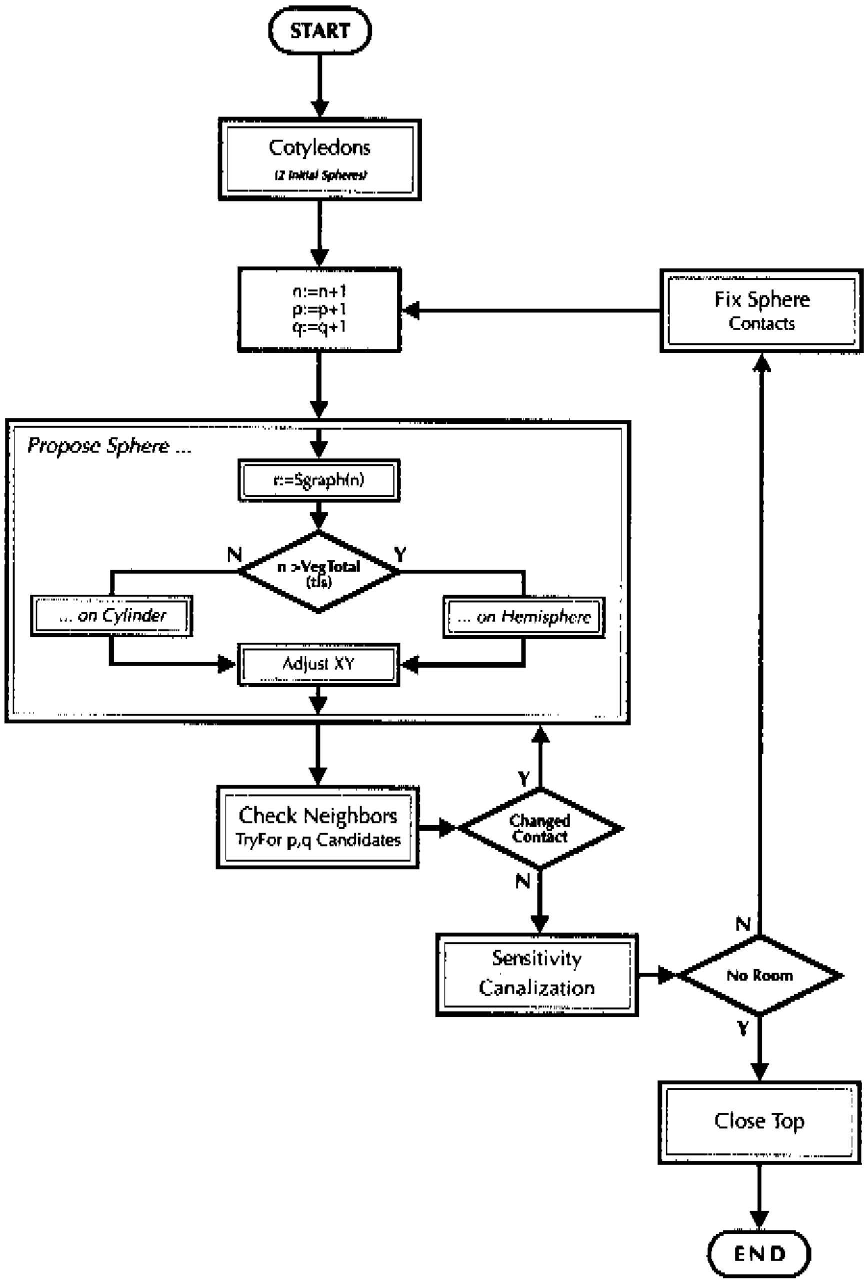

4 Vital Calculation Routines

in '*ApexS*' 3.05 - 120594

Globals

Integers	n, p, q	ordinal number of sphere with contacts
Booleans	ChangedContact	verifying the changing of contacts
	NoRoom	verifying the room left on the extreme apical tip
Singles	x, y, z, r	cartesian coordinates of center M and radius of sphere(n)
	d, a	polar coordinates
	xi, yi, zi	xi: x-difference between support spheres p and q
	xm, ym, zm	new sphere has M on circle (xm,ym,zm,ww)
	ww, ww2	circle radius M(xm,ym,zm) between support spheres; ww^2
	rp, rq	rp: sum of radii of spheres n and p; rq of n and q
	swi, swj	3D-distance between support spheres; Z-projection
	df	compression-factor for sphere-compression/-repulsion
	dc	rounding value
String	Candidate	replacing support sphere, expressed in n, p, q

Subroutines and functions

PatternCalculation	CheckNeighbors	CloseTop
Cotyledons	TryFor	Sgraph
ProposeSphere	FixSphere	AdjustXY
Cylinder	Sensitivity	Contacts
HemiSphere	Canalization	

In order to simplify the judging, several text presentations are used:

underscored, large	subprogram or function
underscored	reference to subprogram or function
italics	remark

[4] VITALE REKENROUTINES

in '*ApexS*' 3.05 · 120594

Globale variabelen

Integers	n, p, q	rangnummer van bol met contacts
Booleans	ChangedContact	al of geen wijziging in een der draagbollen
	NoRoom	al of geen restruimte op de uiterste apicale top
Singles	x, y, z, r	as-coördinaten van middelpunt M en straal van bol(n)
	d, a	poolcoördinaten
	xi, yi, zi	xi: x-verschil tussen draagbollen p en q
	xm, ym, zm	nieuwe bol heeft M op cirkel (xm,ym,zm,ww)
	ww, ww2	cirkelradius met M(xm,ym,zm) tussen draagbollen; ww^2
	rp, rq	rp: som van radii van bollen n en p; rq van n en q
	swi, swj	3D-afstand tussen draagbollen; Z-projectie
	df	compressie-factor voor bol-indrukking/-afstoting
	dc	afrondingsgrootte
String	Candidate	vervangende draagbol, uitgedrukt in n, p, q

Subroutines en functies

PatternCalculation	CheckNeighbors	CloseTop
Cotyledons	TryFor	Sgraph
ProposeSphere	FixSphere	AdjustXY
Cylinder	Sensitivity	Contacts
HemiSphere	Canalization	

Om de leesbaarheid te verbeteren, zijn meerdere tekstpresentaties gebruikt:

onderstreept, groot	subprogramma of functie
onderstreept	verwijzing naar subprogramma of functie
cursief	toelichting

5 VITAL TRANSLATION FORMULAE

and particular Drawing Algorithms

All *ApexS*-subprograms are shared by *ApexD*, except *'Polygon'* and *'Growing'*. This is due to the influence of (i) a different use of the gnomonic principle and (ii) combination of theories like 'The Morphogenic Unit' (G.A. Pieters) with the existence of contact spheres in the present theories.

In the Dislodgement Model, spheres are stacked top-down, which requires a 'negative'-definition for the ***internode-leaf unit*** (see references in the author's article CREATING PHYLLOTAXIS: THE STACK AND DRAG MODEL). Growth simulation in this model follows the starting principles, so a structure develops from the top and expands downwards. Units dislodge each other in a continued process that does not end up with flowering; cotyledons are not defined.

In *'Growing'*, *ApexS* shows different aspects of vegetative and generative growth. From two spherical cotyledons, a cylindrical stem and a phyllotactic pattern on it are generated at the same time. The process ends with a hemispherical (apical) stacking of primordia. When there is no room left, this is indicated by an auditive signal. The structure develops any inflorescence with or without canalization, and radial and axial displacements are responded by coloring.

In order to simplify the judging, several text presentations are used:

<u>underscored, large</u>	subprogram or function
italics	remark

[5] Vitale TranslatieFormules

en bijzondere TekenRoutines

Alle subprogramma's worden zowel in *ApexD* als in *ApexS* gebruikt, behalve *'Polygon'* en *'Growing'*: deze zijn specifiek geënt op het Stack-and-Drag Model. Dit komt, doordat polygonen ('raten') worden gedefinieerd op basis van theorieën als 'The Morphogenic Unit' (G.A. Pieters) en het gegeven van 'contacts', of draagunits (-bollen) in de onderhavige theorie.

In het Dislodgement Model wordt vanaf de top gestapeld, hetgeen een 'negatief'-definitie vereist voor de eenheid internode-blad. Groeisimulatie in dit model volgt de uitgangspunten, zodat een structuur vanuit de top ontstaat en uitdijt. Hierbij is verdringing te constateren. Er is geen evidente bloei, er zijn geen duidelijke zaadlobben.

ApexS toont met *'Growing'* meerdere facetten van vegetatieve en generatieve groei. Gelijktijdig met een cilindrische 'stengel' vanuit twee sferische 'zaadlobben' ontstaat een phyllotactisch patroon. Wanneer de structuur-in-aanleg geen nieuwe 'primordia' meer kan vormen in de top van de hemisferische 'apex', wordt dat aangegeven met een hoorbaar signaal. De structuur dijt uit, eventueel ontluikt een knop en kleuring volgt radiale (en axiale) verplaatsingen. Er zijn vele bloeiwijzen mogelijk, met zwakke tot sterke canalisatie.

Om de leesbaarheid te verbeteren, zijn meerdere tekstpresentaties gebruikt:

<u>onderstreept, groot</u>	subprogramma of functie
cursief	toelichting

Program Files *'ApexS' 3.05*

Software versions:
'ApexD/Demo', 'ApexD/Standard', 'ApexD/Scientific', 'ApexS/Demo', 'ApexS/Standard', 'ApexS/Scientific'.

Programs
- run in the *MS-Windows*-environment
- are smaller than 0.4 MByte.

Sub PatternCalculation ()

——*Program core. p is ordinal of the support unit of unit(n), counterclockwise with respect to unit(n) and pos. X and Y axis. q is ordinal of the other support unit ('contact'). tls (total stem) is the number of vegetative units, or : the user defined number of spheres on the cylinder. tl is the total number of units (vegetative and reproductive), which is a result of the calculation below. CheckTimes is the user defined number of checks for intersecting of spheres.*

-----*Hart van het programma. p is rangnummer van draagunit, ('contact'), tegen de klok in t.o.v. unit(n) en pos. X- en Y-as. q is rangnummer van de andere van de beide draagunits van unit(n). tls (total stem) is het aantal vegetatieve units, ofwel: het (door gebruiker bepaalde) totaal aantal bollen op de cilinder. tl is het totaal aantal units (vegetatief en reproductief), pas bekend na onderstaande berekning. CheckTimes is het door gebruiker ingevoerde aantal checks voor het snijden van bollen.*

```
Dim i As Integer
 Cotyledons
 Do
  n = n + 1: p = p + 1: q = q + 1
  Do
   ProposeSphere
   CheckNeighbors
   i = i + 1
  Loop While ChangedContact And i < CheckTimes
  Sensitivity
  Canalization
  If n > tls Then
   If n > ArraySize Or z > zz(tls) + 1 + dc Or NoRoom Then Exit Do
——dc is rounding
——dc is afronding
  End If
  FixSphere
 Loop
 If n > 2 Then tl = n - 1
 CloseTop
End Sub
```

Sub Cotyledons ()

——*This subprogram has the same significance as: 'ProposeSphere' + 'Cylinder'/'HemiSphere' (stem/apical dome) + 'FixSphere'. Here, two initial spheres are defined as seedlobes. They are lying face to face on the cylinder (stem) at elevation z=0 . In this exceptional case, the user may disable the S-growthcurve temporary: SeedOne = True, or equalize the cotyledons, but dependent on the S-curve: SeedEqual = True.*

-----*Dit subprogramma staat op gelijk nivo met 'ProposeSphere' + 'Cylinder'/'HemiSphere' (stem/apical dome) + 'FixSphere'. Hier worden twee startbollen als zaadlobben gedefinieerd. Ze liggen op hoogte z=0, tegenover elkaar op de cilinder (stengel). De gebruiker kan de S-curve voor deze uitzonderlijke units 'uitzetten': SeedOne = True, of de 'zaadlobben' gelijk houden, maar volgens de S-curve: SeedEqual = True.*

```
n = 0
pp(n) = 0: qq(n) = 0: aa(n) = 0
rr(n) = 0: dd(n) = 0: xx(n) = 0: yy(n) = 0: zz(n) = 0
n = 1
If SeedOne = True Then
 r = 1
```

```
-----The Lucas series may arise spontaneously, without the need for a special variable.
-----De Lucasreeks kan blijkbaar spontaan ontstaan, zonder dat daarvoor een bijzondere variabele is.
 Else
  If SeedEqual = True Then r = Sgraph(1, 2) Else r = Sgraph(1, 1)
 End If
 d = 1: x = 1: y = 0: z = 0
 p = 0: q = 0: a = 0
 pp(n) = p: qq(n) = q: aa(n) = a
 rr(n) = r: dd(n) = d: xx(n) = x: yy(n) = y: zz(n) = z
 n = 2
 If SeedOne = True Then r = 1 Else r = Sgraph(1, 2)
 d = 1: x = -1: y = 0: z = 0
 p = 1: q = 0: a = pi
 pp(n) = p: qq(n) = q: aa(n) = a
 rr(n) = r: dd(n) = d: xx(n) = x: yy(n) = y: zz(n) = z
End Sub
```

Sub ProposeSphere ()

```
-----This is the common part of / before fixing spheres on cylinder or hemisphere. In the do-loop, the problem of too  much room between both support units is dissolved. wi is the square of the 3D distance between centers (wj: 2D).
-----Dit is het gemeenschappelijk gedeelte van en vóór bolplaatsing op cilinder of hemisfeer. In de do-loop wordt het probleem opgelost van een eventueel te grote ruimte tussen de beide draagunits. wi is kwadraat van 3D-afstand middelpunten (wj: 2D).
 Dim wi, wj, ai As Single
 xi = xx(q) - xx(p)
 yi = yy(q) - yy(p)
 zi = zz(q) - zz(p)
 wj = xi * xi + yi * yi
 wi = wj + zi * zi
 swi = Sqr(wi)
 swj = Sqr(wj)
 r = Sgraph(1, n)
 Do
  rp = r + rr(p) * df   'ipv df:   (1 + (df - 1) * fq)
-----Fresh units react stronger on df.
-----Versere units reageren sterker op df.
  rq = r + rr(q) * df   '(1 + (df - 1) * fp)
  If rp + rq < swi + dc Then r = 1.1 * r Else Exit Do
-----In the case of too wide the room for sphere placement , the sphere is oversized temorary (until definite fixing). The factor 1.1 is arbitrary.
-----Is het plaatsingsgat te ruim, vergroot dan de nieuwe unit tijdelijk tot aan einde definitieve plaatsing. De factor 1.1 is willekeurig.
 Loop
 ai = (wi + rp * rp - rq * rq) / (2 * swi)
 ww2 = rp * rp - ai * ai
-----Circle (xm,ym,zm,ww), with M(n) on it.
-----Cirkel (xm,ym,zm,ww), waarop M(n) ligt.
 xm = xx(p) + xi * ai / swi
 ym = yy(p) + yi * ai / swi
```

```
 zm = zz(p) + zi * ai / swi
 ww = Sqr(ww2)
 If n <= tls Or zz(p) < zz(tls) Or zz(q) < zz(tls) Then Cylinder Else HemiSphere
 AdjustXY
End Sub
```

Sub Cylinder ()

-----Iteration process, to find M of the next sphere to be proposed. ww is circle radius with M(xm,ym,zm) between the support spheres. The circle intersects the cylinder: ww^2=aj^2+zj^2. dc gives the rounding, normally dc=10^(-3).

-----Iteratieproces, om M te vinden van de nieuw voor te stellen bol. ww is cirkelradius met M(xm,ym,zm) tussen de draagbollen. De cirkel snijdt de cilinder in het gezochte punt; ww^2=aj^2+zj^2.
dc geeft de afrondingsprecisie, normaliter is die 10^(-3).

```
 Dim xzs, yzs, xsw, ysw, sw As Single
 Dim aj, zj, za, zb As Single
 If n > tls + p + q Then Beep
```

-----Warning: the user may abort the calculation for spheres are not stacked correctly on the hemisphere .
-----Waarschuwing: onderbreek de berekening: te lang op cilinder.

```
 xzs = xi * zi / (swi * swj)
 yzs = yi * zi / (swi * swj)
 xsw = xi / swj
 ysw = yi / swj
 sw = swj / swi
```

-----Until this point: condensed describtions to speed up the iteration loop.
-----Tot hiertoe verkorte omschrijvingen ter bespoediging van het itereren hieronder.

```
 za = 0
 zb = ww
 Do While Abs(za - zb) > dc
  zj = (za + zb) / 2
  aj = Sqr(ww2 - zj * zj)
  x = xm - aj * ysw - zj * xzs
  y = ym + aj * xsw - zj * yzs
  z = zm + zj * sw
  If x * x + y * y < 1 Then zb = zj Else za = zj
 Loop
End Sub
```

Sub HemiSphere ()

-----Direct calculation of M of the next sphere to be proposed.
-----Directe berekening van M van de nieuw voor te stellen bol.

```
 Dim aj, zj As Single
```

-----First, counting from the hemisphere's elevation.
-----Eerst de hemisfeerhoogte rekenen vanaf de cilindertop.

```
 zm = zm - zz(tls)
```

-----ww is circle radius with M(xm,ym,zm) between the support spheres. This circle intersects the hemisphere: ww2=aj^2+zj^2.

-----ww is cirkelradius met M(xm,ym,zm) tussen de draagbollen. Deze cirkel snijdt de hemisfeer in het gezochte punt; ww2=aj^2+zj^2.

```
 m1 = 2 * zi * (xm * xi + ym * yi) / (swi * swj) - 2 * zm * swj / swi
```

```
m2 = ww2 - 1 + xm * xm + ym * ym + zm * zm
m3 = 2 * (xm * yi - ym * xi) / swj
di = m1 * m1 * ((m1 * m1 + m3 * m3) * ww2 - m2 * m2)
 -----di is discriminant of the equation / van vergelijking (m1^2+m3^2)*zj^2+2*m2*m3*zj+m2^2-m1^2*ww2=0.
zj = (-m2 * m3 + Sqr(di)) / (m1 * m1 + m3 * m3)
aj = Sqr(ww2 - zj * zj)
x = xm + zj * yi / swj - aj * zi * xi / (swi * swj)
y = ym - zj * xi / swj - aj * zi * yi / (swi * swj)
z = zm + aj * swj / swi
z = z + zz(tls)
-----Now, add z on the cylinder elevation.
-----Nu z weer optellen bij de cilinderhoogte.
End Sub
```

Sub CheckNeighbors ()

-----The environment of the just proposed sphere is systematically 'combed out' in order to prevent lower situated spheres from intersecting. Intersection candidates are tested by calling subprogram TryFor. The call TryFor is followed by the ordinal numbers of the support sphere and the candidate in question. If a sphere is intersecting indeed, then (from TryFor) the Boolean ChangedContact will be TRUE.

-----Systematisch wordt rond de juist-voorgestelde bol de directe omgeving 'uitgekamd', om het snijden van aanwezige (lager liggende) bollen te voorkomen. Kandidaten voor snijden worden getest door het aanroepen van subprogramma TryFor. De aanroep TryFor wordt gevolgd door de rangnummers van de te bekijken draagbol en de kandidaat. Blijkt een bol te snijden, dan krijgt (vanuit TryFor) de Boolean-variabele ChangedContact de waarde TRUE.

```
 ChangedContact = False
 If p > q Then
  TryFor q, q + n - p
  If Not ChangedContact Then
   TryFor p, q + q - p
   If Not ChangedContact Then
    TryFor p, p + q - n
   End If
  End If
 ElseIf p < q Then
  TryFor p, p + n - q
  If Not ChangedContact Then
   TryFor q, p + p - q
   If Not ChangedContact Then
    TryFor q, q + p - n
   End If
  End If
 End If
 If Not ChangedContact Then
  TryFor p, pp(q) + n - q
  If Not ChangedContact Then
   TryFor q, qq(p) + n - p
   If Not ChangedContact Then
    TryFor p, pp(p) + n - p
    If Not ChangedContact Then
     TryFor q, qq(q) + n - q
```

```
    End If
   End If
  End If
 End If
End Sub
```

Sub TryFor (ActualContact As Integer, ProposedContact As Integer)

----For intersection, the testsphere ProposedContact is tested by distance and size. The actual support sphere ActualUnit may have to be replaced by sphere ProposedContact.

----De testbol ProposedContact wordt via afstand en grootte bekeken op snijden met bol n. De in het geding zijnde draagbol ActualUnit moet eventueel vervangen worden door bol ProposedContact.

```
 Dim rsum, xdif, ydif, zdif As Single
 If ProposedContact = p Or ProposedContact = q Or ProposedContact = n Then Exit Sub
 If p = qq(n - 1) + 1 Or q = pp(n - 1) + 1 Then Exit Sub
 If n - p > 2 And n - q > 2 And p = qq(n - 1) And q = pp(n - 1) Then Exit Sub
 rsum = r + df * rr(ProposedContact)
 xdif = x - xx(ProposedContact)
 ydif = y - yy(ProposedContact)
 zdif = z - zz(ProposedContact)
 If rsum * rsum > xdif * xdif + ydif * ydif + zdif * zdif + 2 * dc Then
  If zz(ProposedContact) + rr(ProposedContact) > .5 * (zz(p) + zz(q)) Then
   ActualContact = ProposedContact
   ChangedContact = True
  End If
 End If
End Sub
```

Sub FixSphere ()

-----Calculation results are put in arrays. For example, elevation z of sphere number n is zz(n). Not z(n), for the programming language does not accept similar names for arrays and zero-dimensional varables. In Angle, cartesian coordinates are translated into polar coordinates.

----Rekenresultaten worden in arrays opgeslagen. Bijvoorbeeld: hoogte z bij bol nummer n wordt geschreven als zz(n). Niet z(n), want de programmeertaal accepteert gelijke namen voor array en variabele niet. In Angle worden cartesische coördinaten in poolcoördinaten omgezet.

```
 Angle
 Contacts
 r = Sgraph(1, n)
----in the case of temorary oversizing of unit n
-----voor het geval een te groot gat de unit voor de berekening tijdelijk vergrootte
 rr(n) = r
----Not rr(n), for in that case Construction (which visualizes the calculation process) will not work.
-----Moet via r, anders loopt Construction (een visualisatie van de calculatie) fout.
 pp(n) = p: qq(n) = q
 xx(n) = x: yy(n) = y: zz(n) = z: dd(n) = d: aa(n) = a
End Sub
```

Sub Sensitivity ()

----A new position is determined by sensitivity for the highest ring of spheres. The new x and y avoid a 'wild' placement. A new z is between: the preceeding z and the mean of the preceeding z and the z before that

one. se is the ring's location, which depends on the number of some preceeding spheres. Low values for se predict placement by many feed-backs - higher values result in r-fluctuations, mistakes, very low and high placements are allowed, there is little feed-back with earlier events. see 'anneau initial' (Buvat.R)

-----Aan de hand van de sensitiviteit voor de hoogste bollenkrans wordt een nieuwe plaatsing bepaald. De nieuwe x en y voorkomen een 'wilde' (niet tussen p(n-1)+1 en q(n-1)+1) plaatsing. Een nieuwe z ligt tussen: de vorige z en: het gemiddelde van de vorige z en z daarvoor. se duidt de PLAATS van de ring, afhangend van een aantal voorgaande bollen. ring vloeiend omhoog. lage se: voorspelbare plaatsing, rekenwerk is van beperkte invloed door overbemeten feed-back. hoge se: sterke r-schommelingen, fouten gemakkelijk, diepe en hoge elementen toegestaan, dus weinig feed-back met voorgaande gebeurtenissen. zie 'anneau initial' (Buvat.R., zie pp. 66 en 83 in Steeves & Sussex)

```
Dim i, j As Integer
NoRoom = False
i = Abs(p - q)
j = 0
Do While j < i
 j = j + 1
```

-----Changing after sensitivity for the lower i spheres, not for the spheres n-1, n-2, etc). If lower spheres had positive checks, then the dislodged spheres will have influence - rated to position distance. In the other case, not.

-----Wijziging naar gevoeligheid voor de onderliggende i bollen (niet voor de voorgaande bollen n-1, n-2, enz). Wanneer er in de berekening van de onderliggende i bollen via checks is gewijzigd, dan hebben de verdrongen bollen invloed - en dat in evenredigheid van plaats. In het andere geval niet.

```
  x = .5 * ((1 + se) * x + (1 - se) * .5 * (xx(pp(n - j) + j) + xx(qq(n - j) + j)))
  y = .5 * ((1 + se) * y + (1 - se) * .5 * (yy(pp(n - j) + j) + yy(qq(n - j) + j)))
```

-----Is there room left on the top?

-----Is er nog ruimte op de top?

```
  If n > tls And d < 2 * r Then
   dxi = (x - xx(n - j)) ^ 2
   dyi = (y - yy(n - j)) ^ 2
   dzi = (z - zz(n - j)) ^ 2
   rri = r + rr(n - j)
   If dxi + dyi + dzi < rri ^ 2 Then NoRoom = True: Exit Sub
  End If
 Loop
 AdjustXY
End Sub
```

Sub Canalization ()

-----Canalization is structural (concentric) ring formation in phyllotaxis. The ring's maximum elevation z depends on z(unit), d en r. If a new unit has a little (decided by ca) elevation above the existing ring, then it is pulled in the ring. A relatively low position will be corrected by neighbors. High values for ca makes the ring thin. zca is canalization elevation. If placement is far too high, zup corrects this. All vital geometrical variables such as alfa, beta, gamma, and delta are outlined in 'Conceptions of the Stack and Drag Model'.

-----Canalisatie is (concentrische) ringenvorming in phyllotaxis. De maximaal mogelijke hoogte z van een ring hangt af van z(unit), d (afstand unit-as) en r (unitstraal). Indien nieuwe unit niet heel duidelijk (wat dat is, bepaalt ca) hoger, dan in ring. Een relatief lage plaatsing wordt gecorrigeerd (naar buren). (0<=)ca(<=1) duidt de BREEDTE (scherpte) van de ring aan en evt zelfs afwezigheid ervan (ca=0). ring schoksgewijs omhoog. Hoge ca: smalle zone, waarboven plaatsing is toegestaan (binnen grens van r. als correctie); lage ca: brede zone. zca is canalizatiehoogte; zup is correctiewaarde bij veel te hoge plaatsing. alfa = hoek op de hemisfeer van de voorgaande unit. beta = hoek op de hemisfeer van de actuele unit. gamma =

*ca*rr(n-1)/r(hemisfeer) = hoek, waarbeneden canalisatie wordt geforceerd. delta = r+rr(n-1) = hoek tussen M(n-1) en rr(n-1)+r = hoek bovenkant voorgaande unit + r.*

```
Dim alfa, beta, gamma, delta As Single
 zca = (1 + Sqr(se)) * zz(n - 1) / 2 + (1 - Sqr(se)) * z / 2
 zup = ca * zca + (1 - ca) * z
 If n <= tls Then zz(tls) = zz(n - 1)
 ----cylinder----cilinder
 alfa = Atn((zz(n - 1) - zz(tls)) / dd(n - 1))
 beta = Atn((z - zz(tls)) / d)
 gamma = Atn(ca * rr(n - 1))
 delta = Atn(r + rr(n - 1))
 If beta < alfa + gamma Then
----canalization of lower error zone
----canalisatie van onderste 'error zone'
  z = zca
  AdjustXY
 ElseIf beta >= alfa + delta Then
----canalization of upper error zone
----canalisatie van bovenste 'error zone'
  z = zup
  AdjustXY
 End If
End Sub
```

Sub CloseTop ()

-----As for the last sphere, take the top with radius 0. For honeycomb shapes, count this sphere several times, with different p and q. In the procedure which draws honeycombs, the number tlt is cited. It gives tls plus the necessary number of closing 'units'. dc is rounding, read dc=0.

----Neem als laatste bol de top met radius 0. Tel deze laatste 'bol' enkele malen extra, met verschillende p en q, om 'polygons' of 'raten' te kunnen definiëren. Raat = vascular unit = internodial part + leaf part. De topraten zouden anders niet gesloten zijn.) Aantal tlt wordt bij het tekenen van raten aangehaald en is het aantal units tl, plus wat nodig is om te sluiten. dc is de afronding (rekenprecisie). Om problemen (lees: deling door 0) te voorkomen, staat dc voor 0.

```
 Dim dif As Integer
 n = tl: p = pp(tl): q = qq(tl)
 dif = Abs(p - q)
 Do While p < tl + dif And q < tl + dif
  n = n + 1: p = p + 1: q = q + 1
  x = dc: y = dc: z = zmax: d = dc: a = dc: r = dc
  xp(n) = dc: yp(n) = dc: zp(n) = zmax
  xq(n) = dc: yq(n) = dc: zq(n) = zmax
  pp(n) = p: qq(n) = q
  xx(n) = dc: yy(n) = dc: zz(n) = zmax: dd(n) = dc: aa(n) = dc: rr(n) = dc
 Loop
 tlt = n
End Sub
```

<u>Function Sgraph (ig As Integer, i As Integer) As Single</u>

```
-----S-curve for ig= 1, 2, 3: 1 unit radius, 2 axial translation (growth), 3 radial translation (growth). b is 'base'minimum, c is coefficient grade, h is halflife.
-----S-curve, voor ig= 1, 2, 3: 1 unitradius (relatie met de receptacle-radius), 2 axiale translaties (groei), 3 radiale translaties (groei). De S-curve wordt beschreven door b, c en h. b is 'base' minimum, c is coeff grade, h is halflife
 Sgraph = 1 - (1 - bb(ig)) / (1 + Exp(cc(ig) * (hh(ig) - i)))
End Function
```

<u>Sub AdjustXY ()</u>

```
-----Keeping z, x and y are placed exactly on their receptacle.
-----x en y worden precies op cilinder of hemisfeer geplaatst, bij behoud van hoogt z.
 Dim OldDistance As Single
 OldDistance = Sqr(x * x + y * y)
 If n > tls Then
  d = Sqr(1 - (z - zz(tls)) ^ 2)
  x = x * d / OldDistance
  y = y * d / OldDistance
 Else
  d = 1
  x = x / OldDistance
  y = y / OldDistance
 End If
End Sub
```

<u>Sub Contacts ()</u>

```
-----Intersection coordinates of the spheres n and p, and of spheres n and q.
-----Raakpuntcoördinaten van de bollen n en p, resp n en q.
 xp(n) = x + (xx(p) - x) * r / rp
 yp(n) = y + (yy(p) - y) * r / rp
 zp(n) = z + (zz(p) - z) * r / rp
 xq(n) = x + (xx(q) - x) * r / rq
 yq(n) = y + (yy(q) - y) * r / rq
 zq(n) = z + (zz(q) - z) * r / rq
End Sub
```

Sub Polygon ()

```
Dim n, p, q, o, f, nva, nta As Integer
nva = nv: nta = nt
If nv < 3 Then
 nv = 3
ElseIf nv = tl Then
 nv = tlt
End If
If nt < 3 Then
 nt = 3
ElseIf nt = tl Then
 nt = tlt
End If
n = nv
Do While Sgn(ns) * n <= Sgn(ns) * nt
 p = pp(n): q = qq(n): o = pp(q): f = qq(p)
 x0 = xscreen(p): y0 = yscreen(p): x1 = xmorescreen(n): y1 = ymorescreen(n)
 x2 = xscreen(q): y2 = yscreen(q)
 x3 = xscreen(o): y3 = yscreen(o)
 x4 = xscreen(f): y4 = yscreen(f)
 x5 = xpscreen(n): y5 = ypscreen(n): x6 = xqscreen(n): y6 = yqscreen(n)
 x7 = xpscreen(q): y7 = ypscreen(q): x8 = xqscreen(p): y8 = yqscreen(p)
 If p = o Or q = f Then
  If q > p Then
   Call triangle(n, p, q, x0, y0, x1, y1, x2, y2, x5, y5, x6, y6, x7, y7)
  Else
   Call triangle(n, q, p, x2, y2, x1, y1, x0, y0, x6, y6, x5, y5, x8, y8)
  End If
 ElseIf o = f Then
  If intercel(p, q) / intercel(n, o) < vi Then
   Call quadrangle(n, p, q, o, x0, y0, x1, y1, x2, y2, x3, y3, x5, y5, x6, y6, x7, y7, x8, y8)
  Else
   Call quadrangle(q, o, n, p, x3, y3, x2, y2, x1, y1, x0, y0, x7, y7, x6, y6, x5, y5, x8, y8)
  End If
 Else
  If o > f Then
   x9 = xpscreen(o): y9 = ypscreen(o)
   If intercel(p, q) / intercel(n, o) < vi Then
    Call pentangle(n, p, q, f, o, x0, y0, x1, y1, x2, y2, x3, y3, x4, y4, x5, y5, x6, y6, x7, y7, x8, y8, x9, y9)
   Else
    Call pentangle(n, q, p, o, f, x2, y2, x1, y1, x0, y0, x4, y4, x3, y3, x6, y6, x5, y5, x8, y8, x7, y7, x9, y9)
   End If
  Else
   x9 = xqscreen(f): y9 = yqscreen(f)
   If intercel(p, q) / intercel(n, f) < vi Then
    Call pentangle(n, q, p, o, f, x2, y2, x1, y1, x0, y0, x4, y4, x3, y3, x6, y6, x5, y5, x8, y8, x7, y7, x9, y9)
   Else
    Call pentangle(q, n, o, p, f, x1, y1, x2, y2, x3, y3, x4, y4, x0, y0, x6, y6, x7, y7, x9, y9, x5, y5, x8, y8)
   End If
  End If
 End If
 Draw.Figure(fi).DrawWidth = contour
 Draw.Figure(fi).ForeColor = kc
 Draw.Figure(fi).Line (x6, y6)-(x1, y1): Draw.Figure(fi).Line -(x5, y5)
 n = n + ns
Loop
nv = nva: nt = nta
End Sub
```

Sub Growing ()

```
Dim yvDummy, zvDummy, dvDummy, xsDummy, b3, h3, c3, tt, ttt, UnitTipMax as Single
Dim UnitTipDummy,LinkDDummy, LinkZDummy, UnitLengthDummy, UnitDiffDummy As Single
Dim nvDummy, ntDummy, nsDummy, ntkDummy, t, tstep As Integer
yvDummy = yv: zvDummy = zv: dvDummy = dv: xsDummy = xs
b3 = bb(3): h3 = hh(3): c3 = cc(3)
LinkDDummy = LinkD:  LinkZDummy = LinkZ
UnitLengthDummy = UnitLength:  UnitDiffDummy = unitdiff:  UnitTipDummy = UnitTip
UnitTipMax = UnitTip + .1
nvDummy = nv:  ntDummy = nt:  nsDummy = ns:  ntkDummy = ntk
Draw.Figure(0).AutoRedraw = True
Draw.Figure(1).AutoRedraw = True
tstep = tl / steps
t = 2: nv = 1
Do
 tt = t / tls
 If t < tls Then tt = Int(tl * tt) Else tt = tl
 nt = tt:  ntk = nt
 ttt = (t / tl)
 zv = zvDummy * ttt
 If Grow.Checkdv.Value = 1 Then
  yv = zv * yvDummy / dvDummy
  dv = zv
 Else
  yv = yvDummy * ttt
  dv = dvDummy * ttt
 End If
 xs = xsDummy * ttt
 bb(3) = b3 * ttt
 'hh(3) = h3 * ttt
 cc(3) = c3 * ttt
 LinkD = LinkDDummy * ttt + 10 * (1 - ttt): LinkZ = LinkZDummy * ttt
 UnitLength = UnitLengthDummy * ttt: UnitDiff = UnitDiffDummy * ttt ^ 2
 UnitTip = UnitTipDummy * ttt + UnitTipMax * (1 - ttt)
 If spheres.rvlink.Value = 1 Then linkradius
 transcalculation
 colorcalculation
 Draw.Figure(fi).Visible = True
 fig = Abs(fig - 1)
 fi = fig
 Draw.Figure(fi).Visible = False
 Draw.Figure(fi).Picture = LoadPicture()
 Select Case shapeitem
 Case "sphere"
  sphere
 Case "needle"
  needle
 Case "leaf"
  leaf
 Case "contact"
  contact
 Case "polygon"
  polygon
 Case "n_q"
  n_q
 Case "n_p"
  n_p
 Case "p_q"
  p_q
 Case "n_z"
  n_z
 Case "n_m"
```

```
  n_m
  End Select
  If t - tstep < tls And t >= tls Then Beep
  bb(3) = b3: hh(3) = h3: cc(3) = c3
  If t < tl - tstep Then
   t = t + tstep
  ElseIf t < tl Then
   t = tl
  Else
   Exit Do
  End If
 Loop
 yv = yvDummy: zv = zvDummy: dv = dvDummy: xs = xsDummy
 UnitLength = UnitLengthDummy: unitdiff = UnitDiffDummy: UnitTip = UnitTipDummy
 LinkD = LinkDDummy: LinkZ = LinkZDummy
 If spheres.rvlink.Value = 1 Then linkradius
 nv = nvDummy: nt = ntDummy: ns = nsDummy: ntk = ntkDummy
 colorcalculation
 transcalculation
 Draw.Figure(fl).Visible = True
 Draw.Figure(Abs(fig - 1)).Visible = False
 Beep
End Sub
```

Sub Drawing ()

```
 Select Case ShapeItem
 Case "sphere"
  sphere
 Case "needle"
  needle
 Case "leaf"
  leaf
 Case "contact"
  contact
 Case "polygon"
  polygon
 Case "n_q"
  n_q
 Case "n_p"
  n_p
 Case "p_q"
  p_q
 Case "n_z"
  n_z
 Case "n_m"
  n_m
 End Select
End Sub
```

Sub contact ()

```
Dim n, p, q, o, f, po, qf, ff, oo, nva, nta As Integer
 nva = nv: nta = nt
 If nv < 3 Then
  nv = 3
 ElseIf nv = tl Then
  nv = tlt
 End If
 If nt < 3 Then
  nt = 3
 ElseIf nt = tl Then
  nt = tlt
```

```
End If
n = nv
Do While Sgn(ns) * n <= Sgn(ns) * nt
 k = kk(n)
 p = pp(n): q = qq(n): o = pp(q): f = qq(p): po = pp(o): qf = qq(f)
 x5 = xpscreen(n): y5 = ypscreen(n): x6 = xqscreen(n): y6 = yqscreen(n)
 x7 = xpscreen(q): y7 = ypscreen(q): x8 = xqscreen(p): y8 = yqscreen(p)
 x9 = xpscreen(o): y9 = ypscreen(o): x10 = xqscreen(f): y10 = yqscreen(f)
 If q = f Then
  ABC x5, y5, x6, y6, x8, y8, k
 ElseIf p = o Then
  ABC x5, y5, x6, y6, x7, y7, k
 ElseIf o = f Then
  ABCD x5, y5, x6, y6, x7, y7, x8, y8, k
 ElseIf f = po Then
  ABCDE x5, y5, x6, y6, x7, y7, x9, y9, x8, y8, k
 ElseIf o = qf Then
  ABCDE x5, y5, x6, y6, x7, y7, x10, y10, x8, y8, k
 ElseIf po = qf Then
  ff = p - (n - q)
  oo = q - (n - p)
  If ff <> f And oo <> o Then
   rff = rr(n) + rr(ff)
   xff = xx(n) + (xx(ff) - xx(n)) * rr(n) / rff    'pool, <>contact
   yff = yy(n) + (yy(ff) - yy(n)) * rr(n) / rff
   zff = zz(n) + (zz(ff) - zz(n)) * rr(n) / rff
   x13 = xt + dv * sgraph(3, n) * xff + xs * sgraph(2, n) * zff / zmax
   y13 = yt + yv * sgraph(3, n) * yff + zv * zmax * sgraph(2, n) * zff / zmax
   x14 = xqscreen(ff): y14 = yqscreen(ff)
   x15 = xpscreen(ff): y15 = ypscreen(ff)
   ABCD x13, y13, x6, y6, x7, y7, x14, y14, k
   ABCD x13, y13, x5, y5, x8, y8, x15, y15, k
  Else
  ABCDEF x5, y5, x6, y6, x7, y7, x9, y9, x10, y10, x8, y8, k
  End If
 ElseIf qf = pp(po) Then
  x11 = xpscreen(po): y11 = ypscreen(po)
  ABCDEFG x5, y5, x6, y6, x7, y7, x9, y9, x11, y11, x10, y10, x8, y8, k
 ElseIf po = qq(qf) Then
  x12 = xqscreen(qf): y12 = yqscreen(qf)
  ABCDEFG x5, y5, x6, y6, x7, y7, x9, y9, x12, y12, x10, y10, x8, y8, k
 End If
 n = n + ns
Loop
nv = nva: nt = nta
End Sub
```

Sub ABC (xa, ya, xb, yb, xc, yc, k)

```
 If Shaping.FillCheck.Value = 1 Then
  poly xc, yc: poly xa, ya: poly xb, yb
  fillpoly k
  Draw.Figure(fi).ForeColor = kc
 Else
  Draw.Figure(fi).ForeColor = k
 End If
 Draw.Figure(fi).DrawWidth = contour
 Draw.Figure(fi).Line (xa, ya)-(xb, yb): Draw.Figure(fi).Line -(xc, yc): Draw.Figure(fi).Line -(xa, ya)
End Sub
```

Sub ABCD (xa, ya, xb, yb, xc, yc, xd, yd, k)

```
If Shaping.FillCheck.Value = 1 Then
 poly xd, yd: poly xa, ya: poly xb, yb: poly xc, yc
 fillpoly k
 Draw.Figure(fi).ForeColor = kc
Else
 Draw.Figure(fi).ForeColor = k
End If
Draw.Figure(fi).DrawWidth = contour
Draw.Figure(fi).Line (xa, ya)-(xb, yb)
Draw.Figure(fi).Line -(xc, yc): Draw.Figure(fi).Line -(xd, yd): Draw.Figure(fi).Line -(xa, ya)
End Sub
```

Sub ABCDE (xa, ya, xb, yb, xc, yc, xd, yd, xe, ye, k)

```
If Shaping.FillCheck.Value = 1 Then
 poly xe, ye: poly xa, ya: poly xb, yb: poly xc, yc: poly xd, yd
 fillpoly k
 Draw.Figure(fi).ForeColor = kc
Else
 Draw.Figure(fi).ForeColor = k
End If
Draw.Figure(fi).DrawWidth = contour
Draw.Figure(fi).Line (xa, ya)-(xb, yb)
Draw.Figure(fi).Line -(xc, yc): Draw.Figure(fi).Line -(xd, yd): Draw.Figure(fi).Line -(xe, ye)
Draw.Figure(fi).Line -(xa, ya)
End Sub
```

Sub ABCDEF (xa, ya, xb, yb, xc, yc, xd, yd, xe, ye, xf, yf, k)

```
If Shaping.FillCheck.Value = 1 Then
 poly xf, yf: poly xa, ya: poly xb, yb: poly xc, yc: poly xd, yd: poly xe, ye
 fillpoly k
 Draw.Figure(fi).ForeColor = kc
Else
 Draw.Figure(fi).ForeColor = k
End If
Draw.Figure(fi).DrawWidth = contour
Draw.Figure(fi).Line (xa, ya)-(xb, yb): Draw.Figure(fi).Line -(xc, yc): Draw.Figure(fi).Line -(xd, yd)
Draw.Figure(fi).Line -(xe, ye): Draw.Figure(fi).Line -(xf, yf): Draw.Figure(fi).Line -(xa, ya)
End Sub
```

Sub ABCDEFG (xa, ya, xb, yb, xc, yc, xd, yd, xe, ye, xf, yf, xg, yg, k)

```
If Shaping.FillCheck.Value = 1 Then
 poly xg, yg: poly xa, ya: poly xb, yb: poly xc, yc: poly xd, yd: poly xe, ye: poly xf, yf
 fillpoly k
 Draw.Figure(fi).ForeColor = kc
Else
 Draw.Figure(fi).ForeColor = k
End If
Draw.Figure(fi).DrawWidth = contour
Draw.Figure(fi).Line (xa, ya)-(xb, yb): Draw.Figure(fi).Line -(xc, yc): Draw.Figure(fi).Line -(xd, yd)
Draw.Figure(fi).Line -(xe, ye): Draw.Figure(fi).Line -(xf, yf): Draw.Figure(fi).Line -(xg, yg)
Draw.Figure(fi).Line -(xa, ya)
End Sub
```

Sub poly (ByVal X As Single, ByVal Y As Single)

```
polyx(ppoly) = X
polyy(ppoly) = Y
ppoly = ppoly + 1
End Sub
```

Sub fillpoly (k)

```
Draw.Figure(fi).DrawWidth = linewidth
Dim n, i, xpix, ypix, pix as integer
Dim ia As Single
n = 0
Do While n < ppoly - 2
 If Shaping.ExitPicture.Visible = True Then Exit Do
 xpix = Abs(polyx(n + 1) - polyx(n + 2))
 ypix = Abs(polyy(n + 1) - polyy(n + 2))
 If ypix > xpix Then pix = ypix Else pix = xpix
 i = pix
 While i > 0
  ia = i / pix
  Draw.Figure(fi).Line (polyx(0), polyy(0))-(ia * polyx(n + 1) + (1 - ia) * polyx(n + 2), ia * polyy(n + 1) + (1 - ia) * polyy(n + 2)), k
  i = i - linewidth * filldensity
 Wend
 n = n + 1
Loop
ppoly = 0
End Sub
```

Function intercel (ByVal i As Integer, ByVal j As Integer) As Single

```
intercel = Sqr((xx(i) - xx(j)) ^ 2 + (yy(i) - yy(j)) ^ 2 + (zz(i) - zz(j)) ^ 2) - rr(i) - rr(j)
End Function
```

Sub triangle (n As Integer, p As Integer, q As Integer, x0, y0, x1, y1, x2, y2, x5, y5, x6, y6, x7, y7)

```
Dim x56, y56, x78, y78, vz As Single
x56 = x5 + x6: y56 = y5 + y6
vs = .5 * vw - 1: vs = vs - .0012 * vs * Sqr(tl): vz = .5 - 2 * vs
x10 = vz * x56 + 4 * vs * x7
y10 = vz * y56 + 4 * vs * y7
If Shaping.FillCheck.Value = 1 Then
 poly x0, y0: poly x5, y5: poly x10, y10: poly x7, y7
 fillpoly (kk(p))
 poly x2, y2: poly x7, y7: poly x10, y10: poly x6, y6
 fillpoly (kk(q))
 poly x1, y1: poly x6, y6: poly x10, y10: poly x5, y5
 fillpoly (kk(n))
 Draw.Figure(fi).ForeColor = kc
Else
 Draw.Figure(fi).ForeColor = kk(n)
End If
Draw.Figure(fi).DrawWidth = contour
For j = 1 To vw
 vs = .5 * vw - j: vs = vs - .0012 * vs * Sqr(tl): vz = .5 - 2 * vs
 If vs >= 0 And vs <= .25 Then        Hier zit een variabele.
  x10 = vz * x56 + 4 * vs * x7
  y10 = vz * y56 + 4 * vs * y7
  Draw.Figure(fi).Line (x5, y5)-(x10, y10): Draw.Figure(fi).Line (x6, y6)-(x10, y10)
  Draw.Figure(fi).Line (x7, y7)-(x10, y10)
 End If
Next j
End Sub
```

Sub quadrangle (n As Integer, p As Integer, q As Integer, o As Integer, x0, y0, x1, y1, x2, y2, x3, y3, x5, y5, x6, y6, x7, y7, x8, y8)

```
Dim x56, y56, x78, y78, vz As Single
x56 = x5 + x6: y56 = y5 + y6: x78 = x7 + x8: y78 = y7 + y8
vs = .5 * vw - 1: vs = vs - .0012 * vs * Sqr(tl): vz = .5 - vs
x10 = vz * x56 + vs * x78
y10 = vz * y56 + vs * y78
```

```
x11 = vs * x56 + vz * x78
y11 = vs * y56 + vz * y78
If Shaping.FillCheck.Value = 1 Then
 poly x0, y0: poly x5, y5: poly x10, y10: poly x11, y11: poly x8, y8
 fillpoly (kk(p))
 poly x3, y3: poly x8, y8: poly x11, y11: poly x7, y7
 fillpoly (kk(o))
 poly x2, y2: poly x6, y6: poly x10, y10: poly x11, y11: poly x7, y7
 fillpoly (kk(q))
 poly x1, y1: poly x5, y5: poly x10, y10: poly x6, y6
 fillpoly (kk(n))
 Draw.Figure(fi).ForeColor = kc
Else
 Draw.Figure(fi).ForeColor = kk(n)
End If
Draw.Figure(fi).DrawWidth = contour
For j = 1 To vw
 vs = .5 * vw - j: vs = vs - .0012 * vs * Sqr(tl): vz = .5 - vs
 If vs >= 0 And vs <= .25 Then
  x10 = vz * x56 + vs * x78
  y10 = vz * y56 + vs * y78
  x11 = vs * x56 + vz * x78
  y11 = vs * y56 + vz * y78
  Draw.Figure(fi).Line (x5, y5)-(x10, y10): Draw.Figure(fi).Line (x6, y6)-(x10, y10)
  Draw.Figure(fi).Line (x10, y10)-(x11, y11): Draw.Figure(fi).Line (x7, y7)-(x11, y11): Draw.Figure(fi).Line (x8, y8)-(x11, y11)
 End If
Next j
End Sub
```

<u>Sub pentangle (n As Integer, p As Integer, q As Integer, f As Integer, o As Integer, x0, y0, x1, y1, x2, y2, x3, y3, x4, y4, x5, y5, x6, y6, x7, y7, x8, y8, x9, y9)</u>

```
 Dim x56 y56, x89, y89, vz As Single
 x56 = x5 + x6: y56 = y5 + y6: x89 = x8 + x9: y89 = y8 + y9
 vs = .5 * vw - 1: vs = vs - .0012 * vs * Sqr(tl): vz = .5 - vs
 x10 = vz * x56 + vs * x7 + .5 * vs * x89
 y10 = vz * y56 + vs * y7 + .5 * vs * y89
 x12 = .5 * vs * x56 + vs * x7 + vz * x89
 y12 = .5 * vs * y56 + vs * y7 + vz * y89
 x11 = vs * x56 + vz * (x7 + x12)
 y11 = vs * y56 + vz * (y7 + y12)
 If Shaping.FillCheck.Value = 1 Then
  poly x0, y0: poly x5, y5: poly x10, y10: poly x11, y11: poly x12, y12: poly x8, y8
  fillpoly (kk(p))
  poly x4, y4: poly x8, y8: poly x12, y12: poly x9, y9
  fillpoly (kk(f))
  poly x3, y3: poly x7, y7: poly x11, y11: poly x12, y12: poly x9, y9
  fillpoly (kk(o))
  poly x2, y2: poly x6, y6: poly x10, y10: poly x11, y11: poly x7, y7
  fillpoly (kk(q))
  poly x1, y1: poly x5, y5: poly x10, y10: poly x6, y6
  fillpoly (kk(n))
  Draw.Figure(fi).ForeColor = kc
 Else
  Draw.Figure(fi).ForeColor = kk(n)
 End If
Draw.Figure(fi).DrawWidth = contour
For j = 1 To vw
 vs = .5 * vw - j: vs = vs - .0012 * vs * Sqr(tl): vz = .5 - vs
 If vs >= 0 And vs <= .25 Then
  x10 = vz * x56 + vs * x7 + .5 * vs * x89
  y10 = vz * y56 + vs * y7 + .5 * vs * y89
  x12 = .5 * vs * x56 + vs * x7 + vz * x89
```

```
  y12 = .5 * vs * y56 + vs * y7 + vz * y89
  x11 = vs * x56 + vz * (x7 + x12)
  y11 = vs * y56 + vz * (y7 + y12)
  Draw.Figure(fi).Line (x5, y5)-(x10, y10): Draw.Figure(fi).Line -(x6, y6)
  Draw.Figure(fi).Line (x10, y10)-(x11, y11): Draw.Figure(fi).Line -(x12, y12)
  Draw.Figure(fi).Line (x7, y7)-(x11, y11)
  Draw.Figure(fi).Line (x8, y8)-(x12, y12): Draw.Figure(fi).Line -(x9, y9)
 End If
Next j
End Sub
```

Sub transcalculation ()

```
Dim ddif, zdif, r As Single
Dim n, p, q As Integer
drel en zrel: maximale positieve radiale, resp. axiale translatie.
rrmax = 0: drel = 0: zrel = 0
ddmax = 0
zzmax = 0
For n = 0 To tlt
 If Spheres.rtrans.Value = 1 Then
  rrr(n) = RadTrans(n) * rr(n)
 Else
  rrr(n) = rr(n)
 End If
 If rrr(n) > rrmax Then rrmax = rrr(n)
 xxx(n) = RadTrans(n) * xx(n)
 yyy(n) = RadTrans(n) * yy(n)
 zzz(n) = AxTrans(n) * zmax
 aaa(n) = aa(n)
 ddd(n) = RadTrans(n) * dd(n)
 x = xxx(n): y = yyy(n): z = zzz(n): r = rrr(n): p = pp(n): q = qq(n)
 rp = r + rrr(p): rq = r + rrr(q)
 If rp > 0 And rq > 0 Then
  xxp(n) = x + (xxx(p) - x) * r / rp
  yyp(n) = y+ (yyy(p) - y) * r / rp
  zzp(n) = z + (zzz(p) - z) * r / rp
  xxq(n) = x+ (xxx(q) - x) * r / rq
  yyq(n) = y+ (yyy(q) - y) * r / rq
  zzq(n) = z + (zzz(q) - z) * r / rq
 End If
 If n > tls Or TheModel = "D" And n > 0 Then
  xmean(n) = (xmean(n - 1) * (n - 1) + x) / n
  ymean(n) = (ymean(n - 1) * (n - 1) + y) / n
 End If
 'Wat is de grootste radiale translatie naar buiten toe?
 ddif = ddd(n) - ddd(n - 1)
 zdif = zzz(n) - zzz(n - 1)
 If ddif > drel Then drel = ddif
 If zdif > zrel Then zrel = zdif
 If ddmax < ddd(n) Then ddmax = ddd(n)
 If zzmax < zzz(n) Then zzmax = zzz(n)
Next n
End Sub
```

Sub colorcalculation ()

```
Kleurenberekeneing volgt translaties (axiale tot radiale: ColorMode) op de voet,
tenzij deze koppeling door de gebruiker wordt teruggedrongen via ColorBalance.
colormode:    kleuring volgens axiale tot radiale translaties [top/base tot center/perifery]
colorbalance: kleuring volgens translaties tot kijkafstand [voor-achter, bepaald door aa(n)]
colorbalance=1  top/p(6)-base/c(5), ofwel (d+z)    maximaal gehonoreerd
colorbalance=0  front(0)-back(1)                   maximaal gehonoreerd
colormode=1     radiale translaties                maximaal gehonoreerd.
```

```
colormode=0    axiale translaties                         maximaal gehonoreerd
color 2 is accentkleur
d- en z- TransRel geven relatieve positieve translaties.
(bv: bloemhooldbodem, als negatieve translatie -in model naar binnen-: dTransRel=0;
bloemhoofdbodem, met sterke translatie: dd(n) - ddd(n)=groot)
 Dim n, ii As Integer
 Dim jj, d, z, a As Single
 AssignColors
 If TheModel = "D" Then ii = -1: jj = 1 Else ii = 1: jj = .5        "D" Dislodgement Model
 For n = nvk To ntk
  d = ColorMode * (ii * dTransRel(n) + jj + .5 * (dd(n) - ddd(n)) - ddd(n) / ddmax)
  z = (1 - ColorMode) * (1 - zzz(n) / zmax)            '' ((zz(n) - zzz(n)) / zmax  + zTransRel(n))
  a = Sin(aa(n))
  GetColor n, d, z, a
 Next n
 kk(0) = kk(1)
 For n = tl To tlt
  kk(n) = kk(tl)
 Next n
End Sub
```

<u>Sub AssignColors ()</u>

```
Om bij Colors-instellingen behorende berekening te garanderen:
 Red(colornumber) = Colors.RedBar.Value
 Green(colornumber) = Colors.GreenBar.Value
 Blue(colornumber) = Colors.BlueBar.Value
 kc = Colors.showcolor(3).BackColor
 kg = Colors.showcolor(4).BackColor
 If kg <> Draw.Figure(fig).BackColor Then Draw.Figure(fig).BackColor = kg
End Sub
```

<u>Sub GetColor (I As Integer, radial As Single, axial As Single, tangential As Single)</u>

```
 Dim RedPart, GreenPart, BluePart, C1, C2 As Integer
 Dim  Part, Rest As Single
 Part = Balance(radial + axial, tangential)
 If Part > 1 Then
  Part = 1
 ElseIf Part < 0 Then
  Part = 0
 End If
 Rest = 1 - Part
 If I Mod kd = 0 Then
  '2,2 zijn de indices van SignColor
  C1 = 2: C2 = 2    'SignColor
 Else
  '5,6 zijn de indices van TranslationColor
  C1 = 5: C2 = 6    'dzMaxColor
 End If
 RedPart = Part * Balance(Red(C1), Red(0)) + Rest * Balance(Red(C2), Red(1))
 GreenPart = Part * Balance(Green(C1), Green(0)) + Rest * Balance(Green(C2), Green(1))
 BluePart = Part * Balance(Blue(C1), Blue(0)) + Rest * Balance(Blue(C2), Blue(1))
 kk(I) = RGB(RedPart, GreenPart, BluePart)
End Sub
```

<u>Function Balance (ByVal Color1, ByVal Color2) As Single</u>

```
 Balance = ColorBalance * Color1 + (1 - ColorBalance) * Color2
End Function
```

Function Sgraph (ByVal ig As Integer, ByVal I As Integer) As Single

```
S-curves, voor ig= 1, 2, 3:
1 unitradius (relatie met de receptacle-radius)
2 axiale translaties (groei)
3 radiale translaties (groei)
De S-curve wordt beschreven door b, c en h.
b is 'base' minimum, c is coeff grade, h is halflife
 Sgraph = 1 - (1 - bb(ig)) / (1 + Exp(cc(ig) * (hh(ig) - i)))
End Function
```

Function AxTrans (n As Integer) As Single

```
 AxTrans = (1 - sgraph(2, n)) * (zz(n) / zmax) ^ LinkZ
End Function
```

Function RadTrans (n As Integer) As Single

```
 RadTrans = sgraph(3, n) * dd(n) ^ LinkD
End Function
```

Function diff (n As Integer) As Single

```
ananas:        UnitDiff = 0, dus differentiatie naar z = 0 en naar d = (ddmax-ddd(n))
zonnebloem:    UnitDiff = 1, dus differentiatie naar z = (1-zzz(n)/zzmax) en naar d = 0
zowel bij kleine als grote ddd groot blad
correctie bij hoog (in de top) --- klein blad
andere correcties axiaal
 Dim zpart, zrest, dpart, drest, upart, urest As Single
 zpart = zzz(n) / zzmax
 zrest = 1 - zpart
 dpart = ddd(n)
 drest = 1 - dpart
 upart = 5 * (zpart + dpart) * UnitDiff
 urest = 5 - upart
 diff = upart * zrest * dpart ^ upart + urest * zpart * drest ^ upart
End Function
```

Function dTransRel (n As Integer) As Single

```
 Dim ddif As Single
 If ddd(pp(n)) < ddd(qq(n)) Then ddif = ddd(n) - ddd(pp(n)) Else ddif = ddd(n) - ddd(qq(n))
 If ddif > 0 Then dTransRel = ddif / drel / ddmax Else dTransRel = 0
End Function
```

Function zTransRel (n As Integer) As Single

```
 Dim zdif As Single
 If zzz(pp(n)) < zzz(qq(n)) Then zdif = zzz(n) - zzz(pp(n)) Else zdif = zzz(n) - zzz(qq(n))
 If zdif < 0 Then zdif = 0
 zTransRel = 1 - zdif / zrel / zmax
End Function
```

Sub rotate (ByVal n, ByVal a)

```
Maak de structuur rond t.o.v. de Z-as.
 xx(n) = dd(n) * Cos(a)
 yy(n) = dd(n) * Sin(a)
 x = xx(n): y = yy(n): r = rr(n): p = pp(n): q = qq(n)
 rp = r + rr(p): rq = r + rr(q)
 xp(n) = x + (xx(p) - x) * r / rp
 yp(n) = y + (yy(p) - y) * r / rp
 xq(n) = x + (xx(q) - x) * r / rq
 yq(n) = y + (yy(q) - y) * r / rq
End Sub
```

```
Sub transquare ()
Maak de structuur vierkant t.o.v. de Z-as.
 Dim n As Integer, an As Single
 For n = 2 To tl
  an = aaa(n) - 2 * pi * Int(aaa(n) / pi / 2)
  If an > pi4 And an <= 3 * pi4 Then
   x = dd(n) * xx(n) / yy(n)
   y = dd(n)
  ElseIf an > 3 * pi4 And an <= 5 * pi4 Then
   x = -dd(n)
   y = -dd(n) * yy(n) / xx(n)
  ElseIf an > 5 * pi4 And an <= 7 * pi4 Then
   x = -dd(n) * xx(n) / yy(n)
   y = -dd(n)
  Else  'If aa(n) > 7 * pi4 And aa(n) <= pi4 Then
   x = dd(n)
   y = dd(n) * yy(n) / xx(n)
  End If
  xx(n) = x
  yy(n) = y
 Next n
End Sub

Function xscreen (n As Integer) As Single
 xscreen = xb + dv * xxx(n) - xs * zzz(n) / zmax
End Function

Function yscreen (n As Integer) As Single
 yscreen = yb + yv * yyy(n) - zv * zzz(n)
End Function

Function xpscreen (n As Integer) As Single
 xpscreen = xb + dv * xxp(n) - xs * zzp(n) / zmax
End Function

Function ypscreen (n As Integer) As Single
 ypscreen = yb + yv * yyp(n) - zv * zzp(n)
End Function

Function xqscreen (n As Integer) As Single
 xqscreen = xb + dv * xxq(n) - xs * zzq(n) / zmax
End Function

Function yqscreen (n As Integer) As Single
 yqscreen = yb + yv * yyq(n) - zv * zzq(n)
End Function

Function xmorescreen (n As Integer) As Single
bladtop
 xmorescreen = xb + dv * xxx(n) + dv * xx(n) * diff(n) * rr(n) * unitlength - unittip * xs * zzz(n) / zmax
End Function

Function ymorescreen (n As Integer) As Single
bladtop
 ymorescreen = yb + yv * yyy(n) + yv * yy(n) * diff(n) * rr(n) * unitlength - unittip * zv * zzz(n)
End Function
```

iii COMPUTER PROGRAMS *'APEXS'* AND *'APEXD'* COMPARED

1 PROGRAM FLOW OF *'APEXD'*

2 PROGRAM FLOW OF *'APEXS'*

The block diagrams of 'ApexD' and 'ApexS' show basic model differences.

For theoretical principles, see Chapter 4, CREATING PHYLLOTAXIS: THE STACK AND DRAG MODEL. For detailed algorithms, see Appendage ii, COMPUTER PROGRAM *'APEXS'*: KEY ALGORITHMS.

1 PROGRAM FLOW OF *'APEXD'*

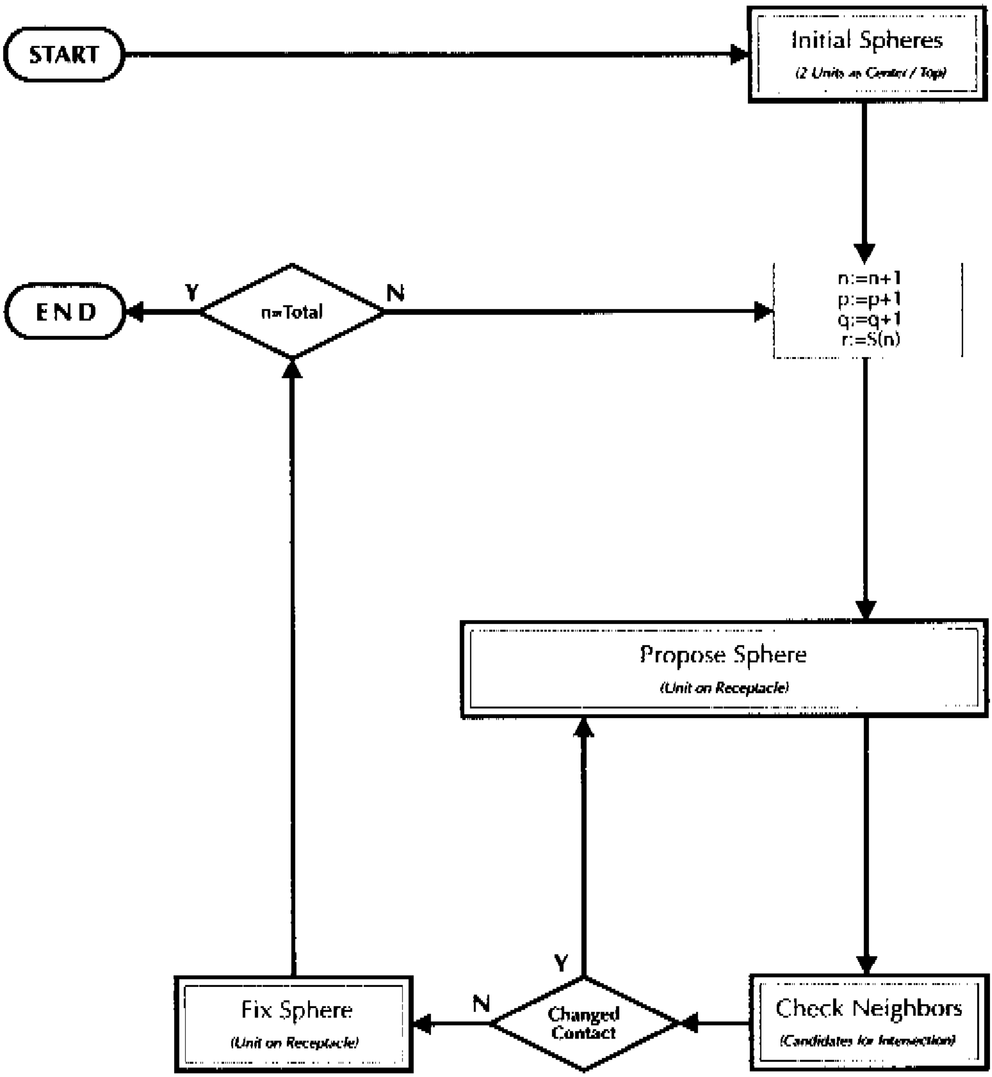

2 Program flow of '*ApexS*'

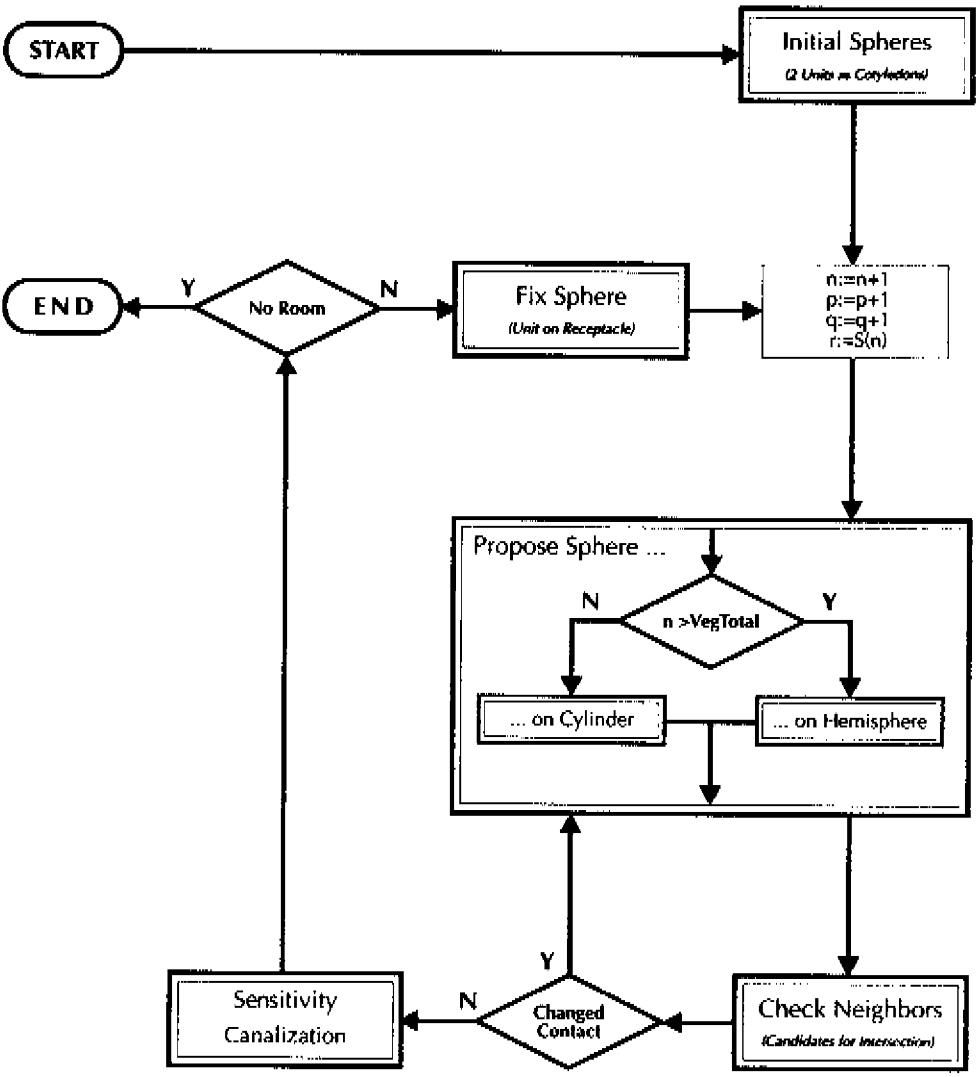

iv RESULTS OF '*APEXD*' AND '*APEXS*': STRUCTURES, GRAPHS, TABLES

1 EXAMPLES OF DISLODGEMENT STRUCTURES

2 EXAMPLES OF STACK AND DRAG STRUCTURES

1 Examples of Dislodgement structures

1.1 Stacking similar spheres on a paraboloid receptacle

The pattern starts with a hexagonal close-packing on the top, but continues with a declining phyllotactic arrangement.

1.2 Simulation of early development of Microseris Pygmaea

Scanning Electron Microscope photographs and approximations via computer program *'ApexD'* are compared.

1.3 Planar structures with different patterns and shapes

In the structures shown, the underlaying patterns and their origins are scarcely traceable. This illustrates the pattern veiling effect of translations and transfigurations.

1.4 Dome structures

While the top configuration of Dislodgement structures is orderly generated as the starting point for the entire pattern, the Dislodgement Model couples complexity with controlled regularity in augmenting numbers of phyllotactic sequences.

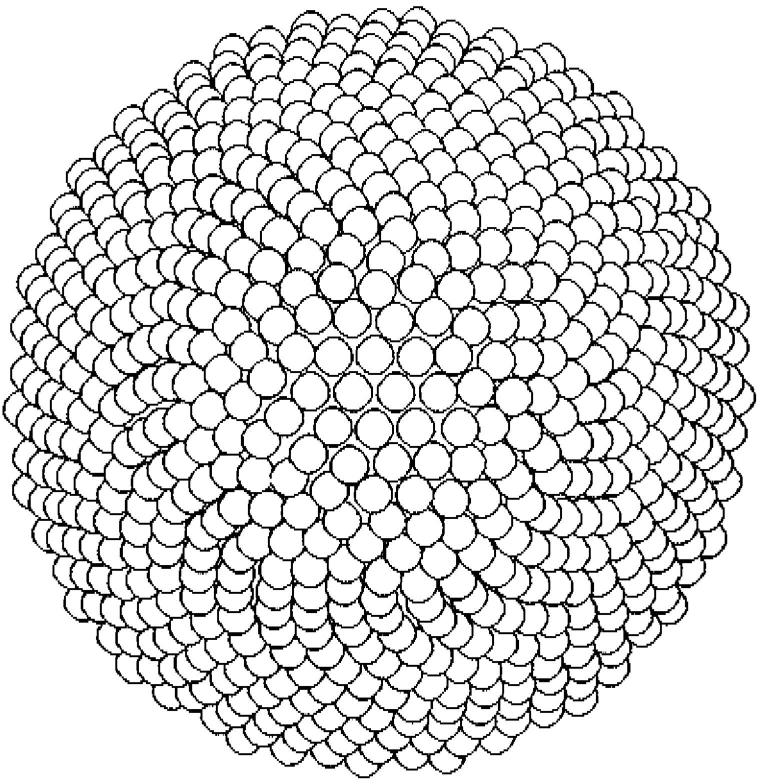

I.1 Similar spheres fill a paraboloid receptacle, showing a gradual transition from the hexagonal (flat plane dense packing) pattern to (in this case) a Fibonaccian pattern. In fact, the central spheres have also Fibonacci-neighbors; numbering the spheres would reveal this.

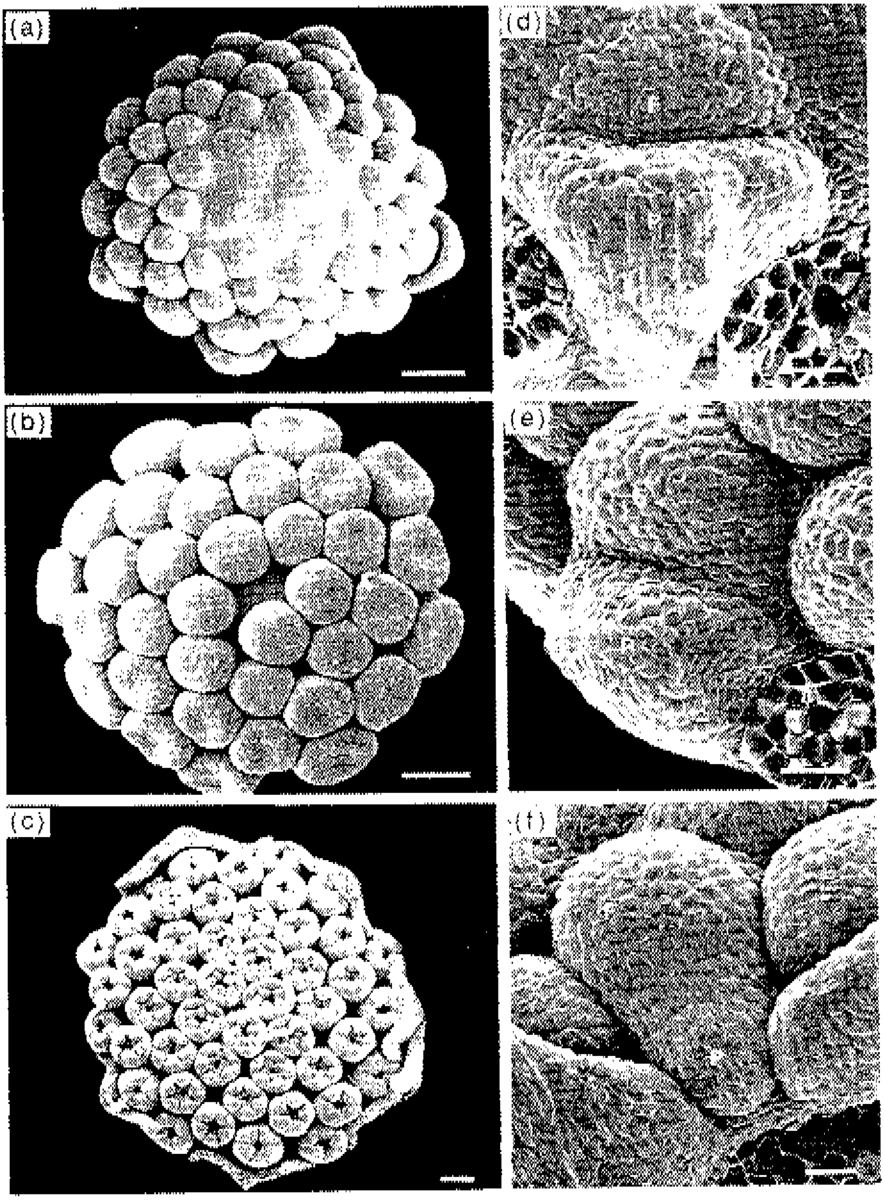

1.2a Early development of *Microseris Pygmaea*: SEM photographs (J. Battjes, 1994).

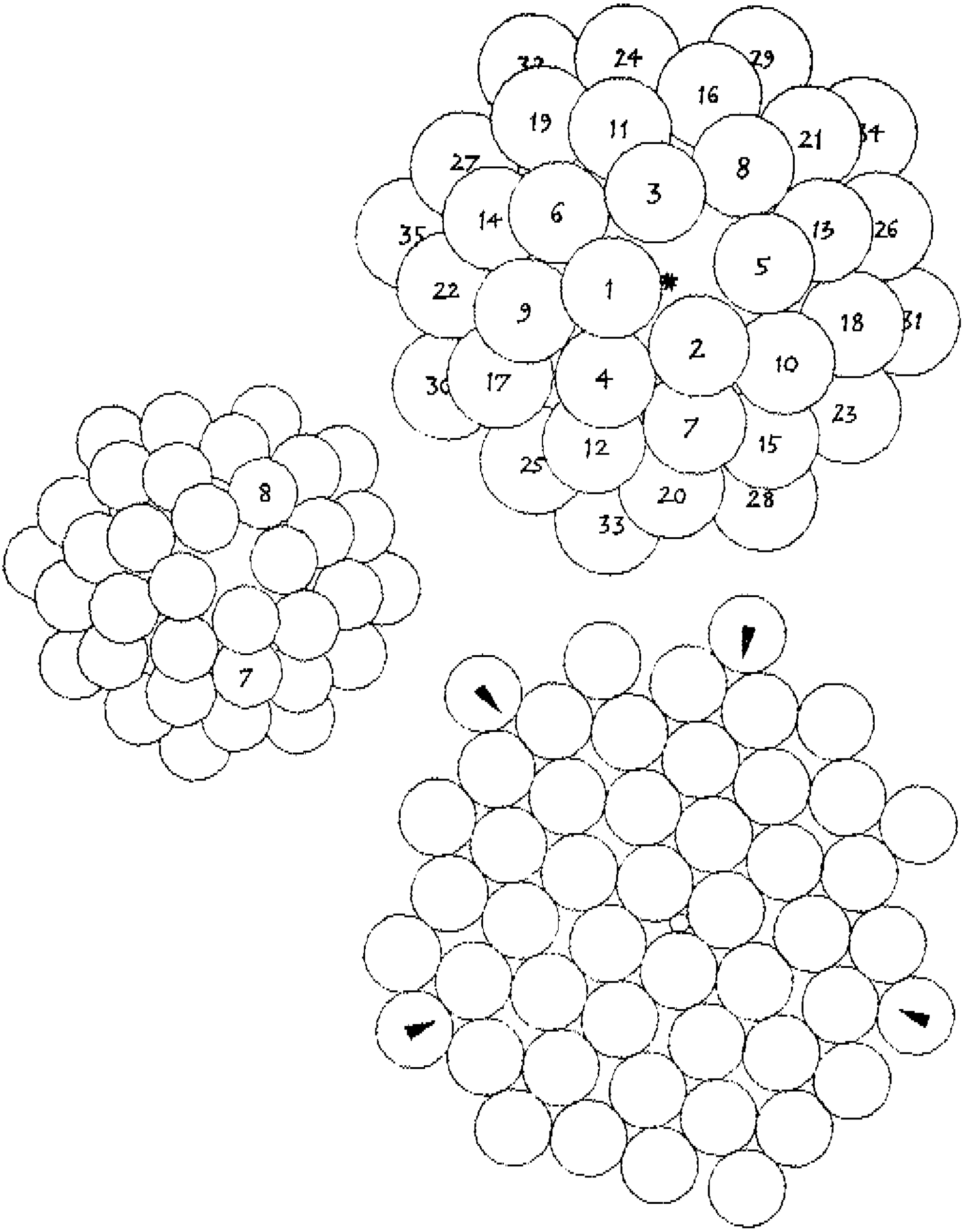

1.2b (top) Modeled structure of photograph *b* (see Fig 1.2a, previous page) which shows deviations at *n=7* and *n=8*, at the same scale and magnified. *(below)* Simulation of photograph *c*. The central additional unit defines the room between the central units which are constructed first in the Dislodgement Model.

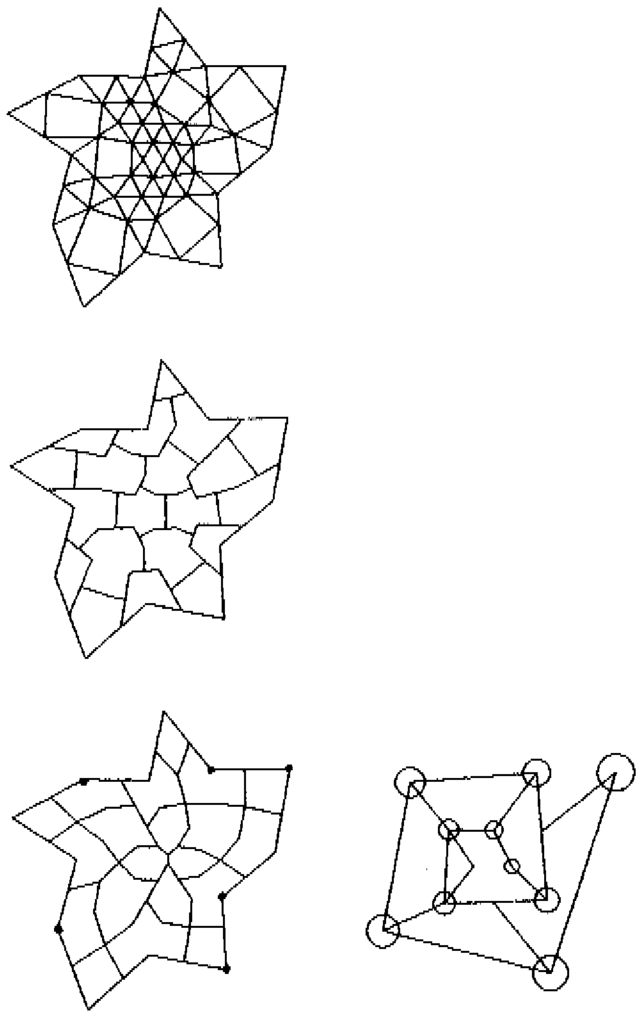

1.3 (pp 6-13) Planar structures with different patterns and shapes.
Illustrating the concealing character of *shape* (or differentiation) 'on top of' ***pattern***, the structures are presented without explanation.

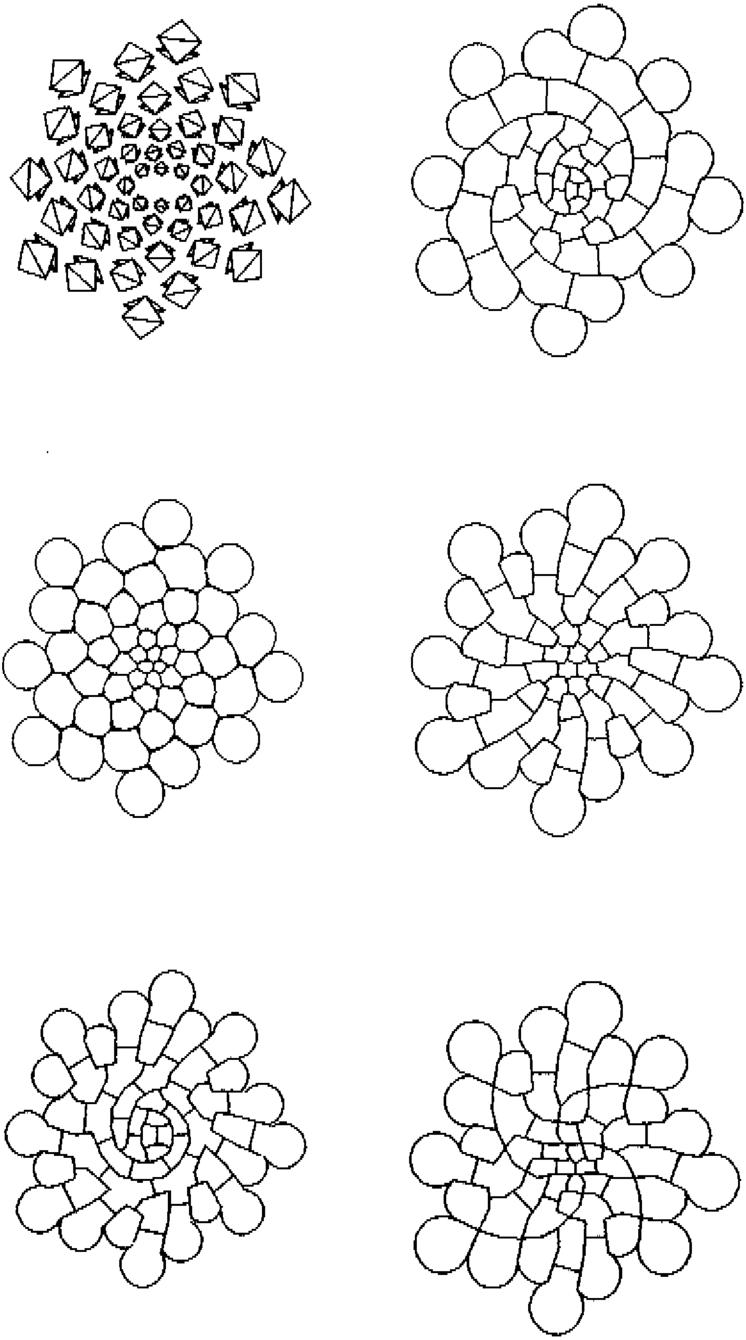

RESULTS OF '*APEXS*' AND '*APEXD*' iv.7

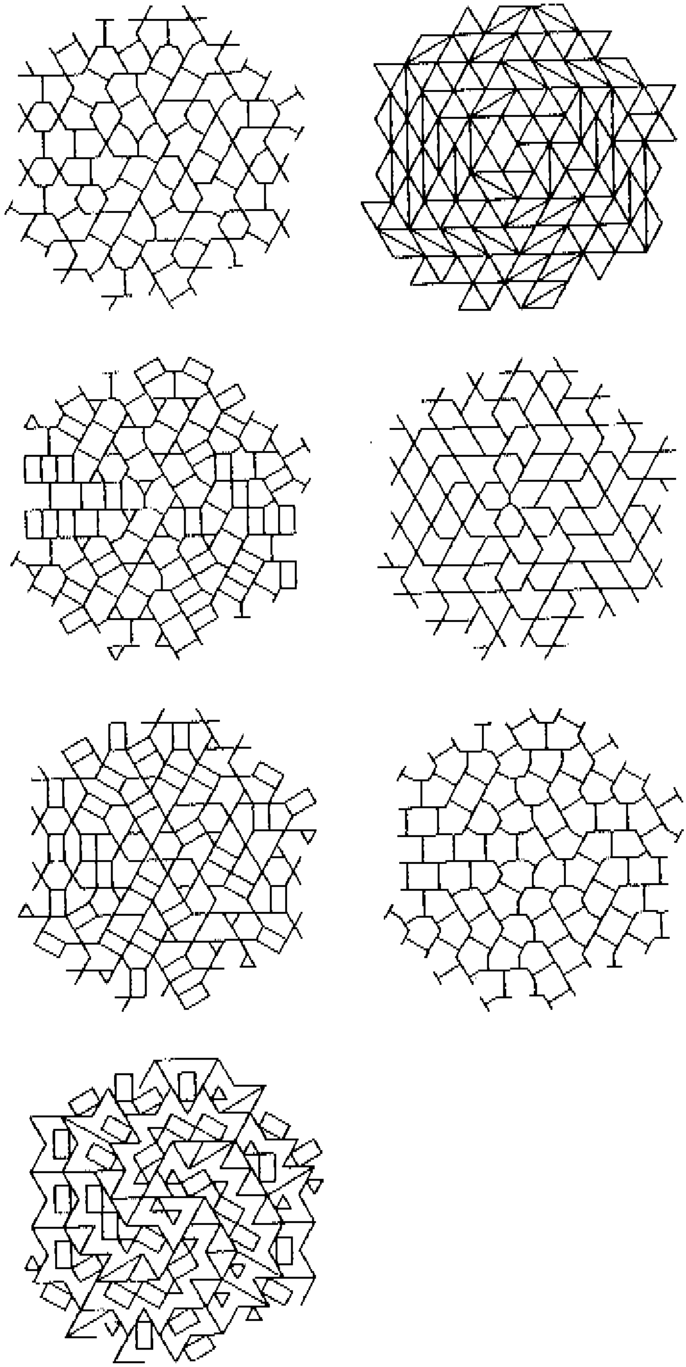

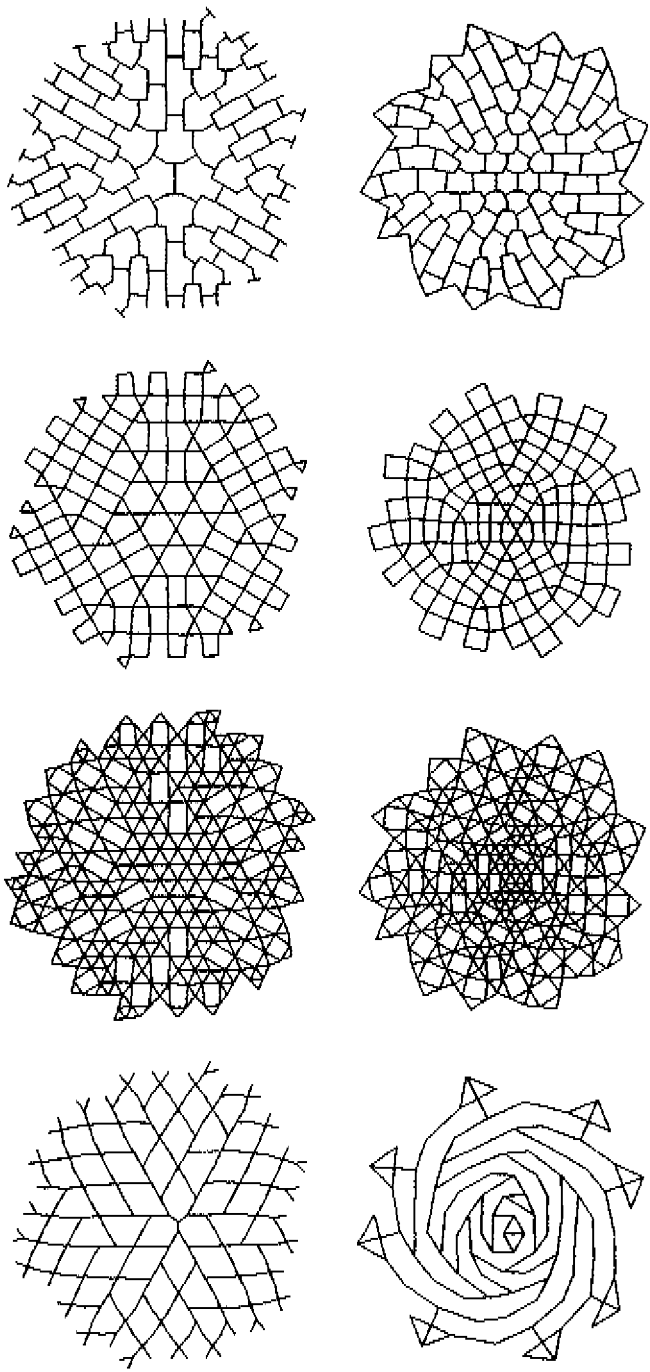

RESULTS OF '*APEXS*' AND '*APEXD*' iv.9

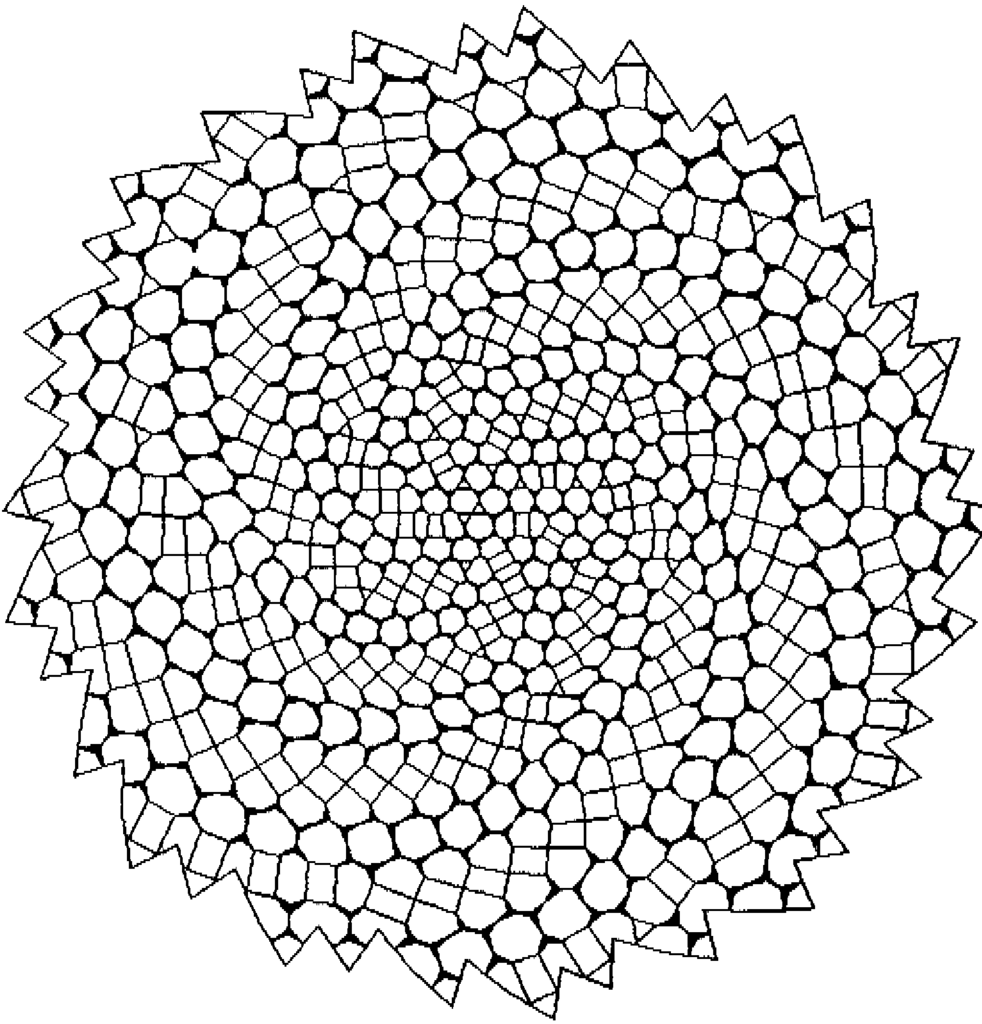

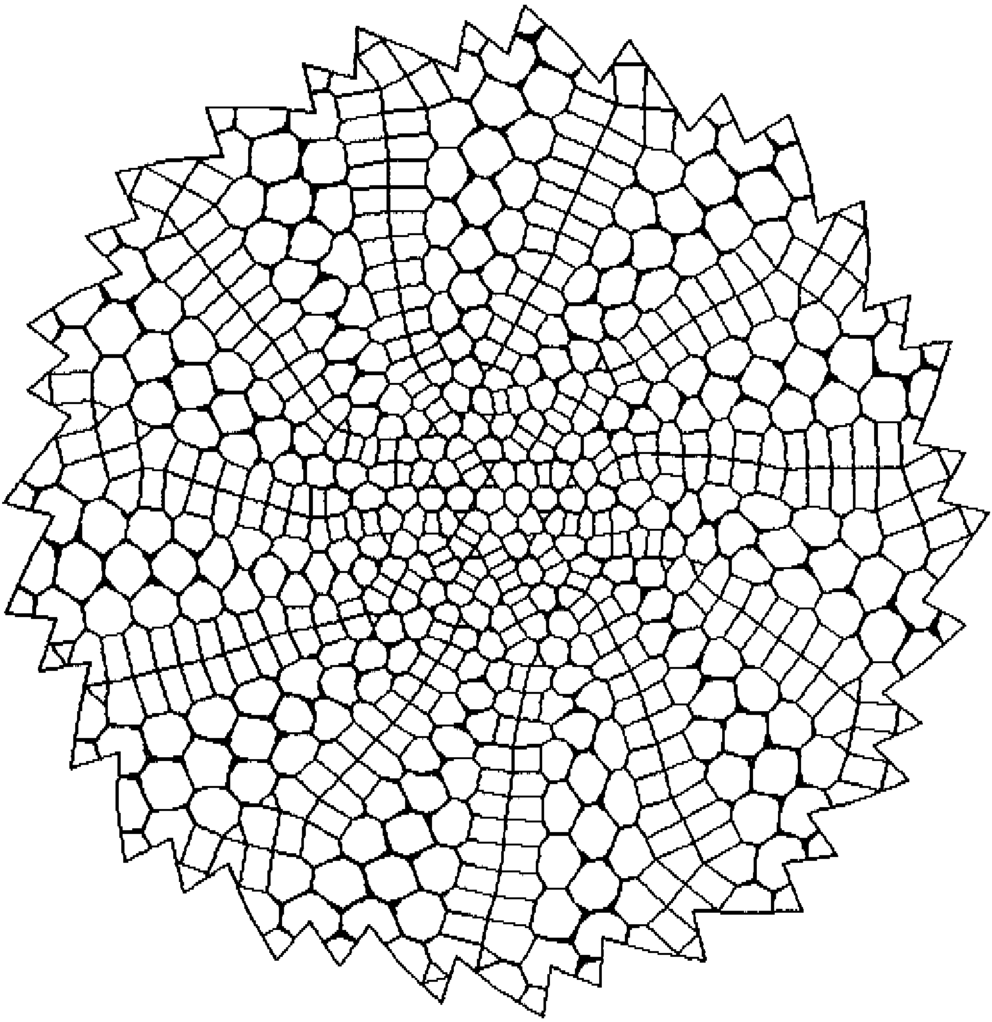

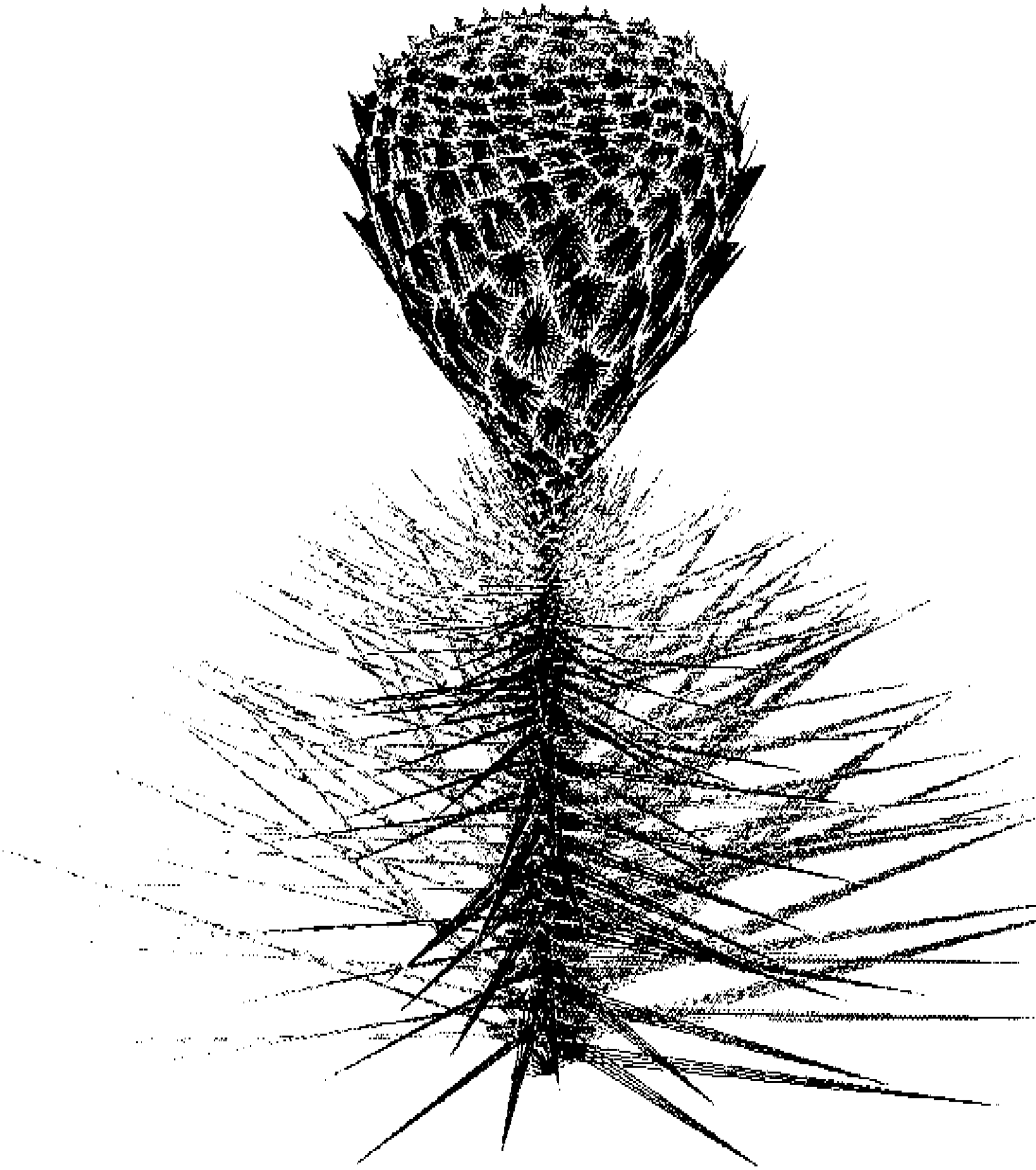

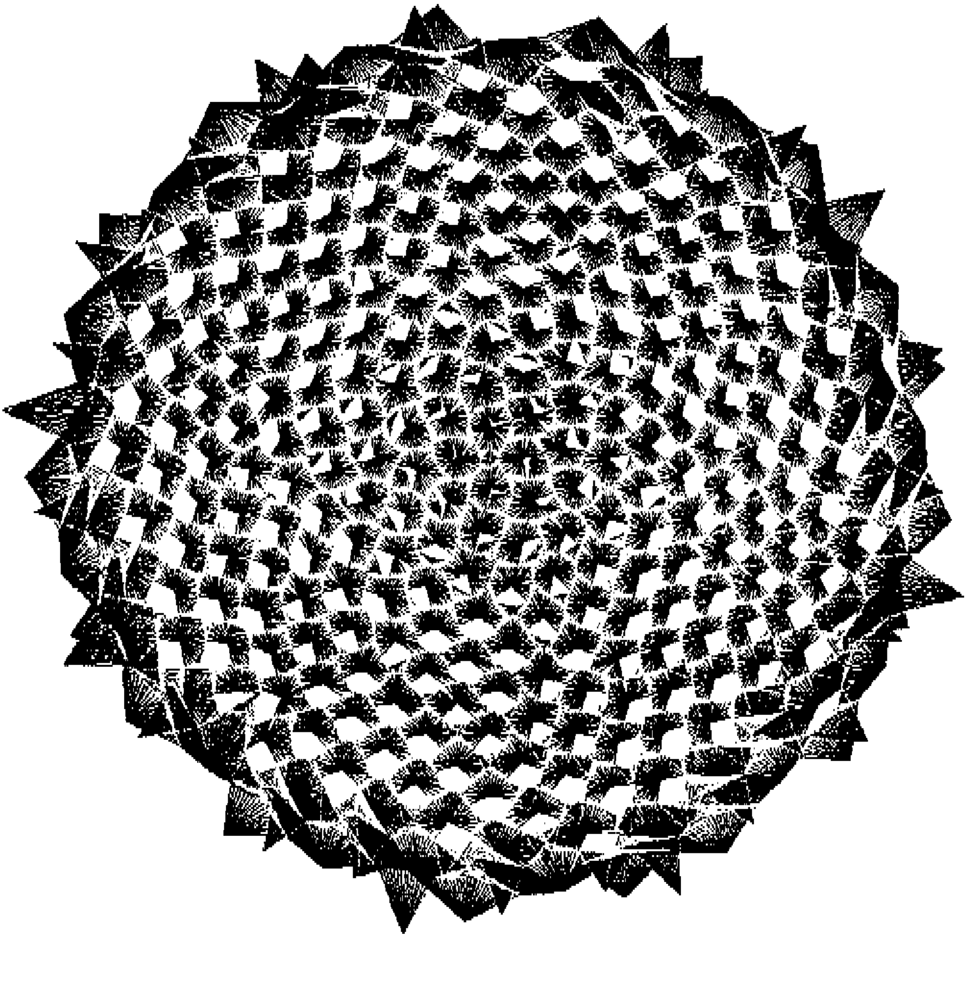

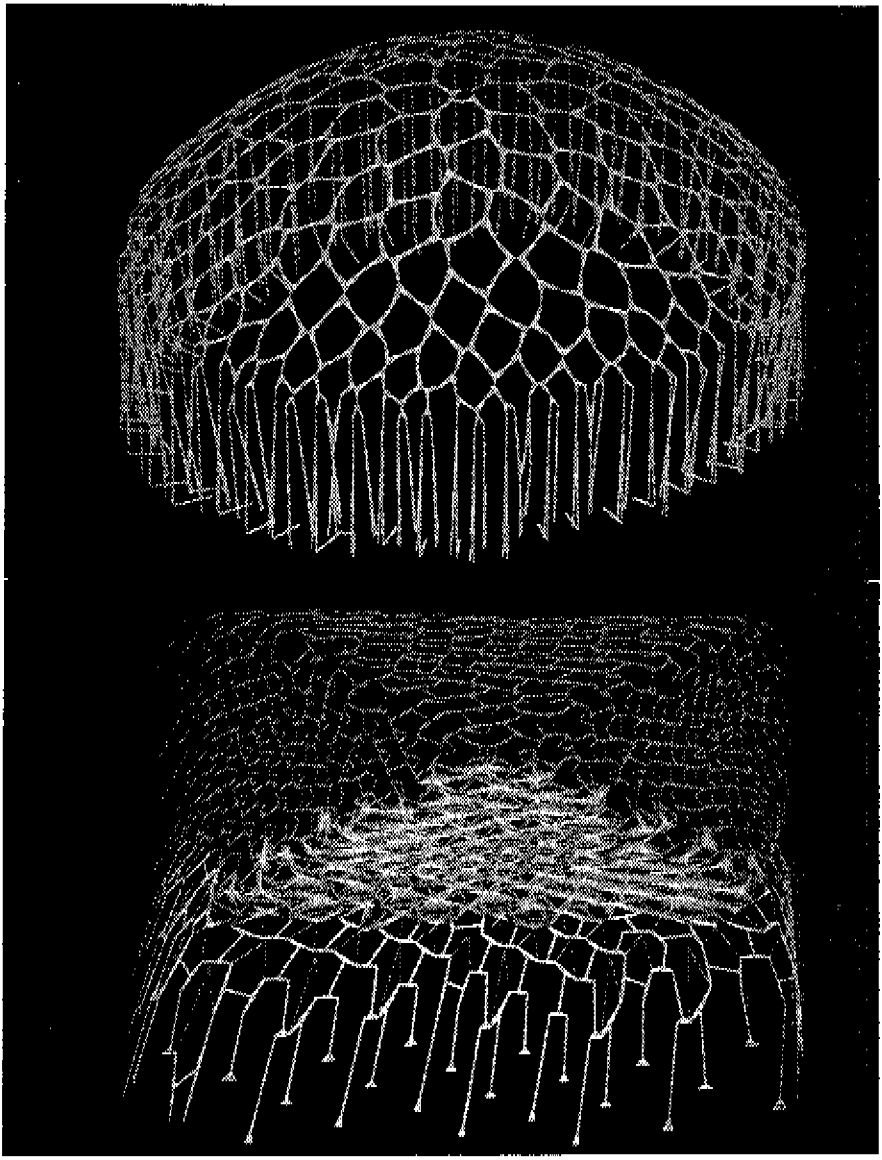

***1.4** (pp 14-23)* Spatial structures with different patterns and shapes.
(Most of the pictures shown are screen photographs.)

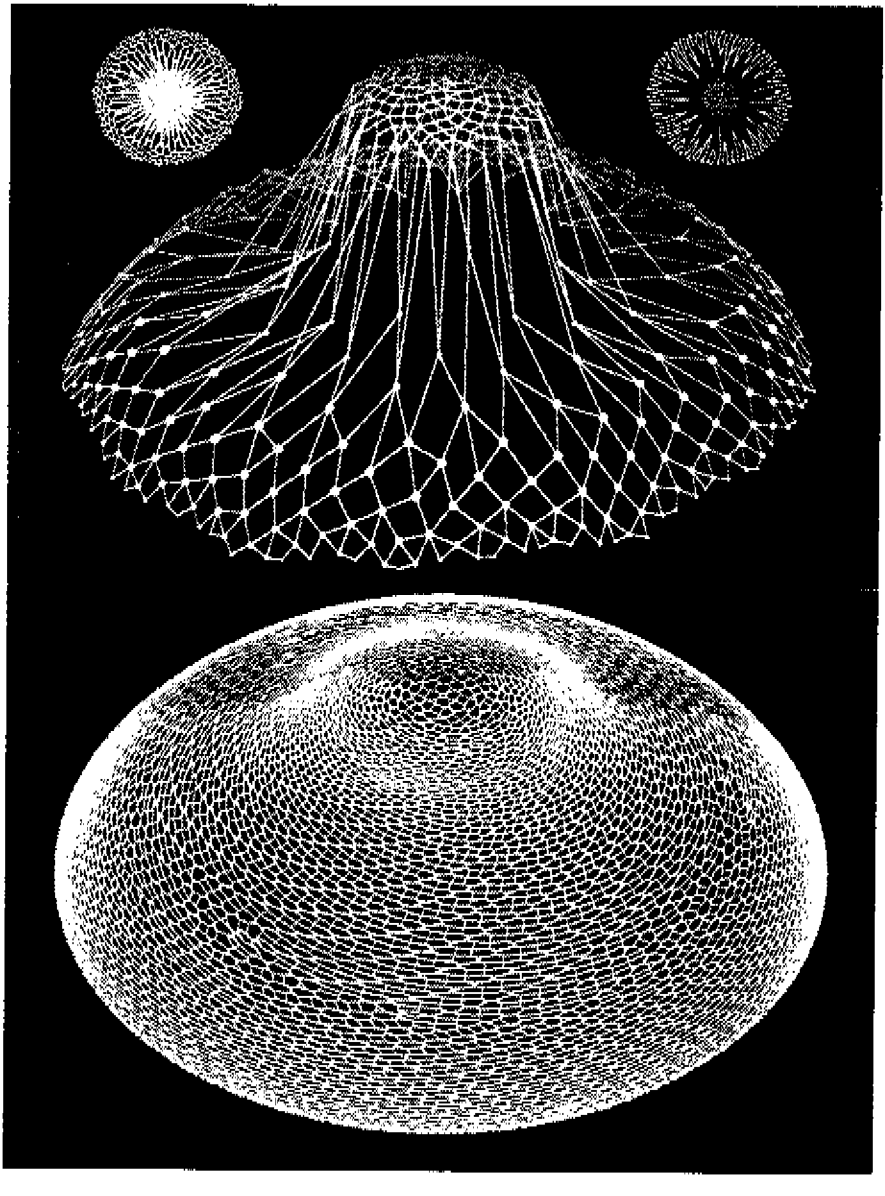

Results of '*ApexS*' and '*ApexD*'

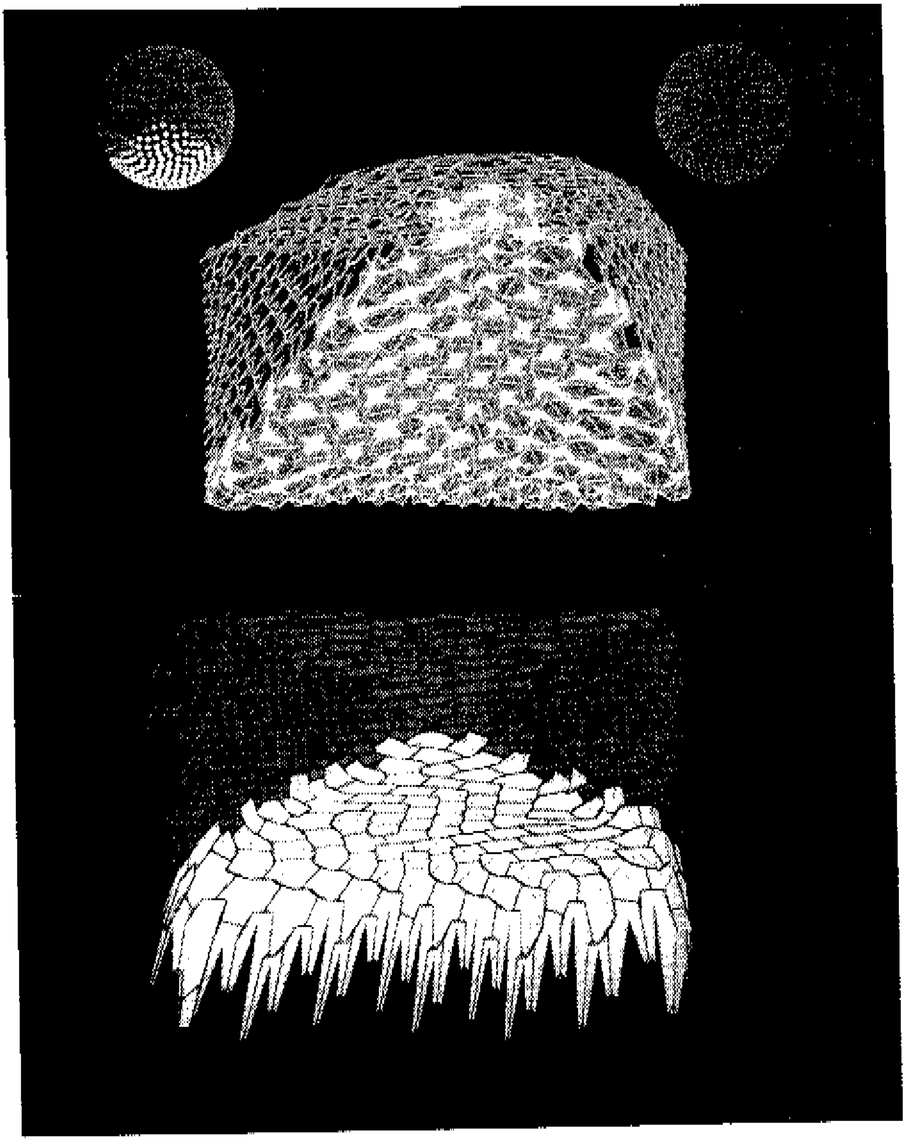

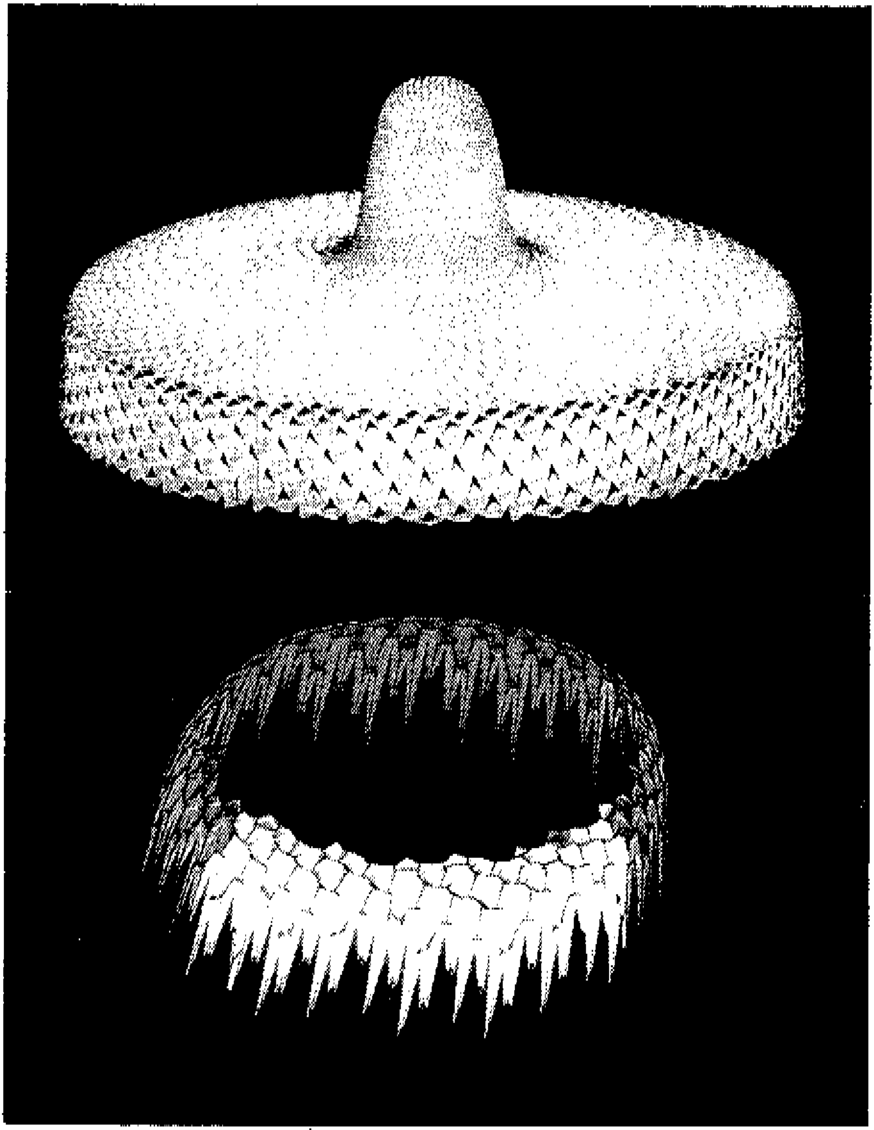

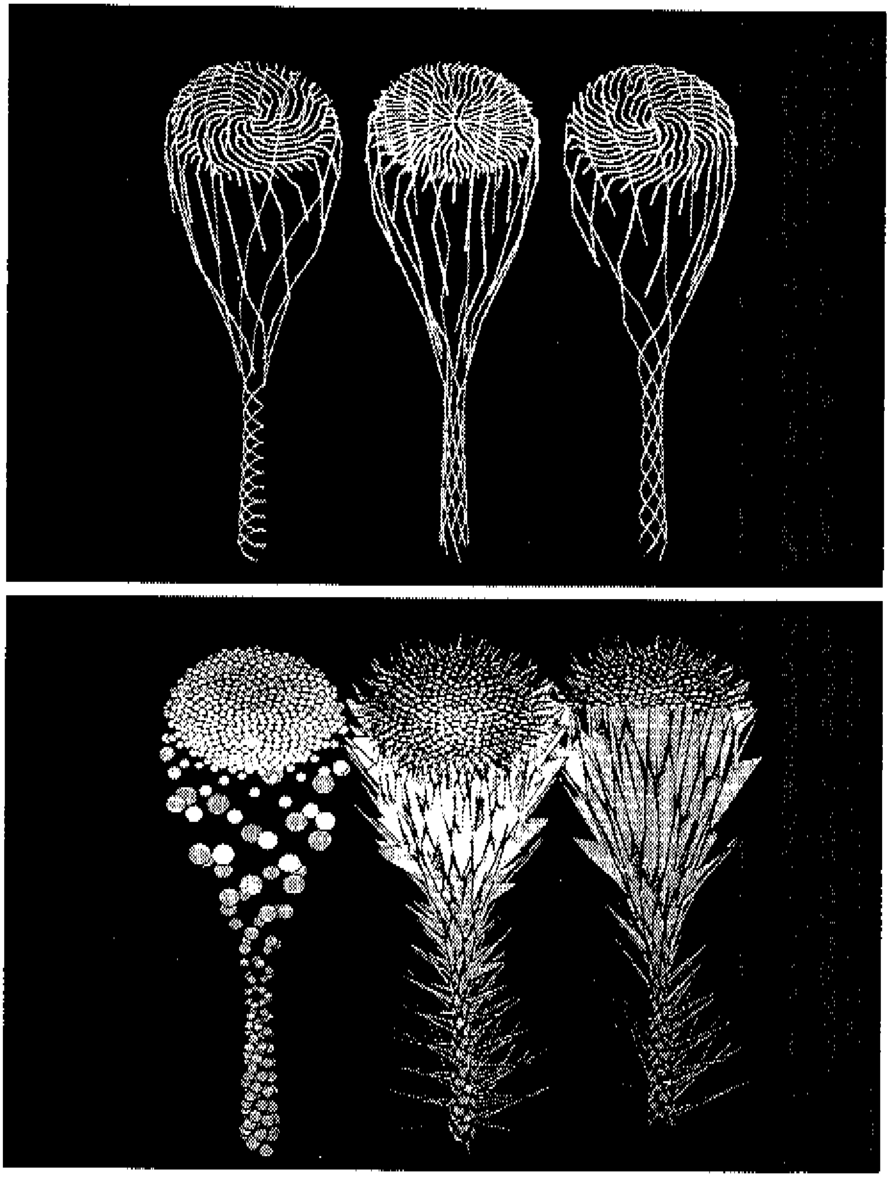

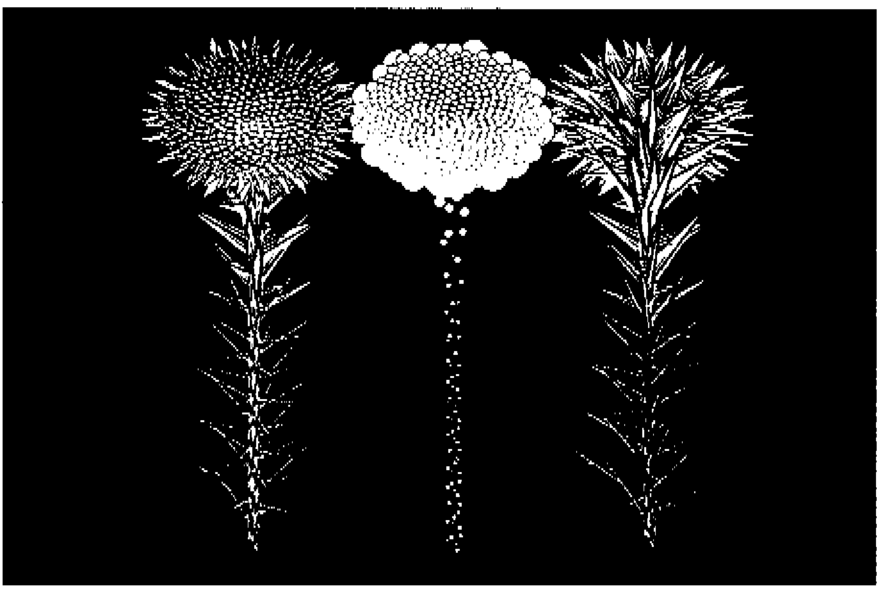

RESULTS OF *'APEXS'* AND *'APEXD'* iv.19

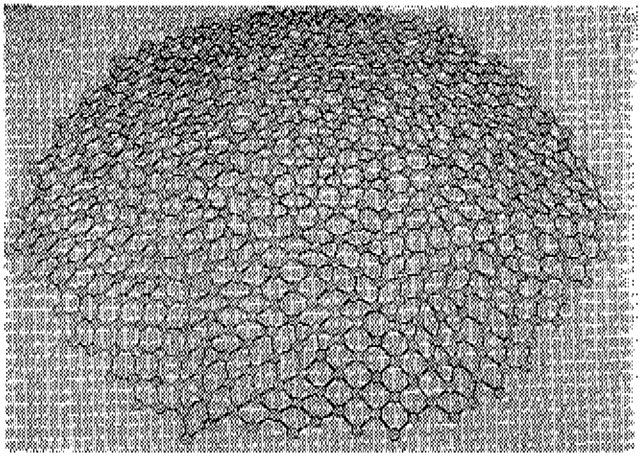

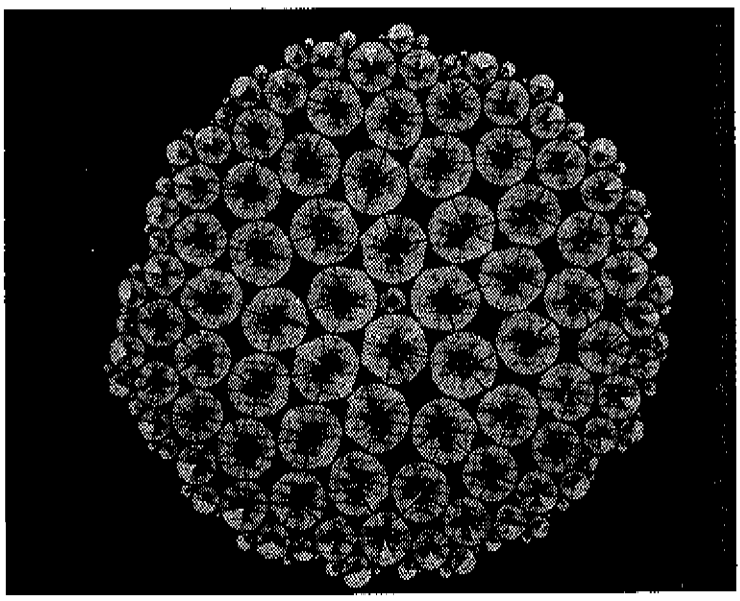

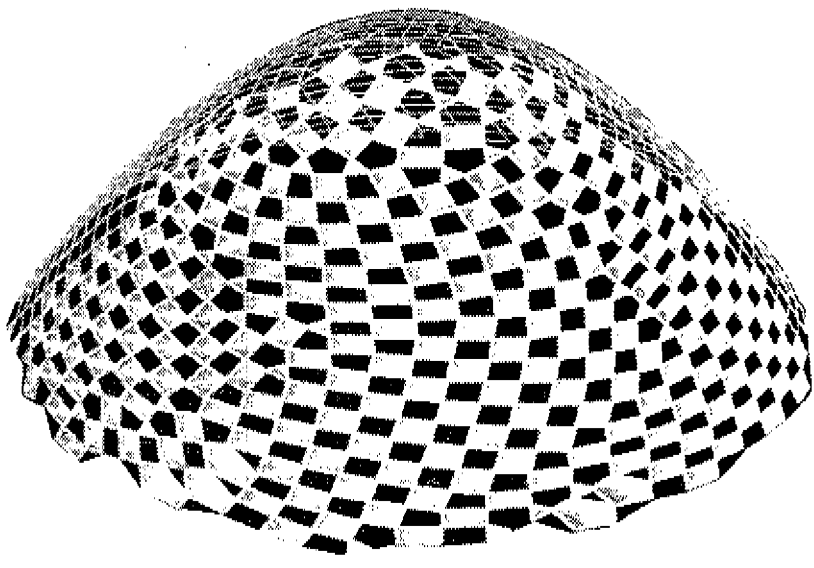

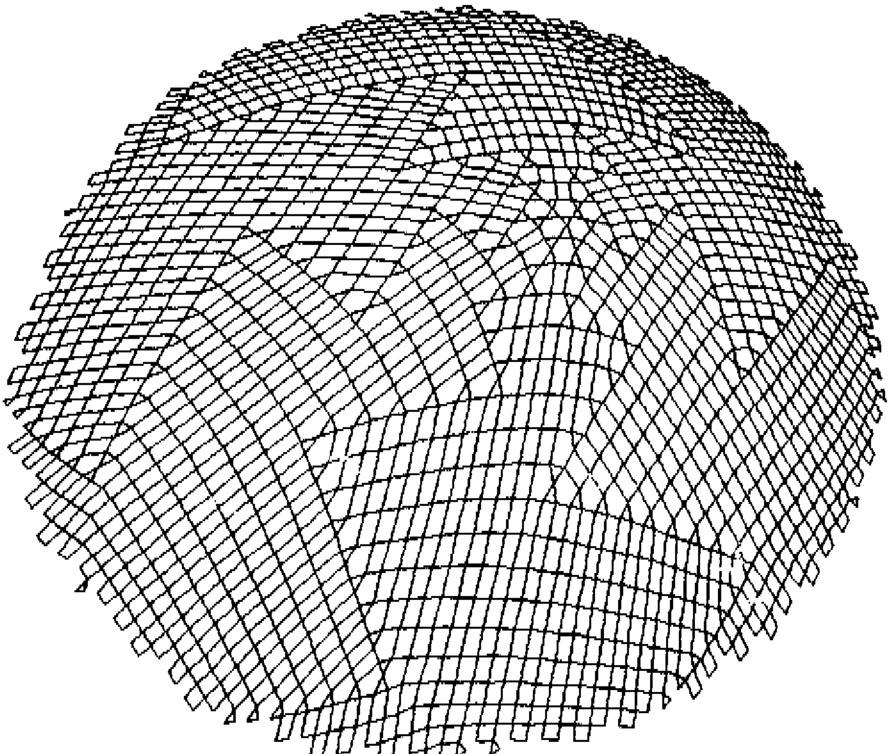

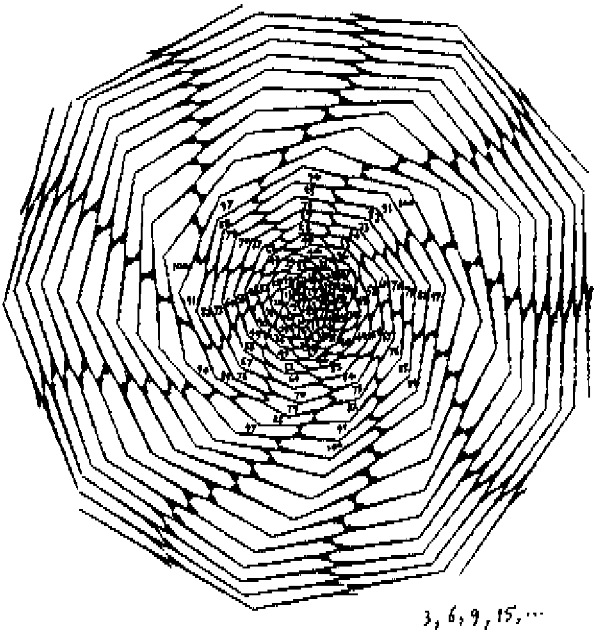
3, 6, 9, 15, ...

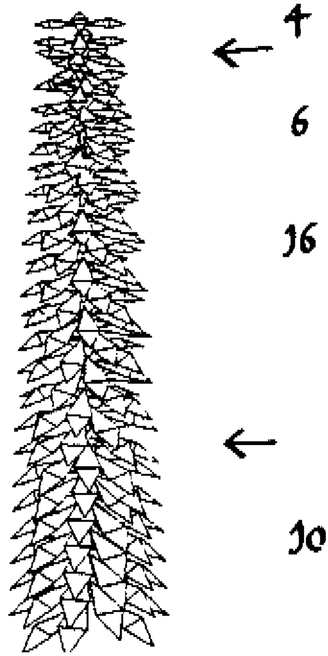
4
6
16
10

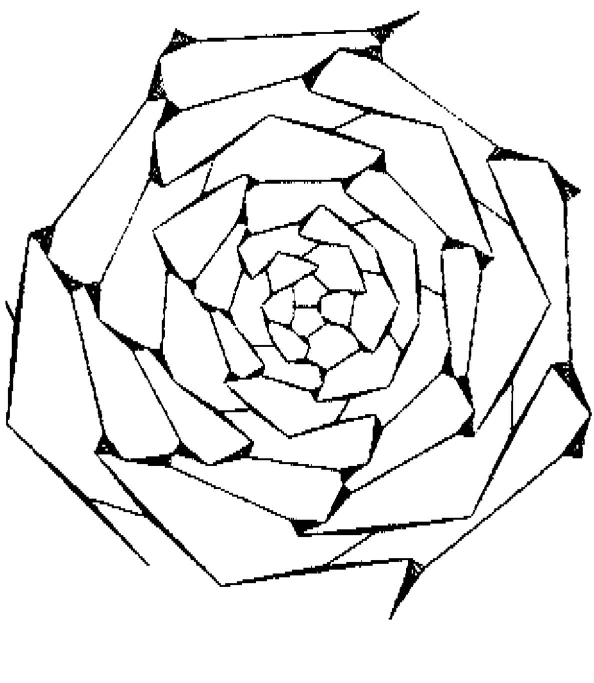

2 *Examples of Stack and Drag structures*

2.1 *Simulation of some existing and virtual plant structures*

Below, the 15 structures as discussed in Chapter 4, 'CREATING PHYLLOTAXIS: THE STACK AND DRAG MODEL' are outlined by graphical and numerical output of the computer program *'ApexS'*. Table and graph legends are similar and easy comparable between simulations:

(total numb units) *(units on cylinder)*	inflor/***specif***
TABLE (description of numerical presentation)	
GRAPH (description of graphical presentation)	

2.2 *A remarkable 'bug'*

'Frac21' shows spontaneous branching caused by a computer programming ***bug*** which had to be eliminated, for spheres may not be stacked outside the predefined receptacle.

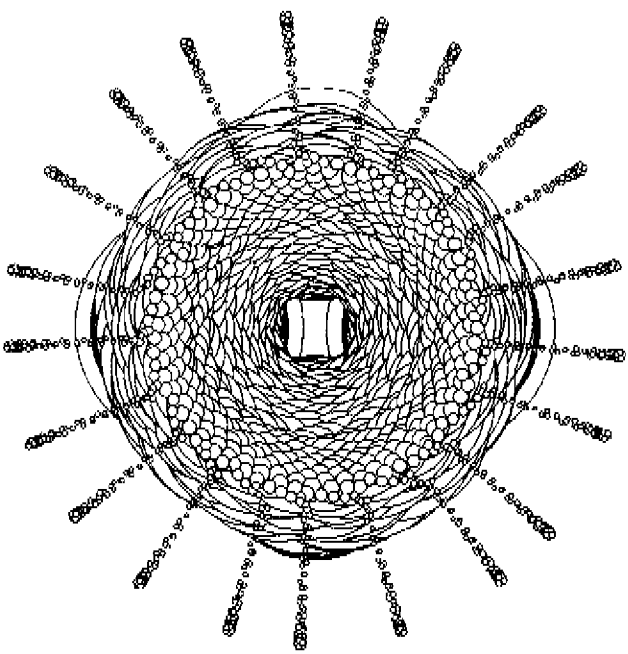

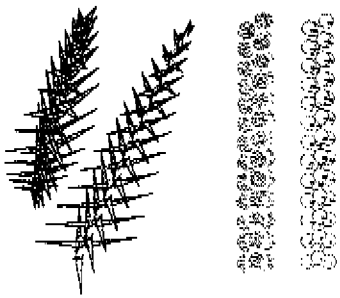

veg/***dec***	unit range 1-50 *vegetative part 1-50*
GRAPH	
elevation of unit(n) related to the centers of the two initial units	

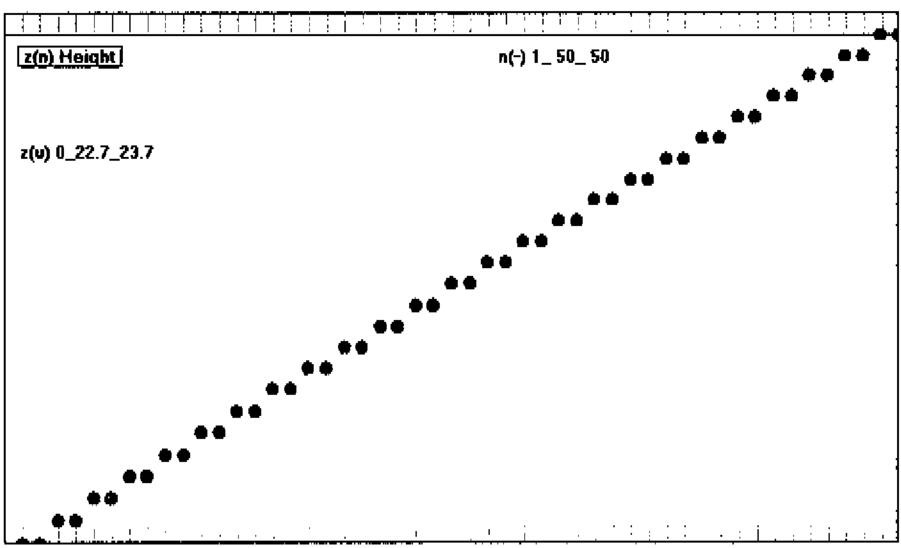

unit range 1-40 *vegetative part 1-40*	veg/***gibb***

GRAPH

divergence angle (center independent deduced from 3 successive units with ordinals n+a, n, n-a), a=1

GRAPH

unit radius r(n)

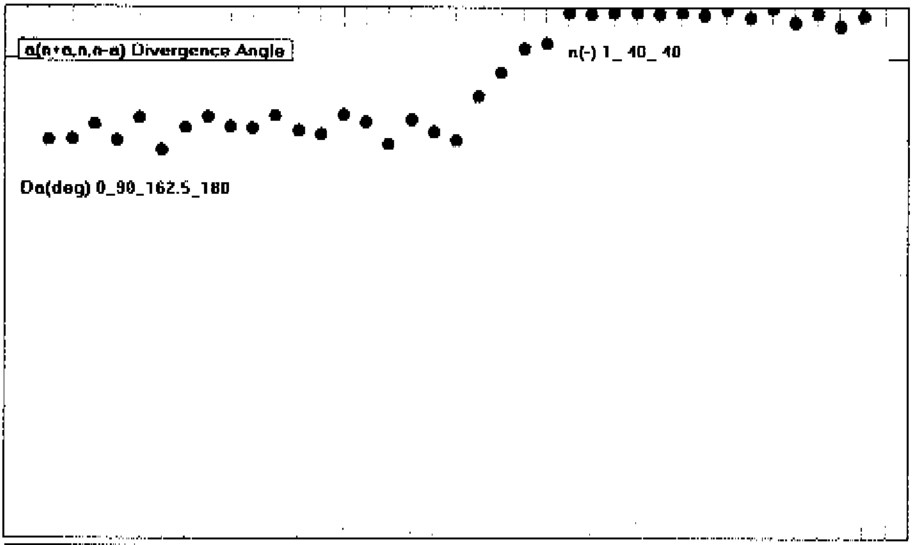

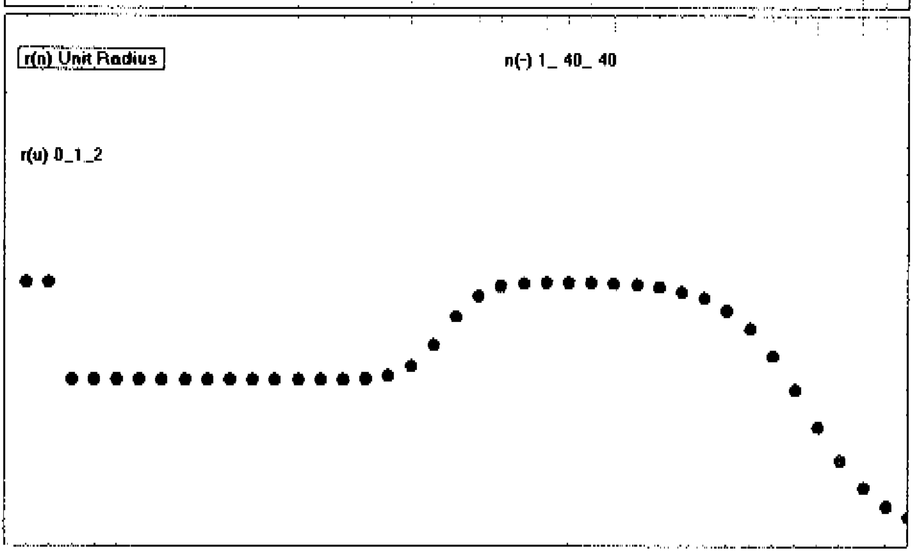

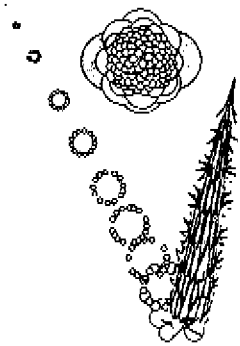

veg/***canal***	unit range 1-113 *vegetative part 1-30*

TABLE

changings in support units (or contacts) p(n) and q(n)

GRAPH

divergence angle (center independent deduced from 3 successive units with ordinals n+a, n, n-a), a=8

001		*021*	q→p+q-n	041		061	p→p+n-q	081		101	
002		*022*		042		062		082	p→p+q-n	102	
003		*023*		043		063		083		103	
004	p→q+q-p	*024*		044		064		084		104	
005		*025*		045	p→p+n-q	065		085		105	
006	q→p+q-n	*026*		046		066	p→p+q-n	086		106	
007		*027*		047		067		087	p→p+n-q	107	
008	q→q+n-p	*028*		048		068		088		108	q→q+n-p
009		*029*	p→p+q-n	049		069		089		109	
010	q→p+q-n p→p+q-n	*030*		050		070		090		110	
011	p→p+n-q	031		051		071		091		111	
012		032	p→p+n-q	052		072		092		112	
013	p→p+q-n	033		053	p→p+q-n	073		093		113	p→p+n-q
014		034		054		074	p→p+n-q	094			
015		035		055	q→p+q-n	075		095	p→p+q-n		
016		036		056		076		096			
017		037	p→p+q-n	057		077		097			
018		038		058	q→q+n-p	078		098			
019		039		059		079		099			
020		040		060		080		100	p→p+n-q		

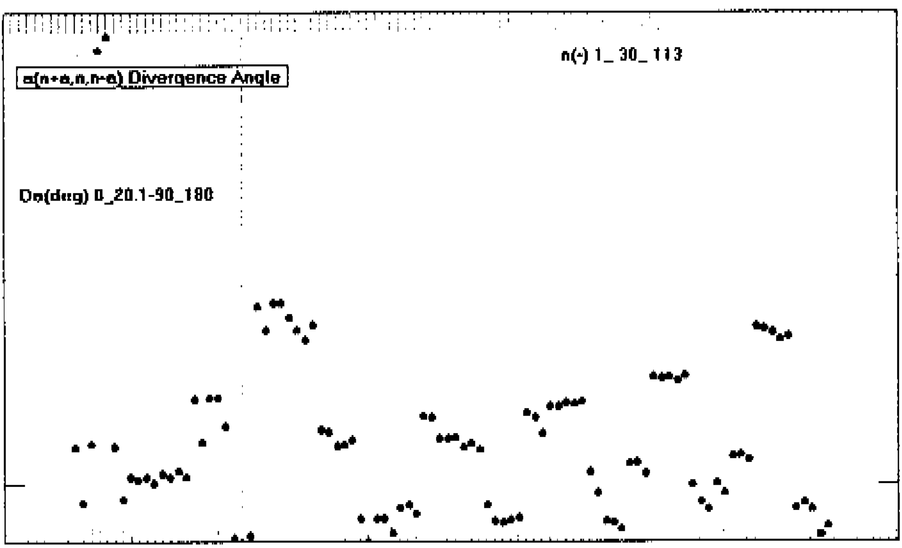

unit range 1-32 *vegetative part 1-10*	flow/*8532*

TABLE

distance of unit's center from the z-axis

GRAPH

radial distance d(unit center, z-axis)

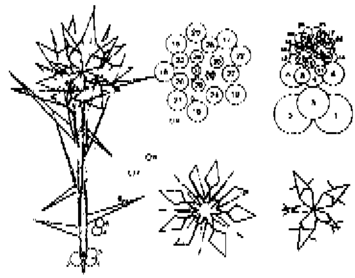

001	*0.100*	021	0.797
002	*0.100*	022	0.800
003	*0.100*	023	0.361
004	*0.100*	024	0.364
005	*0.100*	025	0.364
006	*0.100*	026	0.364
007	*0.100*	027	0.366
008	*0.100*	028	0.126
009	*0.100*	029	0.127
010	*0.100*	030	0.127
011	*0.100*	031	0.033
012	0.100	032	0.034
013	0.100		
014	0.166		
015	0.783		
016	0.792		
017	0.794		
018	0.792		
019	0.795		
020	0.795		

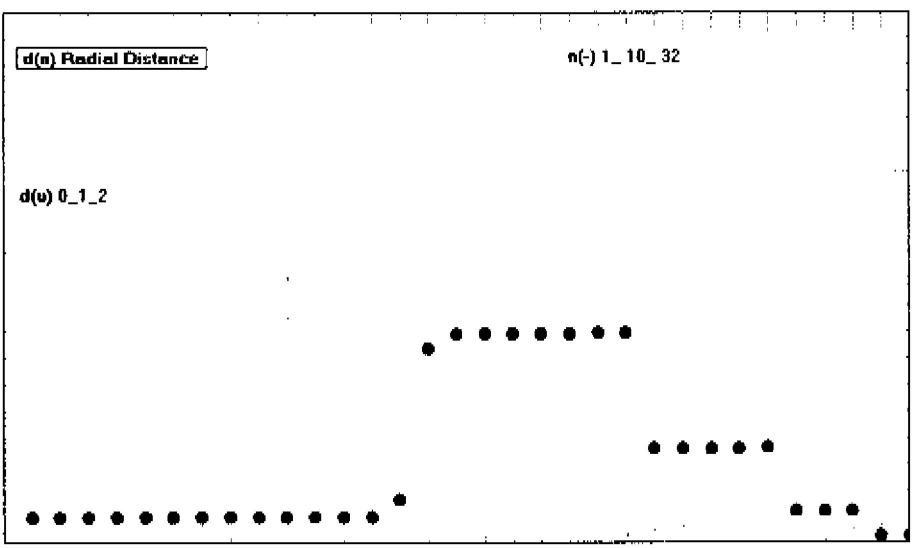

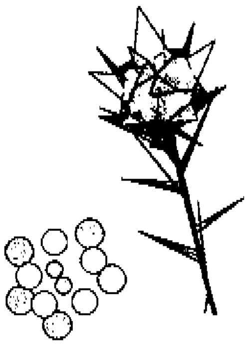

flow/52	unit range 1-24 *vegetative part 1-10*
TABLE	
distance of unit's center from the z-axis	
GRAPH	
support units (or contacts) with ordinals p and q of unit(n)	

001	*0.050*	021	0.636
002	*0.050*	022	0.637
003	*0.050*	023	0.186
004	*0.050*	024	0.186
005	*0.050*		
006	*0.050*		
007	*0.050*		
008	*0.050*		
009	*0.050*		
010	*0.050*		
011	0.050		
012	0.050		
013	0.918		
014	0.921		
015	0.921		
016	0.924		
017	0.925		
018	0.630		
019	0.634		
020	0.636		

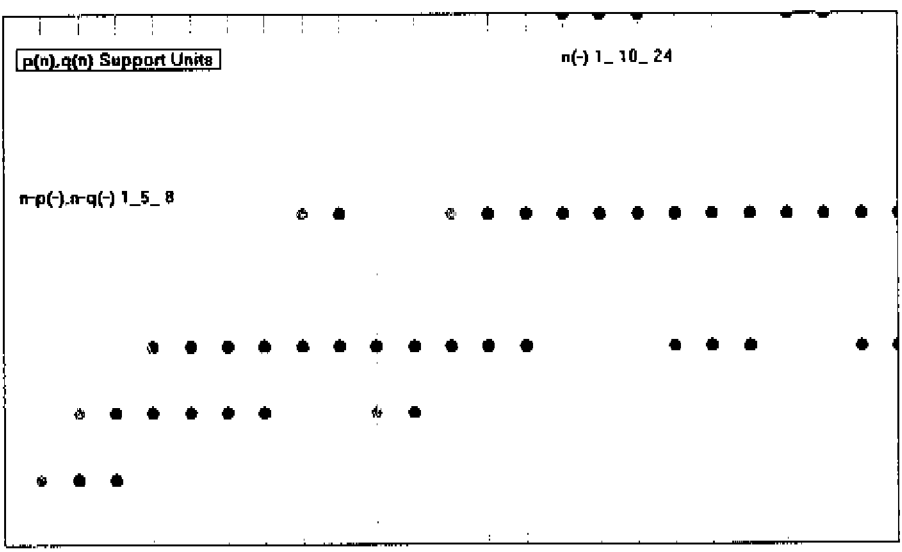

unit range 1-16
vegetative part 1-5

flow/***333***

TABLE

distance of unit's center from the z-axis, as different from that of unit(n-1), related to max difference

GRAPH

radial distance is d(unit center, z-axis); relative radial distance is {distance(n) - distance(n-a)}, a=1

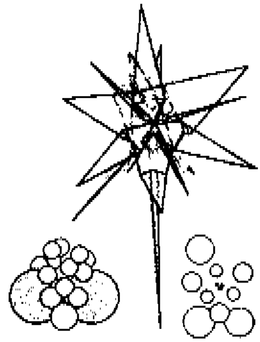

001	
002	*0.000*
003	*0.002*
004	*1.000*
005	*0.002*
006	0.000
007	0.000
008	-0.423
009	0.000
010	0.000
011	-0.346
012	0.000
013	0.000
014	-0.402
015	0.000
016	0.000

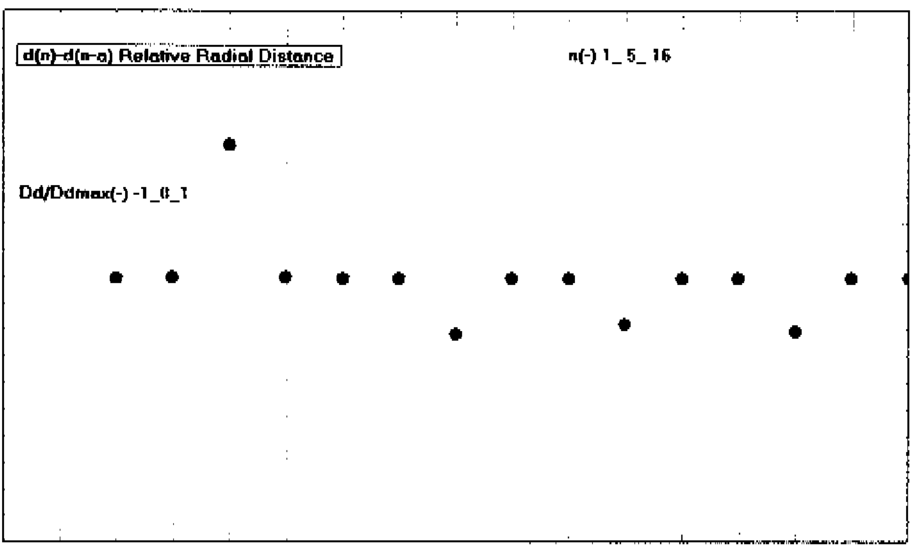

flow/***1313***	unit range 1-79 *vegetative part 1-20*

GRAPH

radial distance d(unit center, z-axis)

GRAPH

divergence angle (center independent deduced from 3 successive units with ordinals n+a, n, n-a), a=5

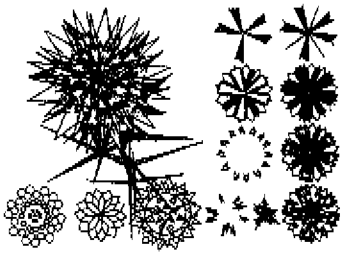

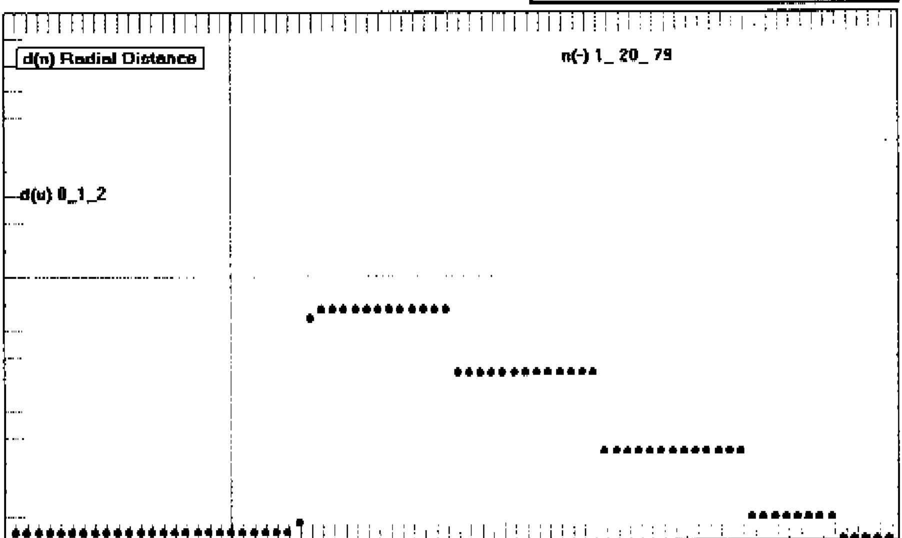

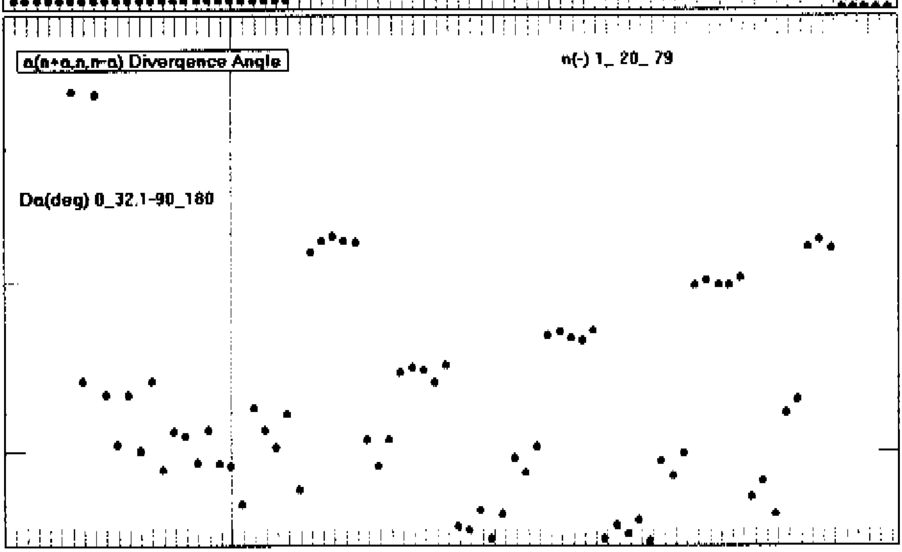

unit range 1-142
vegetative part 1-100

flow/***wild***

GRAPH

changings in support units (or contacts)
p(n) and q(n) of unit(n)
NB graph is an unrolled cylinder

GRAPH

unit(n)-stem ratio is
radius(n) / distance(center(n) to z-axis)

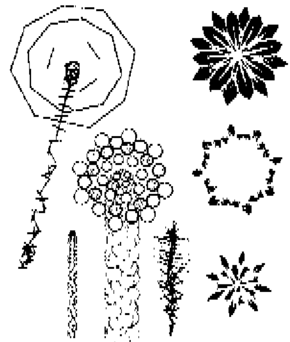

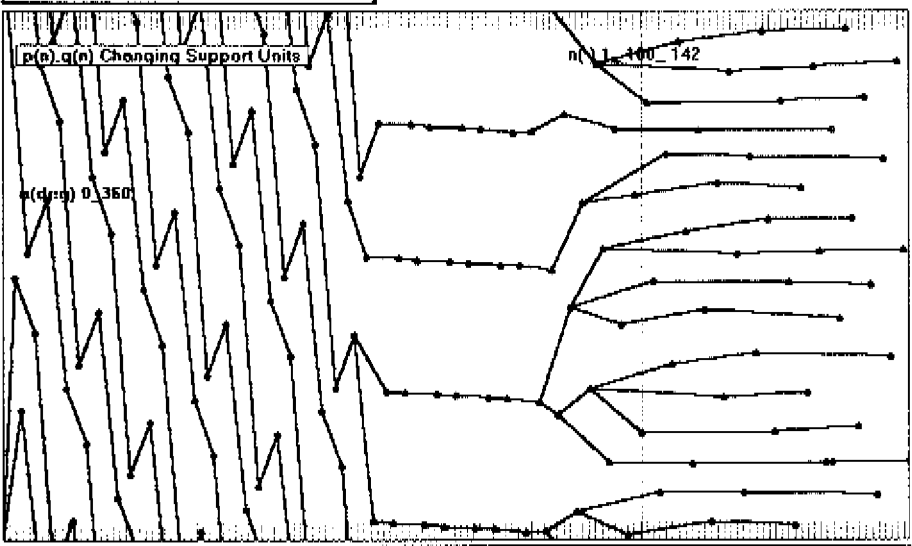

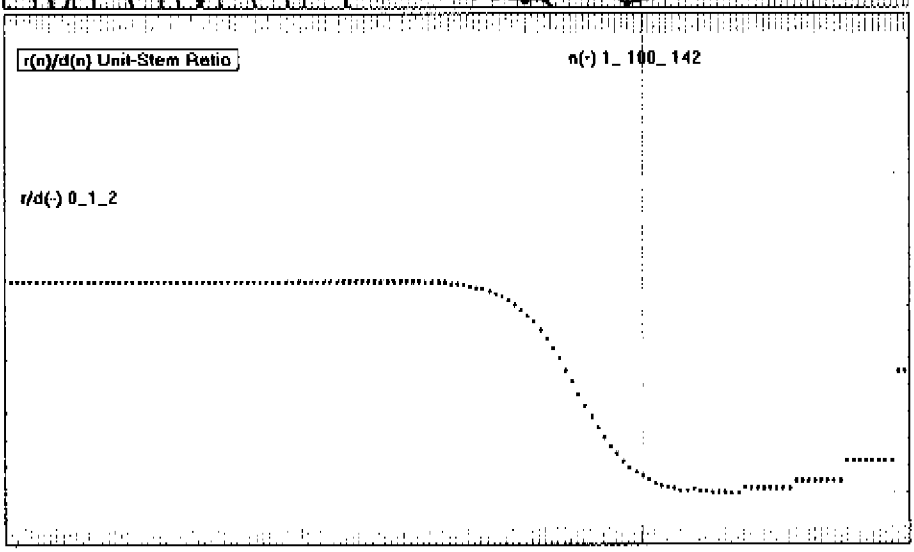

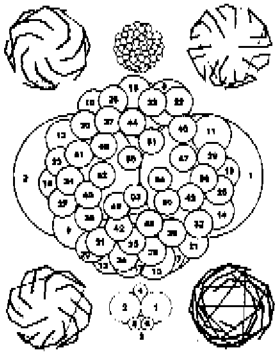

comp/***lucas***	unit range 1-55 *vegetative part 1-20*

TABLE

difference between ordinals of unit n and each of both support units (or contacts) p(n) and q(n)

GRAPH

unit(n)-stem ratio is
radius(n) / distance(center(n) to z-axis)

001	-	-	021	007	011	041	007	011
002	*001*	*002*	022	007	011	042	007	011
003	*001*	*002*	023	007	011	043	007	011
004	*003*	*002*	024	007	011	044	007	011
005	*003*	*002*	025	007	011	045	007	011
006	*001*	*005*	026	007	011	046	007	011
007	*001*	*004*	027	018	011	047	007	011
008	*007*	*004*	028	018	004	048	007	011
009	*007*	*004*	029	018	011	049	007	011
010	*003*	*004*	030	018	011	050	007	011
011	*003*	*004*	031	007	011	051	007	011
012	*003*	*004*	032	018	011	052	007	011
013	*003*	*004*	033	018	011	053	007	004
014	*003*	*004*	034	007	011	054	007	011
015	*003*	*004*	035	007	011	055	007	011
016	*007*	*004*	036	007	011			
017	*007*	*004*	037	007	011			
018	*007*	*004*	038	007	011			
019	*007*	*004*	039	007	011			
020	*007*	*011*	040	007	011			

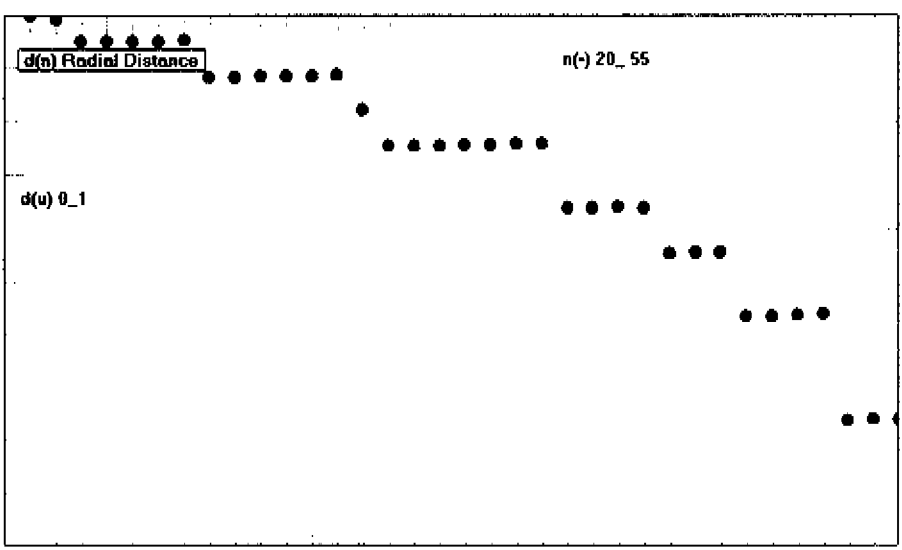

unit range 1-105
vegetative part 1-20

comp/***sun1***

TABLE

divergence angle in degrees (center independent deduced from 3 successive units with ordinals n+a, n, n-a), a=1

GRAPH

unit(n)-stem ratio is
radius(n) / distance{center(n) to z-axis}

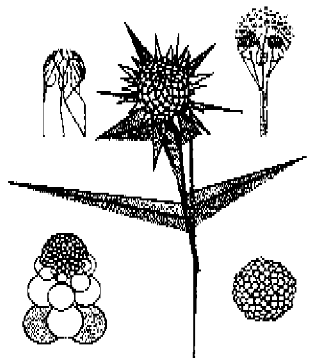

001	-	021	139.72	041	141.96	061	142.00	081	138.42	101	137.67
002	*134.25*	022	136.43	042	138.95	062	140.81	082	139.84	102	139.58
003	*135.75*	023	136.69	043	135.93	063	136.77	083	139.35	103	136.05
004	*130.97*	024	134.63	044	136.57	064	133.37	084	136.56	104	135.50
005	*139.16*	025	133.61	045	135.38	065	134.65	085	135.12	105	-
006	*128.74*	026	133.81	046	135.43	066	133.32	086	138.73		
007	*136.49*	027	138.23	047	139.51	067	136.77	087	138.55		
008	*140.29*	028	143.39	048	140.43	068	139.03	088	137.58		
009	*131.58*	029	139.18	049	140.23	069	140.92	089	138.62		
010	*150.42*	030	136.10	050	136.86	070	140.31	090	138.40		
011	*138.27*	031	136.75	051	133.81	071	137.19	091	137.64		
012	*128.15*	032	135.74	052	134.96	072	134.06	092	130.62		
013	*134.65*	033	135.70	053	134.64	073	138.12	093	137.15		
014	*133.28*	034	141.49	054	138.43	074	140.02	094	139.60		
015	*138.31*	035	138.87	055	139.23	075	139.48	095	139.09		
016	*142.23*	036	136.77	056	138.25	076	136.60	096	137.55		
017	*139.15*	037	136.36	057	138.69	077	134.93	097	137.94		
018	*136.74*	038	134.13	058	136.84	078	137.85	098	136.86		
019	*138.76*	039	136.00	059	134.58	079	133.70	099	140.98		
020	*141.07*	040	139.21	060	138.88	080	135.93	100	137.68		

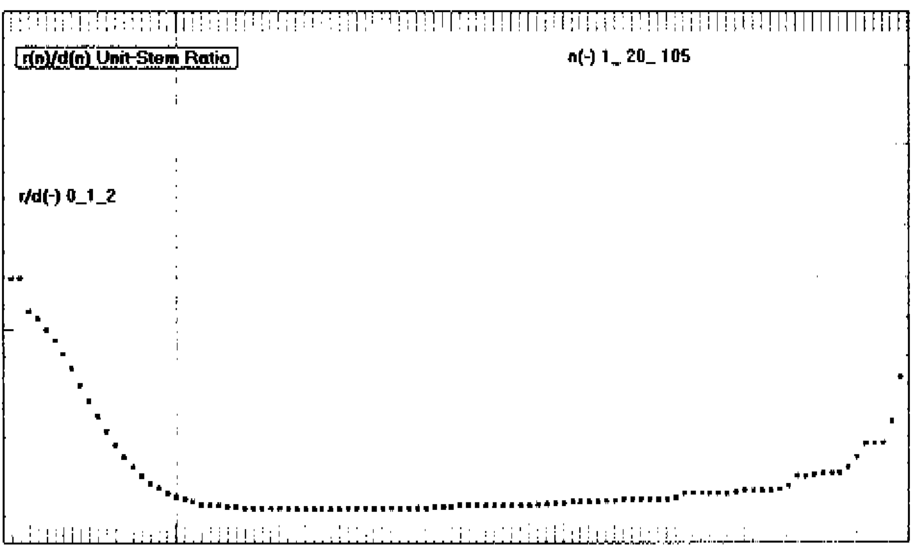

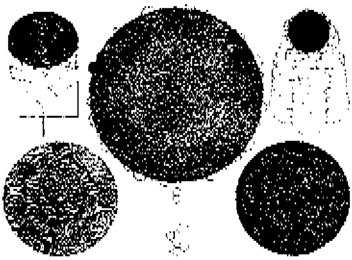

comp/***sun2***	unit range 1-5942 ***vegetative part 1-80***

GRAPH

support units (or contacts) with ordinals p and q of unit(n)

GRAPH

divergence angle (center independent deduced from 3 successive units with ordinals n+a, n, n-a), a=1

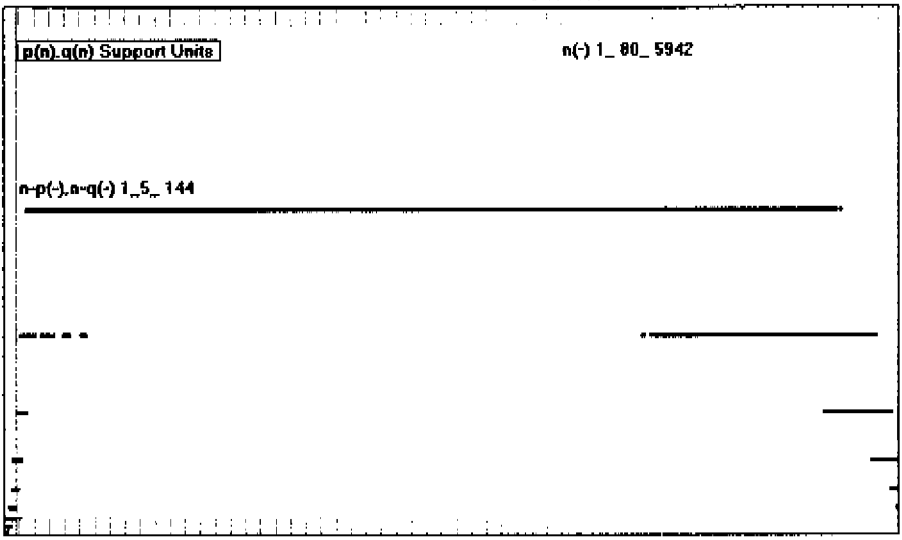

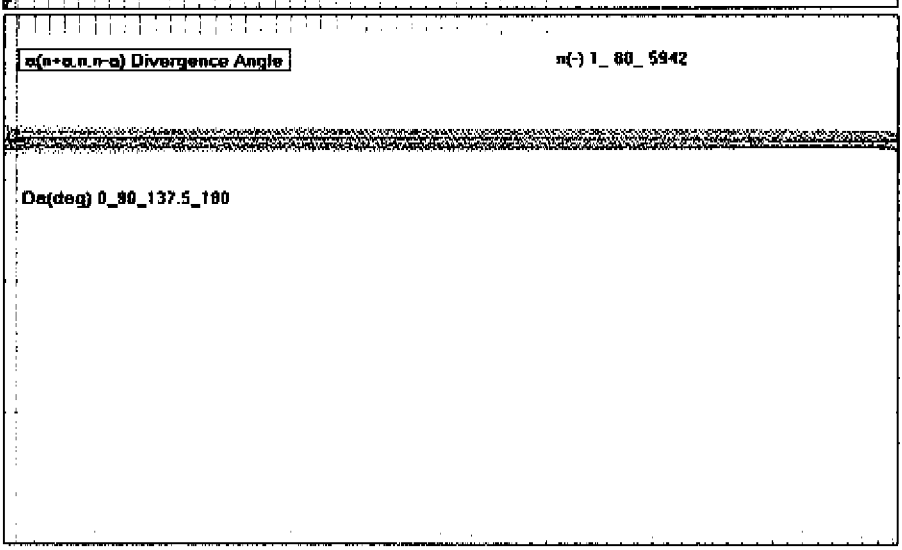

unit range 1-67
vegetative part 1-10

comp/***micr***

GRAPH

divergence angle (center independent deduced from 3 successive units with ordinals n+a, n, n-a), a=1

GRAPH

divergence angle (center ralated deduced from 2 successive units with ordinals n, n-a), a=1

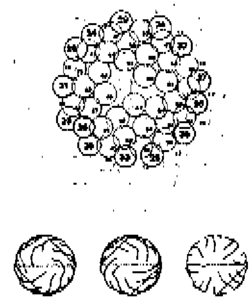

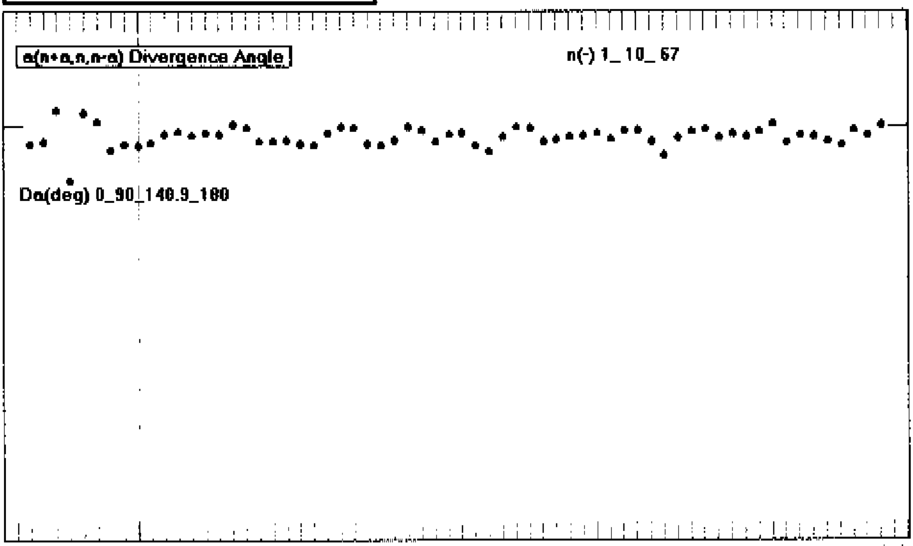

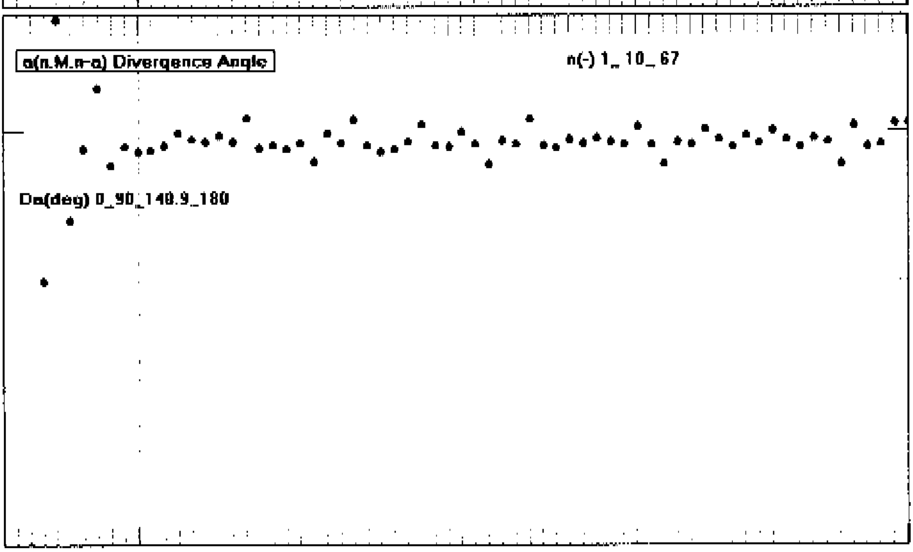

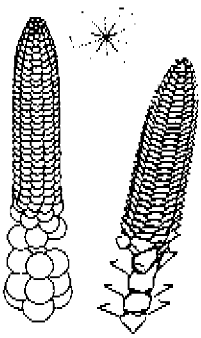

spike/***maize***	unit range 1-311 *vegetative part 1-300*

GRAPH

changings in support units (or contacts) p(n) and q(n) of unit(n)
NB graph is an unrolled cylinder

GRAPH

divergence angle (center independent deduced from 3 successive units with ordinals n+a, n, n-a), a=1

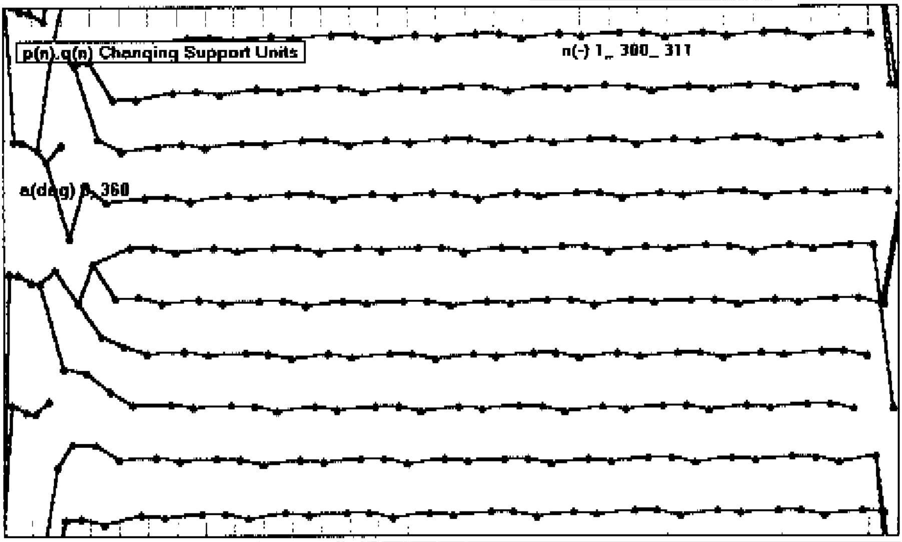

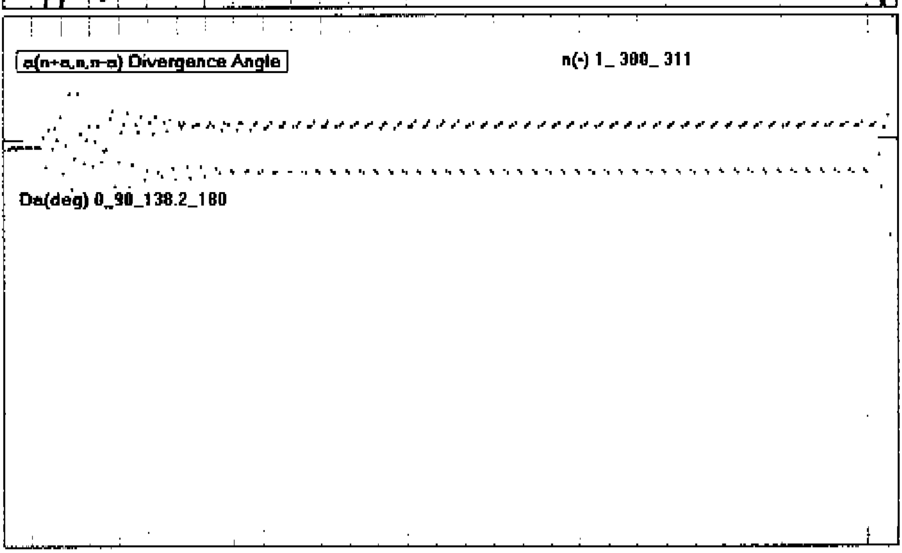

unit range 1-202 *vegetative part 1-200*	cost/***costus***
GRAPH	
divergence angle (center independent deduced from 3 successive units with ordinals n+a, n, n-a), a=2 *NB* 2 spheres form a sickle shaped unit	

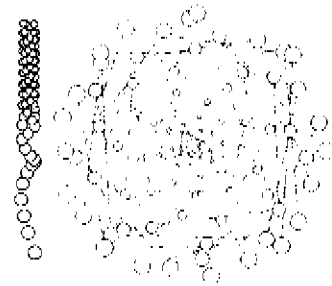

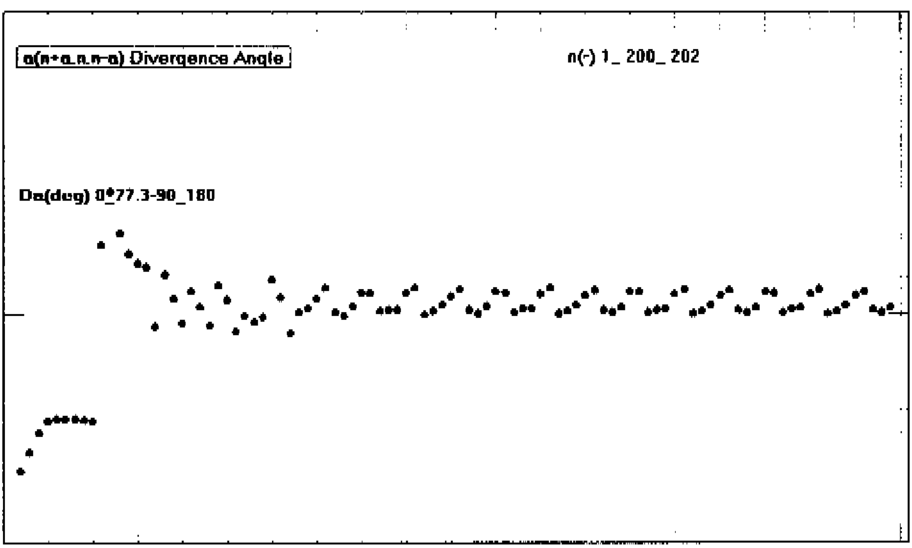

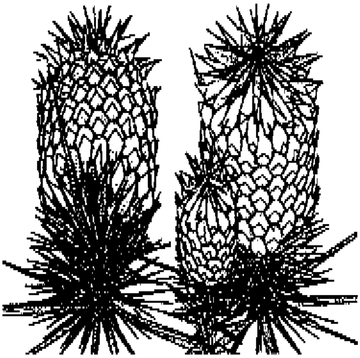

fruit/***pinapp***	*unit range 1-261* *vegetative part 1-200*

GRAPH

radial distance is d(unit center, z-axis), relative radial distance is {distance(n) - distance(n-a)}, a=8

GRAPH

divergence angle (center independent deduced from 3 successive units with ordinals n+a, n, n-a), a=8

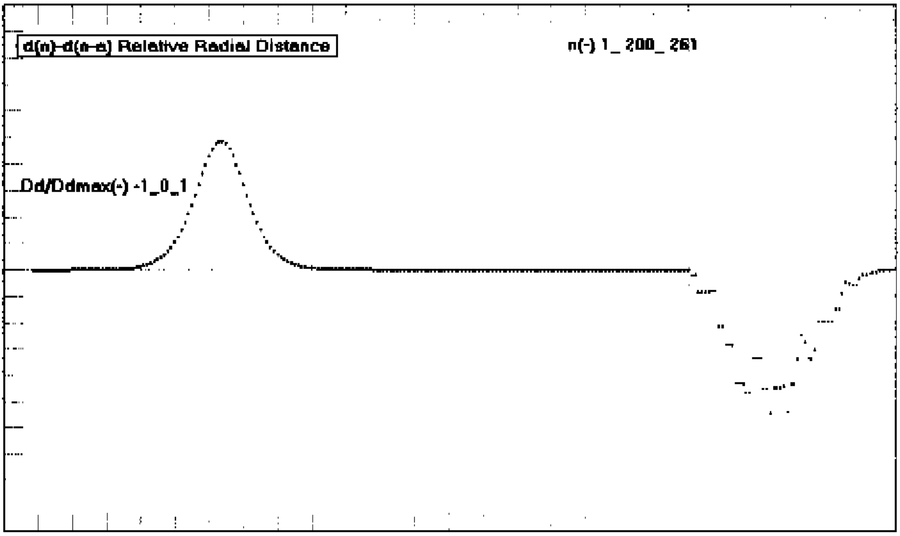

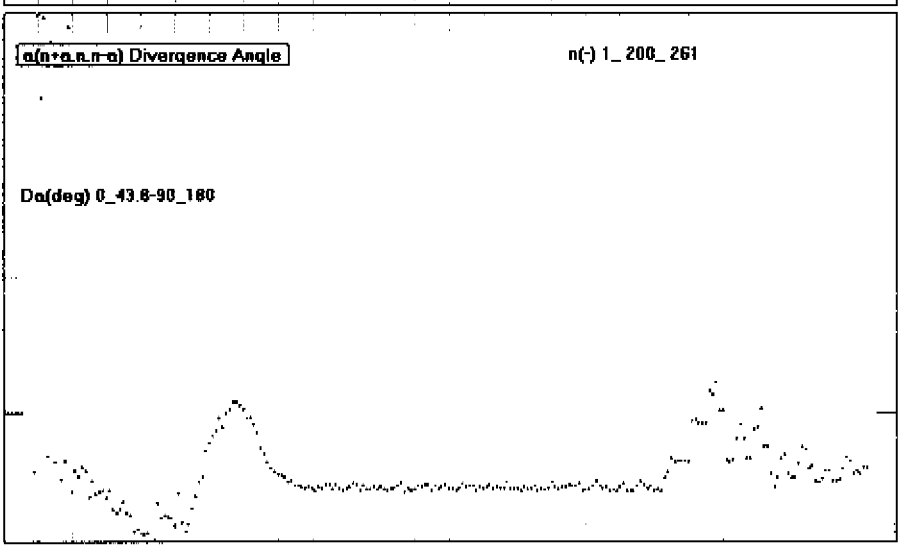

V EDITING SOME RESULTS BY SOLID MODELING

1 EXAMPLES OF DISLODGEMENT STRUCTURES

2 EXAMPLES OF STACK AND DRAG STRUCTURES

Withour comments, several results of the computer programs *'ApexD'* and *'ApexS'* are presented as ray-traced solids*. Note the main difference between the models: The Dislodgement structures are top-down stackings and the Stack and Drag Model produces structures which are stacked from base to top.

As a guide, see:

Basics in the Stack and Drag Model, Chapter 4 'CREATING PHYLLOTAXIS: THE STACK AND DRAG MODEL', *Section 5, p.12 (Fig 12)*

Conceptions of the Stack and Drag Model, Appendage ii 'COMPUTER PROGRAM *'APEXS'*: KEY ALGORITHMS', *Section 2, p.4*

* All solids, except the very first one (by Lucien Havermans, from *'ApexD'*), were generated by René de Kruyf (PTH-contract, Eindhoven, Holland) from results of *'ApexD'* (1x) and *'ApexS'*.

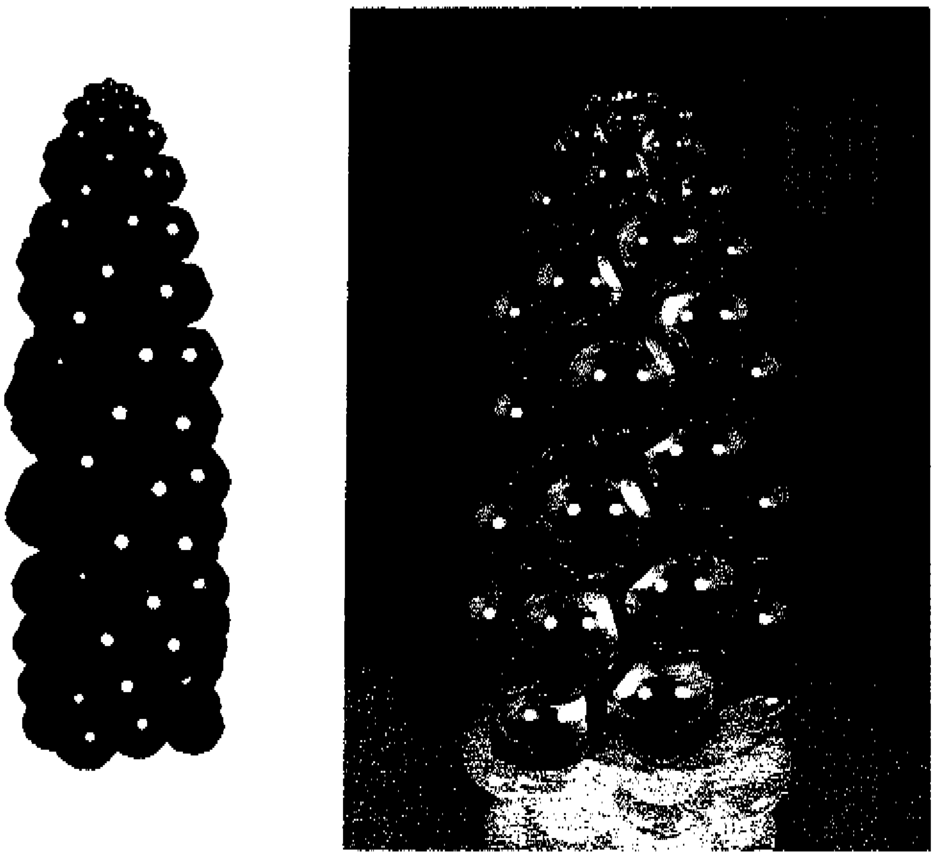

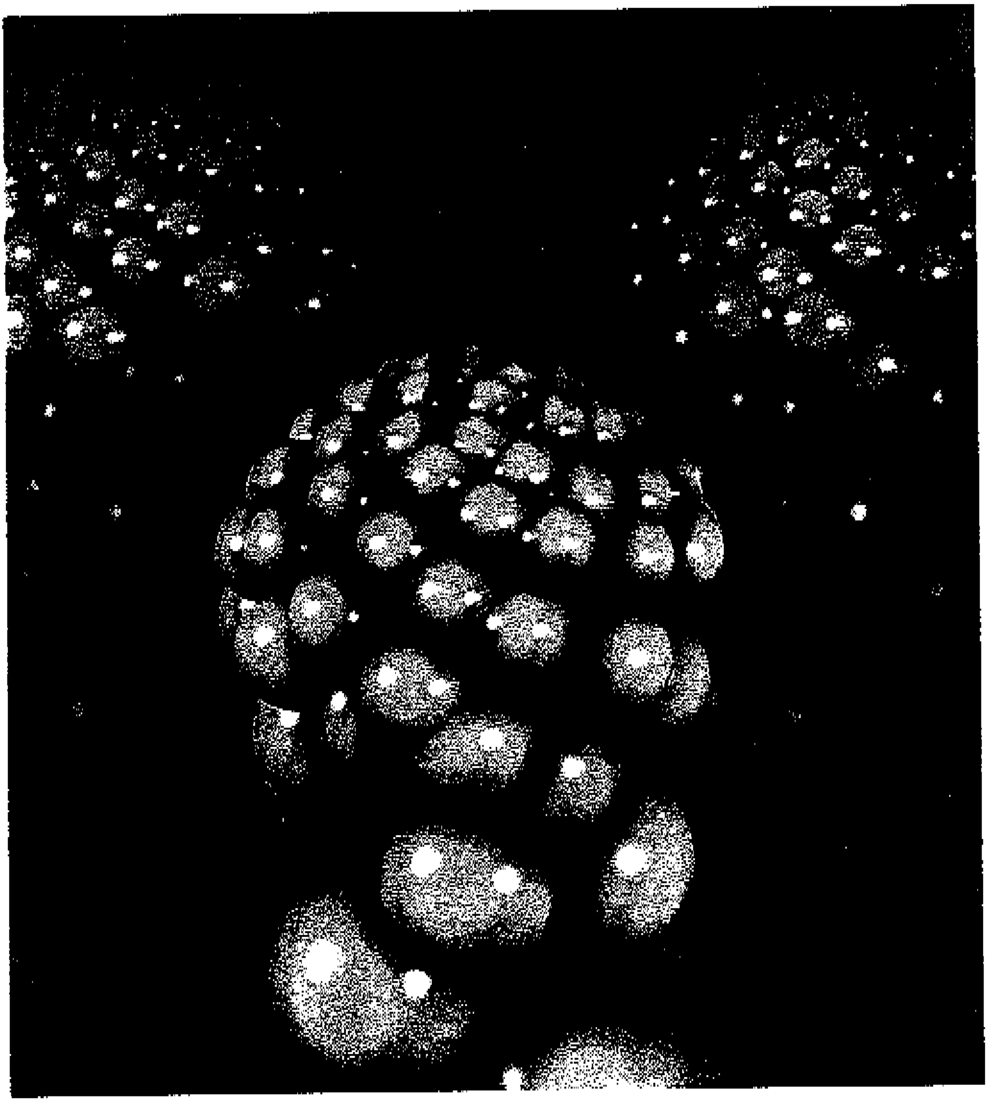

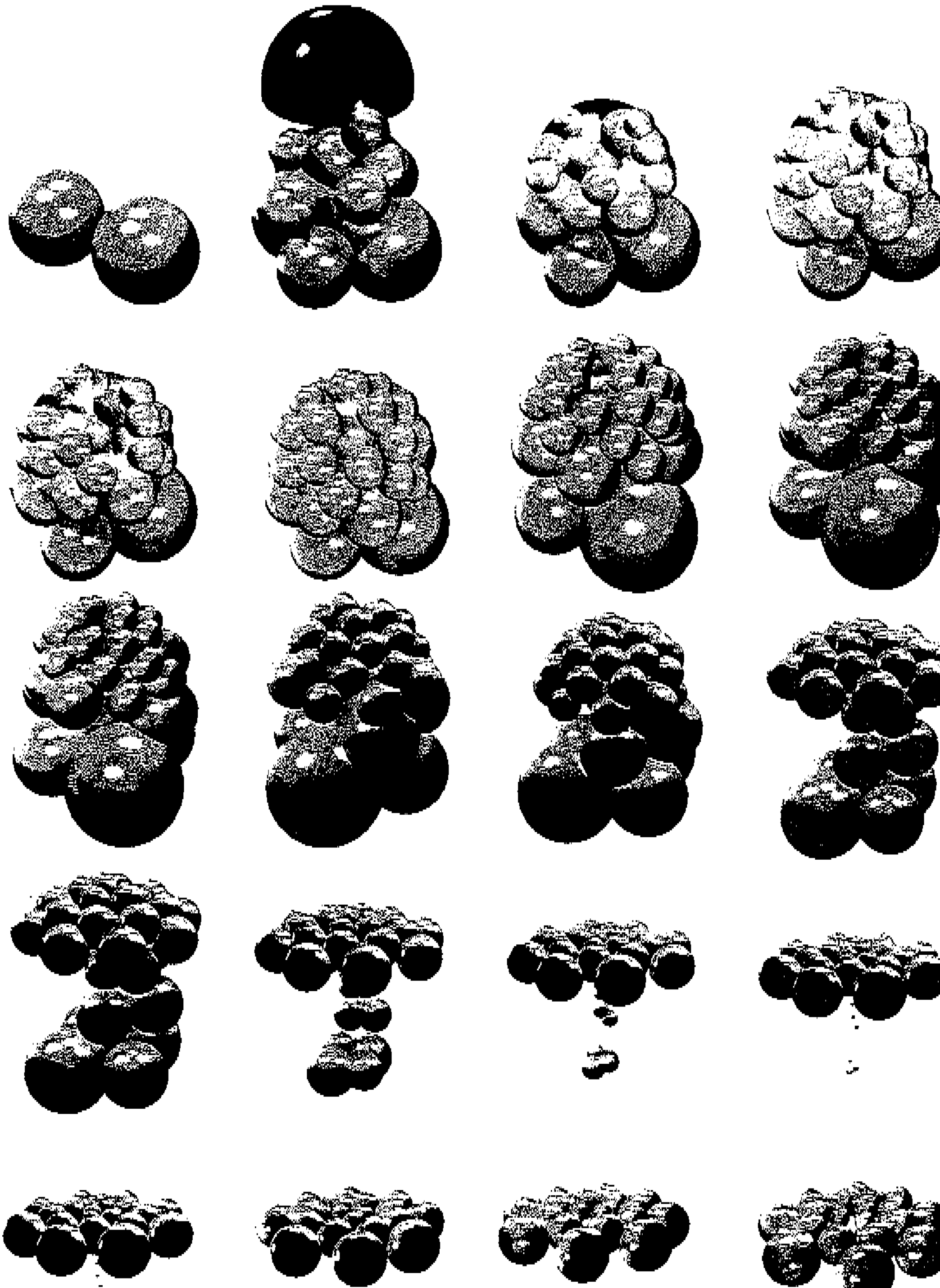

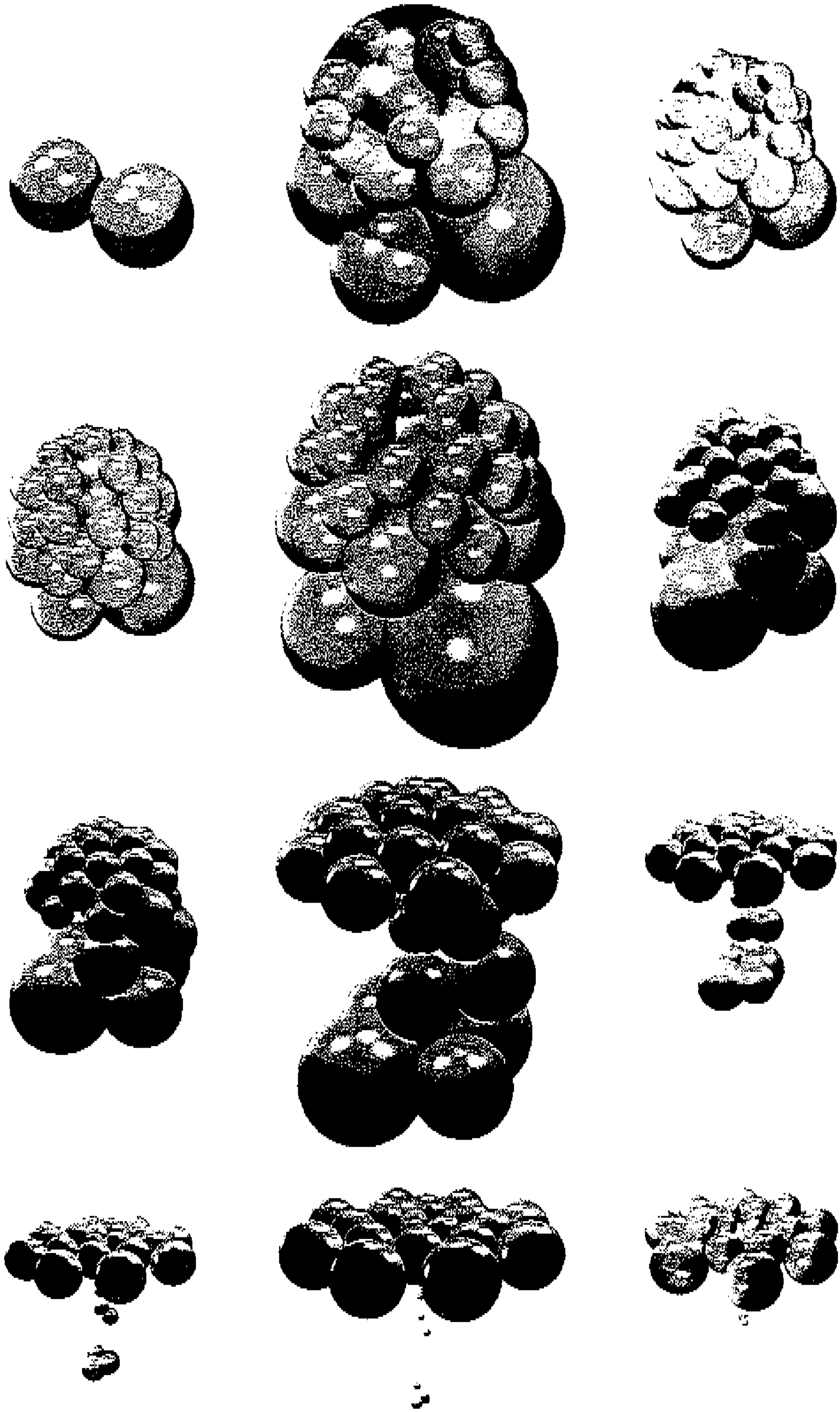

EDITING SOME RESULTS OF '*APEXS*' BY SOLID MODELING

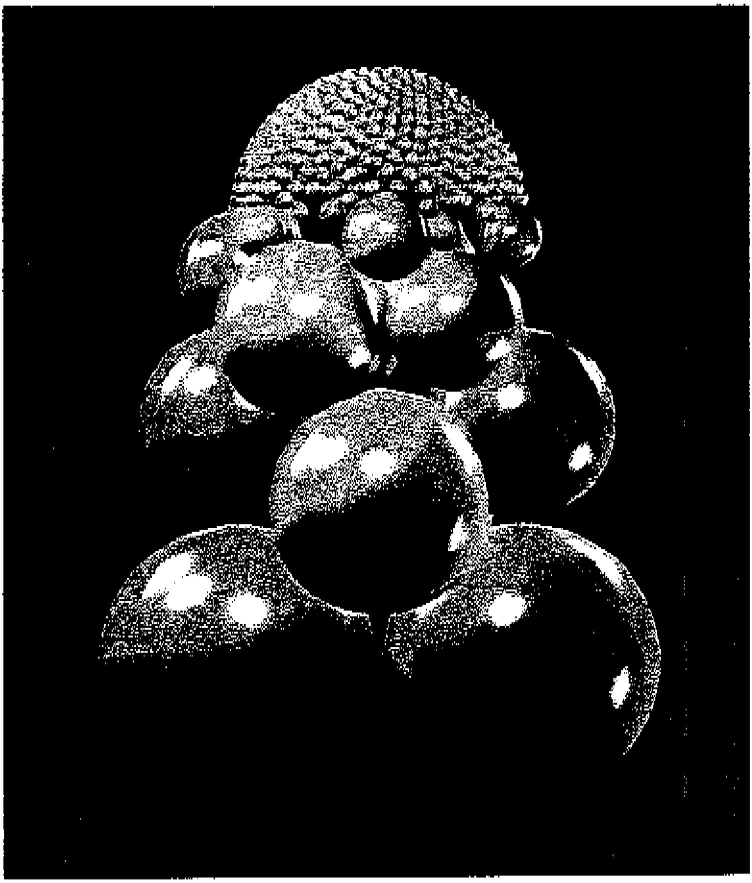

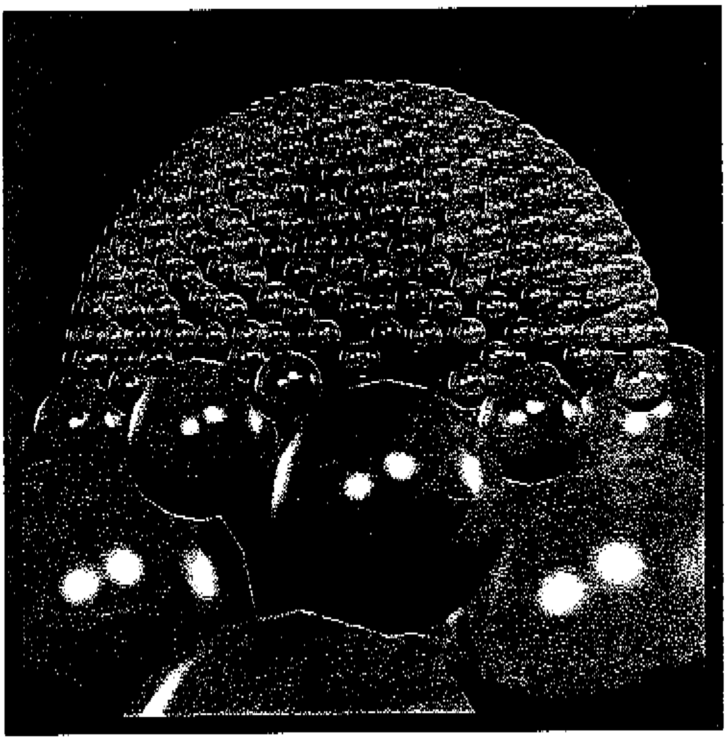

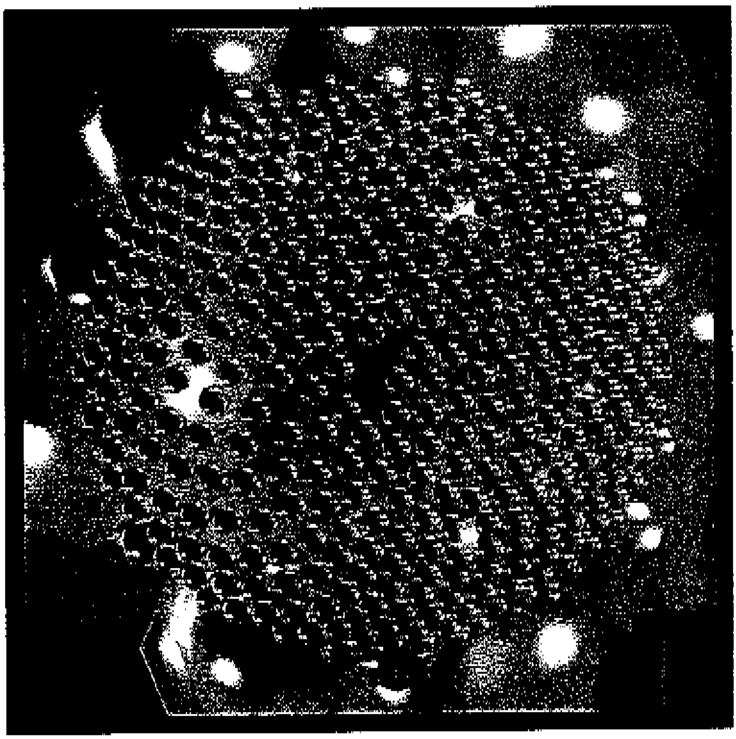

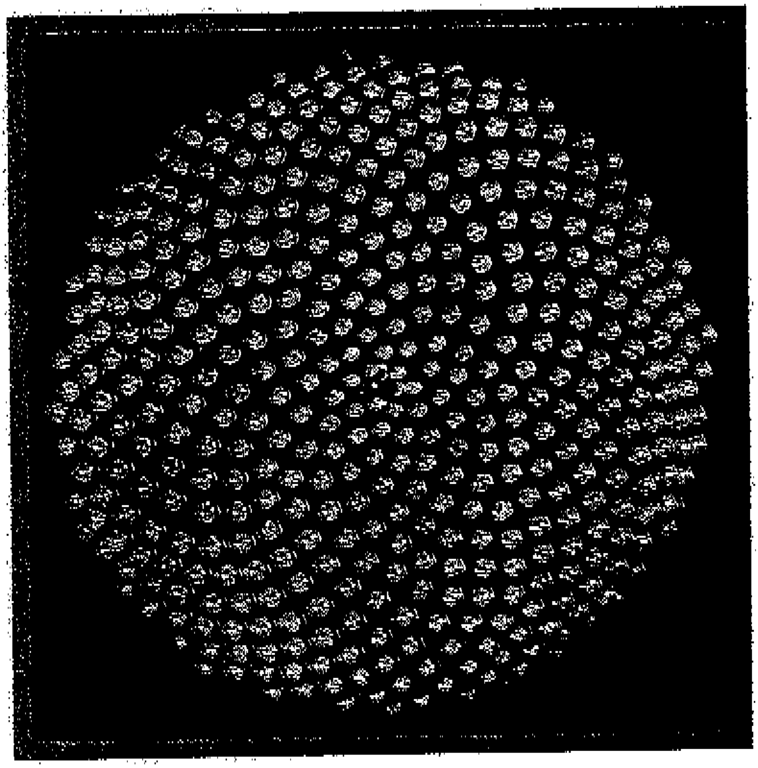

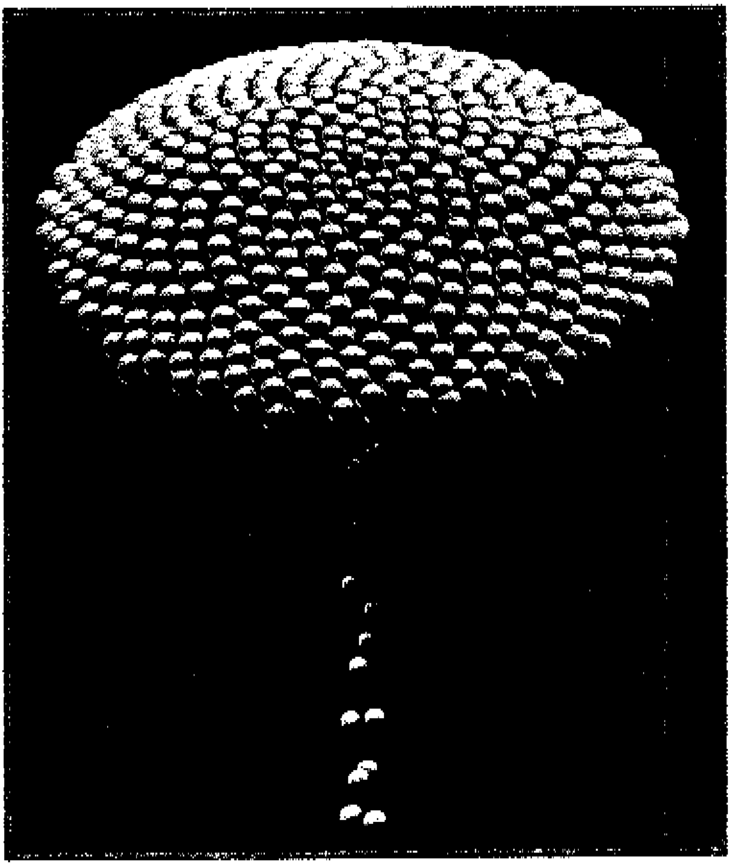

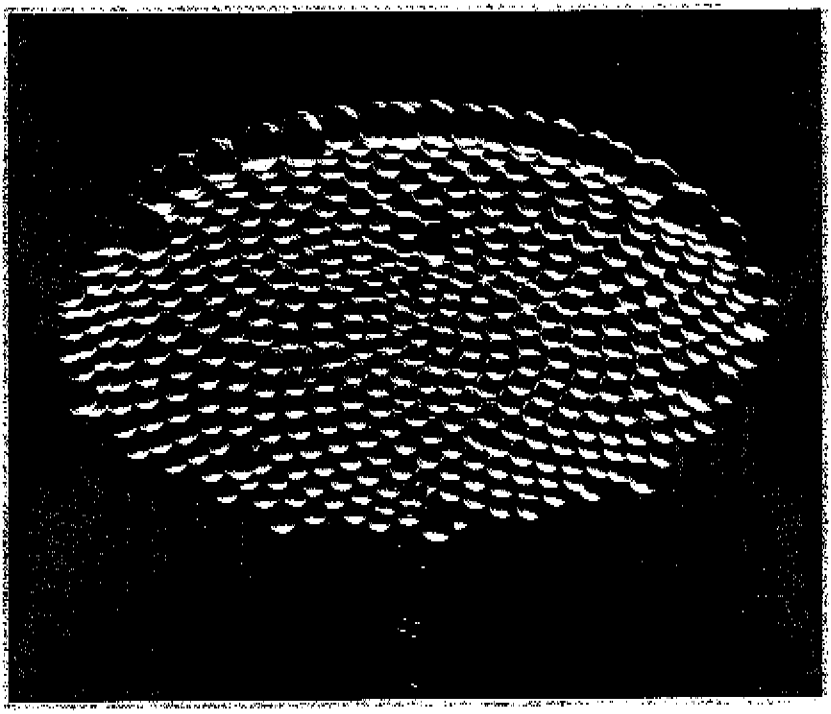

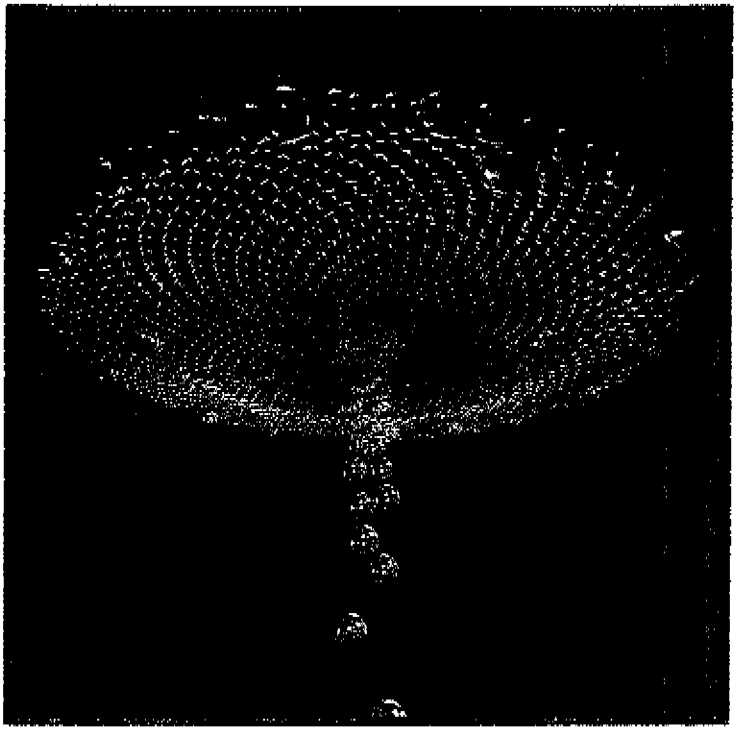

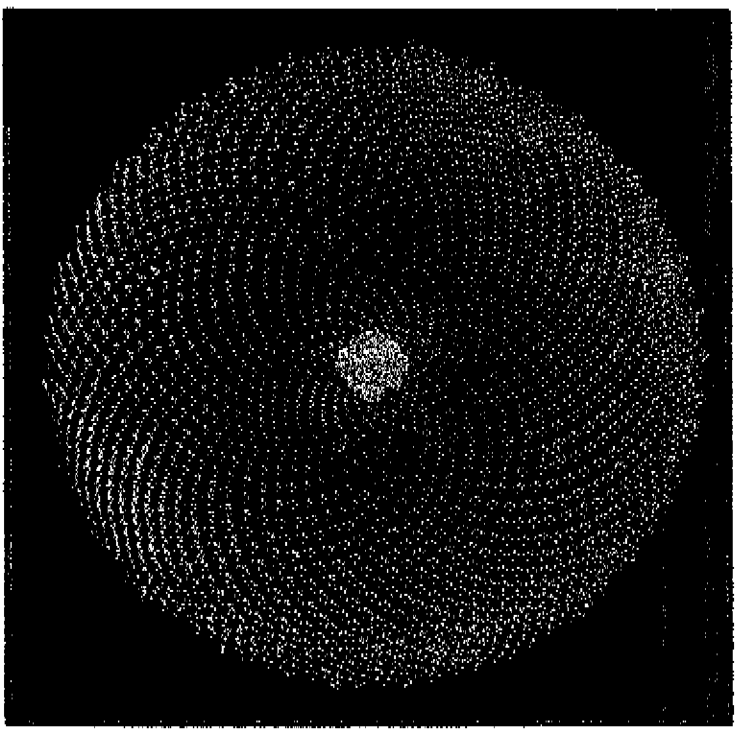

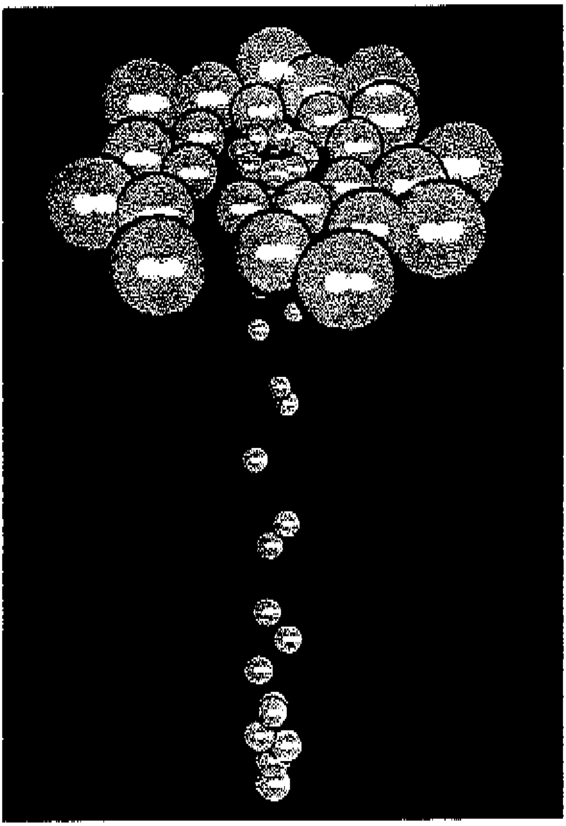

DANKBETUIGINGEN
ACKNOWLEDGEMENTS

Voor gedachtenwisselingen en inhoudelijke aansporingen dank ik:
For exchanges of thoughts and incitements as regards content I thank:

mathematics, informatics, crystallography
R. Barluschke, F. van der Blij, B. Doukmak, L. Havermans, J. Kant, R. de Kruyf, F. van der Linden, J. van Suchtelen, J. Verhoosel, H. Wagter

systematic botany
K. Bachmann, J. Battjes, M. de Boer, L. Camps, W. van Heel, D. Houtgraaf, R. Jean, E. Lammens, A. Lindenmayer†, R. van der Meijden, G. Mitchison, A. Pieters, R. Rutishauser

architecture, building construction, plastic art
R. Blok, M. Daru, R. Daru, W. Huisman, G. Koevoets, P. de Kort, H. Rutten, P. Schmid, E. Vastert

general
Marike Camps

Dit multidisciplinaire onderzoek werd ondersteund door:
This multidisciplinary research has been supported by:

development time
Stichting Hoger Onderwijs Zuid-Nederland

personal support
Projectgroep CAD-CAE van de Pedagogisch Technische Hogeschool Nederland

supervision and environment
Technische Universiteit Eindhoven, Universiteit van Amsterdam

equipment for development and presentation
Stichting Zuid-Nederland tot Ontwikkeling en Opleiding Bouwnijverheid

RECOMMENDED LITERATURE

For specific references, see Chapters 2 (p.22), 3 (p.14), 4 (p.23), and Appendage i (p.5).

Phyllotaxis, L-systems, fractals

(1) J. Battjes, N.O.E. Vischer, and K. Bachmann, Capitulum Phyllotaxis and Numerical Canalization in Microseris Pygmaea, American Journal of Botany, Vol.80(4), pp.419-428, 1993

(2) M.J.M. de Boer, Anal. and Comp. Generation of Division Patterns in Cell Layers Using Developm. Algorithms, Thesis (Utrecht) 1989

(3) J. Briggs, F.D. Peat, The Turbulent Mirror, Harper & Row (N.Y.) 1989

(4) R. Buvat, Structure, Évolution et Functionnement du Méristème Apical de Quelques Dicotylédones, Ann. Sci. Nat. Bot., Ser.11.13, pp.199-300, 1952

(5) S. Douady and Y. Couder, Phyllotaxis as a Physical Self-Organized Growth Process, Physical Review Letters, Vol.68, No.13, pp.2098-2101, 1992

(6) G. Van Iterson, Mathematische und Mikroskopisch-Anatomische Studien über Blattstellungen, Gustav Fischer Verlag, Jena, 1907

(7) R.V. Jean, Phyllotactic Pattern Generation: A Conceptual Model, Ann. Bot. (London) 61, 1988

(8) A. Lindenmayer, Development Algorithms: Lineage Versus Interactive Control Mechanisms, in: Development Order: Its Origins and Regulation, S. Subtelny & P.B. Green, Eds., Alan R. Liss (N.Y.) 1982

(9) B.B. Mandelbrot, The Fractal Geometry of Nature, Freeman (N.Y.) 1983

(10) G.J. Mitchison, Phyllotaxis and the Fibonacci Series, Science, Vol.196, pp.270-275, 1977

(11) P. Prusinkiewicz, A. Lindenmayer, The Algorithmic Beauty of Plants, Springer Verlag (N.Y.) 1990

(12) R. Rutishauser, Blattstellung und Sprossenentwicklung bei Blütenpflanzen, J. Cramer (Vaduz) 1981

(13) d'Arcy W. Thompson, On Growth and Form, Cambridge University Press (London) 1917

(14) F.M.J. Van der Linden, Creating Phyllotaxis, The Dislodgement Model, Math. Biosci. (N.Y.) 100, 1990

(15) F.M.J. Van der Linden, The Dislodgement Model Improved, (manuscript) 1994

(16) F.M.J. Van der Linden, Creating Phyllotaxis, The Stack and Drag Model, Math. Biosci. (N.Y.) 1995

(17) F.M.J. Van der Linden, Phyllotactic Patterns for Domes, Space Structures (London), Vol.9, 1994

(18) F.M.J. Van der Linden, De hoek van 137,5°, NRC-Handelsblad (Rotterdam) 24-1, 1991

(19) F.M.J. Van der Linden, Der Winkel von 137.5°, (Übersetzung NRC) 1991

(20) F.M.J. Van der Linden, Het Geheim van de Zonnebloem, Jonas 21 (Amsterdam), no.16, 1991

Euclidic geometry, (bio-)constructions

(1) A.C. Edmondson, M. Senechal, G. Fleck, J. Wechsler, A.L. Loeb, Shaping Space, A Polyhedral Approach, Birkhäuser (Boston) 1988

(2) S. Hildebrandt, A. Tromba, Mathematics and Optimal Form, Freeman (N.Y.) 1985

(3) K. Miyazaki, An Adventure in Multidimensional Space, John Wiley & Sons (N.Y.) 1983

(4) W. Nachtigall, Phantasie der Schöpfung, Hoffmann und Campe Verlag (Hamburg) 1974

(5) G.A. Pieters and M.E. Van der Noort, The Morphogenic Unit: The Essence of Morphogenesis, Dept. of Plant Physiol. Research, Agricult.University Wageningen (The Netherlands), paper

(6) P.S. Stevens, Patterns in Nature, Little, Brown & Company (Boston) 1974

(7) R. Williams, The Geometrical Foundation of Natural Structure, Dover Publications (N.Y.) 1979

Systematic botany

(1) R.F. Lyndon, Plant Development - The Cellular Basis, Unwin Hyman (London) 1990

(2) G.A. Pieters, M.E. van den Noort, The Morphogenic Unit: The Essence of Morphogenesis (Wageningen)

(3) T.A. Steeves and I.M. Sussex, Patterns in Plant Development, Cambridge University Press, (Cambridge) 1991

(4) O. Zeller, Blütenknospen - Verborgene Entwicklungsprozesse im Jahreslauf, Urachhaus (Stuttgart) 1983

Other relevant publications of F.M.J. van der Linden

(1) Handboek Modulair Bouwen *(Manual for Modular Building)* (with Ir. A.M. de Jong, Ir. J.J.L.M. de Bondt and others), Waltman en VGBouw (Delft) 1990

(2) Architectuurgeschiedenis *(History of Architecture)* (with Ir. A.M. de Jong and Ir. G.J. van Zantvoort), SMD (Delft) 1995

CURRICULUM VITAE

FRANK MARIA JOZEF VAN DER LINDEN

De belangrijkste stappen richting/bezijden dit proefschrift en enkele blijde gebeurtenissen:
The author's main steps towards/beside this thesis and some happy events:

1953 Born 28 december in Eindhoven, Netherlands
1971 Graduation HBS-b at the St-Joriscollege, Eindhoven
1972 One year Biology at the Nijmegen University
1977 Stating the Problem: *"How to draw the sunflower seeds without the use of any curve?"*
1978 First prize architectural *(Tzónis-)* competition *'Towards a non-oppressive architecture'*
1979 Graduation Building Science, Architectural Design, Eindh. Uni. of Technology
1980 Office for Architecture and Graphic Arts: Van der Linden, Vastert, Ooms
1980 First algorithm with touching circles
1982 First computer aided efforts to generate phyllotactic patterns, with R. Barluschke
1984 Lecturer at the PTHN (Pedagogic Highschool of Technology Netherlands)
1985 First successful computer simulation
1986 Married with Marike Camps
1986 Support of the first phyllotactic model by A. Lindenmayer| and F. van der Blij
1987 Daughter Karianne
1987 Computer calculated 'dislodging' of 3500 circles from a center outwards
1988 Computer program *'Spiral'* draws planar and spatial vegetative patterns
1990 Son Mick
1990 Manual for building practice *'Modular Building'*, co-authorship
1990 *'Creating Phyllotaxis: The Dislodgement Model'* in Mathematical Biosciences (N.Y.)
1991 Son Otto
1991 a.o. *'Gnomonic Growth'* and *'The Angle of 137.5°'* in NRC Handelsblad (Holland)
1992 Architectural office: Van der Linden & De Jong
1992 Start of the doctoral study *'Phyllotactic Patterns for Domes'* at the Eindh. University
1992 Adjustment of the model after criticism of J. Battjes and K. Bachmann
1993 Computer program *'ApexS'* draws patterns from seed to flower
1994 *'Phyllotactic Patterns for Domes'* in Space Structures (London)
1994 Manuscript *'Creating Phyllotaxis: The Stack and Drag Model'*
1994 Study-book *'History of Architecture'*, based on architectural items, co-authorship
1994 Doctoral degree

STELLINGEN

bij het proefschrift van
Frank M.J. van der Linden

PHYLLOTACTIC PATTERNS FOR DOMES

- De Gulden Snede is geen streven van de (levende) natuur - het is een onnatuurlijk getal.
- Het Stapel- en Trek-model reduceert het bijzondere probleem van phyllotaxis tot het algemene probleem van celdifferentiatie door het wiskundige probleem te isoleren en op te lossen.
- Het ondergeschikt-zijn van phyllotaxis aan de draagconstructie van planten maakt het geschikt zijn van phyllotactische patronen voor bouwkundige constructies minder aannemelijk.
- Experimenten met rechthoeken in allerlei verhoudingen, die een voorkeursrechthoek moeten opleveren, zijn gedoemd tot mislukken, wanneer proefpersonen niet kunnen kiezen uit een reeks rechthoeken liggende staaf---vierkant---staande staaf.
- Maatsystemen, die ruimtes en massa's architectonisch willen helpen harmoniëren, zijn vaker een leidraad voor onervaren buitenstaanders, dan een gereedschap voor inventieve architecten.
- Intuïtie vormt de basis van wetenschap, ratio vormt wetenschappelijke theorieën.
- Intuïtie en emotie zijn de grootste drijfveren en tevens de grootste remmers van culturele, dus ook technologische en wetenschappelijke ontwikkelingen.
- Hoe abstracter een verklaring voor het fenomeen mens voor iemand is, hoe minder hanteerbaar die is in zijn dagelijkse doen en laten.
- De meeste activiteiten van de mens als individu bedreigen de mens als soort.
- Proefschrift-stellingen vormen een manier van uiten, zoals poëzie, muziek, schilderijen en moppen: je kunt ze niet toelichten zonder concessies te doen aan de boodschap.
- Het ontwerpproces (een proces van synthese, startend met een programma-van-eisen en een idee, zich ontwikkelend van grof naar fijn) verschaft na spiegeling een didactische kapstok voor (analyserende) lessen in de bouwtechniek.
- Waar in enig onderwijs computergestuurd wordt ontworpen is een cursus Oplossend Schetsen onontbeerlijk.
- Beide vertrekken vanaf een programma-van-eisen en beeldvorming, maar op de TUE divergeert de differentiatie architectuur naar het papieren prijsvraagontwerp, terwijl op de PTH de differentiatie bouwkunde convergeert naar het technische ontmoetingsdetail.
- Fouten in je achtertuin zijn aandoenlijk - fouten in je phyllotaxis-ontwerpende software zijn ergerlijk.
- Het geloof, dat een stukje vlees, wanneer het ter plaatse van de koningskamer in een Cheops-piramidemodel wordt bewaard, eerder uitdroogt dan rot, heeft vooral aanhangers onder vrouwen en droogscheerders.